

Building Services and Energy Efficiency

Modernizing and increasing performance of Building Services

Iași, Romania
July 2nd, 2020 - July 3rd, 2020

EDITOR-IN-CHIEF
Vasilică Ciocan

Editors:

Andrei Burlacu

Valeriu Sebastian Hudişteanu

Gabriela Covatariu

Nelu-Cristian Cherecheş

PREFACE

Modernizing and increasing performance of Building Services represents the theme of Building Services and Energy Efficiency Conference (BSEE), July 2-3, 2020

The Building Services and Energy Efficiency (BSEE) Conference is an event that has become traditional in the world of civil engineering, since 1990. The main organizer is the Gheorghe Asachi Technical University of Iasi, Faculty of Civil Engineering and Building Services. Every year, the conference presents issues of new scientific research as well as the companies' needs for creating new organizational solutions. The BSEE Conference covers all scientific and technological aspects of civil engineering and building services field: energy efficiency, building services, computer-aided design, and engineering, computational fluid dynamics, building services performance analysis, building services monitoring and management, heat and mass transfer, lighting systems, energy storage, renewable energy, enhancing sustainability and resilience of building services, numerical analysis in civil engineering, BIM.

The building services and equipment have become essential elements in the construction of buildings to ensure the conditions of interior comfort. In a fast-evolving society, information is an essential element for the progress of economic-social activities, and the Conference of Building Services and Energy Efficiency represent the place where the exchange of information and ideas for the sustainable development of the built environment and its facilities takes place.

The BSEE Conference accepts review articles, original scientific articles, and cases from the field of civil engineering and building services – mechanical engineering, electrical engineering, and materials. All papers in BSEE Conference are first peer-reviewed and only accepted articles that have not yet appeared in a printed or electronic issue are published.

The 2020 Edition of the BSEE conference was organized online as a result of the special situation created by the pandemic COVID-19. Started as an epidemic in Wuhan, Hubei Province of China, in December 2019, COVID-19 was declared a pandemic by the World Health Organization on 12 March 2020, when there were more than 125,000 cases of infected people from 118 countries and regions of the world. The health system crisis generated many other crises in economy, business, education, culture and society. Most of the universities were forced to close their regular classes and to switch all their activities online. As a direct result, all the international conferences organized by

universities had to be online. Our conference made no exception. During the first day of the conference we had three Guest Speakers for the Plenary Session: professor Chérifa ABID from Aix-Marseille Université, France, professor Gawęł ŻYŁA from Rzeszów University of Technology, Poland and professor Pierre-Olivier LOGERAIS from Université Paris-Est Créteil Val de Marne - Université Paris 12, France. Their presentations covered such topics as learning and unlearning in time of crises, knowledge risks and the importance of cybersecurity.

During the day of the conference, there were presented 30 papers with contributors from 5 countries. The papers were presented within the following sessions during two days:

Day 1 - Thursday, 2nd July, 2020

Plenary Session I

Keynote Speaker - Chérifa ABID, Aix-Marseille Université, France

Moderator - Victoria Cotorobai & Andrei Burlacu

Plenary Session II

Keynote Speaker - Gawęł ŻYŁA, Rzeszów University of Technology, Poland

Moderator - Cristian Chereches & Catalin Galatanu

Day 2 - Friday, 3rd July, 2020

Plenary Session III

Keynote Speaker - Pierre-Olivier LOGERAIS, Université Paris-Est Créteil Val de Marne - Université Paris 12, France

Moderator - Sebastian Valeriu Hudişteanu & Marius Balan

The selected papers from the Building Services and Energy Efficiency Conference (BSEE) will be considered for publication. The Proceedings of the 2020 Building Services and Energy Efficiency Conference is published under Sciendo Publishing House and will be indexed in various international databases, especially SCOPUS and the Web of Science (WOS) and other known international databases.

Conference President
Assoc. Prof. PhD. Vasilică Ciocan

Honorary Committee

- **Prof. Jacques PADET** - Emeritus Professor, Université de REIMS – France, Doctor Honoris Causa, Gheorghe Asachi Technical University of Iasi, Romania
- **Prof. Liviu DUMITRESCU** - Honorific President of the AIIR Romania

Scientific Committee

- **Pierre-Olivier LOGERAIS**, Université Paris-Est Créteil Val de Marne - Université Paris 12, France
- **Engin GEDIK**, Karabuk University, Turkey
- **Alina Adriana MINEA**, Gheorghe Asachi Technical University of Iasi, Romania
- **Norayr BENOHANIAN**, American University of Armenia, Armenia
- **Ionut Cristian SCURTU**, "Mircea cel Batran" Naval Academy, Romania
- **Mebarek-Oudina FATEH**, Université de Skikda, Algeria
- **Ilinca NASTASE**, Technical University of Civil Engineering of Bucharest, Romania
- **Chérifa ABID**, Aix-Marseille Université, France
- **Bogdan UNGUREANU**, Imperial College London, United Kingdom
- **Catalin Viorel POPA**, Université de Reims Champagne-Ardenne, France
- **Artak HAMBARIAN**, American University of Armenia, Armenia
- **Nelu Cristian CHERECHEȘ**, Gheorghe Asachi Technical University of Iasi, Romania
- **Gawel ŻYLA**, Rzeszów University of Technology, Poland
- **Gabriela COVATARIU**, Gheorghe Asachi Technical University of Iasi, Romania
- **Lucian Constantin UNGUREANU**, Technical University of Berlin, Germany
- **Michal KRAJCIK**, Slovak University of Technology in Bratislava, Slovakia
- **Andrei BURLACU**, Gheorghe Asachi Technical University of Iasi, Romania
- **Arthur KHALATYAN**, American University of Armenia, Armenia
- **Sebastian Valeriu HUDIȘTEANU**, Gheorghe Asachi Technical University of Iasi, Romania
- **Kamil ARSLAN**, Karabuk University, Turkey
- **Emilian Florin TURCANU**, Gheorghe Asachi Technical University of Iasi, Romania
- **Alper ERGÜN**, Karabuk University, Turkey
- **Marius Costel BALAN**, Gheorghe Asachi Technical University of Iasi, Romania
- **Sébastien GUENNEAU**, UMI CNRS-Imperial Abraham de Moivre, United Kingdom
- **Diana ANCAȘ**, Gheorghe Asachi Technical University of Iasi, Romania
- **Georges ZISSIS**, UNIVERSITÉ TOULOUSE III - Paul Sabatier, France
- **Cătălin-Daniel GĂLĂȚANU**, Gheorghe Asachi Technical University of Iasi, Romania
- **Cristiana CROITORU**, Technical University of Civil Engineering of Bucharest, Romania

- **Laurent CANALE**, UNIVERSITÉ TOULOUSE III - Paul Sabatier, France
- **Iulian GHERASIM**, Gheorghe Asachi Technical University of Iasi, Romania
- **Aliz Éva MÁTHÉ**, Technical University of Cluj-Napoca, Romania
- **Florin BODE**, Technical University of Cluj-Napoca, Romania
- **Tiberiu CATALINA**, Technical University of Civil Engineering of Bucharest, Romania
- **Razvan Silviu LUCIU**, Gheorghe Asachi Technical University of Iasi, Romania
- **Cristina Mihaela Câmpian**, Technical University of Cluj-Napoca, Romania
- **Victoria COTOROBAI**, Gheorghe Asachi Technical University of Iasi, Romania
- **Adrian GLIGOR**, University of Medicine, Pharmacy, Science and Technology of Târgu Mureș, Romania

Steering Committee

- **Theodor Mateescu**, Gheorghe Asachi Technical University of Iasi
- **Vasilică Ciocan**, Gheorghe Asachi Technical University of Iasi
- **Marina Verdeș**, Gheorghe Asachi Technical University of Iasi
- **Mihai Profire**, Gheorghe Asachi Technical University of Iasi
- **Cătălin-Daniel Gălățanu**, Gheorghe Asachi Technical University of Iasi
- **Andrei Burlacu**, Gheorghe Asachi Technical University of Iasi
- **Victoria Cotorobai**, Gheorghe Asachi Technical University of Iasi
- **Cătălin-George Popovici**, Gheorghe Asachi Technical University of Iasi
- **Diana Ancaș**, Gheorghe Asachi Technical University of Iasi
- **Nelu-Cristian Cherecheș**, Gheorghe Asachi Technical University of Iasi
- **Iulian Gherasim**, Gheorghe Asachi Technical University of Iasi
- **Răzvan-Silviu Luciu**, Gheorghe Asachi Technical University of Iasi
- **Marius-Costel Balan**, Gheorghe Asachi Technical University of Iasi
- **Sebastian Valeriu Hudișteanu**, Gheorghe Asachi Technical University of Iasi
- **Florin-Emilian Țurcanu**, Gheorghe Asachi Technical University of Iasi
- **Elena Crețu**, Gheorghe Asachi Technical University of Iasi
- **Gheorghe Avram**, DAS Iasi
- **Angela Avram**, DAS Iasi
- **Lidia Cărăuș**, DAS Iasi

Table of contents

	Page
1. Ion-Costinel MAREȘ, Tiberiu CATALINA, Andrei ISTRATE, Tiberius DICU and Alexandra CUCOȘ EXPERIMENTAL RESEARCH OF MITIGATION SYSTEMS FOR CONTROLLING AND REDUCING RADON EXPOSURE IN RESIDENTIAL BUILDINGS DOI: 10.2478/9788395720413-001	1
2. Ionut Cristian SCURTU, Amin Moslemi PETRUDI and Masoud RAHMANI PARAMETRIC OPTIMIZATION AND CALCULATION OF VIBRATIONS INTRODUCED BY PROPULSION INSTALLATION DOI: 10.2478/9788395720413-002	14
3. Catalin BAILESCU and Vlad IORDACHE EXPERIMENTAL INVESTIGATION ON THE SOUND PRESSURE LEVEL FOR DIFFERENT ACOUSTIC TREATMENT OF BOILER ROOMS DOI: 10.2478/9788395720413-003	29
4. Vinceriuc MIOARA and Tarlea GRATIELA NUMERICAL AND EXPERIMENTAL ANALYSIS OF THE MV3T REFRIGERANT DOI: 10.2478/9788395720413-004	44
5. George MARDARE and Gratiela TARLEA STUDY CASE REGARDING THE IMPROVEMENT OF ENERGY AND ECOLOGICAL PERFORMANCE OF A HEAT PUMPS DOI: 10.2478/9788395720413-005	52
6. Catalin SIMA, Catalin TEODOSIU and Charles BERVILLE MESH INDEPENDENCY STUDY FOR A SOLAR GLAZED TRANSPIRED COLLECTOR DOI: 10.2478/9788395720413-006	60

7. Larisa-Georgiana POPA

**INFLUENCE OF SHADING SYSTEMS ON ENERGY
PERFORMANCE OF BUILDINGS WITH LARGE GLAZING
AREAS**

DOI: 10.2478/9788395720413-007

69
8. Tiberiu CATALINA and Alexandra-Elena FERARU

**EXPERIMENTAL STUDY OF THE EFFECT OF AIR
PURIFIERS ON THE INDOOR AIR QUALITY INSIDE OF AN
APARTMENT**

DOI: 10.2478/9788395720413-008

84
9. Ioan Silviu DOBOȘI, Ștefan DUNĂ and Cristina TĂNASĂ

**BUILDING ENERGY MODELING OF A STUDENTS’
RESIDENCE IN TIMIȘOARA**

DOI: 10.2478/9788395720413-009

93
10. Sheeja NAIR, Ionuț Cristian SCURTU and Sebastian Valeriu
HUDIȘTEANU

**INTEGRATED HEALTH MONITORING & DISINFECTING
SYSTEM FOR ORGANIZATIONS AND SOCIETIES**

DOI: 10.2478/9788395720413-010

104
11. Antonios TSIKALAKIS, Georges ZISSIS, Laurent CANALE, Yiannis
KATSIGIANNIS, Sarintip TANTANEE, Deny HAMDANI, Shobhakar
DHAKAL, Sivanappan KUMAR, Hoang Nam Kha NGUYEN, Trung
Hung VO, Sarjiya SARJIYA and Salvador Suarez GARCIA

**SETTING AN INNOVATIVE MASTER DEGREE ON ENERGY
SUPPLY FOCUSING ON ISOLATED AREAS – THE MESFIA
ERASMUS+ PROJECT**

DOI: 10.2478/9788395720413-011

120
12. Tiberiu CATALINA, Robert GAVRILIUC and Corina GHERASIM -

**NUMERICAL SIMULATION OF A HYBRID SOLAR
GEOTHERMAL ENERGY SYSTEM USED FOR AN ENERGY
POSITIVE BUILDING**

DOI: 10.2478/9788395720413-012

129

13. Sebastian Valeriu HUDIȘTEANU, Nelu-Cristian CHERECHEȘ, 137
 Cătălin-George POPOVICI, Marina VERDEȘ, Vasilică CIOCAN,
 Marius-Costel BALAN and Florin-Emilian ȚURCANU
**ANALYSIS OF THE COOLING EFFECT ON THE EFFICIENCY
 OF THE PHOTOVOLTAIC PANELS**
 DOI: 10.2478/9788395720413-013

14. Robert Ștefan VIZITIU, Andrei BURLACU, Chérifa ABID – DAVID, 154
 Alexandru ȘERBAN, Marina VERDEȘ, Vasilică CIOCAN and Marius
 BRĂNOAEA
**EXPERIMENTAL INVESTIGATION ON THE OPTIMUM
 FILLING RATIO OF HEAT PIPES USED FOR HEAT
 RECOVERY SYSTEMS**
 DOI: 10.2478/9788395720413-014

15. George TARANU, Ligia Mihaela MOGA and Ionut Ovidiu TOMA 162
**ENERGY EFFICIENCY MONITORING OF AN EARTH-
 SHELTERED HOUSE AFTER 4 YEARS OF USE**
 DOI: 10.2478/9788395720413-015

16. Marius BRĂNOAEA, Andrei BURLACU, Vasilică CIOCAN, Marina 172
 VERDEȘ, Florin Emilian ȚURCANU and Robert Ștefan VIZITIU
**A NUMERICAL ANALYSIS ON RADIANT FLOOR HEATING
 SYSTEMS WITH INTEGRATED PHASE CHANGE MATERIALS**
 514-BSEE 2020
 DOI: 10.2478/9788395720413-016

17. Laura DUMITRESCU, Radu-Aurel PESCARU, Irina BARAN and Irina 184
 BLIUC
**INCREASING THE ENERGY PERFORMANCE OF NON-
 RESIDENTIAL BUILDINGS BY THERMAL INSULATION OF
 WALLS ON THE INTERIOR SURFACE**
 DOI: 10.2478/9788395720413-017

18. Victoria COTOROBAI, Theodor MATEESCU, Mihai PROFIRE, Ioan 197
 Cristian COTOROBAI and Sebastian Valeriu HUDIȘTEANU
DESIGN STRATEGIES FOR "nZEB"
 DOI: 10.2478/9788395720413-018

19. Victoria COTOROBAI, Ioan Cristian COTOROBAI, Silvana BRATA, Ionuț-Cristian BRANCA and Ana- Diana ANCAȘ
METAMATERIALS FOR "nZEB" BUILDINGS
DOI: 10.2478/9788395720413-019 213

20. Ana-Maria TOMA, George TARANU, Takahiro NISHIDA, Aliz Éva MÁTHÉ, Cristina-Mihaela CÂMPIAN, Melito BACCAY and Ionut-Ovidiu TOMA
ASSESSING THE SEISMIC PERFORMANCE OF A R.C. FRAME STRUCTURE BY NUMERICAL SIMULATIONS – AN EFFICIENT TOOL FOR A SUSTAINABLE FUTURE
DOI: 10.2478/9788395720413-020 231

21. Marius-Costel BALAN, Marina VERDEȘ, Vasilică CIOCAN, Sebastian Valeriu HUDIȘTEANU, Florin-Emilian ȚURCANU, Andrei BURLACU and Adrian GROSU
PERFORMANCE OF VENTILATION AND SMOKE EXHAUST SYSTEMS IN CASE OF FIRE IN UNDERGROUND PARKING LOTS: CASE STUDY
DOI: 10.2478/9788395720413-021 241

22. Gabriela COVATARIU and Daniel COVATARIU
IoT CONTRIBUTORS FOR BUILDINGS ENERGY EFFICIENCY
DOI: 10.2478/9788395720413-022 257

23. Ladislau RADERMACHER and Theodor MATEESCU
STUDY ON THE BEHAVIOR OF HDPE (HIGH-DENSITY POLYETHYLENE) PIPES BURIED, UNDER THE EFFECT OF AN EXPLOSION
DOI: 10.2478/9788395720413-023 268

24. Florin-Emilian ȚURCANU, Cătălin-George POPOVICI, Marina VERDEȘ, Vasilică CIOCAN, Andrei BURLAC, Sebastian-Valeriu HUDIȘTEANU, Marius Costel BALAN, Larisa ANGHEL -
AIRFLOW AND AIRBORNE PATHOGEN TRANSPORT BY HEATING SYSTEMS IN A CARDIAC INTENSIVE CARE UNIT
DOI: 10.2478/9788395720413-024 276

EXPERIMENTAL RESEARCH OF MITIGATION SYSTEMS FOR CONTROLLING AND REDUCING RADON EXPOSURE IN RESIDENTIAL BUILDINGS

Ion-Costinel MAREȘ¹, Tiberiu CATALINA^{1,2}, Andrei ISTRATE¹, Tiberius DICU² and Alexandra CUCOȘ²

¹Technical University of Civil Engineering of Bucharest/ Faculty of Engineering Installations, Bucharest, Romania

²Babeș-Bolyai” University/ Faculty of Environmental Science and Engineering, Cluj-Napoca, Romania

Abstract. *This article presents the results of implementing a series of methods to mitigate the increased level of radon in multiple existing homes. The subject of this study is represented by techniques and systems to be implemented in pilot houses. From the 1000 house 100 houses from Cluj, Iași, Sibiu, Timiș and Bucharest were selected for monitoring purposes. From these, only 10 were chosen for mitigation. The remediation techniques applied to these pilot houses were active / passive depressurization, local ventilation with heat recovery, centralized ventilation system with heat recovery and installation of a membrane resistant to radon dispersion. In this article one house from Timisoara, and another one from Cluj, were deeply described. The mitigation of the radon level was up to 90% compared to the level measured a year ago.*

Keywords: Indoor air quality, Mitigation systems, Experimental campaign.

1. Introduction

Gaseous pollutants migration from subsurface systems (soils and groundwater) into indoor air represents an important exposure way for human health. These pollutants can become from the natural sources or from spills contaminating the soil or groundwater. Radon gas is by far the most important natural source of ionizing radiation [1, 2]. Radon is a natural radioactive gas, odorless, colorless and flavorless, with a lifecycle of 3.8 days, which arises from the natural decay of uranium in the soil and water. Other important sources would be building materials by exposure to gamma radiation from radionuclides ²²⁶Ra and ²³²Th and their descendants. In 2010, approximately 100.000 deaths and 2,1

million diseases can be attributed to prolonged exposure to high radon values [3]. This gas can easily infiltrate from the soil into the air. Being inhaled, it can cause mutations in human DNA, leading to lung cancer. After smoking, radon is the leading cause of lung cancer. It is reported that between 3-14% of lung cancer cases are due to radon. The possibility to develop lung cancer increases by approximately 16% each time the level is exceeded by 100 Bq/m^3 in case of prolonged exposure. For most of the people, the highest exposure to radon is in their own homes. The level of radon depends on a number of factors such as: the concentration of uranium found in rock and soil substrates; the places wick radon can infiltrate homes; the number of air exchanges per hour, between the inside and the outside of the house (depending on the permeability of the building envelope, the ventilation habits of its occupants [4, 5]. Radon penetration into home can occur through cracks, pores in the floors, leaks, etc [3]. The path of radon atoms from the ground to the air is is exactly represented in the following figure:

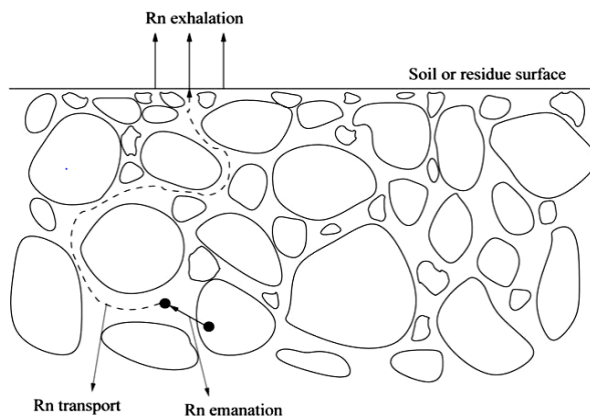


Fig 1- Representation of procees leading to radon discharge to atmosphere [6]

Cosma, Papp [7] have made some radon diagnostic investigation in a radon prone area of Romania to show that the soil is the origin of radon. In order to reduce the radon concentration in the analyzed house, they applied techniques based on the pressurization and depressurization of the building sub soil using an electrical and eolian fan. The results proved that the biggest obtained mitigation efficiency was about 85% [7]. A one year survey study was conducted by Fuente, Rabago [8] in a experimental house from Spain with seriously alarming radon levels to investigate the effectiveness of radon reduction by soil active and passive depressurization. The results showed the permeability characteristics of the house and a link connecting wind velocity and the extraction airflow during passive SD (depressurization system) operation by means of a rotating cowl. A radon reduction efficiency of 85% was achieved [8]. Other many studies showed a good mitigation efficiency for active and passive depressurization systems [9-12]. Another mitigation method for controlling the radon level from the dwellings may be the

installation of a radon-proof membrane, especially in new homes. Coskeran, Denman [13] developed a study that demonstrates that, for low radon level, installing a radon proof membrane may be cost-effective in addressing the dangers to health [13]. In many cases, this method is applied with other remedial technique, as a secondary method [14, 15].

An experimental study on ventilation system in suburban buildings is presented by Merzkirch, Maas [16]. The system overall revealed strong interdependancies among all measured pollutants leading to a highly improved air features and a good comfort [15-17].

The new challenge in reducing energy consumption by retrofitting the existing houses. These energy efficient dwellings lead to the accumulation of many indoor pollutants. A study conducted by Sferle et. al. (2020) describe the relationship between many factors and the indoor air quality [4].

An important research direction is the implementation and experimental testing of various techniques and systems for reducing, preventing and controlling the level of radon in homes. The results of these measurements will lay the foundations of the first guide of good practice [4]. Both beneficiaries and investors will be able to take into account the design of future new constructions, similarly as the improvement of living conditions in existing homes [15]. The main objective of this guide is to reduce the chance of developing lung cancer by establishing medium and long term applicability measures. A study conducted by Istrate, Catalina [18] showed the importance of a mechanical ventilation system to ensure the indoor air quality.

The paper presents: the method, the experimental campaign, results and the comparison of the data anterior and further the mitigation process.

Many studies have been conducted using sub-slab depressurization methods. The novelty of this study is represented by achieving a better indoor air quality simultaneously with radon reduction considering the reduction of energy consumption. The heat can be recovered using heat recovery equipments. The heat transfer into the ventilation flow, can occur in forced and mixed convection [19].

The study comprise a very large number of measurements made in time on several dwellings, more exactly 1000 analysed dwelling. The importance of this study is shown by the health effects which radon mitigation systems brings on the exposed population.

In Romania very few studies have been performed in this branch, even though the radon potential in soil is very high in majority of areas and the exposure risk is imminent.

2. Materials and methods

2.1. Research conducted

Achieving the main objective, creating a healthy environment for occupants, in accordance with the problems related to energy consumption, can be done by implementing some equipment, depending on specifics of each house analyzed, installation possibilities and other barriers that will have to overcome throughout the project. The measurements were conducted following ISO 11665-2:2012 (guidance for measuring radon-222 activity concentration and its short-term decomposing products in air). The sensors have been placed at a height of about 1 m, at approximately 1 m distance from the walls, avoiding area near windows, or other path that can disturb the measurement. The sensors were unmoved for a better accuracy of the measurement. Research in this area has been conducted quite briefly, or only occasionally, on a single house. There are no studies conducted on a larger number of buildings using various radon reduction systems.

2.2. Radon measurement technology in the analyzed dwellings

The continuous measurement of radon level was conducted through an integrated prototype system for monitoring and controlling the interior air quality of the houses (Radon, CO, CO₂, VOC, temperature, pressure, humidity) using remote data transmission. Based on the prototype, the research team developed a number of 100 indoor air quality examination devices, which were installed in 100 houses selected to monitor environmental parameters, according to contractual planning. Of these 100 houses, 10 were selected with the highest values of radon, where energy-efficient equipment to mitigate the radon exposure and other household air pollutants were designed and implemented.

The intelligent indoor air quality examination device (Radon, CO, CO₂, VOC, temperature, pressure, humidity) with remote data transmission, includes the following hardware and software components:

- Radon sensor is using a Tesla TSR2 radon sensor with the specifications in the table below.
- Temperature, pressure, humidity sensors.
- A firmware that allows the acquisition of analog and digital data from sensors, data transmission via Wi-Fi, implementation of control loops and control execution elements.

Table 1

Tesla TSR2 sensor technical specifications

Basic technical parameters:	
Measurement sensitivity	0,15 count/hour/ Bq.m-3 (typically)
Radon scale	5 – 65535 Bq.m-3
Measurement unseureness	15% at 300 Bq.m-3 per 1 hour
Relative humidity scale	10 – 90 %
Temperature scale	-20 to + 60 °C
Radio frequency range	up to 600 m
Records saving interval (probe)	1- 255 minutes, default 1 hour
Memory capacity	150 days
Probe	Li-Ion battery 3.6 V, 2.6Ah
Battery life	>1 year
Radon concentration results display	short-term (1 hour running average)
	long-term (24 hours running average)

2.3. Radon measurements

Radon measurements were performed in two stages. First measurement campaign consisted in passively monitoring for all selected houses using state nuclear track detectors. Detectors were installed into the most inhabited room. To ensure the proper results, each detector was placed and recovered. The second evaluation campaign involved a comprehensive radon detection of each building evaluating some aspects like building tightness, the soil geology, soil permeability, sources of indoor pollution, gamma dose radiation measurements of ground and building materials, the existence of HVAC system, etc. A series of information were collected from the inhabitants, as described in previous works [20]. The prototype measuring device described above was developed by a group of scientists from the Babeş-Bolyai University [21] and installed inside the analysed dwellings to record the indoor air properties (temperature, relative humidity, pressure, CO, CO₂, VOCs and radon) in real-time for up to one year, in order to select 10 pilot house for mitigation measures.

The analysed houses were from the biggest cities of Romania. Over 1000 dwellings from Iaşi, Timiş, Cluj, Bucureşti and Sibiu counties were considered in this study. From these, 100 houses were chosen for detailed measurement as previously described. The annual mean of radon concentration has been calculated to determine the 10 pilot houses suitable for the application of mitigation measures.

Table 2

Average radon level by county

Dwellings	County	Average values/ year
		Bq/m3
10	Iași	215,4
40	Cluj	428,3
17	București	282,9
20	Timiș	265,4
13	Sibiu	264,0

Due to high values of radon measured in the analysed dwellings and the potential of radon in the soil previously investigated [22, 23], in the west of the country, exposing the population to high values of radon is a more imminent necessity. Thus, the pilot houses chosen were 4 from Timiș, 5 from Cluj and only one from Bucharest.

2.4. General mitigation measures

The dwellings were analysed considering a variety of facts to implement the best mitigation solution, customizing every basic system for maximum adaptability. To reach the highest efficiency level, multiple scientific and technical studies were analysed and suitable mitigation systems were designed for every pilot house. The mitigation systems installed were based on building sub-slab depressurization (SSD), radon proof membrane, simple-flow mechanical ventilation with heat recovery, double-flow mechanical ventilation with heat recovery and centralized ventilation with heat recovery.

Active sub-slab depressurization system

This system is based on installing a PVC perforated embossed pipe (100 mm diameter) in a granular fill material, connected to pipeline which ensure the evacuation of contaminating air from the soil by creating a low pressure under the floor. Due to this level of pressure created, the radon gas does not infiltrate into the house, being evacuated outside. To limit the intervention and thus, the cost to install the system, the workers drilled some wholes under the floor from the outside of the house and introduced the suction pipes under the floor.

Radon proof membrane

An efficient method to combat the high level of radon inside the buildings, when the principal provenance of radon into the house is from the soil, is to limit its entries and isolate the sources. A radon proof membrane is used to seal the contact to the soil and limit the radon diffusion inside the house. That method is used mostly in combination with another mitigation system to increase the radon reduction efficiency and a good indoor air quality.

Simple-flow mechanical ventilation with heat recovery

This system consists in drilling a hole into the exterior wall and install the equipment. The principle used consist in driving an air flow from outside to inside from 70 seconds, whereupon the mechanical ventilation reverses its air flow exhausting air from the room for another 70 seconds. The heat recovery equipment recovers an important amount of energy. This method is a cheap and efficient way to mitigate the local rooms when the limit value is not much exceeded.

Double-flow mechanical ventilation with heat recovery

An equipment like the one presented above. The main difference derive from the continuous functioning of airflows, having different ways of intake and exhaust the air ventilated.

Centralized ventilation with heat recovery

This is one of the most complex mitigation methods based on mechanical ventilation, consisting in the installation of a ventilation unit in the attic of the house and ensuring the interconnection of grilles through pipeline routes. The polluted air is exhausted from the bathroom, kitchen and other dirty rooms, and fresh air is introduced in the living spaces like bedroom, living-room, office, etc. The central ventilation unit is equipped with a heat recovery system. This type of equipment provides a very good indoor air quality, removing other pollutants (CO, CO₂, NO_x, VOCs,) and maintaining the interior comfort.

3. Presentation of the dwellings analyzed with the MITIGATION methods

The analyzed house is in Timișoara, Timiș County and it is composed of two parts. The building envelope is relatively tight, the house beingth recently retrofited. The values obtained for the determination of the radon potential in the soil does not exceed severely the reference level, but the radon risk category due to radon concentration does exist. The soil permeability shows a high infiltration risk of radon into the building, values which confirm that the ground is the leading source of radon. Due to exceeding the reference level in the entire dwelling, the centralized ventilation system was recommended.

For mitigation, two ventilation units with heat recovery were installed in the attic of the house to extract contaminated air from the bathroom and kitchen and to introduce fresh air into the living rooms, each one deserving a part of house. In addition to mechanical ventilation of indoor air, other measures such sealing the cover of cellar using silicone and all the visible leaks in the floor which is not sealed from the soil.

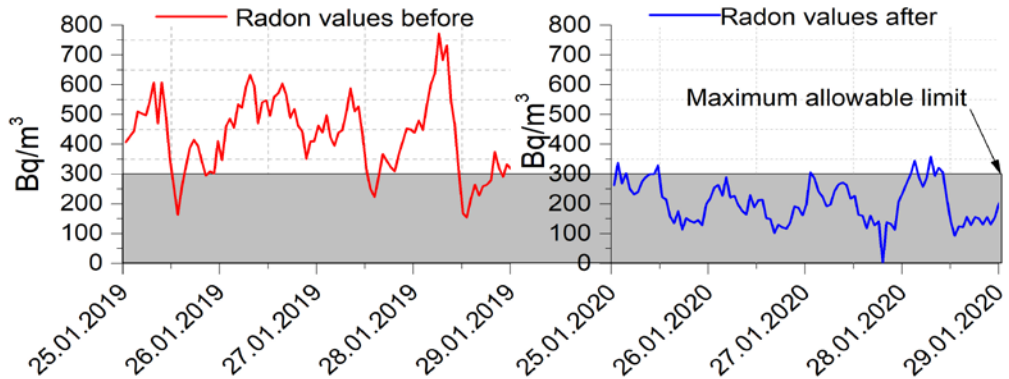


Fig. 2 - The impact of radon remediation system

To express the impact of the improvement of the indoor air quality due to ventilation system, we analyzed two periods of time. First period of time represents the values monitored before any measure was taken when values up to 760 Bq/m^3 were noticed. The variation of radon values express the time when the house occupants opened the windows for natural ventilation. Note that they have been informed with the risk they are exposed. The graph above shows an important fall of radon level from the entire house. The average radon reduction efficiency is about 53% in this case, but the other advantages for using this system are based on the other indoor air quality parameters.

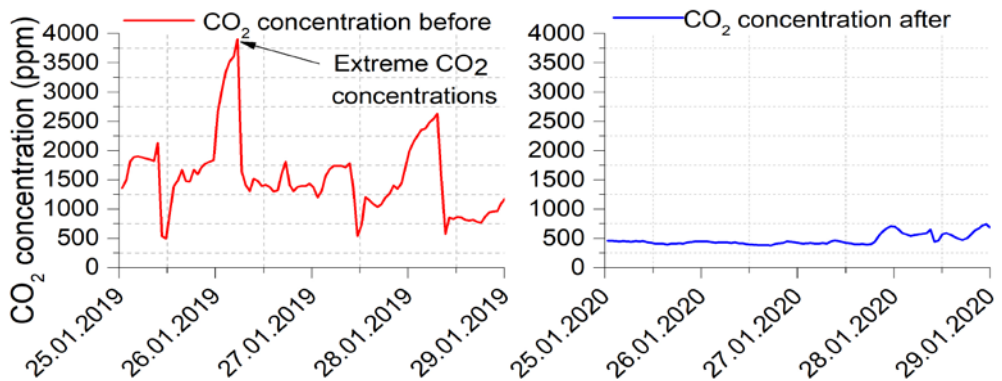


Fig 3 – Mean values of CO_2 concentrations

As described in the graph above the indoor air quality into the analysed dwelling was very harmful for the occupants. Extremely high values of CO_2 were measured reaching values of up to 4000 ppm overpassing 5 times the maximum values. The only times the CO_2 level was lower was during the time the windows were opened. After the mitigation methods have been applied, the CO_2 level has been stabilized with values between 500

ppm and 700 ppm, close to the outdoor concentration. The CO₂ reduction efficiency of the system is around 67%. Due to unnecessary opening of the windows in the wintertime, the comfort level has been improved significantly. The temperature level of the room has been stabilizing to a set point, suffering no more fluctuations. As natural ventilation represented a large amount of energy loss using the heat recovery equipments, the heating costs have been reduced by half.

Another pilot house is a modern building, built in 2008, located in Cluj county. The subject of interest is a ground floor flat with three bedrooms, a living room and a kitchen. There is a small cellar under the bedroom 3 and it is permanently ventilated. During the first and second measurement campaign radon concentration in the cellar was below 70 Bq/m³ and the mean values of radon concentration in the living room varied from 300 Bq/m³ to 450 Bq/m³. Radon concentrations measured at the end of June 2019 were below 100 Bq/m³ in all rooms except of the cellar, where the values around 600 Bq/m³ were discovered. Radon concentrations in the air samples taken from possible entry routes are small; the only exception is a pipe penetration for the radiator in the living room (3,4 kBq/m³). Radon index of foundation soils is low (third quartile is 6 kBq/m³). Based on the measurements, increasing the ventilation flow through the mechanical ventilation will reduce the indoor radon concentration below the reference level. The mitigation system is based on the installation in the outer walls of the bedroom and office of two equipment for single-flow mechanical ventilation, equipped with heat recovery. The synchronization of the devices is done by ensuring the air circulation between the rooms of the house. When one equipment operates on air intake, the other should operate in air exhaust mode. Air circulation between rooms must be ensured. In addition to improve the ventilation all the visible leaks in concrete floor, which are in contact with the soil, were sealed.

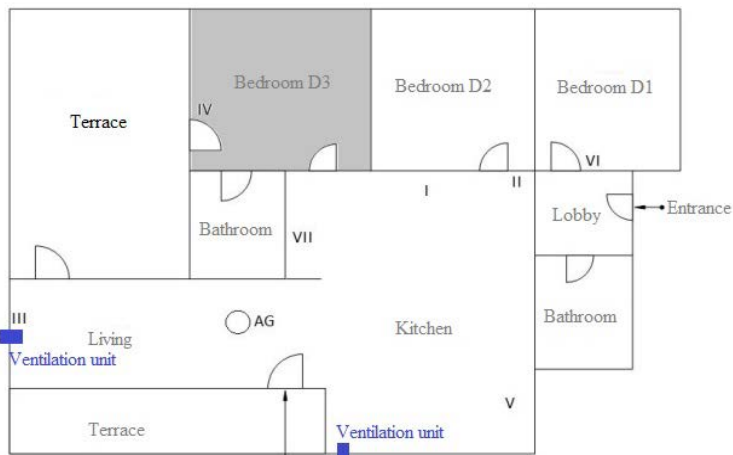


Fig 4 - Position of local ventilation units in the house

After the equipment were installed, we started to oversee the results. The preliminary results showed a improvement of radon level, sufficient to decrease the average level of radon below the limit. The radon reduction efficiency was calculated to be 86% for the analyzed period as it is described in the graph below, maintaining the radon level very low. Due to its costs this system is suitable for mitigation in dwellings where the average radon level is not so much exceeded ($\approx 450 \text{ Bq/m}^3$). As can be observed in the graph below during the accumulation period, very high values were noticed, the limit being outdated almost every time. Due to proper utilization of the system, a better indoor air quality can be assured.

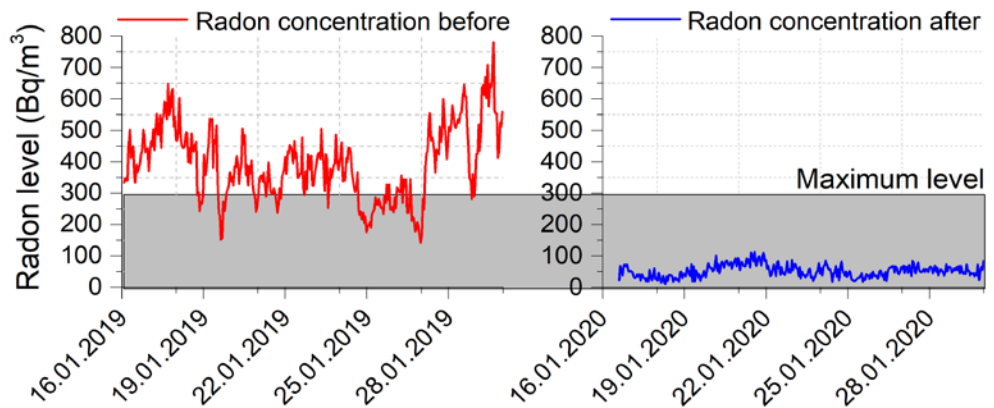


Fig. 5 – The impact of radon mitigation

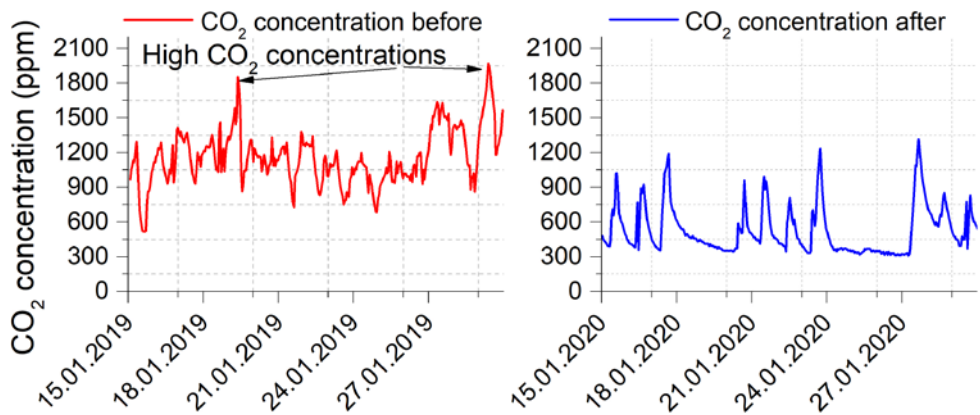


Fig. 6 - The impact of mitigation on CO₂ concentration

This mitigation method improves the air quality, not only decrease the radon level. Thus, the CO₂ level is found in normal concentration after the mitigation solution was applied,

showing values around 530 ppm. The highest CO₂ value was close to 2000 ppm which is a harmful exposure. The CO₂ reduction efficiency is around 55% expressing a better and safe indoor air quality. The fluctuations represented in the graph shows the moment when the occupant opened the window for natural ventilation. The highest values of CO₂ concentrations were found in the morning after accumulation overnight.

Following the mitigation methods applied in all 10 pilot houses, a series of conclusions will determine the advantages and disadvantages for implementing every method due to dwelling characteristics and radon level in the soil and in the water.

Table 3
Mitigation efficiency in the pilot houses

System name	Implemented measures	Mitigation efficiency
Sub-Slab depressurization	Only the SDS system	up to 86%
	Radon proof membrane	up to 95%
	Radon proof membrane + decentralized heat recovery system	up to 95%
Centralized heat recovery ventilation	Ventilation unit installed in the attic	up to 55%
Decentralized heat recovery ventilation	1 reversible flow unit	up to 72%
	2 reversible flow units	up to 86%
	Continuous double flow operation	up to 75%

As observed in the above table, the most efficient method to mitigate the high radon level from existent dwellings is by installing the sub-slab depressurization system, but other pollutants cannot be removed from the indoor air. The utilization of a mechanical ventilation system to mitigate the high radon level can provide an important improvement of indoor air quality and a good comfort for the home occupants. To choose the proper system for radon mitigation a detailed analysis should be conducted.

Conclusions

- According to the measurements made, in most areas of the country the soil has medium or high radon risk values against health of the population.
- The lack of regulations regarding health risk of radon led to this study, one of the aims being the writing of a guide for house owners and constructors.
- The project aimed at designing and implementing solutions to remedy the radon in homes, following the characteristics of buildings, radon level, construction materials, installation and operating costs, energy efficiency.
- The measured data were analysed before and after the implementation of the systems. Data analysis showed that all proposals regarding radon mitigation, had

significant positive results in increasing indoor comfort, more exactly, the radon reduction into the analysed dwellings was between 53 to 86%.

- Into those houses where ventilation mitigation system were applied the CO₂ decreased to a average level between 500 to 700 ppm.
- The average level of radon indoor concentration was reduced below the limit imposed by the national regulations of 300 Bq/m³, creating a safe indoor environment for the house occupants.
- In comparison with the traditional method (natural ventilation through the windows openings), using the energy efficient systems to mitigate the radon level, a significant reduction in energy costs was observed.
- The purpose of these studies is to increase the concern for radon exposure, to test the radon mitigation measures and to increase the radon prevention by implementing the guides into building norms.

Acknowledgement. The authors are grateful for the support provided by the local authorities and the residents who collaborated on this experimental research. The study is part of a large project, with the title “Smart Systems for Public Safety through Control and Mitigation of Residential Radon linked with Energy Efficiency Optimization of Buildings in Romanian Major Urban Agglomerations SMART-RAD-EN” of the POC Programme.

REFERENCES

- [1] Zeeb, H., *WHO handbook on indoor radon: a public health perspective*. 2009: World Health Organization.
- [2] Todea, D., et al., *LUNG CANCER RISK INDUCED BY RESIDENTIAL RADON IN CLUJ AND ALBA COUNTIES, ROMANIA*. Environmental Engineering & Management Journal (EEMJ), 2013. **12**(6).
- [3] WHO, *Radon and health*, 2016, Editor. 2016, World Health Organization
- [4] Sferle, T., et al., *VARIATION OF INDOOR RADON CONCENTRATION WITHIN A RESIDENTIAL COMPLEX*. Radiation Protection Dosimetry, 2020.
- [5] Cosma, C., et al., *Soil and building material as main sources of indoor radon in Băița-Ștei radon prone area (Romania)*. Journal of environmental radioactivity, 2013. **116**: p. 174-179.
- [6] Ishimori, Y., Lange, K., Martin, P., Mayya, Y. S., & Phaneuf, M., *Measurement and calculation of radon releases from NORM residues*. Iaea, 2013.
- [7] Cosma, C., et al., *Testing radon mitigation techniques in a pilot house from Baita-Stei radon prone area (Romania)*. J Environ Radioact, 2015. **140**: p. 141-7.
- [8] Fuente, M., et al., *Radon mitigation by soil depressurisation case study: Radon concentration and pressure field extension monitoring in a pilot house in Spain*. Sci Total Environ, 2019. **695**: p. 133746.
- [9] Groves-Kirkby, C.J., et al., *Domestic radon remediation of UK dwellings by Sub-Slab Depressurisation: evidence for a baseline contribution from constructional materials*. Environ Int, 2008. **34**(3): p. 428-36.
- [10] Abdelouhab, M., B. Collignan, and F. Allard, *Experimental study on passive Soil Depressurisation System to prevent soil gaseous pollutants into building*. Building and Environment, 2010. **45**(11): p. 2400-2406.

- [11] Allison, C., et al., *Radon remediation of a two-storey UK dwelling by active sub-slab depressurisation: Effects and health implications of radon concentration distributions*. Environment international, 2008. **34**(7): p. 1006-1015.
- [12] Jiranek, M., *Sub-slab depressurisation systems used in the Czech Republic and verification of their efficiency*. Radiat Prot Dosimetry, 2014. **162**(1-2): p. 63-7.
- [13] Coskeran, T., et al., *The cost-effectiveness of radon-proof membranes in new homes: a case study from Brixworth, Northamptonshire, UK*. Health Policy, 2007. **81**(2-3): p. 195-206.
- [14] Finne, I.E., et al., *Significant reduction in indoor radon in newly built houses*. J Environ Radioact, 2019. **196**: p. 259-263.
- [15] Khan, S.M., J. Gomes, and D.R. Krewski, *Radon interventions around the globe: A systematic review*. Heliyon, 2019. **5**(5): p. e01737.
- [16] Merzkirch, A., et al., *Field tests of centralized and decentralized ventilation units in residential buildings – Specific fan power, heat recovery efficiency, shortcuts and volume flow unbalances*. Energy and Buildings, 2016. **116**: p. 376-383.
- [17] Merzkirch, A., et al., *A semi-centralized, valveless and demand controlled ventilation system in comparison to other concepts in field tests*. Building and Environment, 2015. **93**: p. 21-26.
- [18] Istrate, M.A., et al., *Experimental measurements of VOC and Radon in two Romanian classrooms*. Energy procedia, 2016. **85**: p. 288-294.
- [19] Laouira, H., et al., *Heat transfer inside a horizontal channel with an open trapezoidal enclosure subjected to a heat source of different lengths*. Heat Transfer-Asian Research, 2020. **49**(1): p. 406-423.
- [20] Florică, Ș., et al., *The path from geology to indoor radon*. Environmental Geochemistry and Health, 2020: p. 1-11.
- [21] Tunyagi, A., et al., *An innovative system for monitoring radon and indoor air quality*. Romanian Journal of Physics, 2020. **65**: p. 803.
- [22] Burghel, B., et al., *The FIRST large-scale mapping of radon concentration in soil gas and water in Romania*. Sci Total Environ, 2019. **669**: p. 887-892.
- [23] Cosma, C., A. Cucos Dinu, and T. Dicu, *Preliminary results regarding the first map of residential radon in some regions in Romania*. Radiat Prot Dosimetry, 2013. **155**(3): p. 343-50.

PARAMETRIC OPTIMIZATION AND CALCULATION OF VIBRATIONS INTRODUCED BY PROPULSION INSTALLATION

Ionut Cristian SCURTU^{1*}, Amin Moslemi PETRUDI² and Masoud RAHMANI²

¹ Mircea cel Batran Naval Academy, Constanta, Romania

² Department of Mechanical Engineering, Tehran University, Iran

Abstract. *Nonlinear vibration issues are of great importance in physics, mechanical structures and other engineering research. Vibration response, stability, and frequencies are the main components of a system's vibration check. Therefore, investigating the effect of different parameters in these sections can be an important step in the design process. In recent years, much research has been done on nonlinear vibrations, and analytical and numerical methods have been used to solve complex nonlinear equations. Equipment and the use of marine structure laboratories for the practical study of the dynamic behavior of vessels require large expenditures, so in order to advance computer science, several software's have been developed and used to model and perform dynamic analysis. In this paper, the mass of the shaft, the motor assembly and the impeller are each examined as a centralized mass and are modelled by ANSYS software. Then, by extracting vibrational equations along the shaft axis and multi-objective optimization with response surface method (RSM), the comparison of the results of this method with the work of other researchers shows that this method has a good accuracy.*

Keywords: Nonlinear Vibration, Ansys, RSM Method, Optimization, Shaft.

1. Introduction

Major advances in the world economy over the past two decades have had a profound impact on the marine construction industry. Therefore, the slightest vibration limit can be dangerous. Reduce vibration levels to ensure the health of the crew, mechanical, electronic systems and ship's steel structures. There are many vibrational factors in a ship, the most important of which are diesel propulsion, propellers, generators,

propellers, and etc. A ship as a complex structure has two types of natural frequencies, one is the natural frequency of the whole structure and the other is the natural frequency. The diesel propulsion system stimulates the entire structure, while the devices can stimulate and intensify the surrounding elements and are unable to stimulate the entire steel structure. There are two completely separate steps, one is the vibration of the ship's engine itself and the solutions involved in repelling it, and the other is the reaction that the steel structure gives to the engine's stimulation, and this is related to the condition of the ship structures themselves. Securing the floating structure from a vibrational point of view is a discussion that begins after minimizing the excitation caused by the engine and securing the body. Ship hydrodynamics involves several topics, one of which is the dynamics of ship in the sea. The sea is an environment in which there are always waves, so ships movements are investigated in the presence of waves, which is called the science of Seakeeping or Dynamics of Marine Vehicles. Designers have always considered prediction of ship movements for ship operational planning and proper use of ship [1].

2. Method (Design and Analysis)

2.1 Analysis of Sources of Excitation

The ships are equipped with the most modern equipment and represent the most complex transport system by sea. Equipped with a large number of equipment and force installations can lead to undesirable phenomena induced by the vibrations of different equipment or their overlap. On-board vibrations negatively influence the strength of various metal constructions, the proper functioning of systems and equipment, the comfort of the crew and passengers. Sources of noise and vibration on board sea and military ships can be divided into two main groups:

- main sources which cause the occurrence of noise and vibrating movements by direct action on the hull, consisting of main engines, auxiliary engines, thrusters, the action of the marine environment on the hull;
- secondary sources that receive movement from the main sources and which in turn become sources of noise and vibration, consisting of the various structural elements of the ship's body (bulkheads, panels, girders, beams, etc.), tree lines, installations with tubing.

The operation of propulsion engines and turbines, diesel generators and related auxiliary installations, makes an important contribution to determining the level of noise and vibration on board the ship. The installed power and the level of induced vibrations can only be compared to similar equipment. Manufacturing technologies, tolerances used,

materials used and design of propulsion installations are important factors in determining the level of vibration induced in the hull. Rolling bearings are important components of rotary machines and must be kept in good condition and replaced whenever the situation so requires. A defect of the ball, inner or outer tread causes the rolling bearing to produce additional vibrations at a frequency equal to the frequency of its defect. Diagnosing rolling bearings by measuring the vibrations produced is important and can reduce the time and cost of maintaining a propulsion installation. Measurements show that, in general, equipment whose maintenance has been careless and whose wear is advanced, the level of vibrations produced in operation is 3-4 times higher than at installation stage. Installations related to main and auxiliary engines also contribute to the increase of noise and vibration on board by the operation of the drive pumps and by the flow of working fluids through the tubing. The metal body of the ship shall be subjected to vibration, in particular from the propulsion system (fig. 5.1): the operation of the propulsion engines or turbines, the operation of the propellers and shaft lines attached to the propulsion system specific to each vessel. An important source of noise and vibration is the action of the sea on the hull of the ship. The spectrum of waves can provide a multitude of frequencies and amplitudes that will directly influence the body of the ship. Changes in the rearing, yield of the propulsion system will indirectly influence the vibrations induced in the hull (fig.1) [2,3].

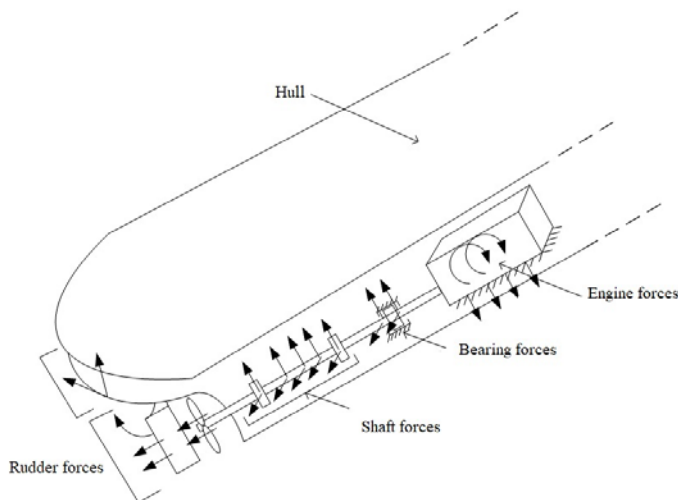


Fig. 1 - Primary sources of excitation to the ship.

2.2 Method Rayleigh

Method Rayleigh used in the study of vibrations of propulsion installations. Using Rayleigh's principle that for conservative systems in vibration after their own way the maximum kinetic energy is equal to the maximum potential energy $E_{p\max} = E_{c\max}$

Results: $p^2 = \frac{U}{K}$ if the deformed shape of the n mode is inserted into the expressions of U and K, the pulsation of that mode is obtained. Thus, in the example considered above, the relationship becomes:

$$p^2 = \frac{EI_y \int_0^1 [Y''(x)]^2 dx}{\rho A \int_0^1 Y^2(x) dx + m Y^2\left(\frac{1}{2}\right)} \quad (1)$$

which:

For $Y(x) = a_1 \phi_1(x) = a_1 \sin \frac{\pi x}{l}$:

$$p^2 = p_1^2 = \frac{\pi^4 EI_y}{2l^3 \left(\frac{M}{2} + m \right)} \quad (2)$$

For $Y(x) = a_2 \phi_2(x) = a_2 \sin \frac{2\pi x}{l}$:

$$p^2 = p_2^2 = \frac{16\pi^4 EI_y}{Ml^3} \quad (3)$$

Usually, the static deformed shape of the bar is used, resulting in a fundamental pulsation of an approximate value, higher than the exact one. The calculation method requires validation of calculations made with rigorous measurements of the equipment studied. The set investigated, including the motor, shaft, propeller and bearings, can be modeled in the simplest way as shown below.

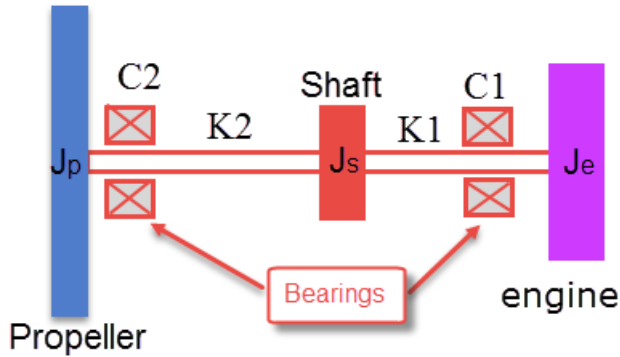


Fig.2 - Schematic diagram of the shaft.

Equivalent differential set equation $I\ddot{\theta} + C\dot{\theta} + K\theta = Q$ it must be written. The free body diagram for the free vibration mode will be as follows.

$$\begin{array}{c}
 \ddot{\theta}_P \theta_P \left(\begin{array}{c} I_p \\ k_2(\theta_S - \theta_P) \end{array} \right) \quad \left(\begin{array}{c} I_s \\ k_2(\theta_S - \theta_P) \end{array} \right) \quad \left(\begin{array}{c} k_1(\theta_e - \theta_S) \\ \ddot{\theta}_e \theta_e \end{array} \right) \quad \left(\begin{array}{c} I_e \\ k_1(\theta_e - \theta_S) \end{array} \right)
 \end{array}$$

$$\begin{bmatrix} I_m & 0 & 0 \\ 0 & I_s & 0 \\ 0 & 0 & I_p \end{bmatrix} \begin{bmatrix} \ddot{\theta}_e \\ \ddot{\theta}_s \\ \ddot{\theta}_p \end{bmatrix} + \begin{bmatrix} k_1 & -k_1 & 0 \\ -k_1 & k_1 + k_2 + k_3 & -k_2 \\ 0 & -k_2 & k_2 \end{bmatrix} \begin{bmatrix} \theta_e \\ \theta_s \\ \theta_p \end{bmatrix} = 0 \quad (4)$$

For free vibrations, which have the single harmonic motion (SHM), it takes the form:

$$\left(-\omega^2 \begin{bmatrix} I_m & 0 & 0 \\ 0 & I_s & 0 \\ 0 & 0 & I_p \end{bmatrix} + \begin{bmatrix} k_1 & -k_1 & 0 \\ -k_1 & k_1 + k_2 + k_3 & -k_2 \\ 0 & -k_2 & k_2 \end{bmatrix} \right) \begin{bmatrix} \theta_e \\ \theta_s \\ \theta_p \end{bmatrix} = \begin{bmatrix} 0 \\ 0 \\ 0 \end{bmatrix} \quad (5)$$

In this relation, ω the natural frequency is twisting and I Moment of inertia and k of the axial stiffness. By calculating the characteristic equation, the natural frequency can be obtained, the characteristic equation of the system is:

$$-\omega^2 \left\{ \omega^4 - \left(k_1 \frac{I_e + I_s}{I_e I_s} + k_2 \frac{I_s + I_p}{I_s I_p} \right) \omega^2 + \left(\frac{k_1 k_2 (I_e + I_s + I_p)}{I_e I_s I_p} \right) \right\} = 0 \quad (6)$$

By solving the equation, the natural frequencies are as follows:

$$\omega = 0 \quad (7)$$

$$\omega^2 = \frac{1}{2} \left(k_1 \frac{l_e + l_s}{l_e l_s} + k_2 \frac{l_s + l_p}{l_s l_p} \right) \pm \sqrt{\left[\frac{1}{4} \left(k_1 \frac{l_e + l_s}{l_e l_s} + k_2 \frac{l_s + l_p}{l_s l_p} \right)^2 - \left(\frac{k_1 k_2 (l_e + l_s + l_p)}{l_e l_s l_p} \right) \right]} \quad (8)$$

The torsional stiffness of each part of the shaft are also calculated as follows:

$$k = \frac{GJ}{l} \quad (9)$$

Which G is the modulus of torsional stiffness, J is the second torque of the surface around the axis of rotation and L is the length of the axes. Frequency changes compared to shaft diameter can be seen in the figure 3.

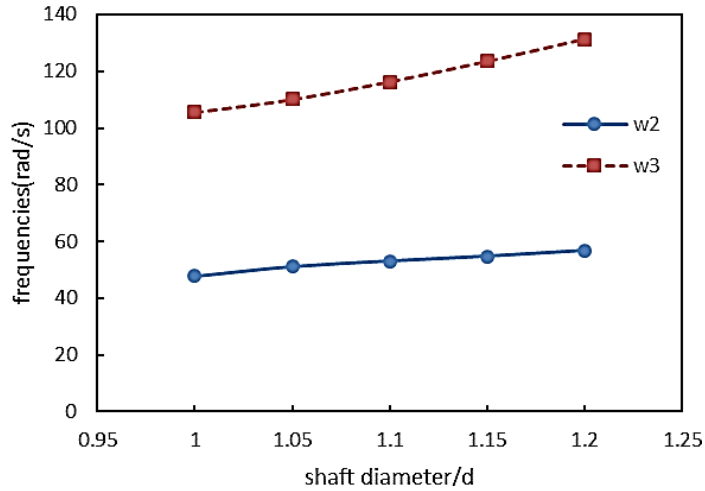


Fig. 3 - Frequency changes compared to shaft diameter.

2.3 Measurement Methods

The measurement of vibrations produced by in-service equipment can be done with the help of diagnostics Toolbox Type 9727, available within the "Mircea cel Batran" Naval Academy. This equipment is accompanied by Pulse Labshop software specifically designed to record and analyzes the results. Diagnostics Toolbox Type 9727 equipment and has uniaxial and triaxle accelerometers that can be mounted in the analysis locations identified on board the vessel following analysis of the sources of excitation present. The records made may be analyzed using the FFT analysis to identify the frequencies and amplitudes present during the measurements [8,9].

3. General Methods of Combating Noise and Vibration

To reduce the vibrations felt at the level of the superstructure, dynamic dampers controlled by computers began to be used, at which a transducer coupled to the line of trees senses the size and phase of the vibrating motion generated by the main engine, transmits it to a unit of calculation which, by comparing with certain preset values, controls the movement of the dynamic absorber so that the vibration level falls within the prescribed limits. The scheme of principle of such a system is shown in the figure below.

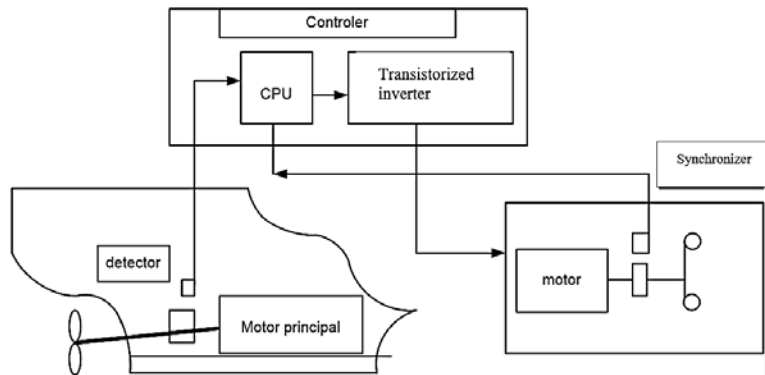


Fig. 4 - Vibration control system with dynamic absorber.

To reduce the roll-over and meandering vibrations of the engine, lateral support of the frame is used with hydraulic dampers [10,11].

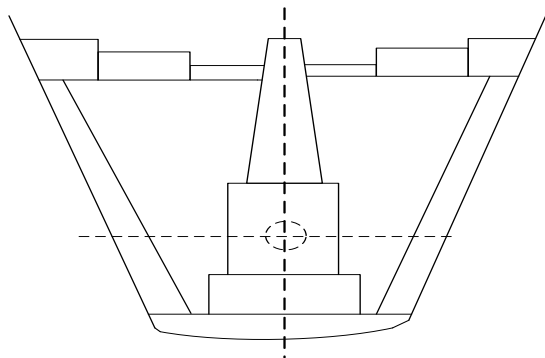


Fig. 5 - Side support of the engine frame.

4. Result and Discussion

The software modelling of the propulsion installation in the calculations presented is done with the help of Ansys Workbench. A classic propulsion system, simplified and reported to equivalent masses as shown in Figure 6, was used in modeling. Software analysis with finite elements must go through the following steps:

- The definition of its structure, its geometric and elastic characteristics, the loads applied and the conditions of resuscitation;
- The choice of the types of finished elements in the program library for the modeling of the structure, taking into account the deformation modes or tensions arising in the elements;
- Discretion of the structure into finite elements, taking into account: geometric dimensions of the structure, elastic characteristics of the material, edge conditions, loads and movements imposed on materials;
- Verification of input data;
- Running the Ansys calculation program;
- Verification of the results obtained in the report generated by the application.

The reference drawing for the study of its own vibration modes of a propulsion installation is shown in Figure 6.

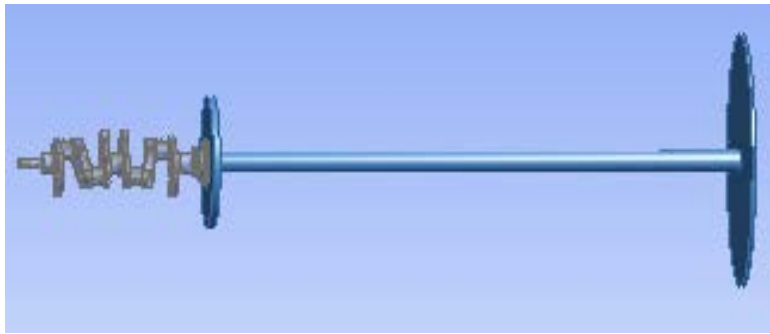


Fig. 6 - Modelling of reference geometry for modes of vibrations.

For analysis we used a specialized program in the finite element method, Ansys Workbench, available within the Naval Academy "Mircea cel Batran". The propulsion system made and used as a model for calculations shall be made of steel with properties as defined in Table 1 [4,5].

Table 1.
Material Properties

Density	7850 kg m ⁻³
Linear dilation coefficient	1.2e-005 C ⁻¹
Specific heat	434 J kg ⁻¹ C ⁻¹
Thermal conductivity	60.5 W m ⁻¹ C ⁻¹
Resistive	1.7e-007 ohm m
Admissible effort	250N/mm ²
Reference temperature	22C
Young mode	2.e+011

Next, we will present how the modal analysis is carried out for the model propulsion plant. Open the calculation program and select the Modal Analysis module. Table 2 can extract the propulsion system's own vibration values and it is recommended to avoid operating at frequencies similar to those obtained in its own vibration modes. Following the calculations, the following displacement distribution diagrams (fig. 3-5) corresponding to the frequencies in the solution present in Table 2 were obtained [6,7].

Table 2
Modal analysis solution and Vibration mode frequencies.

Mod	Frequency[Hz]
1.	0.25216
2.	67.923
3.	68.726
4.	72.949
5.	142.15
6.	143.24

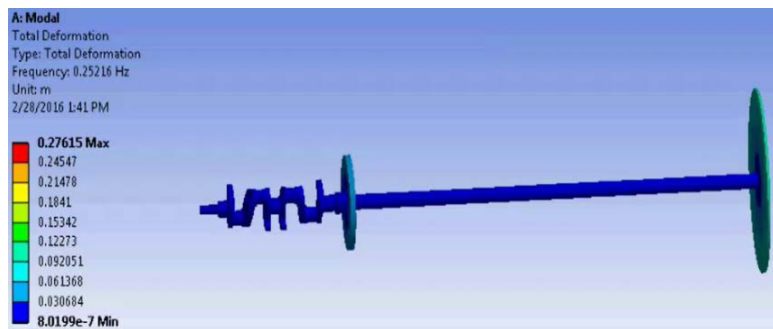


Fig. 7 - Chart of movements at 0.25 Hz frequency.

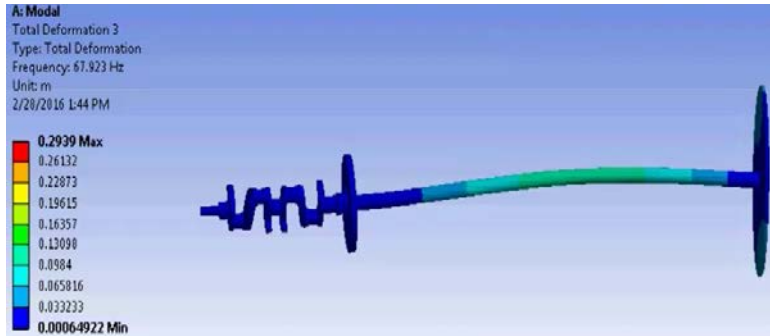


Fig. 8 - Chart of movements at frequency 67.92 Hz.

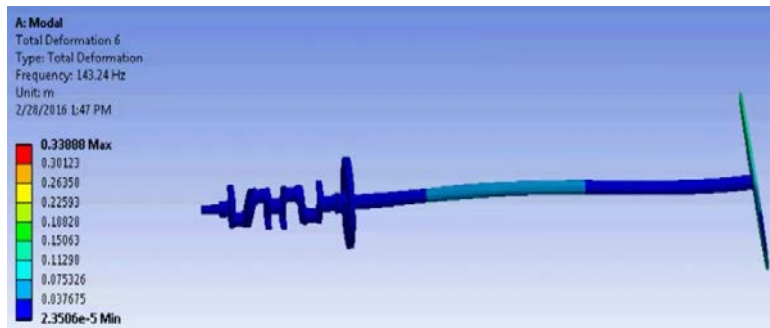


Fig. 9 - Chart of movements at frequency 143.24 Hz.

Following the analysis of the above diagrams, the following can be concluded:

1. The maximum displacement will be searched for the first 6 vibration modes.
2. The maximum amount of effort shall be assessed for each vibration mode.
3. The maximum value of the equivalent tension [N/mm] identified in the Ansys calculations shall be below the flow limit of 250 [N/mm].
4. All of the above leads to the final conclusion that the Ansys analysis may impose conditions and assess very close to the technical reality the phenomena associated with the propulsion installations' own vibrations.

4.1 Parametric optimization

The optimization method is used to solve the optimization problems where the salient points of this optimization method are:

- Effectiveness of this method is retained in non - convex problems.
- With the help of this method, optimum quasi - optimal responses are determined.

The second version of the NSGA algorithm was introduced due to the relatively high sensitivity that the algorithm responds to shared and fitness parameters and other parameters. Answers $i-1$ and $i+1$ the answers before and after are the answer of i , then the distance of the congestion of my answer is as follows:

$$d_i^1 = \frac{f_1(x_{i+1}) - f_1(x_{i-1}))}{f_1^{\max} - f_1^{\min}} \quad (10)$$

$$d_i^2 = \frac{f_2(x_{i+1}) - f_2(x_{i-1}))}{f_2^{\max} - f_2^{\min}} \quad (11)$$

$$d_i = d_i^1 + d_i^2 \quad (12)$$

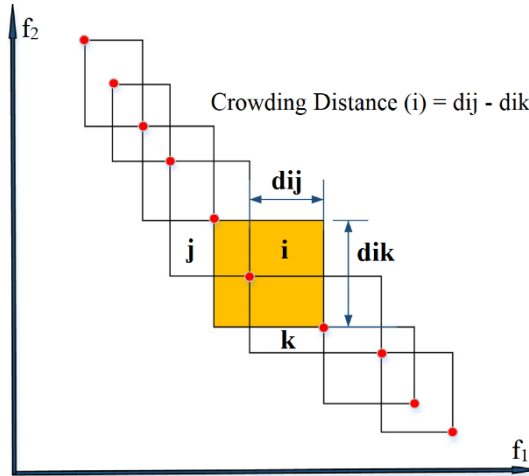


Fig. 10 - Crowding distance in NSGA-II.

To improve answers solvers can use various conditions for solution acceptance [14].

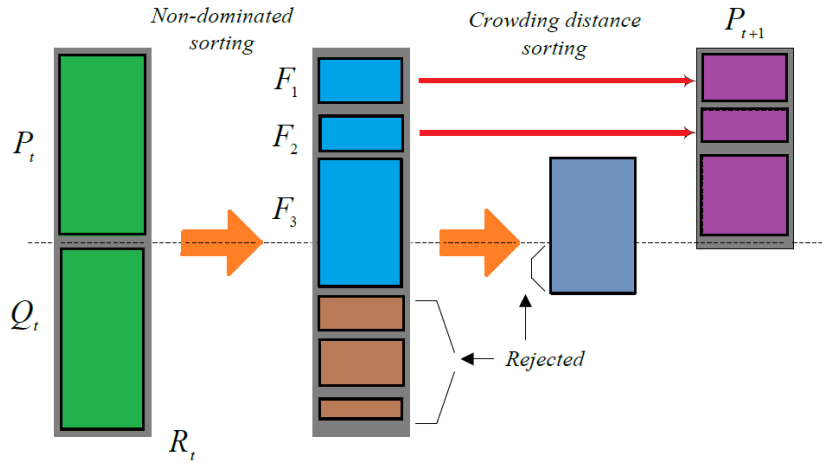


Fig. 11 - The structure of NSGA-II.

Choosing the right solution is a difficult task and must correlate relations and conditions imposed in solving engineering issues. [15].



Fig. 12 - Optimization flowchart.

The response surface methodology (RSM) is a collection of mathematical and statistical techniques to match the experimental data with polynomial models. [16].

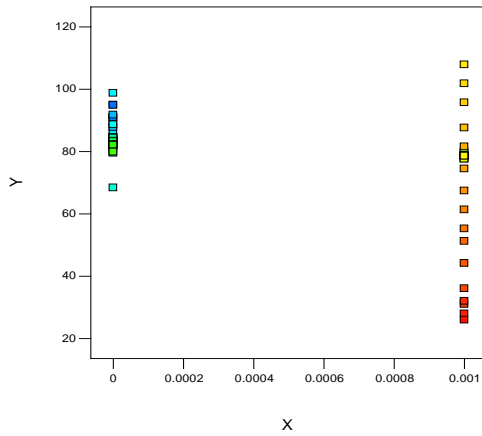


Fig. 13 - Predicted values.

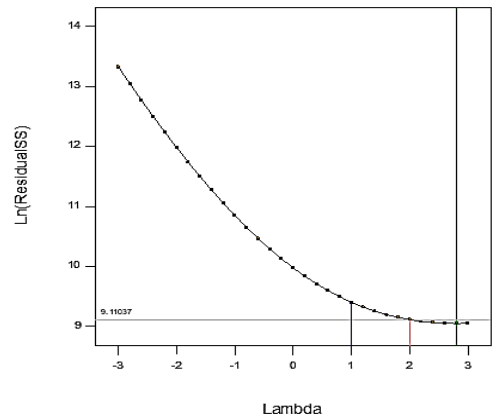


Fig.14 - Power trasforms

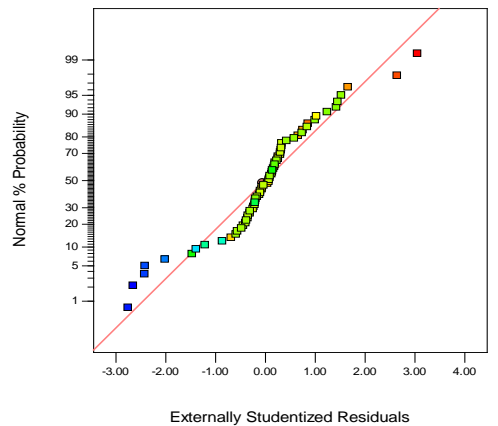
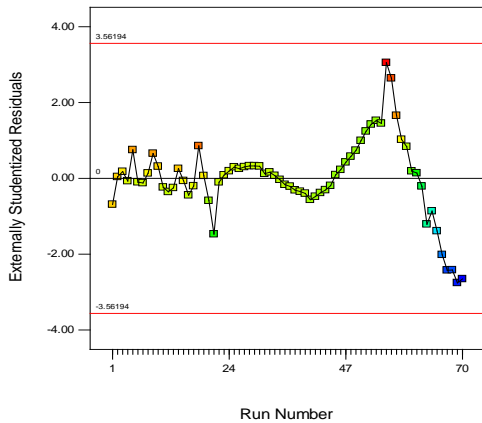


Fig. 15 - Normal probability plot residuals.

5. Conclusion

The experience gained to date in the field of shipbuilding has shown that the main source of excitation of shipbuilding is the propulsion plant through its components: the main engine, the reduction gear, the shaft line and the propeller. The study of the vibration level of the propulsion system must be analysed because of two major effects:

- effects on the physical-psychic performance of the craft operating personnel, increasing the risk of damage due to human error.

- the influence of their level on the state of operation of the propulsion system, collecting global values that reveal the "health" state of the components of the installation or performing spectral analysis to locate and find the cause of the defect. Therefore, by calculating, constantly monitoring and combating the vibration level of the plant, you can minimize the repercussions of stresses and strains induced due to vibration and eventual failure of machine or its ill-effects on humans operating the machine. The comparison of the results of this method with the work of other researchers shows that this method has a good accuracy.

REFERENCES

- [1] A. Moslemi Petrudi, P. Fathi, and M. Rahmani, "Multi-objective Optimization to Increase Nusselt Number and Reduce Friction Coefficient of Water/Carbon Nanotubes via NSGA II using Response Surface Methodology", *J. Mod. Sim. Mater.*, vol. 3, no. 1, pp. 1-14, Mar. 2020.
- [2] Lupchian, M. (2020). Influence of propulsion installation performance on travel efficiency. *Technium: Romanian Journal of Applied Sciences and Technology*, 2(7), 50-53.
<https://doi.org/10.47577/technium.v2i7.1644>
- [3] Crudu, L., Bosoancă, R., & Obreja, D. (2020). A comparative review of the resistance of a 37,000 dwt Chemical Tanker based on experimental tests and calculations. *Technium: Romanian Journal of Applied Sciences and Technology*, 1, 59-66. <https://doi.org/10.47577/technium.v1i.32>
- [4] Turcanu, F.-E., Verdes, M., Ciocan, V., Popovici, C. G., & Hudisteanu, S. V. (2020). The indoor climate modelling and the economic analysis regarding the energetic rehabilitation of church. *Technium: Romanian Journal of Applied Sciences and Technology*, 1, 67-73.
<https://doi.org/10.47577/technium.v1i.116>
- [5] M. Hatami, "Nanoparticles migration around the heated cylinder during the RSM optimization of a wavy-wall enclosure," *Adv. Powder Technol.*, vol. 28, no. 3, pp. 890–899, 2017.
- [6] M. Hatami, M. J. Z. Ganji, I. Sohrabiasl, and D. Jing, "Optimization of the fuel rod's arrangement cooled by turbulent nanofluids flow in pressurized water reactor (PWR)," *Chinese J. Chem. Eng.*, vol. 25, no. 6, pp. 722–731, 2017.
- [7] T. B. Gorji and A. A. Ranjbar, "Thermal and exergy optimization of a nanofluid-based direct absorption solar collector," *Renew. Energy*, vol. 106, pp. 274–287, 2017.
- [8] Radchenko, R., Radchenko, A., Serbin, S., Kantor, S., Portnoi, B. Gas turbine unite inlet air cooling by using an excessive refrigeration capacity of absorption-ejector chiller in booster air cooler. *HTRSE-2018*, 6 p. E3S Web of Conferences 70, 03012 (2018), *HTRSE-2018*, <https://doi.org/10.1051/e3sconf/20187003012>
- [9] Radchenko, A., Mikielwicz, D., Forduy, S., Radchenko, M., Zubarev, A. (2020) Monitoring the Fuel Efficiency of Gas Engine in Integrated Energy System. In: Nechyporuk M., Pavlikov V., Kritskiy D. (eds) *Integrated Computer Technologies in Mechanical Engineering (ICTM 2019)*. *Advances in Intelligent Systems and Computing* (2020), vol 1113. Springer, Cham, pp.361-370. https://doi.org/10.1007/978-3-030-37618-5_31
- [10] Petrudi, A. Moslemi, P. Fathi, and M. Rahmani. "Multi-objective Optimization to Increase Nusselt Number and Reduce Friction Coefficient of Water/Carbon Nanotubes via NSGA II using Response Surface Methodology." *Journal of Modeling and Simulation of Materials* 3, no. 1 (2020): 1-14.

EXPERIMENTAL INVESTIGATION ON THE SOUND PRESSURE LEVEL FOR DIFFERENT ACOUSTIC TREATMENT OF BOILER ROOMS

Catalin BAILESCU¹ and Vlad IORDACHE²

¹CAMBI Research Center, UTCB, Bucharest

²CAMBI Research Center, UTCB, Bucharest

Abstract. *Noise pollution is the cause of many health problems, and the inhabitants of the neighborhoods from crowded cities exposed to high noise is growing in Europe. Noise from thermal power plants represents the main factor of the acoustic discomfort in the residential buildings for the occupants, but also for the people who operate the equipment. The goal of this article is the experimental analysis of the efficiency of acoustic treatment solutions and their effect in reducing the noise level inside thermal power plants. Although the thermal performance and efficiency of the equipment in a boiler room have increased, the noise level produced by thermal power plants has not decreased considerably. Current measurements of the sound level in boiler plants have shown an increase in the noise level due to the fact that modern burners are noisier than old atmospheric burners, the quality of materials of the burner-boiler fixing system is poor and the volume of the boiler space becomes getting smaller. Covering the burner with a housing can reduce the noise at the source because it absorbs the noise at high frequencies. Instead, this measure is less effective in terms of low frequencies which are also the best transmitted by the structure of the building to the apartments. Regarding the chimney, the noise inside it comes from the combustion process and can be a problem in new buildings for which sound insulation or outdoor installation can be recommended. Another solution to reduce the noise level is to remove the noise source. The boiler rooms must be placed from the design stage as far as possible from the apartments, in another building, in the basement of the building or at least there should be a buffer space between the living rooms and bedrooms represented by common spaces, halls, closets, storage spaces, sheds. The results obtained by the experimental comparisons proved to be satisfactory. This article is expected to assist design engineers in improving compliance with legislation, analysis, and optimization of boiler rooms.*

Keywords: Noise pollution, thermal power plant, acoustic treatment, sound level, experimental comparison

1. Introduction

The acoustic behavior of boilers is of major importance in the current context of the development of gas-based domestic heating installations.

On the one hand, modern boilers are equipped with high-performance burners that produce a high level of noise, on the other hand legal and regulatory regulations on noise emissions they become stricter [1]. In the context of these three issues, the topics are of interest: The first is the analysis of the noise from different types of boilers. The difference in noise produced by a modern boiler compared to the old generation boilers with blown air will be investigated [2]. The second subject is the difference in noise produced by the same boiler for different thermal loads [3]. The third topic is the study on the efficiency of noise reduction solutions and the comparison of these methods to reduce it.

Regarding the boilers, there are a lot of parameters that can be potentially influential in amplifying the noise emission [4,5,6,7]. Another purpose of this article is to determine which of these parameters actually have a negligible influence on noise emissions.

2. Analysis of noise protection solutions in boiler rooms

2.1 Scientific goals

Although the thermal performance and efficiency of the equipment in a boiler room have increased, however, noise from thermal power plants did not decrease considerably [13]. Current measurements of sound levels in boiler rooms show a dispersion of these values, dispersion due to:

- the fact that modern burners are noisier than atmospheric burner.
- the quality of the materials, i.e. the burner-boiler torque.
- the most important noise is combustion noise.
- the volume of the boiler room.

To reduce the noise from the source it is necessary to:

- choose the least noisy equipment possible at the same thermal power.
- have a space for the boiler room as large as possible.

This is a useful paper suggesting practical ways to improve well-being of people leaving near noisy thermal plants. This study can be made accessible to engineers and designers so that they can choose the best acoustic treatment solution for the boiler room in their project.

2.2 Measuring techniques

For each experiment, significant efforts were made. The experiments were made applying different class 2-methods for the measurement of the sound power level of the boilers, as there are the measurement in a reverberant room according to ISO 3743, parts

1 and 2 [8,9], and the intensity method described in ISO 9614-1 [10], there were performed at night, during the week and in different cities (Brasov, Ploiesti, Bucharest). Also, approvals were required from the management of the institutions where the measurements were performed.

The measurements were performed by a team of at least three or four people: one person records the gas consumption, another person operates the boiler automation, and the third person performs the noise measurements. Fochists participated in the experiments, automatists, students, teachers, and others to whom I am grateful for their help and effort.

The experiment consisted in the experimental measurement of the noise level in the boiler room using a portable sound meter type 2250 with frequency of 4-22 kHz, software Pulse Lab shop ver 5.1.0 for automatic processing of experimental data, balloons for measuring reverberation time and laser rangefinder for architectural measurements.

For each experiment, the following steps were performed:

- photographs from different angles to analyze architecture
- find acoustic discomfort from external sources (street type, etc.)
- identify the type of absorbent material (type of wall, floor, ceiling)
- identification of boiler type (maximum boiler load, burner type)
- gas meter
- identification of natural gas parameters (pressure, temperature)



a. Gas meter

CT 23 August		wilo	
C21	C22		
0	0		
0	0		
1	0		
1	0		
1	0		
0	1	1 726662,200	626665,578
0	1	2 126669,280	626669,200
1	0	0 626679,200	626680,538
1	1	1 626665,200	626667,155
1	2	2 626674,842	626673,159
2	0	0 626681,200	626681,213
2	1	1 626675,308	626676,525
2	2	2 626671,700	626672,748

b. Operating stage and gas index

Fig. 1 – Notations during the experiment.

- Analyzing the possibility of measuring gas flow.
- Identification of other noise generating equipment (pumps, heat exchangers) heat, chimneys, etc.);
- Identification of acoustic treatment solutions (noise attenuator, solid doors, insulated chimney, boiler detachment, etc.)
- Architectural measurements (room dimensions);
- B & K Type 2250 Portable Acoustic Analyzer (tripod mounting, mounting function, calibration, setting working parameters)
- Using the software Pulse Labshop ver 15.1.0, 25, measurements of noise was performed for 10 seconds at a total of 250 acoustics pressure levels.
- Using Pulse Labshop ver 15.1.0 software, time measurements and reverberation time were measured

Acoustic measurements were downloaded using the BZ5503 software on a workstation with Windows operating system, imported into Excel and added to the experimental database.

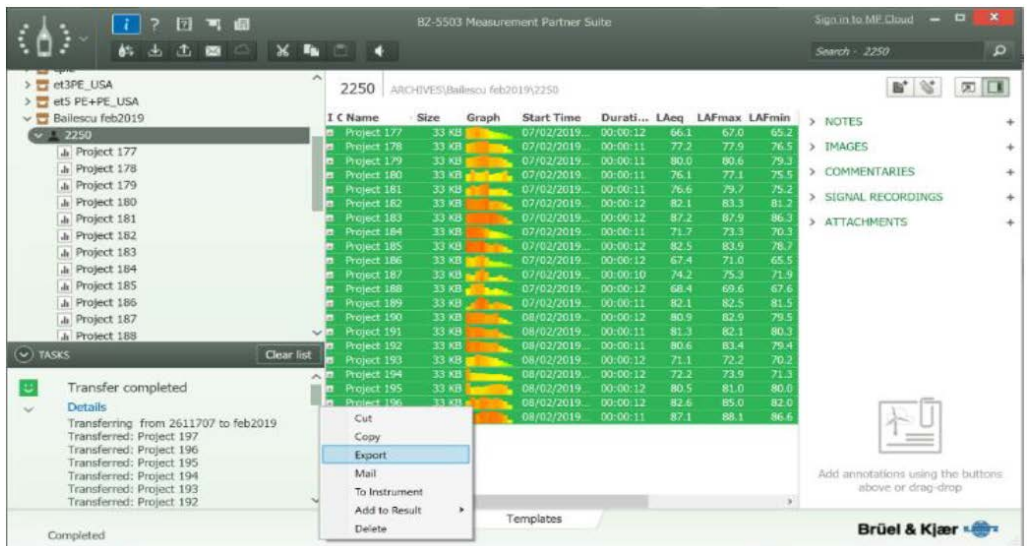


Fig. 2 – Download measured data using BZ-5503 software from Bruel & Kjaer

After the experiment, the following database input values were obtained:

- input data: P_{burner} , $\log_{10}(P_{\text{burner}})$, L_w , V , $\alpha_{125\text{Hz}}$, $\alpha_{250\text{Hz}}$, $\alpha_{500\text{Hz}}$, $\alpha_{1000\text{Hz}}$, $\alpha_{2000\text{Hz}}$, $\alpha_{4000\text{Hz}}$, $\alpha_{8000\text{Hz}}$,
- output data: L_{Aeq} , L_p 63-8000 Hz, T_{20} , T_{30} , EDT.

The thermal power of the boiler is measured at the gas meter, so the thermal power at the connection level, not the useful thermal power (what comes out of the boiler). This thermal power depends on the normal state of the gas (normal pressure and normal temperature), the lower calorific value.

Through several mathematical processing, the following equation for calculating the thermal load produced by the burner was obtained:

$$P_{\text{burner}} = \frac{(I_{1\text{min}} - I_{0\text{min}}) \cdot \frac{p_g + p_{\text{atm}}}{p_{\text{atm}}} \cdot \frac{273.15}{273.15 + t_g}}{60} \cdot 35372 \quad (1)$$

where: P_{burner} is the real thermal load for a duration of 60s [kW]; $I_{1\text{min}}$, is the reading after 60 seconds of the gas index to the meter [m³]; $I_{0\text{min}}$ is the initial index read from the gas meter [m³]; p_g is the methane gas pressure [bar]; p_{atm} is atmospheric pressure [bar]; t_g is methane gas temperature [°C];

2.3 Experimental setup

The actual work package dealing with the investigations on boilers began in autumn 2017. Twenty-nine different boilers were chosen for these testing to cover the most common products that are in use all over Romania. For each thermal power plant, a few 5-12 operating situations was simulated, so that the current database contains 162 real operating situations.

The list of inspected thermal power plants consists of technical spaces located in different cities (Ploiesti, Brasov, Bucharest), and includes from small power plants (wall power plant 40kW) to very high thermal load power plants (3500kW).

To avoid disturbing the experiments due to external noises, all the experiments took place, only at night, between 22:00 and 04:00. The experiments took place over three seasons and in different cities. The first experimental campaign was in the fall of 2017, in UTCB thermal power plants, the second in the spring of 2018, in Ploiesti and Brasov, the third in the summer of 2018 in Bucharest on RADET power plants, and the last one in winter 2019 on RADET power plants, in order to include a boiler operation in higher thermal loads.

2.4 First results

In the following we will graphically represent the limit of the database obtained from the experiments, and then to correctly interpret the physical phenomena that occur inside the thermal power plants during the experiments, we will represent the distributions of the database using MATLAB software and will create thermal power plant classes, which will be explained and represented graphically for a better understanding.

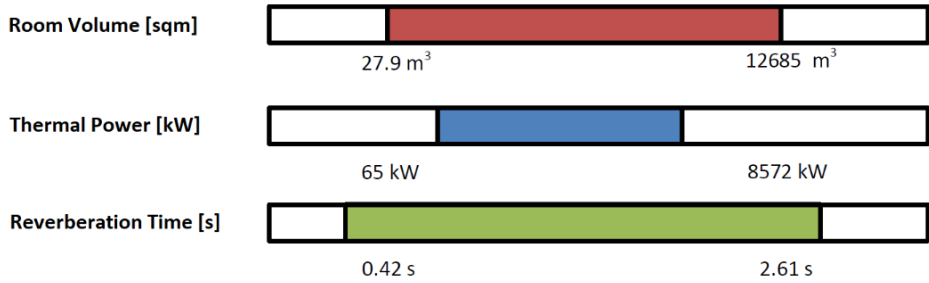


Fig. 3 – Lower and upper limits of the complete database

Thermal power plants from different cities with different thermal loads and architectures were selected in order to observe the influence that the thermal load has on the noise level, but also the comparison with the values imposed by the norms in force.

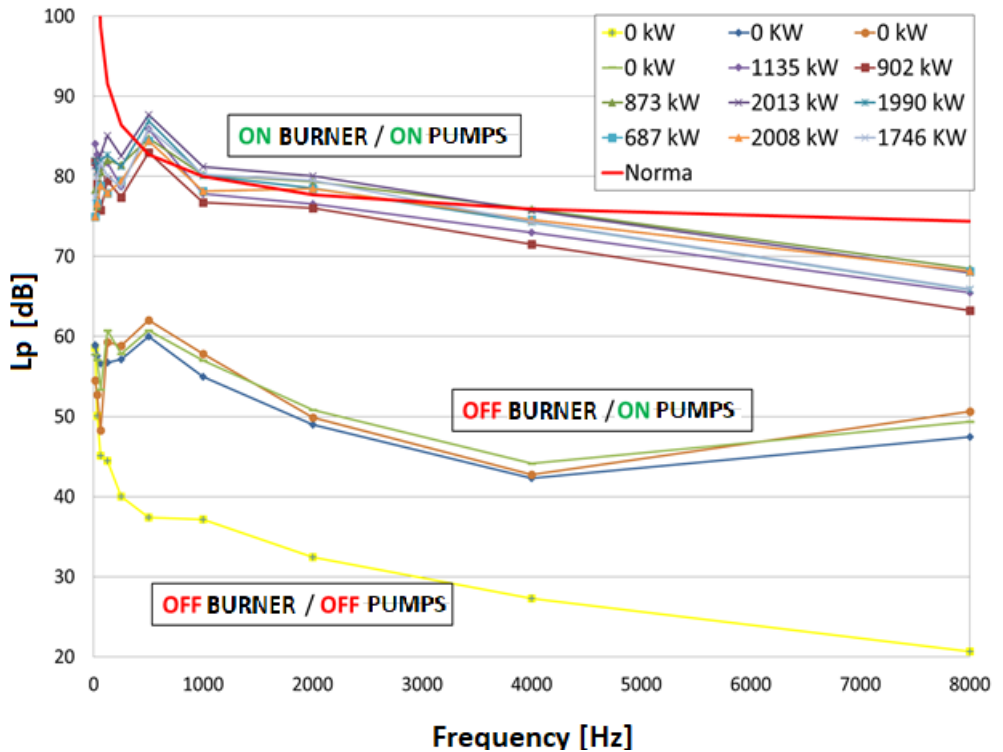


Fig. 4 – Comparison between the noise level for each frequency and CZ80 for CT Bucov

It can be seen from the graph above that the noise level for the situation in which no equipment works (yellow) is below 40dB at each frequency. When starting the pumps (blue, green and brown), the noise level increases up to 57dB at the frequency of

1000Hz.

After starting the burners, the noise level increases above 75dB at 1000Hz and depends to the thermal load. For frequencies between 500 and 4000Hz it exceeds the standard value in more than half of the operation scenarios.

As the first preliminary conclusion it is observed that at very low and very high frequencies, the noise level falls within the prescription imposed by the norm, the noise level exceeds the value from norm between 500 and 3000Hz.

Like the above comparison, an analysis of the equivalent noise level measured for each operating situation was followed, the one indicated in the regulations and the one given in the technical data sheets of the burner manufacturer.

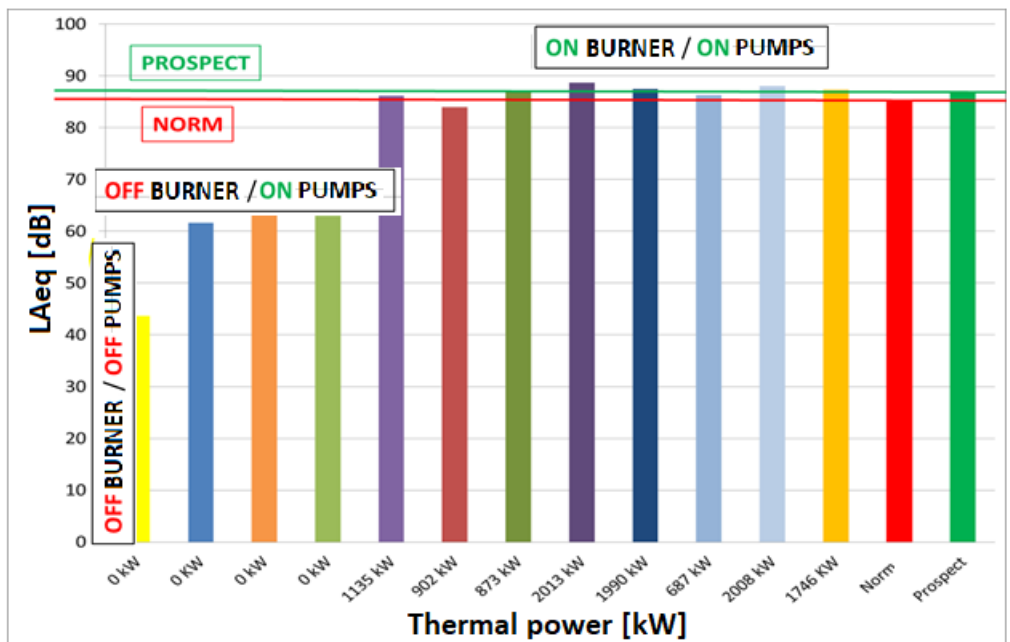


Fig. 5 – Comparison between equivalent noise level, Norm and Prospect for CT Bucov

The bar graph for CT Bucov shows an exceeding of the noise level for all burner operating situations, with one exception at 902kW. The burner prospects indicates a value, above the norms, but close to the actual measured value.

2.5 Outlook

These graphs also highlight the conclusions reached by Hamayon[11,12] as the main noise generating equipment in a technical space such as a boiler room is the burner (noise produced during combustion)[1].

Another important conclusion is that thermal load depends to the noise level, and for high thermal loads it is necessary to obtain a lower value of the noise level to comply with regulations.

3. Noise analysis of acoustic treatment

Boilers equipped with atmospheric air burners are rarely used in new buildings due to their very low efficiency. Modern boilers are equipped with blowers with blown air to ensure the best possible efficiency of the transformation from methane gas to thermal energy.

There is a major difference, up to 23dB, between noise from a modern blower with blown air and that produced by the classic burners with natural draft. This difference is given by noise from the flue gas fan provided in the construction of modern burners.

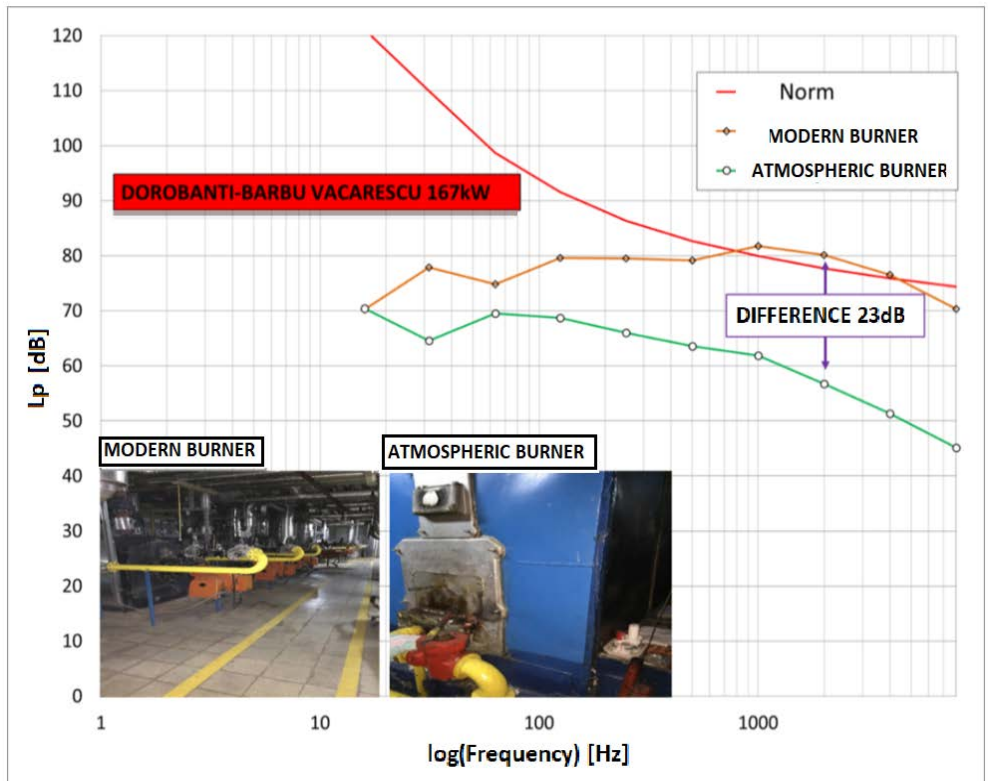


Fig. 6 – Comparison between noise from blower with blown air / atmospheric Dorobanti (blown air) - CT Barbu Vacarescu 167kW (natural draft)

Several comparisons were made between the two different construction types for an operation at the same thermal load and the following table was obtained:

Table 1

Comparisons between boiler burner at same thermal load for different construction type

Nr.crt	Plant1	Plant2	P _{burner} [kW]	LA _{eqAI} [dBA]	LA _{eqAA} [dBA]	Δ LA _{eq} [dBA]
1	AI DOROBANTI	AA BARBU VACARESCU	167	86.1	66.05	20.05
2	AI DOROBANTI	AA FLOREASCA	71	82.45	57.48	24.97
3	AI TURTURELE	AA FLOREASCA	294	79.93	75.83	4.1
4	AI MOZART	AA FLOREASCA	637	76.81	76.8	0.01
5	AI DOROBANTI	CM STOIAN	180	83.62	49.61	34.01
$\mu \Delta LA_{eqAA - AI}$ [dBA]						12.28
$\mu \Delta LA_{eqAA - CM}$ [dBA]						34.01

Boilers with modern burners (AI) produce up to 12dBA more noise than boiler with atmospheric burners (AA), but are preferable in modern boilers due to much higher efficiency. There is a difference of up to 34dB in addition for the boiler compared to the wall boiler (CM). It is thus highlighted the possibility of reducing noise in technical spaces by using a wall boiler, when it is not necessary to provide high thermal loads.

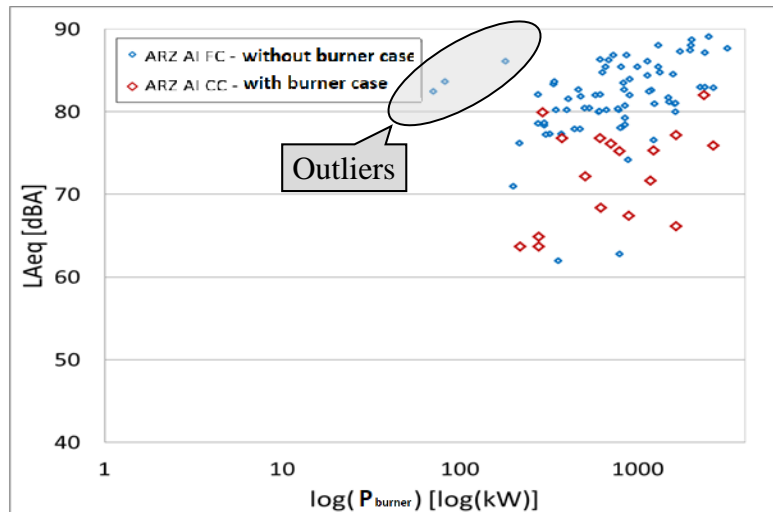


Fig. 7 – Graph of the weighted global equivalent noise level, depending on the thermal load for modern boiler with case (AI CC) and modern boiler without case (AI FC)

Covering the burner with a housing can reduce the noise at the source because it absorbs the noise at high frequencies. Instead, this measure is less effective in terms of low frequencies which are also the best transmitted by the structure of the building to the

apartments. The housing can attenuate noises at low frequencies only if its walls are heavy, which has the disadvantage of making it difficult to move, so difficult to maintain the burner.

The graph above shows that the noise level for burners without housing is higher than for those provided with housing. There is a higher dispersion of the points corresponding to the measurements of the modern burners with blown air with case - AAI CC.

Since the predominant source of noise is the burner, those without the housing are less sensitive to other noise sources, for example pumps, the blue dot cloud is more grouped than those with the housing.

In the following, one of the analyzed solutions will be presented to highlight the effect of the sound-absorbing casing, thus comparing the noise level with / without the sound-absorbing casing for CT Republicii with a real thermal load of 204Kw.

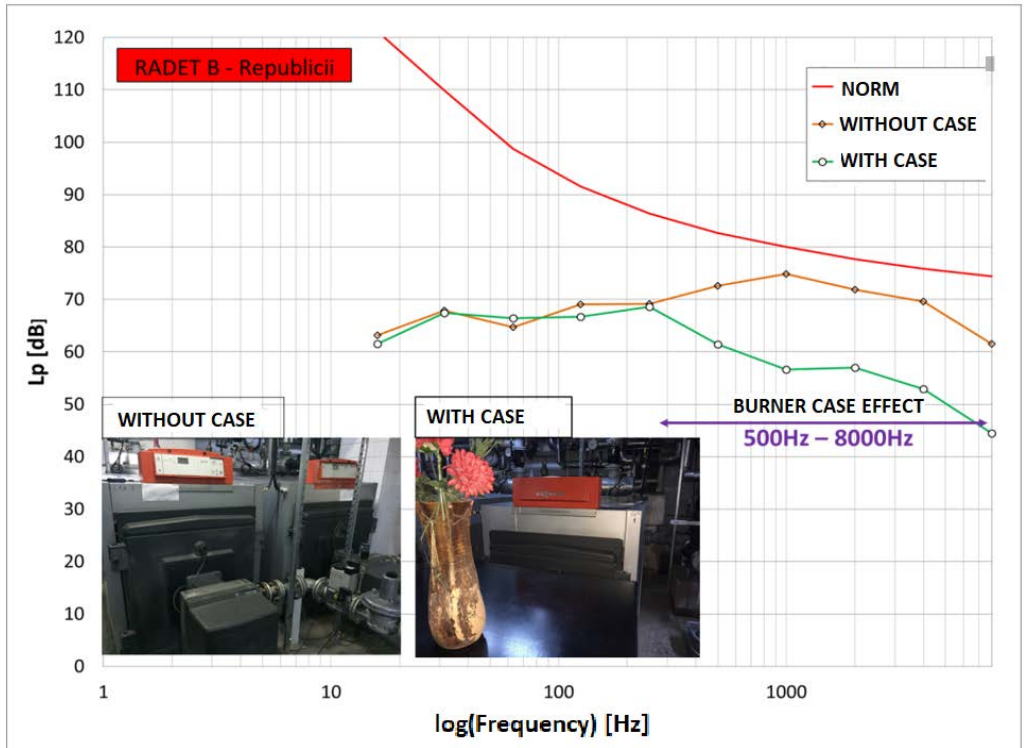


Fig. 8 – Noise level with / without sound-absorbing housing for Republic Republic CT 204kW

A noise level reduction of 14dB is observed for frequencies higher than 500Hz. This acoustic treatment solution is feasible, but attention must be paid to how the housing is sealed to the boiler.

For all sound-absorbing housings, a reduction in noise level of up to 20dB was observed. This reduction had different values because the equipment was operated at different thermal loads, and for the same thermal load the sealing mode of the housings was different (some plants had a very well-sealed housing, others did not have it sealed).

Table 2

Comparisons between boiler equipped with blown air burner, of the same thermal load with and without CASE

$Nr. cr$ t	Plant	P_{burner} [kW]	$LAeqAI$ FC [dBA]	$LAeqAI$ CC [dBA]	$\Delta LAeq$ [dBA]
1	AI - REPUBLICII	276	78.59	64.92	13.67
2	AI - MOZART	609	82.02	76.81	5.21
3	AI - TURTURELE	290	79.93	61.97	17.96
4	AI - DIMITROV AI	399	80.24	76.82	3.42
5	AI - EROILOR I	216	76.18	63.67	12.51
$\mu \Delta LAeq$ [dBA]					10.55

Another acoustic treatment solution identified in 4 measuring points, made in two thermal power plants is represented by acoustic treated walls from an acoustic point of view with sound-absorbing material.

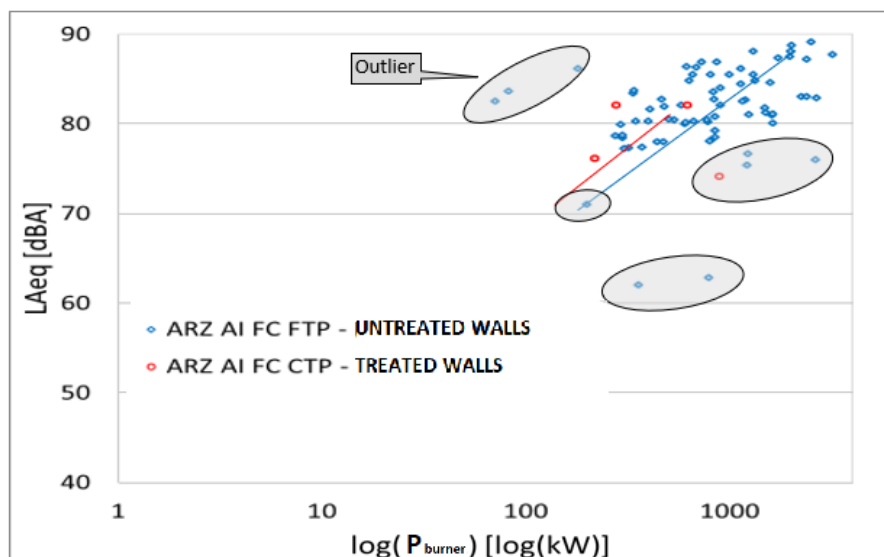


Fig. 9 – Graphical representation of the weighted global equivalent noise level, depending on the thermal load for boiler room with treated and untreated walls

It seems that the trend of these points is above the general trend of the point cloud - for air blowers without AI FC case, but not with a significant influence. Given the insufficient number of measurements, no exact conclusion can be drawn regarding the influence of this parameter on the model.

It seems that the trend of these points is above the general trend of the point cloud - for air blowers without AI FC housing, but not with a significant influence. Given the insufficient number of measurements, no exact conclusion can be drawn regarding the influence of this parameter on the model.

Another acoustic treatment to noisy boiler rooms is the detachment. The high-power boilers required to heat a collective building are large generators of vibration and noise. They must be mounted on their own foundation, a solid concrete, different from the boiler foundation and placed on the support in order to limit the propagation of the vibration of the boiler and its foundation to the rest of the building structure. These supports can be made based on rubber, elastomers, metal springs, etc. Anti-vibration supports must be framed in an equal manner, which ensures that the boiler vibrates properly. The boiler mounted on the anti-vibration supports must not be rigidly connected to the pipes by means of the drums.

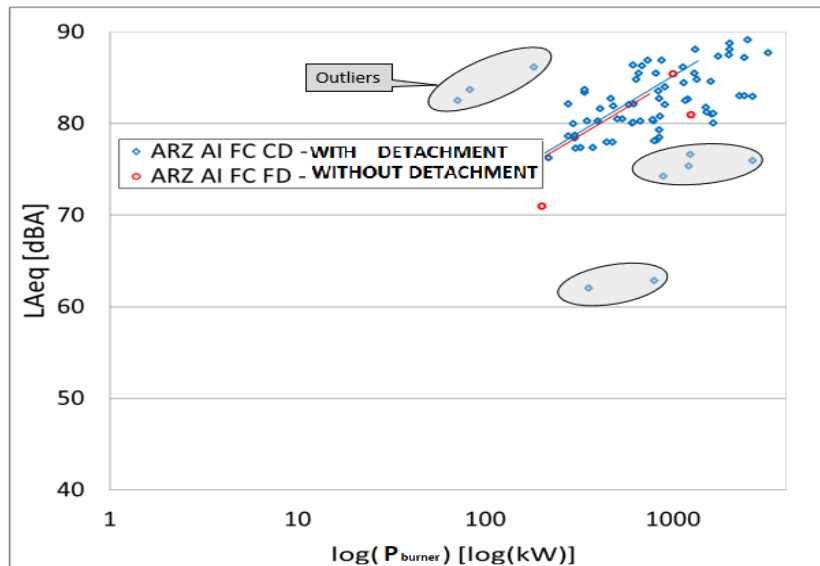


Fig. 10 – Graphical representation of the weighted global equivalent noise level, depending on the thermal load for boiler with/without detachment

The measuring points for blown air burners without housing and without detachment - AAI FC FD are in the noisier stage of the points of blown air burners without housing with detachment - AAI FC CD.

The graph above shows that solid decoupling solutions do not provide significant prediction information of LAeq [dBA].

After removing the outliers, the cloud of points shows or reduced variation.

Another detachment solution for thermal power plants is the boiler foundation. Normally this element must be separated from the concrete slab of the building by a rubber buffer. Detachment through the foundation is used to limit the vibrations transmitted after combustion to the boiler and then to the structure of the building.

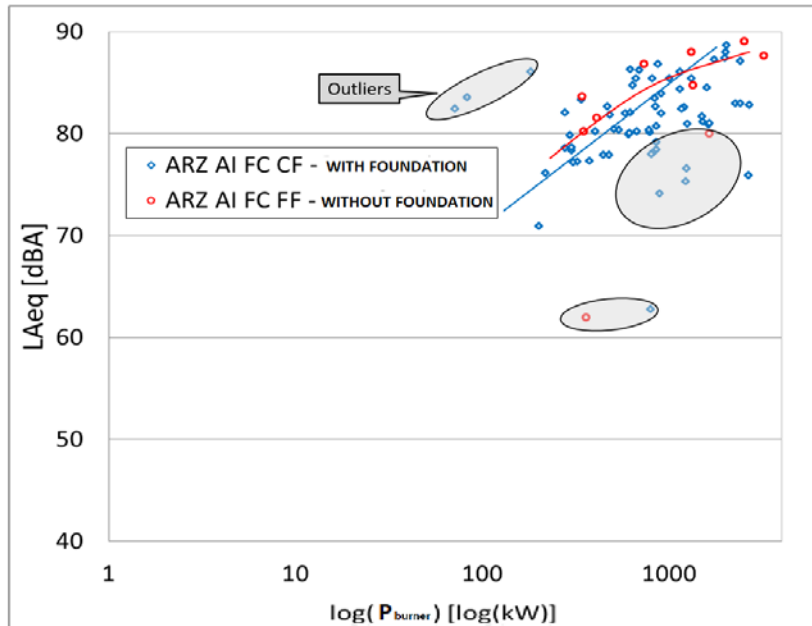


Fig. 11 – Graphical representation of the weighted global equivalent noise level, depending on the thermal load for boiler with/without boiler foundation

It seems that this solution reduces the noise level inside boiler room, so for equal thermal loads, higher noise levels were recorded for measuring points in other thermal power plants. Due to the lack of a larger number of points (minimum 10 measuring points) it is not possible to conclude on the benefits brought by such a positioning of the pumps inside the thermal power plants.

There are other acoustic treatment solutions, less effective for reducing the weighted equivalent global noise level, but useful in reducing the noise level for certain frequencies, for example flexible connection for the burner gas supply pipe (low frequencies) or moving the pumps in rooms adjacent to the space of the thermal power plant (high frequencies).

4. Conclusions

After achieving the experiments, it was found that the equipment that produces a high noise level in a thermal plant is fan of the modern burners, and not pumps or other components of the heating system.

From the analysis made in comparison with the datasheet, there were revealed overtaking of the values given by the producer of the burner, which indicate differences due to faulty equipment settings. Also, in this study were highlighted that the measurements of the noise levels exceeding the maximum value indicated in the norm [1].

According to the results of theoretical studies [5,6], a boiler case near the burner can be used. In addition to this recommendation, other studies have been conducted in this article on the influence of acoustic treatments on noise reduction.

We also demonstrate that it is possible to decrease noise from boiler plant by using other acoustic treatment solutions when it is not possible to mount a burner housing, but in this case the results will be less effective.

The purpose of this paper was to carry out such measurements in different boiler plants to choose the optimal solution for the acoustic treatment of the boiler room. Engineers involved in the design and construction of the installations can use this information for noise reduction when the designed solution or the existing boiler room exceeds the values of acoustic comfort parameters from local regulations.

This study can be made accessible to the wider community, not just scientific community, because it is of pressing importance with the political push to leave a better planet for the future generation.

Acknowledgements. The study was carried out as part of a doctoral thesis from the Faculty of Installations, UTCB, under the coordination of Professor Vlad Iordache

REFERENCES

- [1] Monitorul Oficial al Romaniei (2012). *Normativ privind Acustica în construcții și zone urbane* C125-2013. Romania: Guvernul Romaniei. Ministrul dezvoltării regionale și turismului. (romanian)
- [2] A.I. Abramov, *Improving the environmental safety of CHPs: a textbook for universities* M.: Publishing House of MPEI, 378, 2002
- [3] V.Iordache, T.Catalina, *Experimental investigation on the sound pressure level for a high thermal capacity burner during a running cycle* Applied acoustics 74 (5), 708-717, 2013
- [4] A.M. Drokono, A.E. Drokono, *Noise reduction in power plants. Fundamental and applied problems of engineering and technology* 3, 65–75, 2014
- [5] B.V. Tupov, *Increasing safety of thermal and nuclear power stations energy equipment by reducing noise*. International Conference on Problems of Thermal Physics and Power Engineering 4, 14–16, 2017
- [6] V.B. Tupov, S.A. Semin, B.V. Tupov, A.A. Taratormin, D.A. Rozanov, *Noise barriers for power-plant equipment*. Power Technology and Engineering, 50(6), 649-652, 2017

- [7] S.A. Semin, V.B. Tupov, *Effective measures to reduce the noise from a CHPP and a boiler-house*. Proc. 5Th All-Russia Int. Sci. Pract. Conf. on Noise and Vibration Protection, 268-275, 2015
- [8] ISO 3743-1, *Acoustics; Determination of sound power levels of noise sources; engineering methods for small, movable sources in reverberant fields; part 1: comparison method in hard-walled test rooms*, 1994
- [9] ISO 3743-2, *Acoustics; Determination of sound power levels of noise sources using sound pressure - Engineering methods for small, movable sources in reverberant fields - Part 2: Methods for special reverberation test rooms*, 1994
- [10] ISO 9614-1, *Acoustics; Determination of sound power levels of noise sources using sound intensity; part 1: measurement at discrete points*, 1993
- [11] Hamayon L., *Réussir l'acoustique d'un bâtiment*, Ed. Le Moniteur, Paris, 1996;
- [12] Cyssau, R., Palenzuela, D., Francoise E., *Bruit des equipments*. Collection des guides de l'AICVF, Ed PYC Edition livres, 1997
- [13] V.Iordache, *Acustica cladirii si a instaltiilor*, Matrixrom, Bucuresti, 2007

NUMERICAL AND EXPERIMENTAL ANALYSIS OF THE MV3T REFRIGERANT

Mioara VINCERIUC^{1,2} and Gratiela TARLEA^{1,2}

¹TUCE Bucharest Romania

²RGAR, Bucharest Romania

Abstract. This paper shows a modelling study for mixture MV3T used in an air-water heat pump refrigeration system. The paper has focused on theoretical and experimental data for validation purposes, using ClimaCheck software. Mathematical simulations were done with the EES software. After experimental and mathematical analysis, very good results were obtained for this mixture and thus we validated the cooling capacity and COP. Regarding F-Gas Regulation the optimum alternative for this application is MV3T.

Keywords: refrigerant mixture, heat pump, ecological, COP, GWP.

1. Introduction

At an international level, according to the new legislative Regulations [1], ecological alternatives for refrigerants must be found in order to decrease the global warming potential (GWP).

The refrigerant mixture MV3T is proposed in this validation of mathematical and experimental modelling.

The paper also shows a possible retrofit solution for R134a currently used in heat-pump refrigeration systems [5,7] with low GWP in accordance with EU Regulations.

In table 1 some properties of the new refrigerant mixture are presented [6].

Table 1
Properties of refrigerant mixture retrofit [2]

Refrigerant	MV3T
Critical temperature [°C]	98.06
Critical density [kg/m ³]	493,06
Molar mass [kg/kmol]	108

It is necessary to replace HFC [1] with zero ODP and low GWP refrigerant and such an example is MV3T.

1.1. The operating mode of the air-water equipment.

The equipment uses the ambient air to heat water. Air is drawn in at the top with the help of a fan, led to the evaporator unit and blown out again sideways. It is called an evaporator because the refrigerant in the heat pump circulation evaporates in it.

During evaporation, heat is extracted from the drawn in ambient air, as this is warmer than the medium in the evaporator [8,9]. Even at relatively low temperatures (down to 6° C or - 10 ° C) heat can still take out of the air.

The working fluid is compressed by the compressor and brought up to a higher temperature level. This heat is transferred to the drinking water by the helical tube condenser built into the double casing of the reservoir.

The cooled medium, that is now liquid again, is expanded via the expansion valve, returns to the evaporator and thus is again ready to take up heat.

2. Mathematical model

This chapter focuses on the mathematical modelling of the thermodynamic processes for the air-water heat pump which works with MV3T. The pages describe the parameters of the model [3].

Introduced parameters in the model: evaporating pressure, condensing pressure, external air temperature (T_{amb}), water temperature inlet and outlet of the condenser, air temperature inlet and outlet evaporator, refrigerant temperature inlet and outlet evaporator, refrigerant temperature inlet and outlet compressor, electrical input, wet bubble air temperature (T_{aer_wb}) and mass flow for water and condenser (\dot{V}_{water_cd}), mass flow air evaporator (\dot{V}_{air_ev}) and water specific heat content (c_{p_w}).

After the mathematical models calculation [10] the resulted parameters are: evaporator and compressor refrigerant mass flow (\dot{M}_{r_ev} , \dot{M}_{r_cp}), volumetric ratio (ϵ_{cp_v}), isentropic ratio (ϵ_{cp}), adiabatic ratio (ϵ_{cp_adiab}), compression ratio (r_p), the global coefficient of heat transfer (condenser- AU_{cd} and evaporator AU_{ev}), performance coefficient for cooling (COP_{cool}) and heating (COP_{heat}), condenser (ϵ_{cd}) and evaporator ratio (ϵ_{ev}), evaporator and condenser number of thermal units (NTU_{ev}), (NTU_{cd}), cooling power (\dot{Q}_{ev}), condenser thermal power (\dot{Q}_{cd}), compressor volumetric ratio (r_v), condenser water thermal power (\dot{Q}_{w_cd}), air cooling thermal power (\dot{Q}_{air_ev}).

Mathematical model equations for refrigeration system are:

"Condenser"

"Refrigerant"

$$\text{DELTAT}_{r_ex_cd} = T_{r_sat_ex_cd} - T_{r_ex_cd} \quad (1)$$

"Evaporator"

"Refrigerant"

$$\text{DELTAT}_{r_ex_ev} = T_{r_ex_ev} - T_{r_sat_ex_ev} \quad (2)$$

"Air"

$$T_{\text{dewpoint_air}} = 13 + 273.15 \quad (3)$$

$$T_{\text{amb}} = T_{\text{air_su_ev}} \quad (4)$$

$$c_{p_air} = \text{cp}(\text{AirH2O}, T = T_{\text{air_su_ev}}, D = T_{\text{dewpoint_air}}, P = 101.325) \quad (5)$$

$$Q_{\text{dot_air_ev}} = \frac{V_{\text{dot_air_ev}}}{v_{\text{air_su_ev}} * c_{p_air} * (T_{\text{air_ex_ev}} - T_{\text{air_su_ev}})} \quad (6)$$

$$V_{\text{air_su_ev}} = \text{Volume}(\text{AirH2O}, T = T_{\text{air_su_ev}}, D = T_{\text{dewpoint_air}}, P = 101.325) \quad (7)$$

"Compressor"

$$M_{\text{dot_r_cp}} = M_{\text{dot_r_cd}} \quad (8)$$

$$M_{\text{dot_r_cp}} = M_{\text{dot_r_ev}} \quad (9)$$

$$T_{r_sat_su_cp} = T_{r_sat_ex_ev} \quad (10)$$

$$M_{\text{dot_r_cp}} * h_{r_su_cp} + W_{\text{dot_cp}} - Q_{\text{dot_amb_cp}} = M_{\text{dot_r_cp}} * h_{r_ex_cp} \quad (11)$$

$$V_{\text{dot_s_cp}} = 0.00001528 \quad (12)$$

$$M_{\text{dot_r_cp}} = V_{\text{dot_s_cp}} / v_{r_su_cp} * 2900 / 60 \quad (13)$$

"AU condenser calculation "

$$c_{p_w} = 4.185 \quad (14)$$

$$Q_{\text{dot_cd}} = AU_{\text{cd}} * (T_{\text{cd_mean}} - T_{w_su_cd}) \quad (15)$$

$$\epsilon_{\text{cd}} = 1 - \exp(-NTU_{\text{cd}}) \quad (16)$$

$$NTU_{\text{cd}} = \frac{AU_{\text{cd}}}{C_{\text{dot}_{w_{\text{cd}}}}} \quad (17)$$

" AU evaporator calculation"

$$Q_{\text{dot_ev}} = AU_{\text{ev}} * (T_{\text{ev_mean}} - T_{\text{air_ex_ev}}) \quad (18)$$

$$C_{\text{dot_air_ev}} = V_{\text{dot_air_ev}} / v_{\text{air_su_ev}} * c_{p_air} \quad (19)$$

$$\epsilon_{\text{ev}} = 1 - \exp(-NTU_{\text{ev}}) \quad (20)$$

$$NTU_{ev} = \frac{AU_{ev}}{C_{dot_{air_{ev}}}} \quad (21)$$

$$h_{w_su_cd} = \text{Enthalpy (Water, } P = 250, T = T_{w_su_cd}) \quad (22)$$

$$h_{w_ex_cd} = \text{Enthalpy (Water, } P = 250, T = T_{w_ex_cd}) \quad (23)$$

"Coefficient of Performance"

$$COP_{heat} = \frac{Q_{dot_{cd}}}{W_{dot_{cp}}} \quad (24)$$

$$COP_{cool} = \frac{Q_{dot_{ev}}}{W_{dot_{cp}}} \quad (25)$$

" Equilibrium equation "

$$//Q_{dot_{cd}} = W_{dot_{cp}} + Q_{dot_{ev}} \quad (26)$$

$$Q_{w_cd} + Q_{dot_{amb_cp}} + Q_{dot_{air_{ev}}} = Q_{dot_{cd}} + Q_{dot_{ev}} - W_{dot_{cp}} + Q_{dot_{cp}} \quad (27)$$

Figure 1 presents the Climacheck interface of the mathematical model [4] [11]

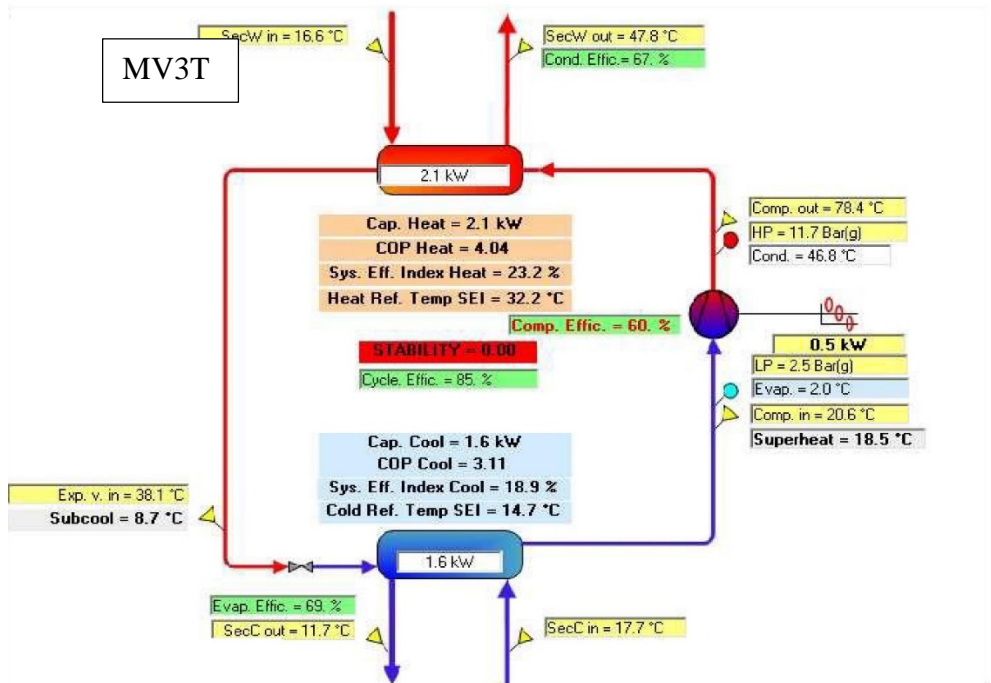


Fig. 1 - The interface of the mathematical model MV3T

3. Experimental data

Figures 3 and 4 show the preliminary performance coefficients (COP) for heating and cooling, experimental data before the heat pump gets in the stability regime.

The acquisition of experimental data, when the system enters into operation (Figure 2) was done with the Climacheck software [4].

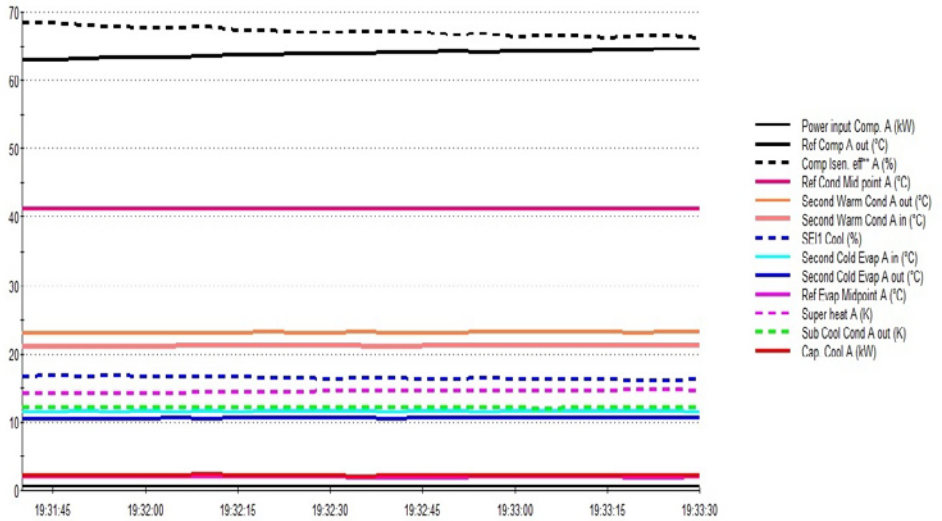


Fig. 2 - Preliminary data acquisition with Climacheck software

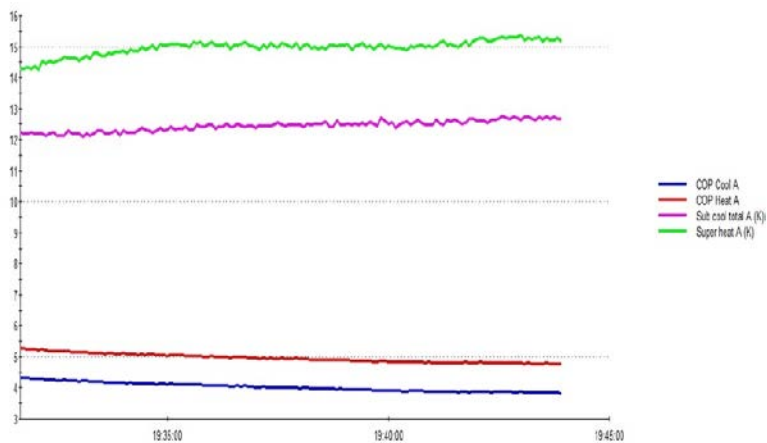


Fig. 3 - Preliminary COP for heating and cooling experimental

Figure 4 shows the cooling COP versus cooling capacity [3]. One can observe the increase of COP with the increase of cooling capacity.

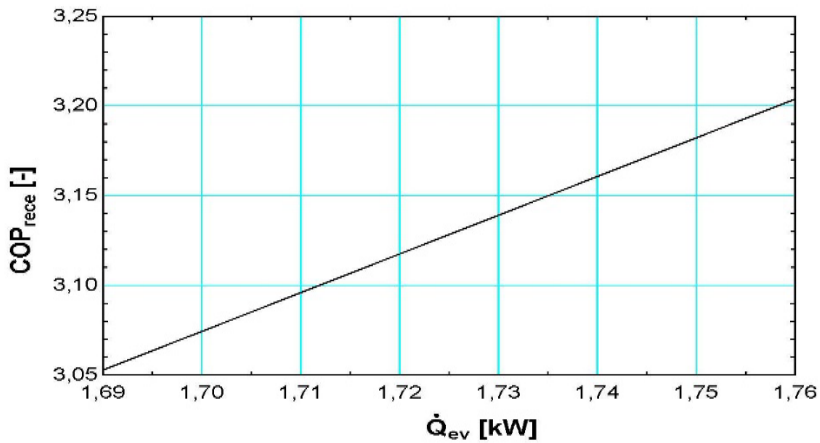


Fig. 4 - Cooling COP versus cooling capacity

Figure 5 presents the normal evolution of COP for cooling and heating in comparison with the compression ratio [3].

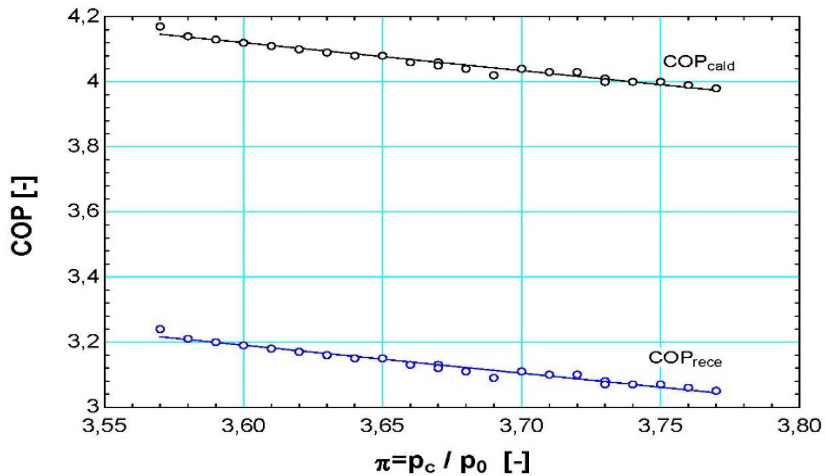


Fig. 5 - Cooling and Heating COP versus compression ratio

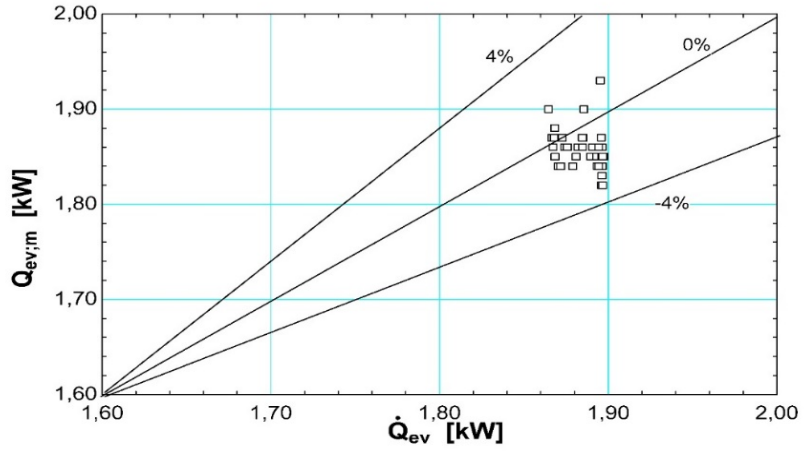


Fig. 6 - Cooling COP versus cooling capacity

Figures 6 and 7 showcase the validation between experimental (measured) and mathematical models (4% accepted technical error).

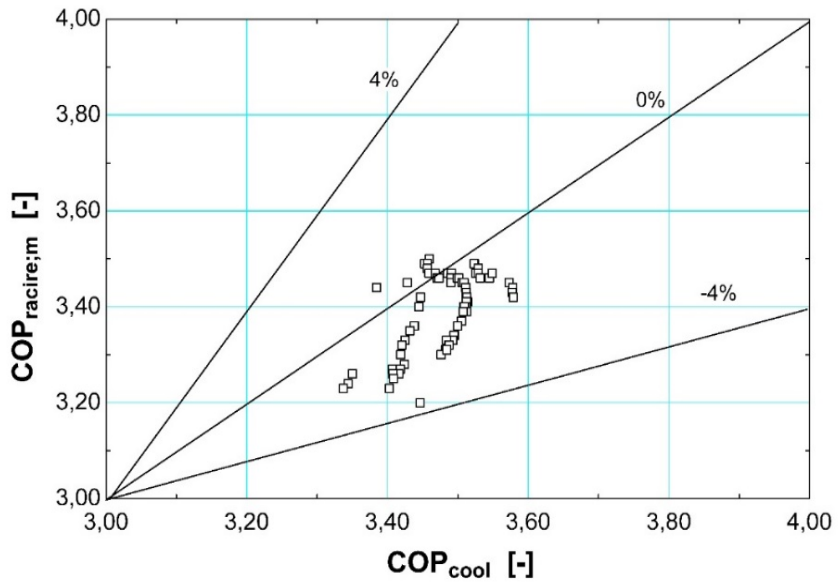


Fig. 7 - Calculated and measured COP cool comparisons

4. Conclusions and validation

In accordance with the international legislations, the optimum alternative for this application, regarding GWP is refrigerant mixture MV3T.

As an example (Figure 6), the heating and cooling COP (cold, hot) is shown here below (experimental measurement versus calculations for MV3T air-water heat pump).

In this study, experimental and mathematical analyses led to very good results for this mixture and the cooling capacity and COP were validated (Figure 6 and Figure 7).

REFERENCES

- [1] Țârlea G. M., Vinceriuc M., *Alternative ecologice ale agentului frigorific R134a*, Revista de Instalatii, I.S.S.N. 2457 – 7456, AIIR 2018.
- [2] Țârlea G. M., Vinceriuc M., Zabet I., Țârlea A., *Water-Air Heat Pump Ecological and Energy - Efficiency Study Case SME Cluj* 2017.
- [3] Țârlea G. M., Vinceriuc M., *Alternative ecologice de agenti frigorifici pentru o pompa de caldura aer-apa*, Volumul Conferintei Tehnico- Stiitifica cu participare internationala, „Instalatii pentru constructii si economia de energie”, Editia XXII, 5-6 iulie Iasi 2012, Editura Societatii Academice "MATEI-TEIU BOTEZ" ISSN 2069-1211.
- [4] Țârlea G., Hera D., Vinceriuc M., *Noul agent frigorific HFO-1234yf*, publicata in volumul Producerea, transportul si utilizarea energiei”, Editia XXVII, Cluj-Napoca 2009 pagina 315-317 Editura Risoprint ISBN 978-973-751-799-9.
- [5] Țârlea G., Hera D., Vinceriuc M., *HFO-1234yf agent frigorific cu potential de incalzire globala (GWP) redus*, publicata in volumul conferintei cu participare internationala „Instalatii pentru constructii si confortul ambiental ”, Editia XVIII, 2-3 aprilie Timisoara 2009, pagina 212-217 Ed.Politehnica ISSN 1842-9491.
- [6] Țârlea G. M., Vinceriuc M., Zabet I., Țârlea A., *R513A AND R1234yf Alternative Replacement of R134a Refrigerant*, a XVII-a Conferinta nationala de Termotehnica, cu participare internationala, noiembrie 2016, Universitatea Transilvania Brasov, categoria B+.
- [7] SR EN378- Refrigerating systems and heat pumps - safety and environmental requirements”, 2016, European standard, CEN.
- [8] Mioara VINCERIUC, Gratiela TARLEA - *Comparative refrigerants study of R134a, R1234YF, MV3T and MV3TN*, 50-International HVAC&R Congress and Exhibition (KGH), 2019, Belgrad
- [9] Gratiela Tarlea, Mioara Vinceriuc, Ion Zabet- *Air-Water Heat Pump Modelling*, 50- International HVAC&R Congress and Exhibition (KGH), 2019, Belgrad
- [10] ***EES Software (Engineering Equation Solver).
- [11] ***ClimaCheck Sweden AB.

STUDY CASE REGARDING THE IMPROVEMENT OF ENERGY AND ECOLOGICAL PERFORMANCE OF A HEAT PUMP

George MARDARE ¹ and Gratiela TARLEA ^{1,2}

¹Technical University of Civil Engineering Bucharest Romania

²Romanian General Association of Refrigeration, Bucharest Romania

Abstract. *The general objective of the study consists in analyzing the possibilities to grow the energy parameters of the heat pumps, under the conditions of ensuring an extended reliability. The specific objective of the study consists in the realization of a original heat pump having an open circuit, having an evaporator realized in a new conception, in the form of a special spiral, with capillary tubes, able to offer superior performances of energetic nature, in the conditions of much greater reliability and the use of a refrigerant with higher ecological performance. The experimental results confirmed the performances obtained by calculation. The conclusion was that the heat pump that uses a capillary heat exchanger guarantees superior performance to the classical installations ensuring electricity savings of up to 50%*

Keywords: heat, refrigerant, performance, environment, heating.

1. Introduction

The current international situation is characterized by a drastic reduction in fossil fuel reserves in conditions where their use has become unacceptably harmful to the quality of the environment, which has generated climate change that if continued at the same rate, will drastically affect life on our planet. In this context, the contemporary world is facing major problems generated both by the nature of fossil fuels and their harmful impact on the environment. Concern about these perspectives and their consequences on global socio-economic developments has led to the emergence of the concept of "sustainable development" designed to streamline the consumption of primary resources and mitigate the consequences of using fossil fuels. [1]

In the EU, the residential housing the generators for aprox 40% of energy loss with proportional consequences in pollution, when using fossil fuels. Under these conditions, the economically efficient, long-term solution for reducing GHG emissions is the use of heat pumps. According to the European EPBD Directive, heat pumps are listed as systems that use renewable energy [2].

Equipment equipped with heat pumps are useful for both conditioning. These equipment absorb heat from the environment and transfer energy to the building. [3] For this reason, heat pumps have many applications [4].

2. Method

The use of capillary tubes as an expansion device was originally used for low-capacity refrigeration machines, such as refrigerators for residential use or air conditioning equipment, [5] due to the advantages of simplicity of equipment, zero maintenance cost and low torque, starting the compressor. Experiments done on evaporators equipped with capillary tubes dates about 20 years back and analyze the system performance according to the size of the capillary. The mentioned studies show that the mass flow in a spiral capillary is lower by up to 5% compared to a straight capillary. Zhou and Zhang (2006) [6] presented an experiment in which they studied the behavior of a serpentine capillary.

The experiments showed that at a 10K sub- cooling, for an enlarge of the dimension of pipe the variation of flow is as shown in the diagram Fig.1.

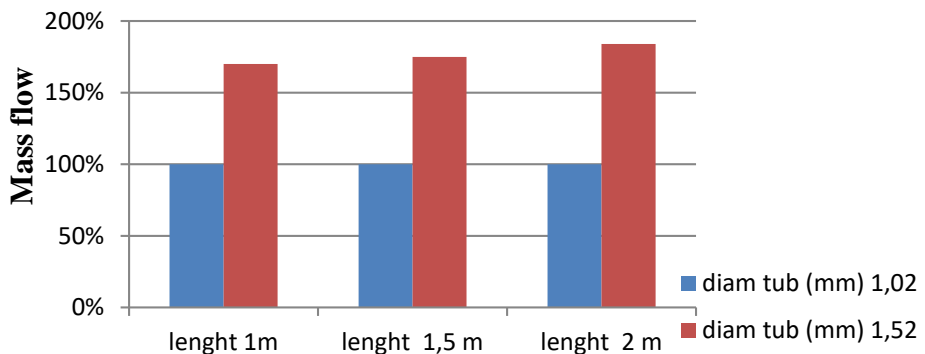


Fig. 1 Diagram of variation length and diameter

To analyze heat pumps efficiency, the coefficient of performance (COP) is used [6]. Generally, for heat pump collectors, horizontal piping systems are used, in ditches dug in the ground with a depth between 1.5-2.5 meters, which requires both a very large area of land and very long lengths. [6]. Usually, the length of the required piping is about 50 m / kW heat of the heat pump. However, this value depends very much on the type of soil, the diameter capillary, and depth of ditch, the flow of the fluid flowing through the pipe, etc. [6].

Bazkiaei. [7] suggested a type for optimizing these horizontal piping systems, using homogeneous profile soils. Esen [8] analyzed performances obtained by a system of

such a evaporator with horizontal pipes and the economic advantages of such a system. Ramniwas [9] found that the exchanger output thermal energy is the determining factor in realization of the best coefficient of performance.

Noorollahi [10] conducted a financial balance sheet for a plant equipped with such equipment for conditioning a greenhouse in Iran. This research led to the idea of using a capillary heat exchanger. Mariem Lazaar [11] conducted research on heating with a capillary heat pump located in the floor of a greenhouse, which provided a temperature of 12 °C during the night. Mejdi Hazami [12] have done research on the use of a capillary heat exchanger that uses seawater.

During the analysis of the cooling coefficient (EER), the R22 refrigerant was used [13]. The condensation temperature in the condenser was at sea level plus 10 °C [14]. Starting from these tests, this work and research represents a novelty regarding the construction and architecture of heat pumps which led to a new heat pump with capillary vaporizer in the form of a special spiral, according to fig.2.

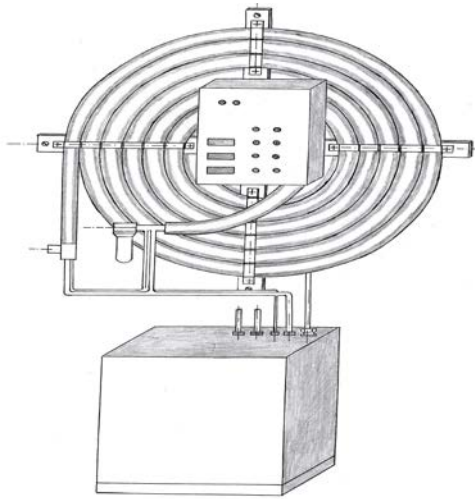


Fig.2 Heat pump with capillary evaporator with spiral shape

At this type of heat pump, the operation is ensured by a battery of capillary tubes, the vaporization control being achieved by temperature control, ensuring the optimal values of sub- cooling and overheating of the refrigerant during the operation cycle, which also contains a heat exchanger regenerative.

3. Results and Discussions

From the analysis of the results obtained from the tests performed, it could be concluded that an increase of the EER performance coefficient of the heat pump was obtained 2.21

times compared to a regular refrigeration unit with heat pump, without capillary. Consequently, the use of this type of heat pump ensures considerable reductions in electricity consumption. Power consumption analysis. As it results from fig.3 and 4, the monthly heating meant a consumption increased, corresponding to an electricity consumption which also increased. Towards the end of the testing time, the heat consumption was 1501.12kw / h and the electricity consumption was 284.97kW / h.

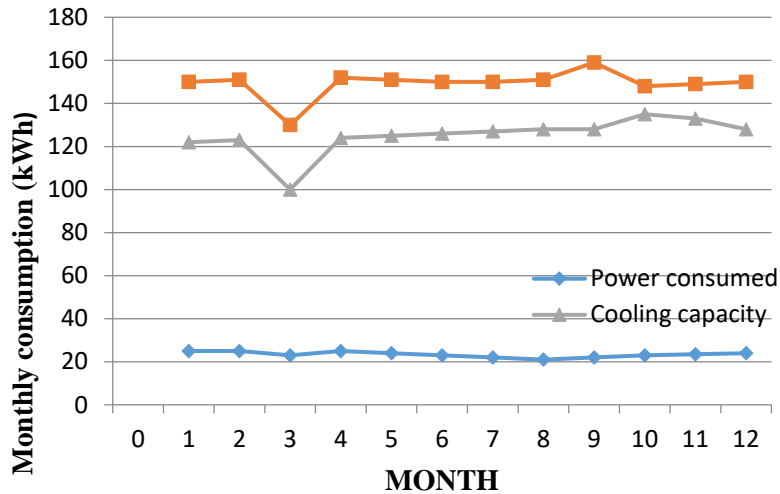


Fig. 3 GSHP monthly heating / cooling / consumption

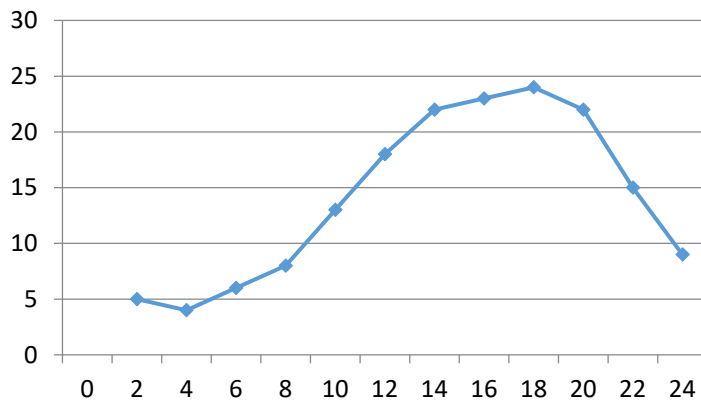


Fig.4. Sea water temperature

In the test performed, the variation of the parameters was according to figure 4.

As it results from fig.3, the energy efficiency was higher during the summer compared to the operation during the winter. It was also found that the COP and EER values

underwent changes for different values of the loading rate. Thus, there are large variations of the COP and EER to the variation of the loading rate from 0.3 to 0.6, COP varying between 3.4 and 5.32 and EER between 3.82 and 6.32. (Fig.5)

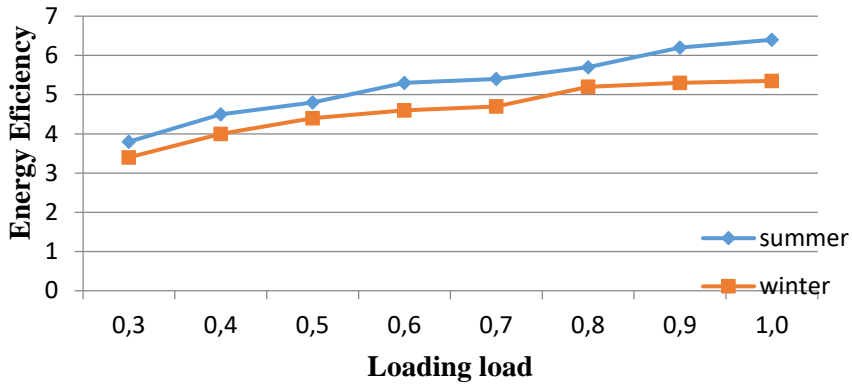


Fig. 5. Variation of energy efficiency depending on the charging rate

As shown in Fig 6, COP increased in direct proportion to seawater temperature. Also, the COP value was higher the lower the temperature difference between the heat source and the thermal load. Regarding the EER variation, it increased in direct proportion to the sea water temperature.

Heating and cooling capacity. The tests performed showed that both the heating capacity of the heat pump and its cooling vary depending on the load of the building.

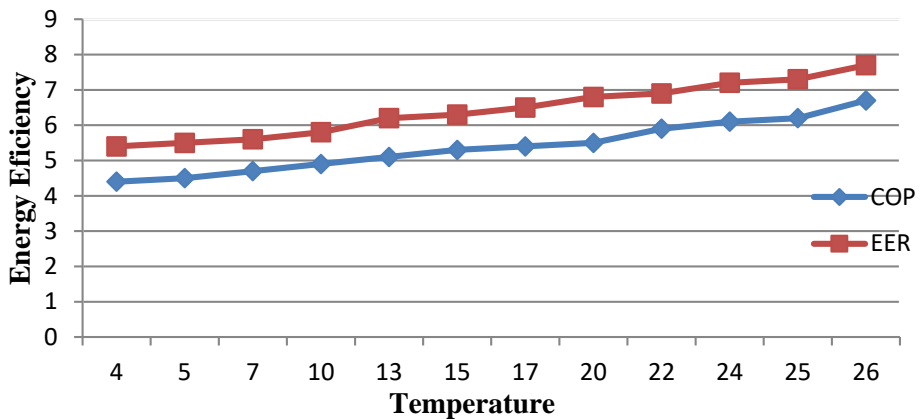


Fig. 6. Variation of energy performance versus sea water temperature

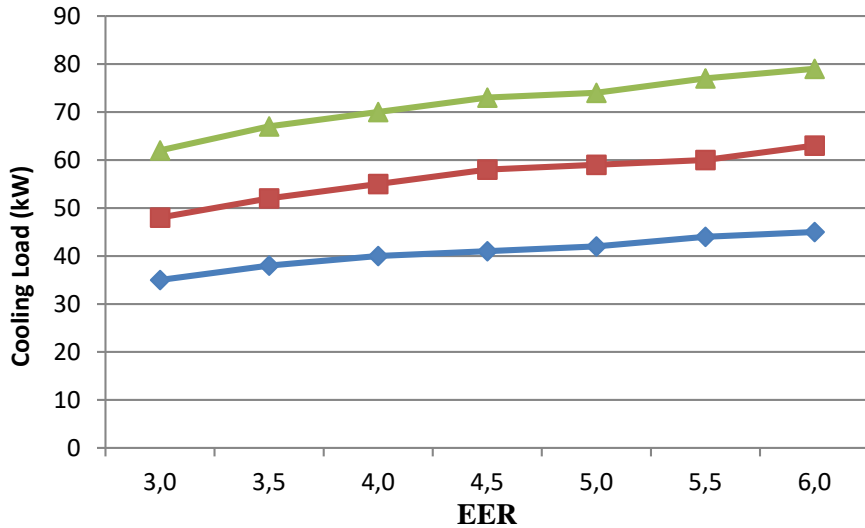


Fig. 7 Variation of cooling load with EER

In Fig 7. one can see that when the cold demand increased, the cooling capacity of the heat pump increased, the EER being slightly ascending.

4. Conclusions

Zhou and co-workers [14] conducted tests on a medium-sized hotel using a capillary heat pump with water as the capillary system, the Qindao River. The hotel had a built area of 500m². The average value of EER was 4.50 and the average value of COP when operating as a heat pump was 4.06. It should be mentioned that the COP / EER values obtained experimentally were lower than the values obtained by theoretical calculation

Thus, the theoretical value of the EER was 5.32 and the theoretical value of the COP was 6.32. It is assumed that the difference would be due to the motivation that the power of the system was too small compared to the required and that the capillary heat exchangers were in time buried in the sand.

These tests analyzed the behavior of heat pumps with capillary heat exchanger in various situations. The malfunctioning modes of the heat pump with capillary winter-for heating and during summer for cooling were analyzed. The following observations resulted:

- The use of heat pumps with capillary heat exchanger in buildings ensures significant reductions in electricity consumption, these reductions being higher during the summer than during the winter;

- Compared to ordinary air conditioners, the electricity consumption obtained by using the capillary heat pump was reduced by up to 1/2, the benefits being significant;

The researches of the heat pumps models having capillary evaporator, made by Zhou and co-workers [14] on the Qindao River where the capillary evaporator was placed on the river bottom as well as the researches of the heat pumps models having capillary evaporator performed by Mejdi Hazami et al. [12] in which the capillary vaporizer was placed in seawater, as well as other similar researches, had as a model the placement of the capillary evaporator in a liquid environment, from which to recover thermal energy. In all these cases, the experiments showed that the practical results obtained were inferior to the theoretical calculations. The conclusion for each case was that the operation of the capillary tube evaporator was severely affected by sand and alluvium deposits both in the case of the vaporizer located on the bottom of the Qindao River and in the case of placing the capillary vaporizer on the seabed.

To avoid the disadvantage generated by alluvial deposits, the authors of the article made a capillary evaporator in the shape of an archimedean spiral, in which water was pumped from a well drilled to the first groundwater level. This personal contribution of the authors was made in order to avoid clogging the capillary tubes with the alluvium in the evaporator. The water from the first groundwater level, used for pumping in the capillary evaporator, is not potable in most cases, being clogged due to pesticides used in agriculture over the years, but this does not affect too much. From the tests performed by the authors in several areas of Romania, the water temperature in the first groundwater level has the value of 11-14°C, with summer-winter temperature variations below 1°C, which allowed the heat pump thus equipped to achieve a performance coefficient higher than 5, very stable coefficient, being influenced by the relatively constant temperature of the water in the groundwater table. The special shape of the capillary evaporator, in which the water circuit does not suffer returns to 90° or 180°, ensures a continuous self-washing of the evaporator, preventing any possibility of clogging it and thus ensures a very high reliability of the evaporator.

- Open circuit water heat pump with capillary vaporizer made as an own contribution in this research, having the vaporizer made in the form of a special spiral, quantifies these energy performances and eliminates the shortcomings of the mentioned researches caused by sand deposits and alluvium on capillaries, which led to the reduction of energy efficiency. This type of capillary evaporator offers extended reliability and increased resistance to clogging by having the phenomenon of continuous self-washing and ensuring a flow section without bottlenecks and returns to 180°, which generates clogging. as is the case with classic heat exchangers.

REFERENCES

- [1] Sarbu I, Sebarchievici C. General review of ground-source heat pump systems for heating and cooling of buildings. *Energy Build* 2014;70:441;
- [2] Arif Hepbasli, M. Tolga Balta. *A study on modeling and performance assessment of a heat pump system for utilizing low temperature geothermal resources in buildings*;
- [3] Byuna JS, Jeonb CD, Jungc JH, Leea J. *The application of photo-coupler for frost detecting in an air-source heat pump*. *International Journal of Refrigeration* 2006;29:191–8.
- [4] M.K. Mittal, Ravi Kumar*, Akhilesh Gupta. *An experimental study of the flow of R-407C in an adiabatic helical capillary tube*
- [5] Zhou, G., Zhang, Y., 2006. *Numerical and experimental investigations on the performance of coiled adiabatic capillary tube*. *Appl. Therm. Eng.* 26, 1106–1111.
- [6] Cho H, Choi JM. *The quantitative evaluation of design parameter's effects on a ground source heat pump system*. *Renew Energy* 2014;65:2e6.
- [7] . Bazkiaei AR, Niri ED, Kolahdouz EM, Weber AS, Dargush GF. *A passive design strategy for a horizontal ground source heat pump pipe operation optimization with a non-homogeneous soil profile*. *Energy Build* 2013;61:39e50.
- [8] Esen H, Inalli M, Esen M. *Technoeconomic appraisal of a ground source heat pump system for a heating season in eastern Turkey*. *Energy Convers Manag* 2006;47:1281e97.
- [9] Ramniwas K, Murugesan K, Sahoo PK. *Optimization of operating parameters of ground source heat pump using Taguchi Method*. In: 23rd IIR Conference, Prague, Czech Republic, August 21e26, 2011.
- [10] Younes Noorollahi, Pedram Bigdelou, Fathollah Pourfayaz, Hossein Yousefi, *Numerical modeling and economic analysis of a ground source heat pump for supplying energy for a greenhouse in Alborz province, Iran*, *J. Clean. Prod.* 131(2016) 145–154.
- [11] Mariem Lazaar, Salwa Bouadila, Sami Kooli, Abdelhamid Farhat, *Comparative study of conventional and solar heating systems under tunnel Tunisian greenhouses: Thermal performance and economic analysis*, *Solar Energy*, Volume 120, October 2015, Pages 620-635.
- [12] Mejdi Hazami, Sami Kooli, Mariem Lazaar, Abdelhamid Farhat, Chekib Kerkani, Ali Belguith, *Capillary polypropylene exchangers for conditioning of museum aquariums (Tunisia)*, *Desalination*, Volume 166, 2004, Pages 443-448.
- [13] Dasare, R. R., & Saha, S. K. (2015). *Numerical study of horizontal ground heat exchanger for high energy demand applications*. *Applied Thermal Engineering*, 85, 252–263.
- [14] P. Zhou, *A study of the operating characteristics of a capillary sea source heat pump system*. 2016, Qingdao Technological University.
- [15] M. Qiao. *Theoretical and experimental study of sea water refrigeration heat pump system*. Tianjin University of Science and Technology, 2006.

MESH INDEPENDENCY STUDY FOR A SOLAR GLAZED TRANSPIRED COLLECTOR

Catalin SIMA^{1,*}, Catalin TEODOSIU¹ and Charles BERVILLE¹

¹First author Technical University of Civil Engineering of Bucharest

Abstract. *Climate change has become a key issue worldwide, making it one of the EU's priorities. One of the answers to this problem is based on the use of technologies working with renewable energy. In this context, air solar collectors represent an interesting solution with low investment cost. In addition, Glazed Transpired Collectors (GTCs) are increasingly developed, one of the studying methods being Computational Fluid Dynamics (CFD) models. Consequently, a mesh independency study has been performed for 6 cases (0.87 to 16.2 million cells) to determine the optimal grid for a prototype of glazed transpired solar wall system. Based on the results achieved, we concluded that the mesh of 5.83 million cells is the optimal discretization as it leads to grid-independent solutions, with the lowest computational resources and minimal CPU time.*

Keywords: renewable energy, air solar collector, CFD model, mesh study

1. Introduction

The building sector is responsible for approximately 40% of final energy use and 36% of CO₂ emissions in the European Union. Fortunately, these figures can be substantially reduced at relatively low cost [1].

According to International Energy Agency (IEA) 2008 reports, CO₂ emissions of the building sector have doubled in 2004 compared to 1971 and they are expected to triple by the year of 2030, reaching 14 Gt of CO₂/year due to increased energy consumption and the continuous economic development [2].

These aspects persuaded the European Union (EU) to apply numerous actions to reduce energy consumption and CO₂ emissions by implementing various measures that reduce pollution and encouraged the use of renewable energy sources. In this context, the concept of “intelligent façades” for buildings represents an interesting approach, more and more used. This is mainly due to the fact that this solution can not only contribute to reducing energy consumption but can also help improve occupant comfort [3].

In the scientific literature, intelligent façades are supposed to include different types: double skin façades (DSFs), double glazed façades, open joint ventilated façades (OJVs), kinetic façades, or solar façades [4].

On the other hand, solar thermal air collectors are often used within intelligent façades solutions. From the constructive point of view, solar thermal air collectors can be classified into several types: opaque solar collectors or transparent (glazed) solar collectors, both with flat absorber or perforated (transpired) absorber [5].

Basically, solar thermal air collectors represent solutions that can be implemented with relatively low investment costs. In addition, the Transpired Solar Collectors (TSCs) are characterized by good results in terms of cost / benefit ratio (reducing energy consumption for heating and ventilation) [6].

In fact, TSC solutions have been analysed for over 35 years, considering that many improvements can still be made regarding their efficiency. TSCs are already used for important buildings in Europe and North America [7,8]. Studies have shown that this type of solar collector is very well suited for direct heating of fresh air, achieving very high efficiencies (up to 72%, according to [9]). Compared with opaque air solar collectors, TSCs have higher efficiency (by 28-50%) under the same working conditions [10,11].

Based on TSCs, the solutions of intelligent façades using Glazed Transpired solar Collectors (GTCs) can attain even better thermal efficiency [12]. Experimental and numerical analyses have shown the applicability of GTCs for space heating or even for improving indoor air quality [12-15].

Consequently, the results of this study are part of a wider research program [16] that aims to optimize (experimentally and numerically) “GTC wall system” solutions, to be used in intelligent façades for different types of buildings.

Basically, the present study is dealing with the GTC numerical model. More exactly, as the approach used is based on the Computational Fluid Dynamics (CFD) technique, the specific aim of this study is focused on the discretization of the computational domain.

It is known that the quality of the mesh properly adapted for a specific case it is of great importance in the quest of obtaining the best numerical results with fewer computational resources and less CPU time.

Therefore, a mesh independence study was carried out in this paper, aiming to identify the grid that can give proper numerical results - uninfluenced by the structure and number of the elements in the mesh.

2. Method

The study of solar thermal air collectors has recently been a major investigation topic at the “Advanced Research Center for Ambiental Quality and Building Physics” (CAMBI) - Technical University of Civil Engineering of Bucharest. Accordingly, TSCs configurations with sophisticated lobed shaped orifices have been subject to in-depth studies [17-21].

On the other hand, it has been demonstrated that the wind is an important parameter that affects the efficiency of the collector [22] but the addition of a glazed layer to the TSCs considerably diminishes the effect of the wind velocity [13].

Furthermore, it has been pointed out that complex geometries and complicated perforations shapes of the absorber do not surely mean significant improvements of GTCs thermal performance [12].

The aspects mentioned above determined the study of a new prototype of solar thermal air collector: GTC with more simple geometry of the plate perforations (Fig. 1).

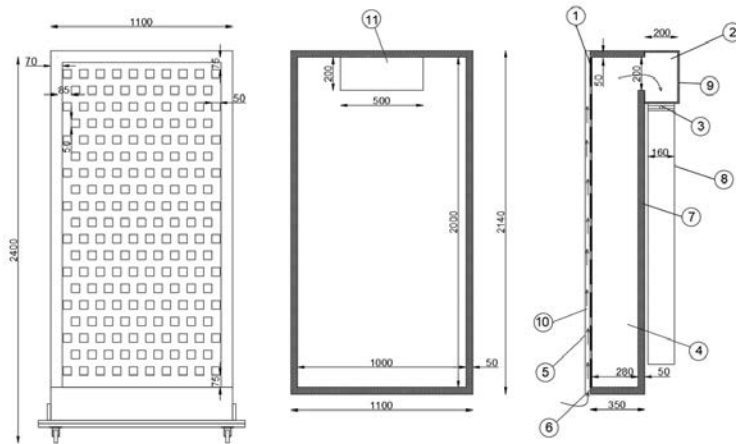


Fig. 1 - Geometry of the “GTC wall system”

1) absorber steel plate (2 mm thickness); 2) plenum; 3) fan; 4) interior cavity; 5) glass (4 mm thickness); 6) air inlet; 7) rockwool thermal insulation (50 mm thickness); 8) air duct (160 mm diameter); 9) plenum rockwool thermal insulation (20 mm thickness); 10) air cavity between glass and absorber; 11) air outlet.

This prototype has been constructed both experimental and numerical using 50 x 50 mm square holes with a regular vertical and horizontal pitch of 50 mm on a 1050 mm x 2000 mm absorber plate. This led to the creation of 181 perforations, disposed as in Fig. 1.

The distance between the glass and the absorber proposed in this first configuration of the prototype was 30 mm (with possibility to have also 40 mm or 50 mm), taken into account that Nahar et al. stated that 40 mm is the optimal gap between the plate and the glass in order to achieve a balance between heat loss due to convection and minimum collector shading [23].

The numerical model was developed using the CFD software ANSYS Fluent and all its components: ANSYS Workbench, ANSYS DesignModeler, and ANSYS Meshing [24].

The first step was the generation of the geometry for the studied GTC (Fig. 1). This was performed in SolidWorks and after this, the geometry was imported into Ansys Workbench (Fig. 2a). The next step was to generate the mesh for the computational domain taken into consideration by means of ANSYS Meshing (Fig. 2b).

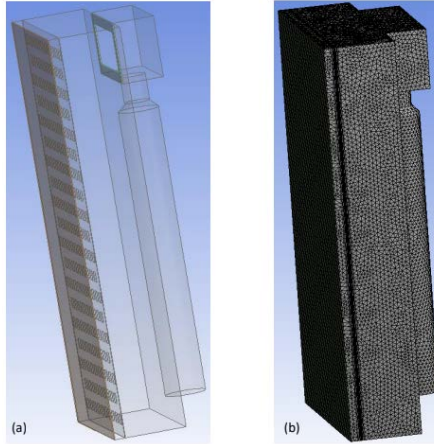


Fig. 1 - Construction of geometry and mesh

As mentioned before, the main objective of this study was to create a discretization that can properly predict the phenomena involving flow and heat transfer within the GTC prototype taken into account, using the lowest possible computational resources and the shortest possible CPU time (mesh independency study). Consequently, in order to determine the proper number of cells for the mesh, several numerical simulations were performed on 6 meshes with 0.87, 1.7, 3.0, 5.83, 9.95, and 16.2 million tetrahedral elements.

Regarding the physical models used within the CFD simulations (steady-state), these were the following:

- airflow modelling: RNG k- ϵ turbulence model with Enhanced Wall Functions for near-wall airflow treatment which can predict with accuracy both the free stream airflow and the airflow through the perforated panel [25];
- radiation modelling: Surface to Surface (S2S) model; solar load was computed using Solar Ray Tracing with an imposed measured Direct Solar Irradiation of 605.7 W/m^2 and Diffuse Solar Irradiation of 150 W/m^2 ; we also used Solar Calculator provided in ANSYS Fluent for the Global Position of the Sun for Bucharest – Romania (where the measurements were carried out).

Finally, the imposed boundary conditions were:

- - air flow through the solar collector: $398 \text{ m}^3/\text{h}$;
- - inlet air temperature: 21.8°C (it is the measured ambient temperature).

3. Results and Discussion

The numerical results are analyzed both from qualitative and quantitative point of view. The quantitative analyze is shown in Table 1, Fig. 3, and Fig. 4.

Table 1
Mean numerical results for the 6 meshes taken into account

Mesh results	Steel plate average temperature (°C)	Air output average temperature (°C)	Air output average velocity (m/s)
0.87 mil	33.87	28.54	3.73
1.7 mil	34.80	28.50	4.29
3 mil	35.04	28.68	3.79
5.83 mil	35.46	28.74	3.71
9.95 mil	35.49	28.68	3.64
16.2 mil	35.65	28.74	3.79

Mesh errors*	Steel plate average temperature (%)	Air output average temperature (%)	Air output average velocity (%)
0.87 mil	4.57	0.52	2.72
1.7 mil	1.96	0.66	17.90
3 mil	1.27	0.01	4.21
5.83 mil	0.08	0.20	2.11
9.95 mil	0.00	0.00	0.00
16.2 mil	-	-	-

* the references taken into account were the values obtained for the finest discretization

Based on values in Table 1, it is observed that there are no notable differences between the 6 meshes, with one exception, the velocity at the output of the collector for the mesh of 1.7 mil.

Fig. 3 describes the longitudinal temperature distribution of the GTC for the 6 meshes. It should be mentioned that, again, there are no clear differences between the results issued from the 6 meshes taken into consideration.

Furthermore, longitudinal velocity contours are shown in Fig. 4, but this time only near the air suction area, which is the most interesting region in terms of air velocity comparisons.

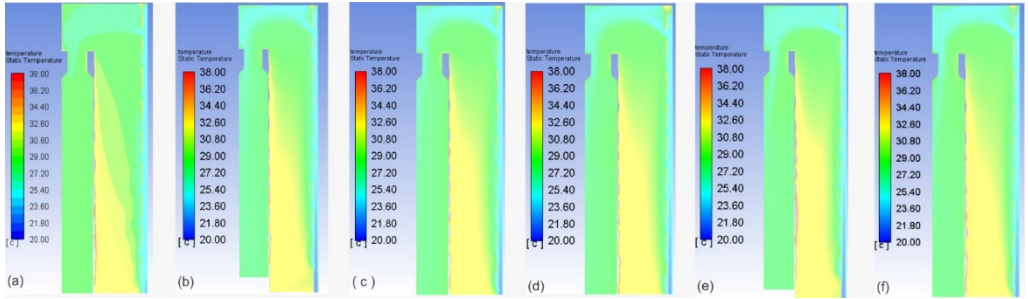


Fig. 3 - Temperature contours
a) 0.87; b) 1.7; c) 3.0; d) 5.83; e) 9.95; f) 16.2 million elements

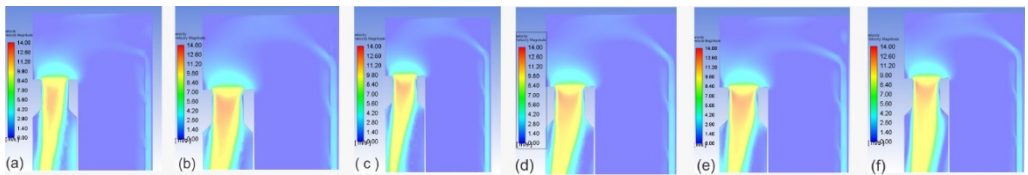


Fig. 4 - Velocity contours
a) 0.87; b) 1.7; c) 3.0; d) 5.83; e) 9.95; f) 16.2 million elements

The graphical representation of air temperature and air velocity in Figs. 3 and 4 showed that 0.87 and 1.7 million elements grids could not properly represent the dynamic of the air through the GTC prototype.

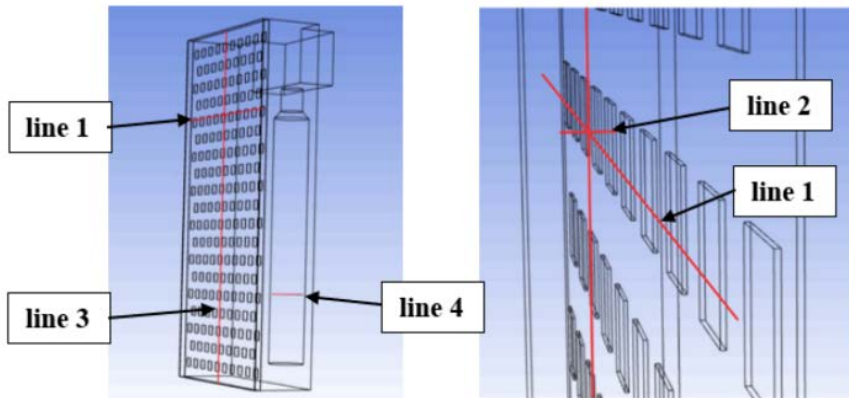


Fig. 5 Position of profiles lines within the GTC prototype

To further investigate, we represented the air velocity and air temperature profiles in various locations within the GTC prototype for the 6 meshes taken into consideration. For this, we extracted the numerical data from the locations depicted in Fig. 5 (4 lines).

Fig. 6 illustrates the qualitative study of air temperature and air velocity profiles that will help us to determine the optimal mesh. It can be seen in Fig. 6a (line 1) that the two coarsest grids (0.87 mil. and 1.7 mil.) are not influenced by the perforated area, while the 3 mil. mesh takes into account only a part of this influence. On the other hand, it can be seen in Fig. 6b (line 2) that the results of the meshes 5.83 mil. and 9.95 mil. almost correspond to the results of the finest mesh of 16.2 mil. For the longitudinal temperature and velocity profiles carried out in the air cavity of the GTC (Fig. 6c – line 3), the same problem as in the first case (line 1) is highlighted for the 0.87 mil, 1.7 mil, and 3 mil. discretizations: their inability to correctly predict the temperature and velocity in the perforated area - characterized by intense heat and mass transfer. The transversal air temperature and air velocity profiles shown in Fig. 6d (line 4 - in the ventilation duct) do not illustrate very well the differences between the 6 meshes taken into account. Therefore, these results can be excluded from the qualitative mesh study.

4. Conclusions

Based on the results achieved, considering both quantitative and qualitative analyses, we concluded that the mesh of 5.83 million elements represents the optimal discretization as it allows reaching grid-independent solutions, with the lowest computational resources and the minimal CPU time.

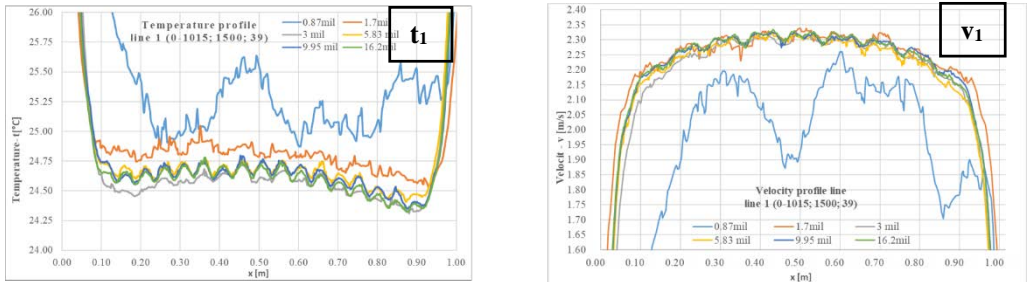


Fig.6a – Temperature and velocity profiles, line 1 ($v_1; t_1$)

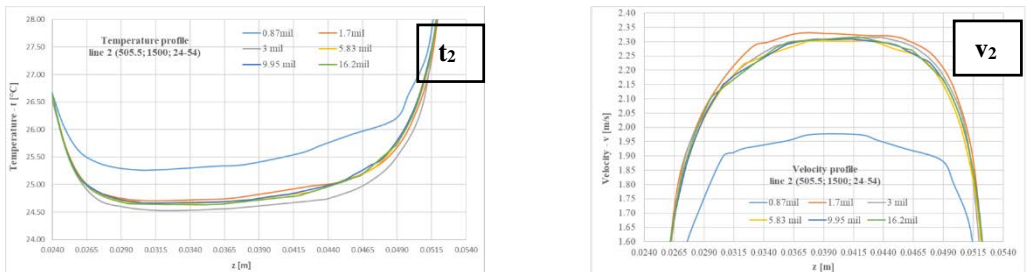


Fig.6b – Temperature and velocity profiles, line 2 ($v_2; t_2$)

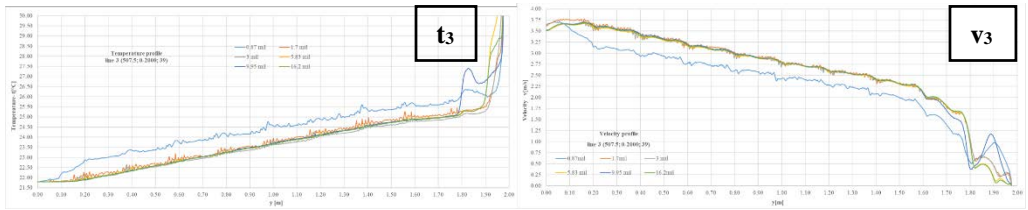


Fig.6c – Temperature and velocity profiles, line 3 (v_3 ; t_3)

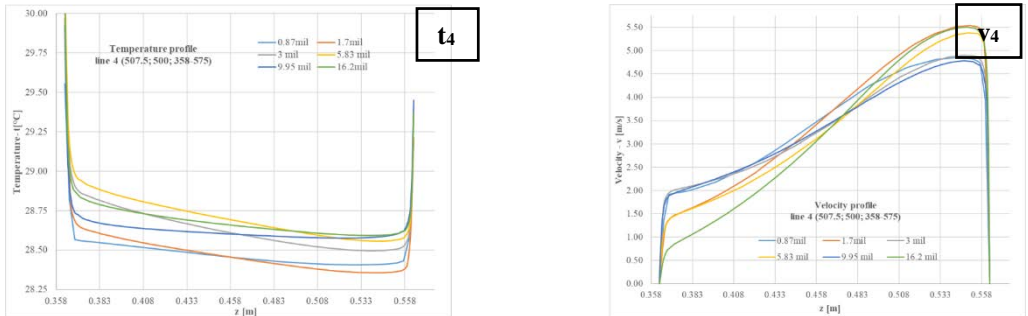


Fig.6d – Temperature and velocity profiles, line 4 (v_4 ; t_4)

Consequently, this grid will be further used in the simulations for the GTC prototype. In addition, this mesh independency study will be followed by the experimental validation of the numerical model, as well as parametric studies concerning the airflow rate through the GTC, the distance between the glass and the perforated plate, and different ambient conditions (air temperature and solar radiation).

Acknowledgments. This work was supported by a grant of the Romanian National Authority for Scientific Research, CNCS – UEFISCDI, project number PN-III-P1-1.2-PCCDI-2017-0391.

REFERENCES

- [1] J. Noailly, “Improving the energy efficiency of buildings: The impact of environmental policy on technological innovation,” *Energy Econ.*, vol. 34(3), pp. 795-806, May 2012.
- [2] <https://www.iea.org>, “Date statistic IEA.org,” webpage, 2019. [Online]. Available: <https://www.iea.org>. [Accessed: 28-May-2020].
- [3] C. E. Ochoa and I. G. Capeluto, “Intelligent facades in hot climates: Energy and comfort strategies for successful application,” in *PLEA 2008 – 25th Conference on Passive and Low Energy Architecture*, Dublin, 22nd to 24th October 2008.
- [4] C. E. Ochoa and I. G. Capeluto, “Strategic decision-making for intelligent buildings: Comparative impact of passive design strategies and active features in a hot climate,” *Build. Environ.*, vol. 43(11), pp. 1829-1839, Nov. 2008.
- [5] C. M. Lai and S. Hokoi, “Solar façades: A review,” *Build. Environ.* vol. 91, pp. 152-165 Sep. 2015,
- [6] X. Wang, B. Lei, H. Bi, and T. Yu, “A simplified method for evaluating thermal performance of unglazed transpired solar collectors under steady state,” *Appl. Therm. Eng.*, vol. 117, pp. 185-192, May

2017.

- [7] C. Brown, E. Perisoglou, R. Hall, and V. Stevenson, "Transpired solar collector installations in Wales and England," in *Energy Procedia*, vol. 48, pp. 18-27, Sep. 2014.
- [8] M. A. Leon and S. Kumar, "Mathematical modeling and thermal performance analysis of unglazed transpired solar collectors" *Sol. Energy*, Vol. 81(1), pp 62-75 Jan. 2007.
- [9] L. H. Gunnewiek, K. G. T. Hollands, and E. Brundrett, "Effect of wind on flow distribution in unglazed transpired-plate collectors," *Sol. Energy*. Vol. 72 (4), pp. 317-325, April 2002.
- [10] M. Belusko, W. Saman, and F. Bruno, "Performance of jet impingement in unglazed air collectors," *Sol. Energy*, 2008. vol. 82 (5), pp 389-398, May 2008.
- [11] H. Y. Chan, J. Zhu, M. H. Ruslan, K. Sopian, and S. Riffat, "Thermal analysis of flat and transpired solar facades," in *Energy Procedia*, vol. 8, pp. 1345-1354, 2014.
- [12] L.X. Gao, H. Bai, S.F. Mao, "Potential application of glazed transpired collectors to space heating in cold climates", *Energy Conversion and Management* Vol. 77, pp. 690-699, Jan. 2014.
- [13] T.T. Zhang, Y.F. Tan, X.D. Zhang, Z.G. Li, "A glazed transpired solar wall system for improving indoor environment of rural buildings in northeast China", *Building and Environ.* vol. 98, pp 158-179, Jan. 2016.
- [14] X.L. Li, C. Li, B.J. Li, "Net heat gain assessment on a glazed transpired solar air collector with slit-like perforations", *Appl. Therm. Eng.* vol. 99, pp. 1-10, 2016.
- [15] W.D. Zheng, B.J. Li, H. Zhang, S.J. You, Y. Li, T.Z. Ye, *Thermal characteristics of a glazed transpired solar collector with perforating corrugated plate in cold regions*, *Energy* vol. 109 pp. 781-790, 2016.
- [16] UEFISCDI: 2018, Intelligent buildings adaptable to the effects of climate change (PN-III-P1-1.2-PCCDI-2017-0391), Executive Unit for Financing Higher Education, Research, Development and Innovation (UEFISCDI), Bucharest, Romania, 2018.
- [17] C. Croitoru, F. Bode, I. Nastase, A. Dogeanu, and A. Meslem, "Innovative solar wall performance study for low energy buildings applications," in *International Multidisciplinary Scientific GeoConference Surveying Geology and Mining Ecology Management, SGEM*, vol. 1(5), 2014.
- [18] C. Croitoru, Nastase I, Bode FI, Meslem A. *Thermodynamic investigation on an innovative unglazed transpired solar collector*. *Solar Energy*, vol. 131, pp. 21–29, 2016.
- [19] A.-S. Bejan, A. Labihi, C.-V. Croitoru, F. Bode, and M. Sandu, "Experimental investigation of the performance of a transpired solar collector acting as a solar wall," in *ISES Solar World Congress 2017 - IEA SHC International Conference on Solar Heating and Cooling for Buildings and Industry 2017*, Proceedings, 2017.
- [20] A.-S. Bejan, F. Bode, C. Teodosiu, C. V. Croitoru, and I. Năstase, "Numerical model of a solar ventilated facade element: Experimental validation, final parameters and results," in *E3S Web of Conferences*, vol. 85, 2016.
- [21] A.-S. Bejan, C. V. Croitoru, and F. Bode, "Preliminary numerical studies conducted for the numerical model of a real transpired solar collector with integrated phase changing materials," in *E3S Web of Conferences*, vol. 111, 2019.
- [22] H. Y. Chan, J. Zhu, and S. Riffat, "Heat transfer analysis of the transpired solar facade," in *Energy Procedia*, vol. 42, pp. 123-132, 2013.
- [23] N. M. Nahar and H. P. Garg, "Free convection and shading due to gap spacing between an absorber plate and the cover glazing in solar energy flat-plate collectors," *Appl. Energy*, vol.7 (1-3), pp. 129-145, Nov. 1980.
- [24] ANSYS, Inc "Fluent 19.0 User Guide".
- [25] F. Bode, A. Meslem, C. Patrascu, and I. Nastase, "Flow and wall shear rate analysis for a cruciform jet impacting on a plate at short distance," *Prog. Comput. Fluid Dyn.*, vol. 20 (3) pp. 169–185, 2020.

INFLUENCE OF SHADING SYSTEMS ON ENERGY PERFORMANCE OF BUILDINGS WITH LARGE GLAZING AREAS

Larisa-Georgiana POPA^{1*}

¹ Arch.PhD, Art&Facts, Suceava

Abstract. *The paper aims at evaluating the energy performance of an average office building characterized by high glazing ratio and various shading degrees. Two hypotheses have been considered and compared: i) the building without shading and ii) the building having a fixed shading system with vertical and horizontal elements. Results show a small increase in heating energy demand of 18,18% because of the blocked heat gains during winter and a significant decrease in cooling energy demand of 80,69%. By using a mobile shading system, the zero energy target can be achieved beginning with the end of March up to the beginning of November (except for one third of July and one third of August).*

Keywords: fixed shading, mobile shading, energy efficiency, office buildings, adaptable envelope.

1. Introduction

Sustainable design is becoming more and more complex due to the need to satisfy increasingly severe requirements related to economic, social and environmental performance - where energy efficiency is essential. Buildings should be closely related to the climate context and the envelope as a moderator between the exterior and the indoor environment is a key element for sustainable design.

An important issue in the case of office buildings is the large glazed façade preferred for both, natural lighting and the idea of openness, as well as to convey a message of transparency and democracy. This leads to overheating during summer and significant heat losses during winter, with high energy consumption for cooling and heating [4]. Studies show that air conditioning systems alone consume 10-60% of the total energy demand for these buildings [7], highlighting an important aspect in terms of energy performance, as they offered solutions to a problem that could be avoided by using efficient shading devices.

The evolution and use of shading elements thus derive from the need to reduce the energy demand of a building [2], the shape of the envelope being designed in order to increase the absorption and reflection of solar radiation by active or passive means. The development of technologies for adaptable envelopes, able to change their characteristics according to the variation of the parameters of the outdoor and indoor environment, is an important step towards optimizing the energy performance of buildings and achieving the nZEB goal, taking into account the global warming.

2. Typology and efficiency of shading systems

In order to reach the green building standard, optimal sun protection is essential to decrease the energy demand for cooling and lighting and therefore to minimize the total energy demand. The glazed surface area and the shading system determine the amount of light that enters the interior space, the cooling energy demand being inversely proportional to the need for artificial lighting [5].

Even though in the Northern Hemisphere the maximum intensity of solar radiation is reached on June 21st and the lowest on December 21st, due to thermal mass, the maximum temperatures are recorded in July and August, and the minimum temperatures in January and February. While a fixed shading system is designed taking into account the geometry and intensity of solar radiation, throughout the year, it proves to be inefficient as it provides the same shading degree in April (when heating is necessary) as in September (when cooling is necessary) [6].

Mobile shading devices can therefore reduce the amount of incident radiation on the glazed surface during the warm season when the sun reaches the maximum altitude and also in autumn when temperatures are high [8]. To draw the geometry of a shading system, graphical or analytical methods can be used [6] in order to reduce the cooling energy demand from mid-spring to autumn, depending on local climatic conditions.

Shading systems can be classified into three formal types: horizontal (Fig. 1), vertical (Fig. 2) and combined (Fig. 3), having considerably different impact on the shading degree [10], as demonstrated by the attached shading masks[3].

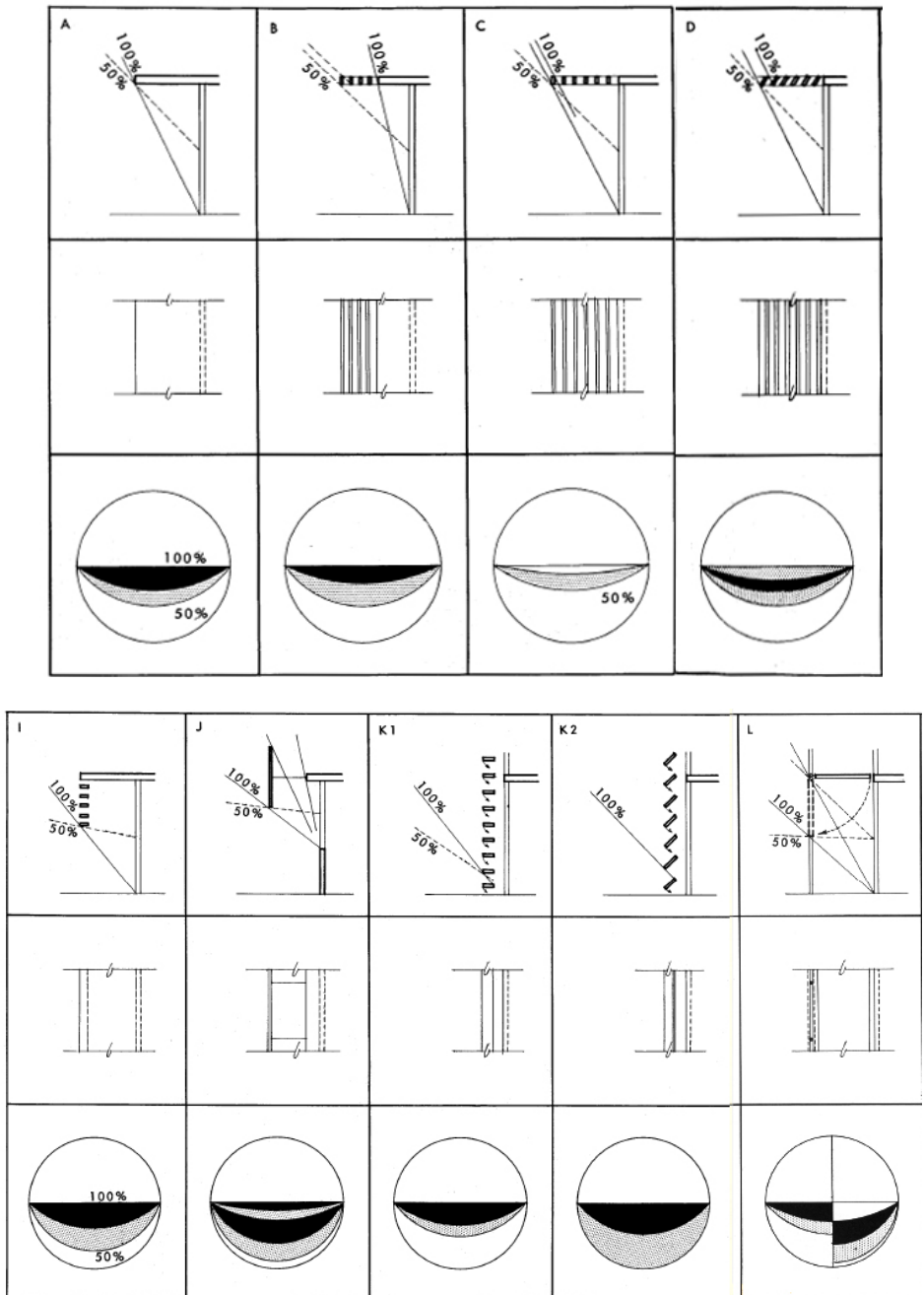


Fig. 1- Shading masks for horizontal shading systems [1]

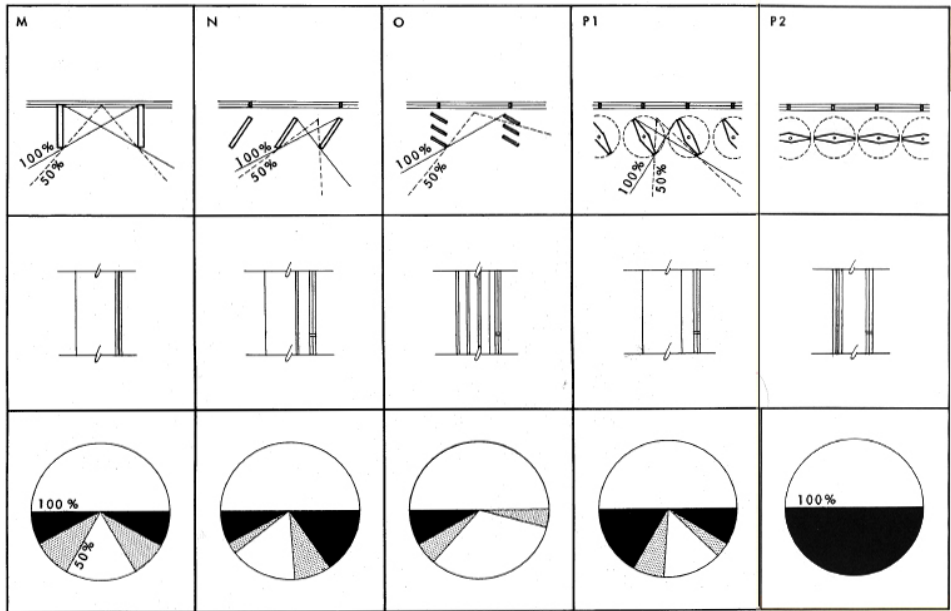


Fig. 2 - Shading masks for vertical shading systems [1]

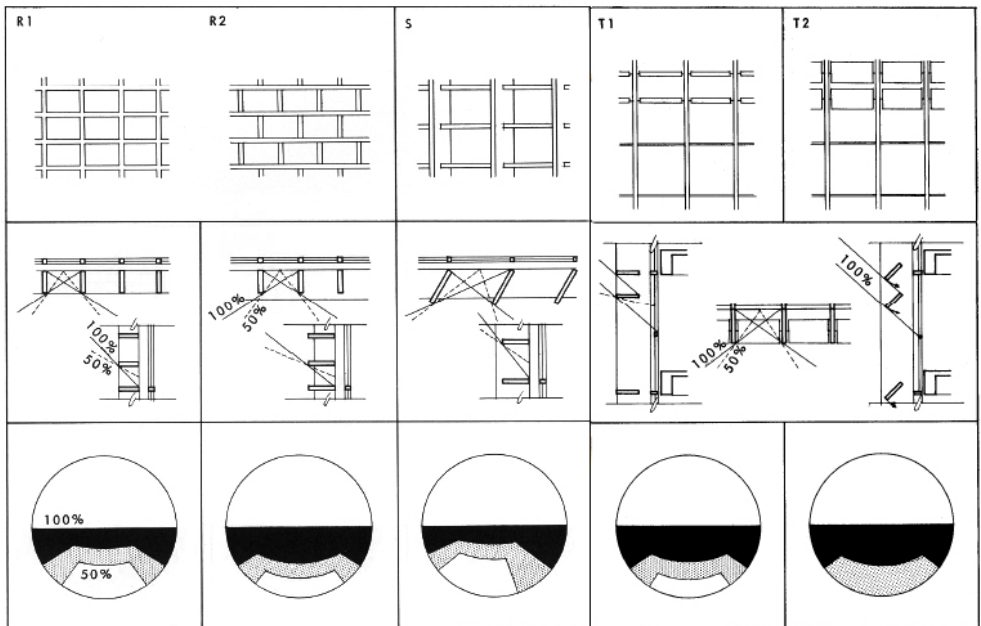


Fig. 3 - Shading masks for combined shading systems [1]

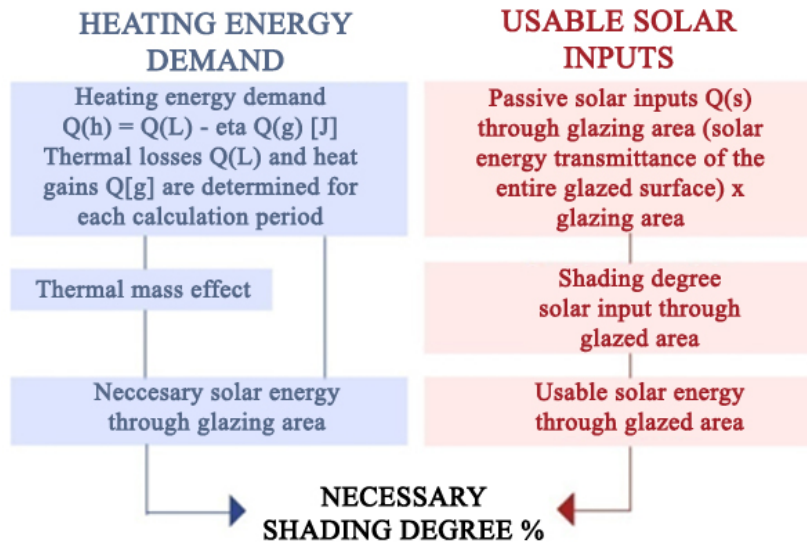


Fig. 4 – Scheme for determining the required degree of shading

Transferred to a solar diagram, the shading criteria define portions of the sky that shading systems must block. The way of determining the required degree of shading is illustrated in Fig. 4. Two solar charts are necessary to illustrate the yearly need for shading due to higher temperatures in the autumn than in the spring.

Unlike fixed shading systems that are designed for shading purposes only, mobile shading systems can also be used to control heat gains, reduce glare and redirect light. Manually operated or mechanized systems offer higher flexibility due to the possibility of retraction or rotation of the elements, which thus meet the conditions of the external environment.

Mobile shading systems have a clear advantage over the fixed ones due to their ability to adapt to a particular climate zone and the requirements of the indoor environment. They can be operated manually or through an automatic system that uses various sensor systems.

3. Case study

In order to determine the contribution of shading systems in optimizing the overall energy efficiency of a building, an office building with large glazing areas on the east, south and west façades was analyzed (Fig. 5) using the PHPP program [12].

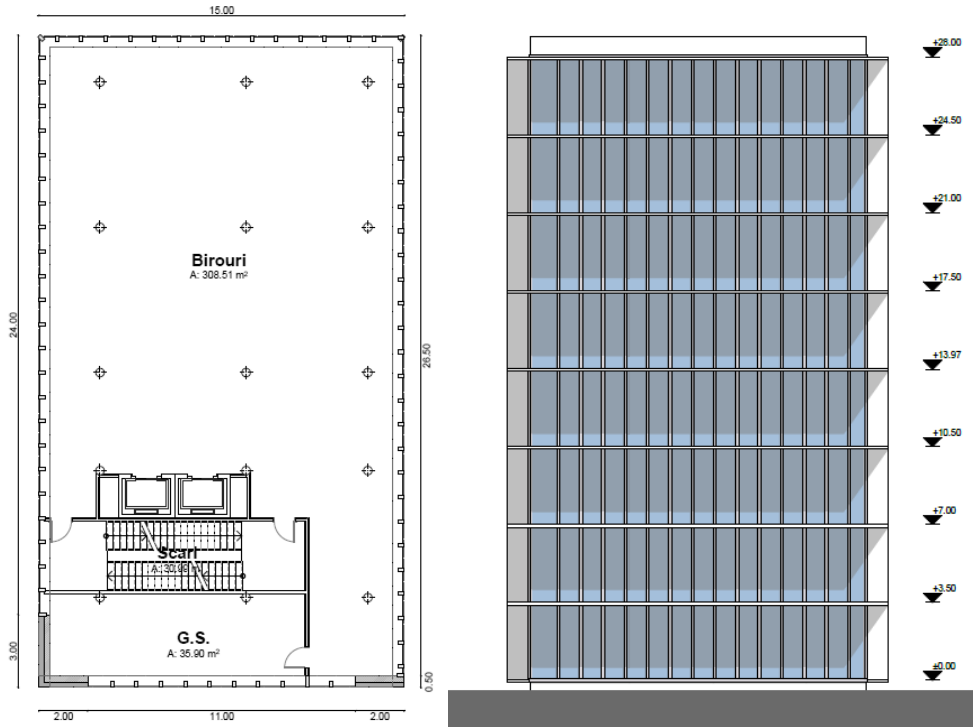


Fig. 5 – Office building – current floor and elevation

Two hypotheses have been evaluated:

- i. the building without shading system;
- ii. the building with a shading system consisting of 2m wide horizontal elements placed at each floor (equivalent to any other horizontal system providing the same shading degree) for the southern façade (Fig. 9) and 1m wide vertical elements placed at 1m from each other (equivalent to any other vertical system providing the same degree of shading) for the eastern and western façades (Fig. 6).
- iii. the shading mask diagram depends on the dimensions, shape in plane and section of the shading elements (Fig. 6), as well as on the cardinal orientation. The efficiency of the shading devices in Fig. 6 and 9 is determined by overlapping the shading mask, the solar diagram and the shading requirement for each previously analyzed façade (Fig. 7, 8 and 10).

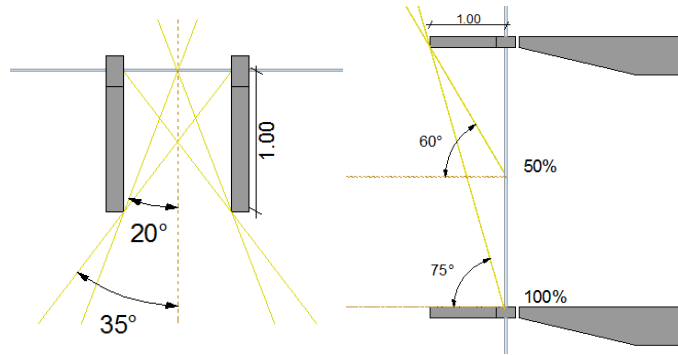


Fig. 6 – Horizontal view and elevation of the elements for shading on western and eastern glazed areas

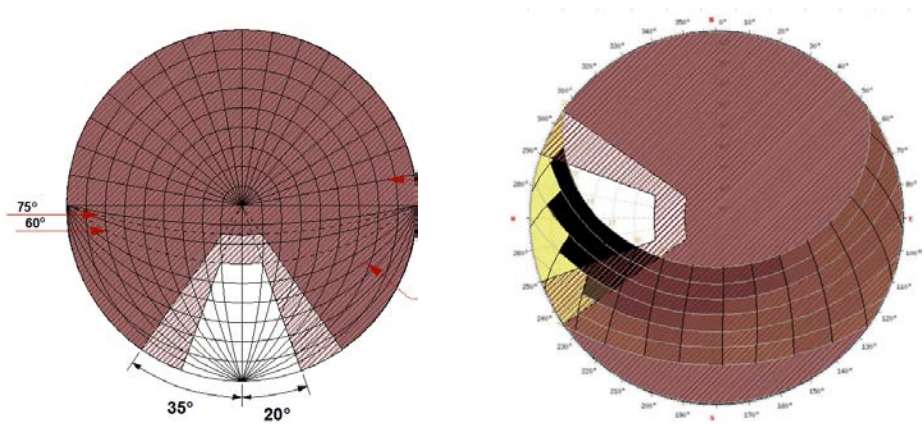


Fig. 7 – Western façade – shading mask overlapping the solar diagram with the shading demand

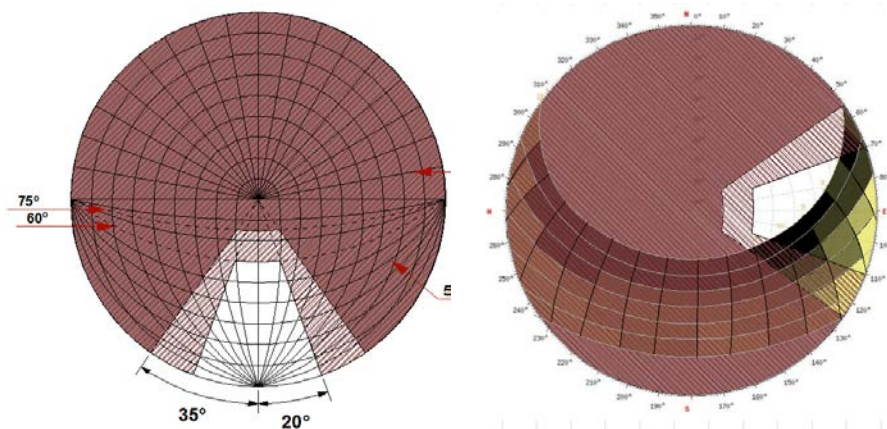


Fig. 8 - Eastern façade – shading mask overlapping the solar diagram with the shading demand

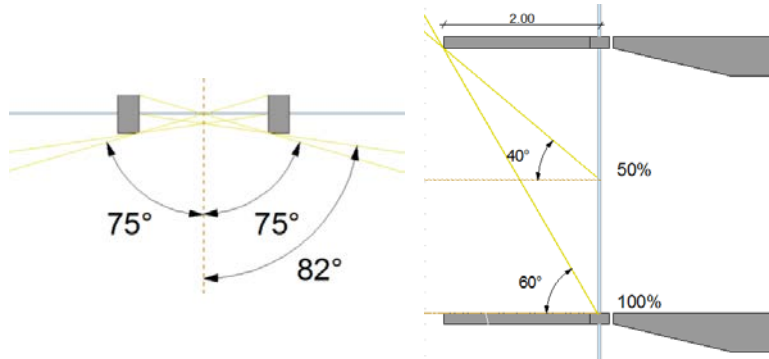


Fig. 9 – Plane and section of shading elements on the southern glazed areas

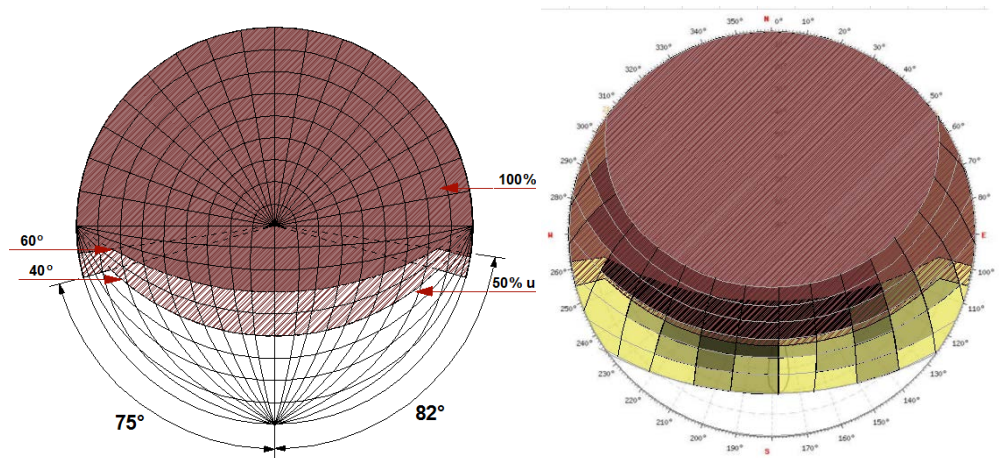


Fig. 10 - Southern façade – shading mask overlapping of solar diagram with the shading demand

For the analyzed office building the shading system can be improved by using inclined vertical elements for the eastern and western façades, which would determine an asymmetrical shading mask and could meet the need for shading, not fulfilled in this case. For the southern façade, the efficiency of the shading system can be optimized by enlarging the compact horizontal console (Fig.9).

The share of the glazed area exposed to direct radiation and the value of solar radiation at glazing level for each shaded façade are shown in Fig. 11.

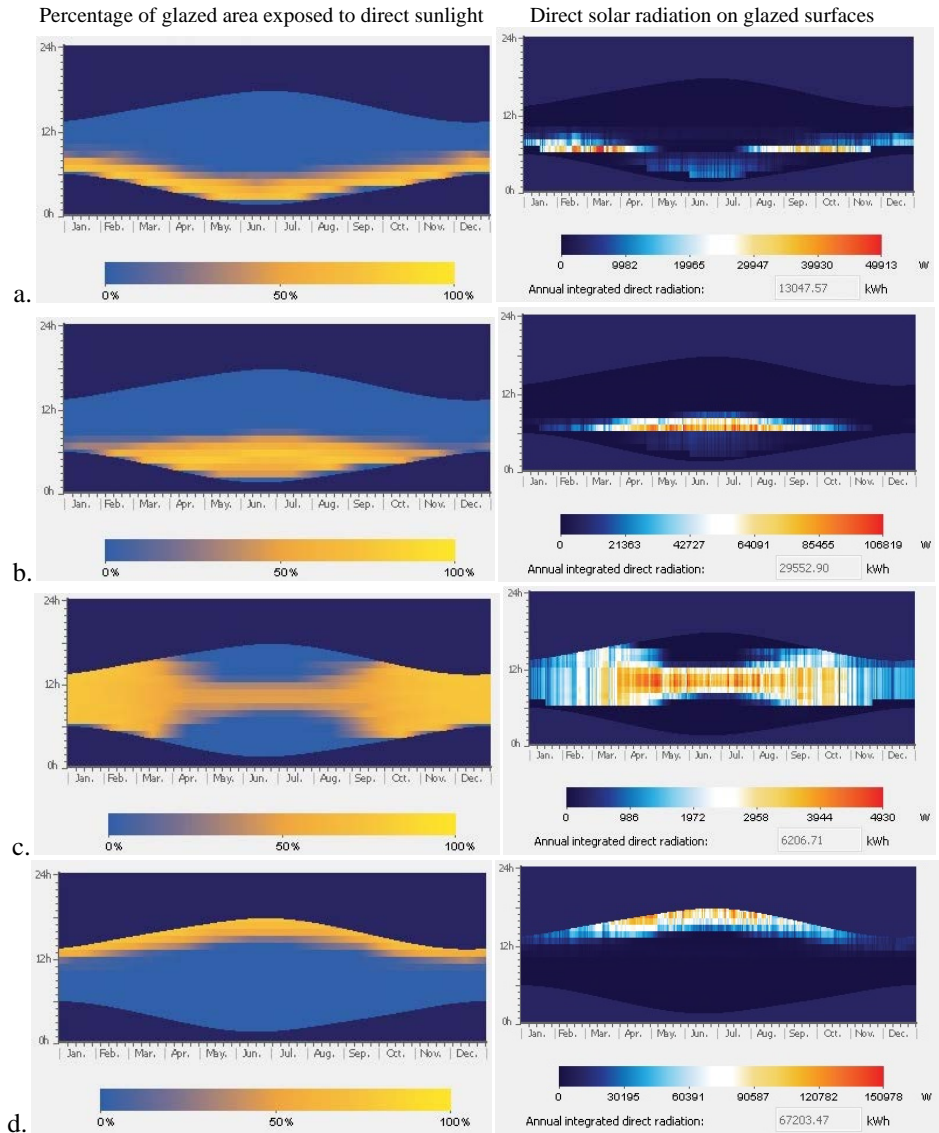


Fig. 11 - Percentage of glazed area exposed to direct radiation and the radiation value for: eastern façade with horizontal (a) and vertical (b) shading system; southern façade with horizontal (c) and vertical (d) shading system

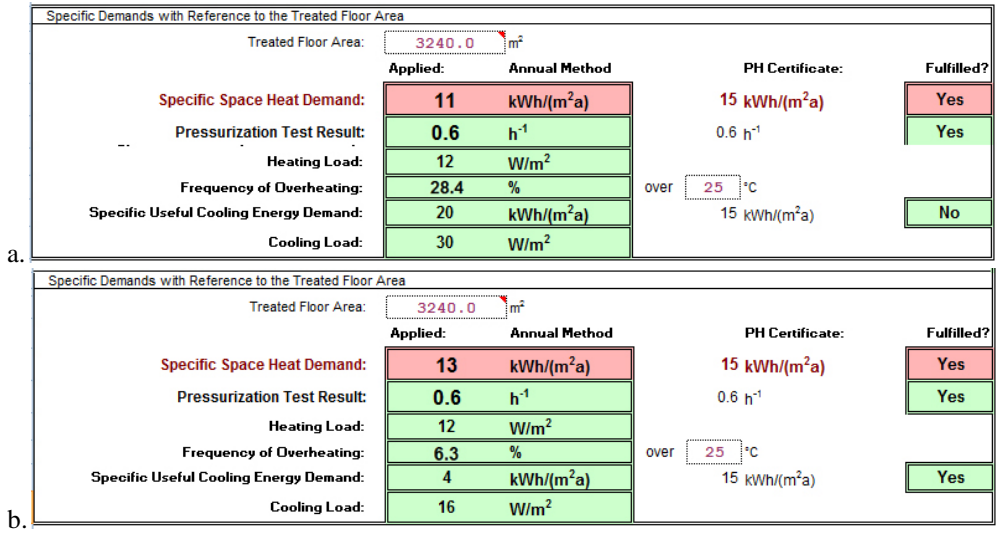


Fig. 12 –PHPP results for the office building: a. without shading system; b. with fixed horizontal shading system

The calculation highlights the increase in heating energy demand from 11 kWh/m²year to 13 kWh/m²year (Fig. 12), as the fixed shading elements block the heat gains during winter (chart Fig. 13). The solar energy use increases from 48% in the first case to 52% in the second case, as the presence of shading elements slightly decreases the heat gains during the summer, from 11 kWh/m²month to 10 kWh/m²month.

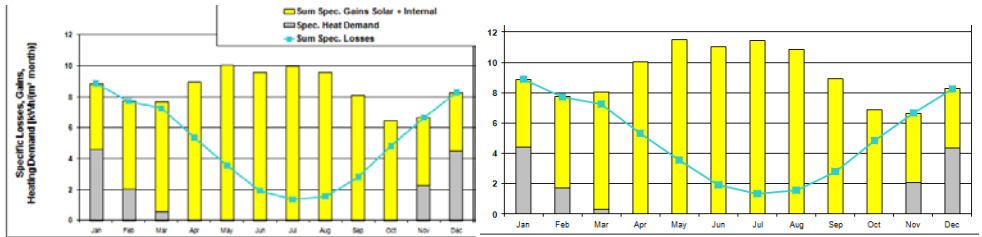


Fig. 13 – Charts of solar inputs and heating energy demand for the office building without shading system and with a horizontal shading system

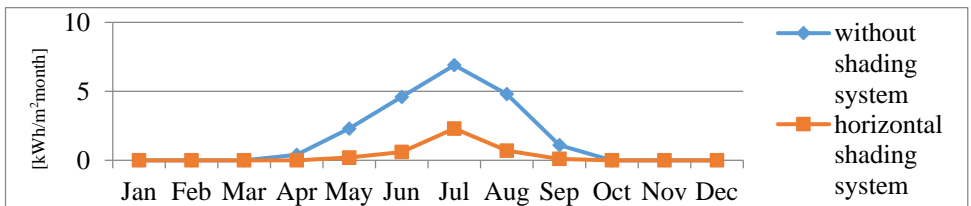


Fig. 14 – Chart of cooling energy demand for the office building without shading system and with a horizontal shading system

Fig. 14 highlights the decrease of the cooling energy demand from 20.2 kWh/m²/year for the building with no shading, to 3.9 kWh/m²/year for the building with horizontal shading system. There is also a reduction to zero for the cooling energy demand in April and a nearly zero cooling energy demand in May (from 2.3 kWh/m²/month to 0.2 kWh/m²/month) and September (from 1.1 kWh/m²/month to 0.1 kWh/m²/month). For July, the month with the highest cooling energy demand, the reduction is of 66.66% due to the shading system (from 6.9 kWh/m²/month to 2.3 kWh/m²/month).

In order to determine the efficiency of the shading systems in terms of yearly heat gains, cooling energy demand and energy performance, the office building was analyzed with the CASAnova program. Fig. 15 shows the results regarding the zero energy hours (time in which no heating or cooling is required to achieve interior comfort) and the energy demand for heating and cooling, for the building with: a. no shading; b. a shading degree of 50% and c. 100% shading degree.

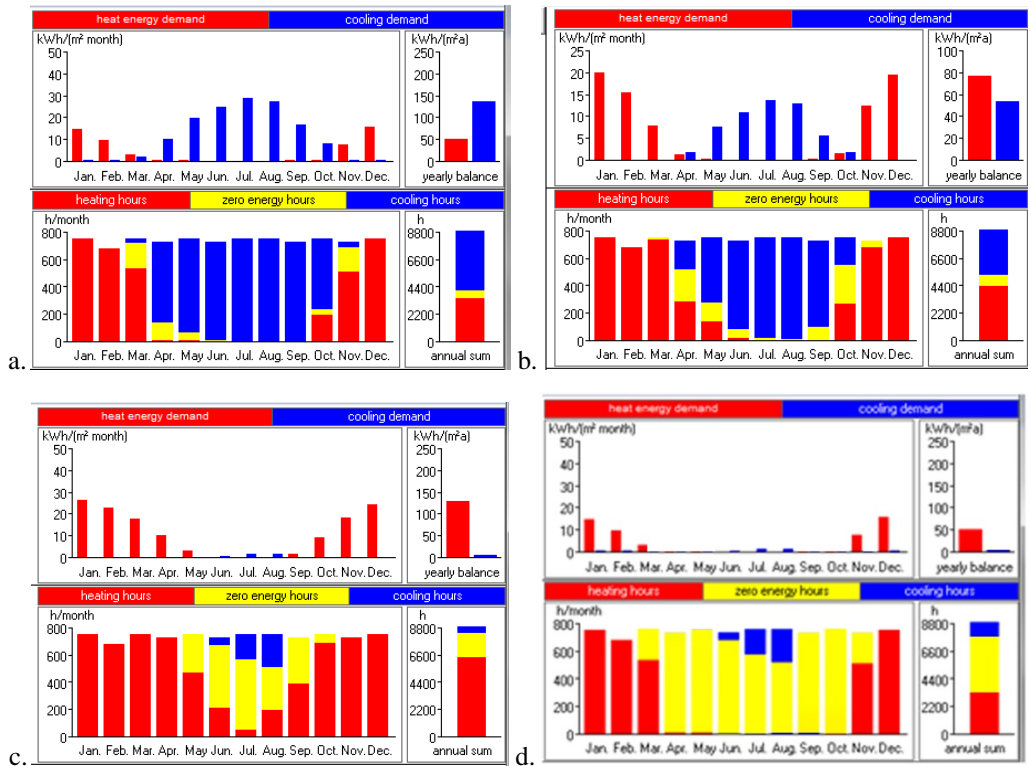


Fig. 15 – Zero energy hours and energy demand for heating and cooling, for the building with: a. 0% ; b. 50% ; c. 100% shading degree; d. increment of zero energy hours by using mobile shading systems

There is a significant increase in the number of zero energy hours by increasing the shading degree, but also an increase in heating energy demand compared to the

cooling energy demand. There are also differences between the cooling and heating energy demand for the months when the sun trajectory is the same. Therefore in April and September when the sun trajectory is similar, excessive shading leads to the need for heating, while in September shading is necessary in the first part of the month to prevent overheating. The charts show the possibility of reaching the zero energy target in the time lapse beginning with the last third of March and ending with the first third of November, by using a mobile shading system that can adjust the shading degree according to the external conditions, except for one third of July and one third of August when the cooling energy demand cannot be reduced to zero.

Fig. 16 indicates the decrease of the maximum cooling load during summer, from 486.3 kW for the building with no shading to 57.4 kW for a 100% shading degree, representing 88.19% reduction. The maximum specific cooling load decreases from 187.6 W/m² to 22.1 W/m².

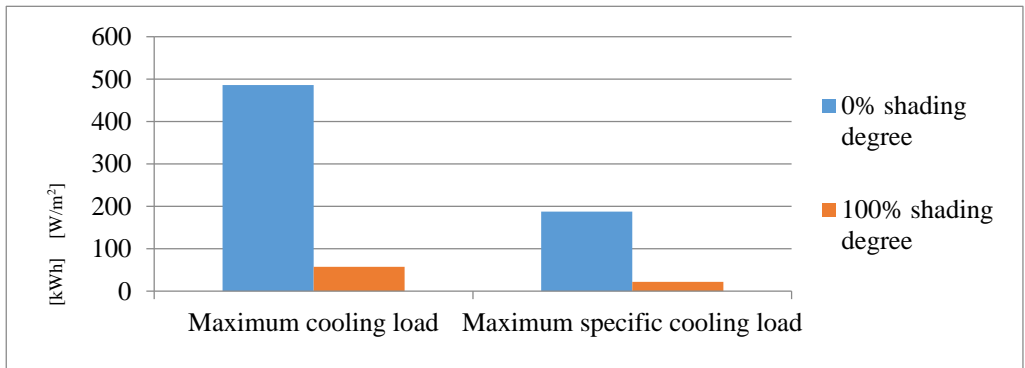


Fig. 16 –The cooling load for the office building with 0% and 100% shading degree

Thus, the exceeding heat flow to be removed from the building and the heat gains are decreasing due to the reduction of solar radiation through the glazed surfaces. Only in June, July and August the cooling energy demand cannot be completely reduced by the use of shading systems, as shown by Fig. 17.

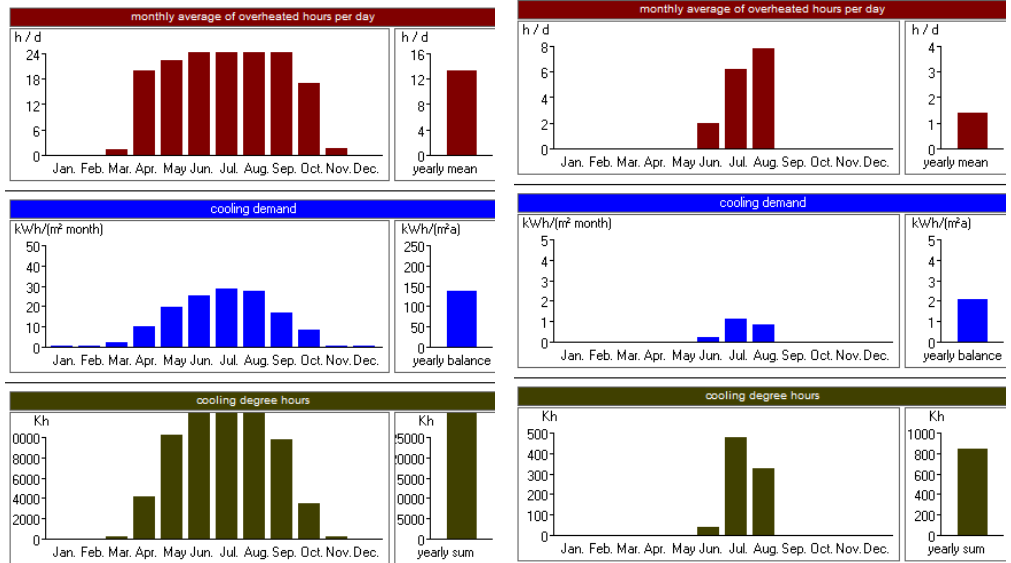


Fig. 17 – Charts of the cooling energy demand and overheating hours for the office building with 0% and 100% shading degree

The use of fixed shading systems increases the heating energy demand by blocking the solar radiation during the cold periods (Fig. 18).

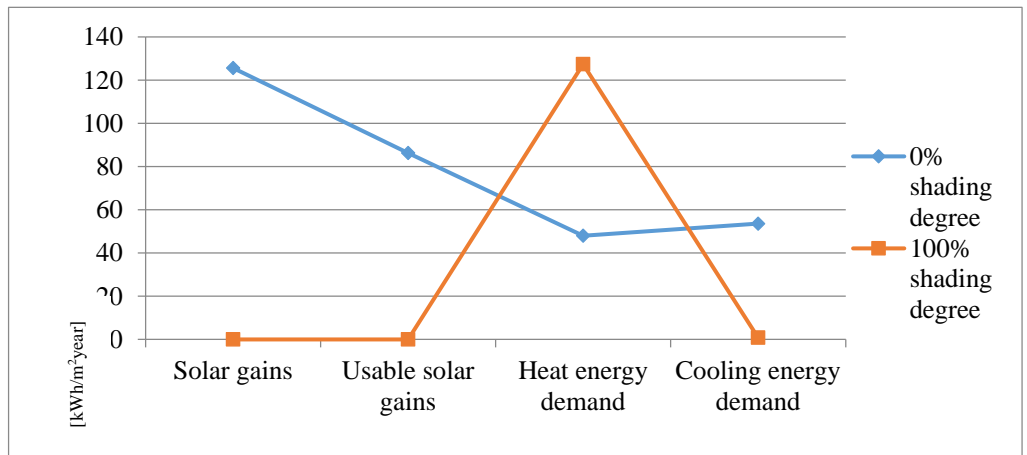


Fig. 18 – Heating and cooling energy demand for the office building with 0% and 100% shading degree

In case of the office building with no shading, the contribution of solar radiation leads to a reduction in heating energy demand and increase in cooling energy demand (Table 1).

Table 1*Variation in heating and cooling energy demand depending on the shading degree*

Shading degree	Heating energy demand	[%]	Cooling energy demand	[%]
0%	48 kW/m ² year	38	133,9 kW/m ² year	100
100%	127,4 kW/m ² year	100	2 kW/m ² year	1,5

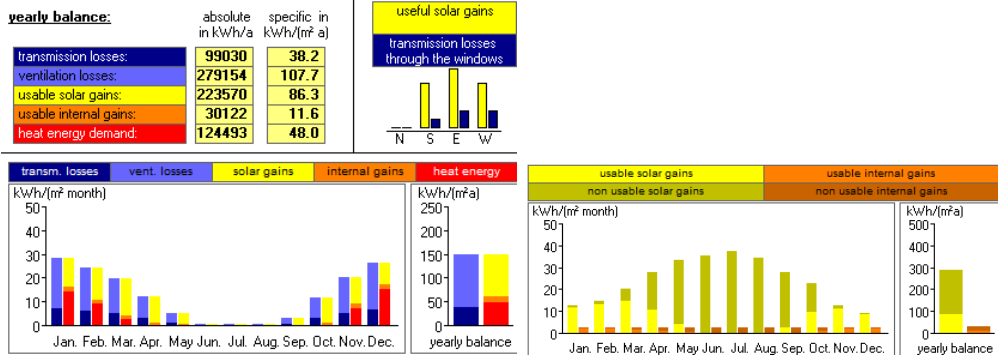
**Fig. 19 – Usable heat gains for the office building with no shading**

Fig. 19 shows the chart of usable heat gains from solar radiation, also highlighting the effectiveness in using mobile shading systems by taking into account the axis of symmetry of the solar trajectory (June 21) and unequal amounts of usable solar energy during the months when the sun trajectory is the same. Capture systems may be incorporated into shading devices in order to exploit unusable solar energy, reducing the total energy consumption of the building from non-renewable resources.

4. Conclusions

The wise choice of the shading system, indispensable for achieving interior comfort in the warm season in buildings with large glazing areas, significantly influences not only the cooling energy demand, but also the heating energy demand. The study carried out on a office building with fixed shading system reveals the following: a significant decrease in cooling energy demand, a slow increase in heating energy demand because of the blocked solar inputs, the potential of a mobile shading system to considerably increment the zero energy hours through adjusting the shading degree and allowing the input of only usable solar energy.

Fixed shading systems were analyzed and evaluated, with their limited performance in terms of meeting the necessary shading degree and the possibility of using solar gains during the cold periods of the year. Although the cooling energy demand decreases through the use of fixed shading systems, the heating energy demand increases.

The mobile shading system, being adjustable, provides the possibility to reach the goal of nearly zero energy demand in the time lapse between the end of March and the beginning of November.

The paper highlights the efficiency of a mobile shading system that can be adapted monthly, compared to a fixed one, on the one hand by avoiding the symmetry of the January-June and July-December periods, and on the other hand, by the possibility of using solar radiation during the cold season and also to block it in the warm season.

A shading system self-adjusting on a daily basis would be more efficient, as it avoids the daily symmetrical values of the shading degree determined by the symmetrical trajectory of the sun (as shown in the shading diagrams). It also offers the possibility to increase the shading degree during the afternoon and to adapt itself to daily outdoor conditions (for example, in a cloudy summer day the shade should not be as high as in a sunny day).

REFERENCES

- [1] A. Olgyay and V. Olgyay, *Solar Control and Shading Devices*, Oxford University Press, London, 1957
- [2] B.A. Limanowski, *Implementation of Window Shading Models into Dynamic Whole-Building Simulation*, Ontario, Canada, 2008
- [3] C. Brown, *Shading Masks and Fenestration Design*, ARCH 140, Architecture 140 Energy and Environmental Management College of Environmental Design, UC Berkeley, 2015
- [4] E. Lee, S. Selkowitz, V. Bazjanac, V. Inkarojrit and C. Kohler, *High-performance Commercial Building Facades*, University of California, Berkley, 2002
- [5] G. Cellai, C. Carletti, F. Sciurpi and S. Secchi, *Transparent Building Envelope: Windows and Shading Devices Typologies for Energy Efficiency Refurbishments*, Building Refurbishment for Energy Performance. A Global Approach, Springer International Publishing, Switzerland, 2014
- [6] L.G. Popa, *Envelope Optimization for Energy-efficient Office Buildings*, Ph.D. dissertation, Department Civil Engineering, Technical University of Cluj-Napoca, 2018
- [7] M. Adam, *The Influence of the solar shading devices on the energy consumed for the office buildings cooling process*, 12th International Multidisciplinary Scientific GeoConference, www.sgem.org, SGEM2012 Conference Proceedings/ ISSN 1314-2704, June 17-23, 2012, Vol. 4, 437 - 444 pp
- [8] M. Hutchins, *High Performance dynamic Shading Solutions for Energy Efficiency and Comfort in Buildings*, Sonnergy Limited, United Kingdom, 2015
- [9] U. Knaack, K. Tillmann, *The Future Envelope 2: Architecture, Climate, Skin*, IOS Press, Amsterdam, Netherlands, 2009
- [10] V. Olgyay, *Design with Climate: Bioclimatic Approach to Architectural Regionalism*, New and Expanded Edition, Princeton University Press, London, 2015
- [11] <http://www.designbuild-network.com/features/featureclimate-control-intelligent-facades/>
- [12] PHPP (Passive House Planning Package)

EXPERIMENTAL STUDY OF THE IMPACT OF AIR PURIFIERS ON THE INDOOR AIR QUALITY INSIDE OF AN APARTMENT

Tiberiu CATALINA^{1,*} and Alexandra-Elena FERARU^{1,2}

¹Technical University of Civil Engineering, Faculty of Building Services Bucharest, Romania

²DAIKIN Central Europe-Romania

Abstract. *The use of air purifiers to filter polluted or contaminated air, seems an interesting solution nowadays. Using an extensive experimental approach, a commercial air purifier was tested under real conditions in-situ. The IAQ was measured in two rooms: living room and bedroom for different air change rates of the air volume. Measurements of PM_{2.5}, PM₁₀, relative humidity, air temperature and sound pressure level were made. It was found that the PM_{2.5} levels are quickly reduced from 20.64 µg/m³ and decreased to 5.58 µg/m³. The research was also focused on the noise levels measurements and it was noticed that in Silent to Low mode (60 and 150 m³/h) the sound pressure levels are under 30 dB. Overall, the use of air purifiers in homes is recommended nowadays.*

Keywords: Air purifier, Purification technology, Experimental measurements, Relative Humidity, Sound pressure measurements, Fine particulate matter, Indoor air, Dust exposure.

1. Introduction

Several plans are made when it comes to reducing the exposure degree to countless factors of biological origin or non-biological. The evolution of air filters brings effective measures and air filtration starts being an important component of environmental control measures. Based on the studies of World Health Organisation, known as “the promoter of health”, we now know that air pollution is the cause of over six million deaths a year and a very important factor when it comes to allergies. Throughout our lives, we spend most of our time indoors, but this doesn’t mean we’re safe from pollution – a mixture of particulate matter (PM) and volatile organic compounds (VOC), make the air inside our homes to be up to five times more polluted than outside. Our homes contain a mix of airborne particles from mould, cleaning products, dust mites, cosmetics and gases from cooking and heating – and as we know, breathing in these pollutants has been linked to serious health conditions, like asthma, other pulmonary diseases and even more serious problems like lung cancer [1]. One of the things people can do to ameliorate the air condition in their homes, is to keep it well ventilated – especially when cooking and cleaning. Dust is a combination of fine particles from both

indoors and outdoors [2], that can be generated from a variety of different sources and processes. Recent studies aim to highlight the impact of ventilation systems and air purifiers on IAQ. An unplanned controlled test evaluated the efficiency of air filters and classic split units for air conditioning in 126 necessitous houses of children with asthma. IAQ was experimentally measured during four seasons. When indoor air quality was monitored, filters reduced PM levels in the child's bedroom by an average of 50% , levels that could be reduced only by using filters [3]. Giving the fact that children are exposed frequently to airborne particles and various pollutants, an experimental action was conducted in several sports arenas in Barcelona). The indoor and outdoor measurements of particle amount and PM concentrations, were fulfilled, as well as indoor measurements of CO₂ and NO₂ levels. The study admits that using air purifiers and keeping windows closed (meaning natural ventilation), can lead to an important reduction when it comes to indoor-to-outdoor accumulation ratios. In the space the indoor-to-outdoor concentrations decreased to 93-95% in the matter of particle number and PM₁₋₁₀, respectively; while in the bigger sport arena, the equivalent reductions were 70% and 84% [4]. Another study of air purifiers, was made to prove the benefits of a HEPA filter in reducing allergic respiratory manifestations. The subjects were 32 patients with never ending rhinitis and asthma symptoms, mostly occurring during winter and fall season, and who were also positive skin tested to house dust or mite extract. The experiment was made with an ENVIRACAIRE air purifier, placed in the bedroom for eight weeks. Randomly, the active filter was used for four weeks, and the following four, a blank one, as a placebo. With the HEPA filter, there was a 70% reduction in the matter of particle number, of 0.3 µm in size. As a conclusion, the study revealed that patients responded positively to the active filter benefits and the overall opinion is that HEPA filters can reduce the symptoms of allergic diseases [5]. In the late years, studies showed that because of fog's and clouded weather growth, pollution increased, which brings suffering to people and affects their health and also social and business life. According to the government of China's environmental communication, cities begun monitoring PM_{2.5} and observed that few reached the standard and almost half of the year, air quality got to 52% of the standard, Beijing being an example. Also, another important noticed fact, was the heavy pollution and the numbers showed 16.2% of days. One more study was made over a six-month period, to record the efficacy of air filters.

The study contained three parts: active air cleaners, placebo air cleaners mixed with allergen-impermeable mattress covers and active air cleaners mixed with allergen-impermeable mattress covers. Allergen proportions in mattress and floor dust were measured before the intervention, and after the three and six months of the experiment. At the end of the six months, the air cleaners were disassembled and the filters showed that substantial amounts of dust and allergens were caught, more precisely, HEPA filtered 70% of 0.3-µm particles and 95% of 1.0-µm particles and the Rota filter, captured small dust particles, at high speed function [6]. Another experiment was held in three elementary schools located in the same district area in the United States, the

main focus being on the indoor pollutants and the level of their concentrations. The measurements took place between October 2013-June 2014. For the three schools, there were 21 classrooms and active air cleaners with HEPA filters were installed in half of the rooms. For the rest of the classrooms, the author chose cleaners with no HEPA filters and no air flow [7]. Measurements took place in three steps, the first taking place before placing the purifiers. A total of 63 samples were collected, on Teflon filters placed inside specimen boxes. Simultaneously, daily outdoor air pollution concentrations were measured at the on the rooftop of the Countway Library at Harvard Medical School. PM_{2.5} particles were collected using a specimen box containing a personal exposure monitor. The first period of measurements took place during cold weather months and it was found that the air in the classrooms with active purifiers across all three schools had lower levels of PM_{2.5} than those classrooms that had no filters. Next period of measurements, which corresponded to warmer months, the air in the classrooms with active purifiers across all three schools had lower levels of PM_{2.5} than the classrooms with no filters. Another study took place in Iran and the main concern were street cleaners, which are mostly exposed to dust inhalation, conducting to respiratory diseases and airway difficulties. The purpose was to evaluate the multiple pulmonary symptoms of 84 cleaners, with other not exposed of individuals, meaning 80 office workers. For each of the participants, pulmonary symptoms were assessed by using an equipment called spirometer. The results showed that the exposed group presented respiratory symptoms higher than in the reference group. Cough was the main issue reported by the exposed group (81%), compared to the other participants (16.3%). Providing street cleaners respiratory protection instruments and also a periodic spirometry, could be an efficient solution in preventing pulmonary damage [8]. The mineral dust of the Sahara desert, may be a serious health threat. Lately, particular interest has been accorded to mineral dust particles, that could lead to real health issues.

The PM deriving from Saharian dust are responsible to multiple causes of mortality and morbidity. The impact of dust is appearing and sufficiently powerful, therefore it requires further study [9]. As found from these previous papers, the use of air purifier to reduce PM levels, seems an appealing solution. In this paper, a home air purifier is analysed to check its impact on indoor air quality and on the overall indoor environment in an apartment.

4. Experimental campaign

The perfect environment for doing a research study on the impact of an air purifier, was to study in-situ and an occupied apartment was the ideal testing situation. The apartment is located in Bucharest, Romania and it is part of a block of apartments of 10 floors. The building has double exposure, one to Pantelimon Boulevard and the second one to a backyard. During the year 2010 the building was thermally rehabilitated, and the old windows replaced along with the closure of the balconies, with double glazing windows. The Pantelimon Boulevard is a source of pollution among which it is mentioned NO_x,

dust particles, noise, etc. In figure 1 it is illustrated a schematic drawing of the apartment and the position of the air purifier, during the two experimental campaigns.

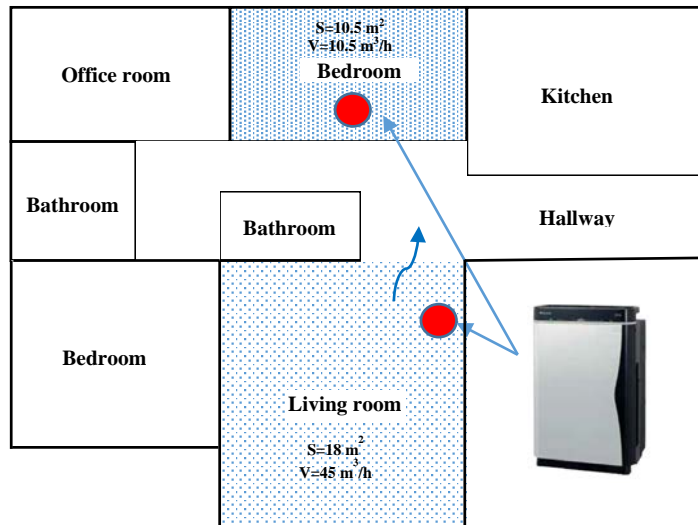


Fig. 1 – Schematic drawing of the campaign used during the experimental tests and the position of measurements

The research was conducted with a home air purifier from Daikin, model URURU, that is designed to remove gaseous air pollutants or convert them to harmless by-products. The air purifier has multiple modes: humidification and air purification. The streamer technology, which decomposes odours and allergens, creates an extensive plasma emission inside the equipment, that allows substantial number of electrons to be generated, thus producing a large oxidative effect. Bacteria and viruses are completely eliminated by the titanium apatite and then eliminated by the photocatalyst. The specifications of the analysed air purifier are listed in Table 1.

The highest air flow rate of the URURU system is $450 \text{ m}^3/\text{h}$ being capable of an air change rate of up to 9 ach for a 20 sqm room, while the minimum is 1.1 ach. The manufacturer specifies also the maximum sound equivalent pressure level, that for the silent mode ($60 \text{ m}^3/\text{h}$) is 17 dB(A) while for the Turbo mode ($450 \text{ m}^3/\text{h}$) can reach up to 50 dB(A). URURU is also capable of humidification of the indoor air with an input of maximum 600 ml/h . The experimental measurements were realized with TESTO 480 for air and relative humidity, with DYLOS 1100 PRO for dust particle measurements and with SVAN 979 class 1 precision sound meter, for sound pressure measurements.

Table 1
Air purifier specifications

Type	Specification
Weight	11
Air flow rate Turbo/H/M/L/Silent	450/330/240/150/60 m ³ /h
Humidifying operation Turbo/H/M/L/Silent	450/330/240/150/120 m ³ /h
Sound pressure level – Air purifier mode Turbo/H/M/L/Silent	50/43/36/26/17 dBA
Sound pressure level – Humidifier mode Turbo/H/M/L/Silent	50/43/36/26/23 dBA
Power input Air purifier Turbo/H/M/L/Silent	0.081/0.035/0.018/0.011/0.008 kW
Power input Humidifier mode Turbo/H/M/L/Silent	0.084/0.037/0.02/0.013/0.012 kW
Humidifier mode Turbo/H/M/L/Silent	600/470/370/290/240 ml/h
Water tank capacity	4.0 litres
Air filter	Polypropylene net with catechin
Dust collecting method	Plasma ionizer/Electrostatic dust collection filter
Dimensions (Height x Width x Depth)	590/395/268 mm

3. Results

As we can see from the measurements made with the air purifier in the living room, the results show the evolution of ambient air quality. At the beginning of measurements, the PM_{2.5} concentration in the living room, showed 20.64 µg/m³ units and a decrease to 5.58 µg/m³ units within 1 hour of system operating at High level and Humidification function ON (330 m³/h or 7.33 ach). The next step was to set the system to stage 2 (Low level – 150 m³/h or 3.33 ach) with humidification mode ON, which maintained the PM_{2.5} under 11 µg/m³, being considered a good ambient air quality. The results were even better during stage 3 and Humidification function OFF, PM_{2.5} reaching the lowest value of 4.2 µg/m³. At the end of the experimental measurements the system was turned on Silent mode (max. 60 m³/h) and the PM_{2.5} average values were found in the range 8 to 13.3 µg/m³. The larger particles PM₁₀ followed the same pattern presented previously, with a maximum value at the beginning of 2.01 µg/m³ and a lower value of 0.1 µg/m³. The air purifier's discharge temperature varied from 24.4 °C during the humidification function, to 25.9 °C. Measurements were taken also for the relative humidity at the exhaust air and interesting information was found. After 1 hour of functioning in Turbo mode and Humidification, the relative humidity increased from 60% to a maximum value of 67.5%, while during the Silent Mode (Stage 1) and no humidification, the humidity stabilized at 57.5%.

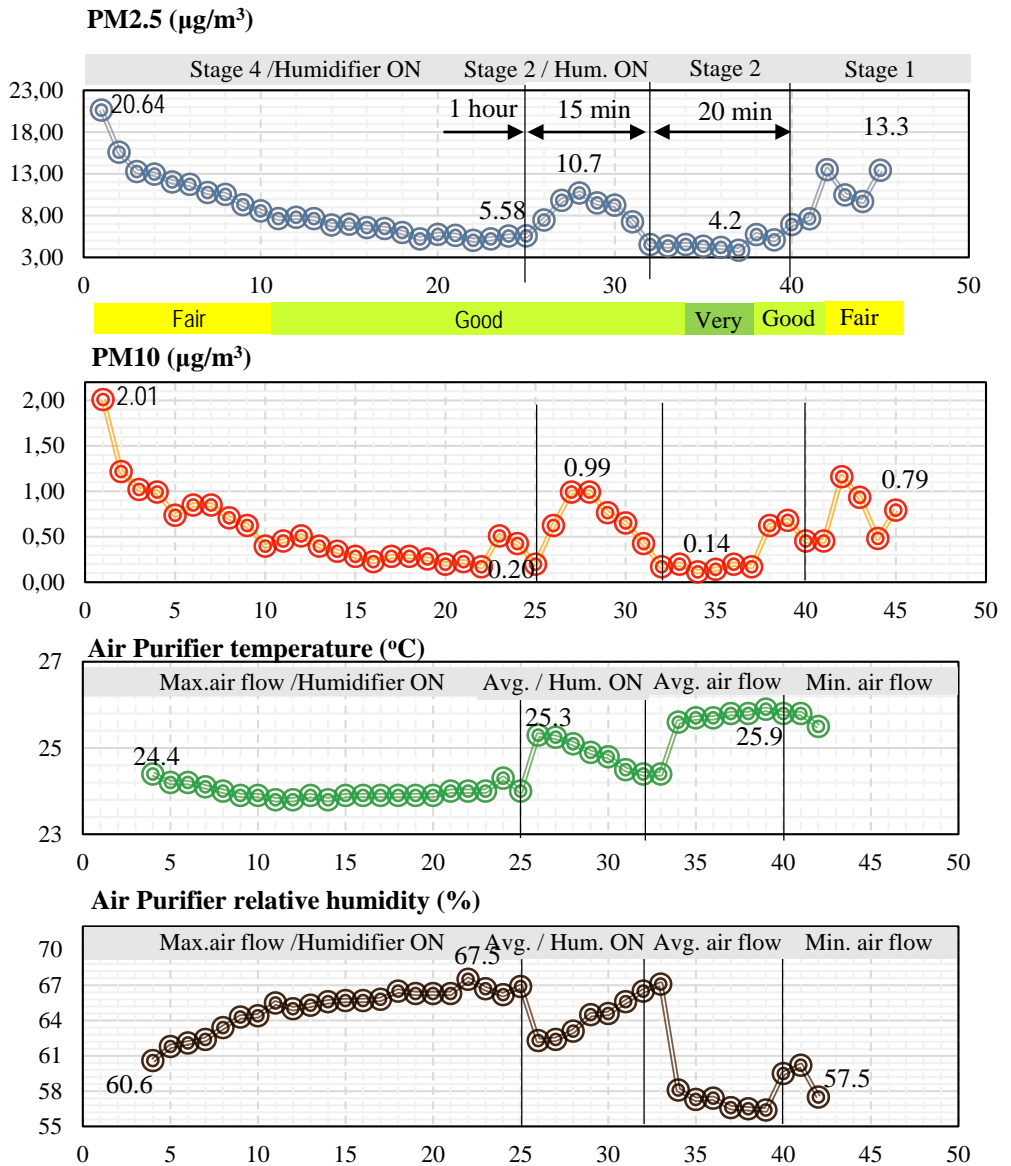


Fig. 2 – PM2.5, PM10, Purifier temperature and relative humidity variations during different stages in the living room

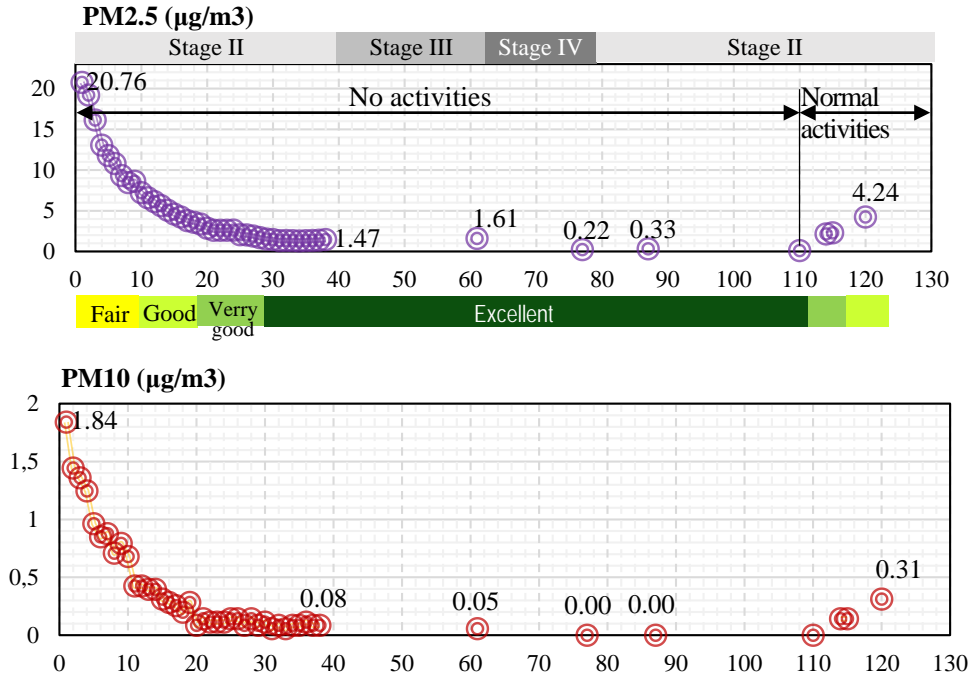


Fig. 3 – PM2.5, PM10 variations during different stages in the bedroom

On the other hand, in the bedroom ($V=27.5\text{m}^3$) the efficiency of the system was even higher, as the PM2.5 decreased in less than 40 minutes from $20.76 \mu\text{g}/\text{m}^3$ to $1.47 \mu\text{g}/\text{m}^3$ for $150 \text{ m}^3/\text{h}$ (5.7 ach) and even more, during stage 4 (High – $330 \text{ m}^3/\text{h}$ or 12.6 ach). However, during normal occupants activities in the room, the PM2.5 slightly increased to $4.24 \mu\text{g}/\text{m}^3$ still being situated in the “green”, zone of good air quality. It is a clear evidence that the system performs better in lower volumes enclosed rooms.

As we spend more than 8 hours/day in the bedroom it is also mandatory to have as well, a good acoustic comfort. The measurements took place in the bedroom during night time, in order to have lowest background noise. It can be observed from Table 2 that for 1000 Hz the sound pressure level is only 9.8 dB, a very low value, confirming that the measurements were correctly executed. Using the sound meter SVAN 979, the air purifier noise level was measured for different stages (1 to 5 / Silent to Turbo). During the Silent mode, the air purifier only slightly increased the noise level in the bedroom and even in Low mode ($150 \text{ m}^3/\text{h}$), the sound levels are still under 30 dB considered an acceptable value for sleeping areas. However, the system is not recommended to be used during night-time in Medium to Turbo mode, as the acoustic comfort is no longer fulfilled.

Table 2
Noise measurements in dB for 1 octave frequency range

Type	Frequency (Hz)							
	31.5	63	125	250	500	1K	2K	4K
Background noise	0.76	5.70	8.37	13.30	10.75	9.88	12.58	14.43
Silent	1.49	4.53	9.87	14.88	12.57	10.93	12.86	14.32
Low	2.13	5.89	17.17	24.30	27.04	26.32	20.73	17.50
Medium	3.68	8.03	24.64	31.20	37.09	38.91	33.22	28.35
High	6.06	12.77	31.63	37.26	44.76	45.47	43.89	37.44
Turbo	11.71	19.26	39.39	44.35	51.49	53.53	50.70	48.49

Figure 4 illustrates the global sound equivalent pressure level, expressed in a single value, measured in dB(A) that corresponds the best to human hearing system. As expected, the air purifier greatly increases the noise level during the Turbo mode with values reaching up to 58 dB(A), but remaining acoustical comfortable in Silent and Low modes.

It can be noticed that for the range of frequencies 31.5 Hz to 250 Hz even in Medium mode (240 m³/h) the sound pressure levels are under 30 dB while for the Turbo mode (450 m³/h) from 125 Hz the maximum sound pressure admissible level are no longer respected. However, the results demonstrates that even with 60 m³/h to 150 m³/h the indoor air is cleaned sufficiently and the noise levels are low.

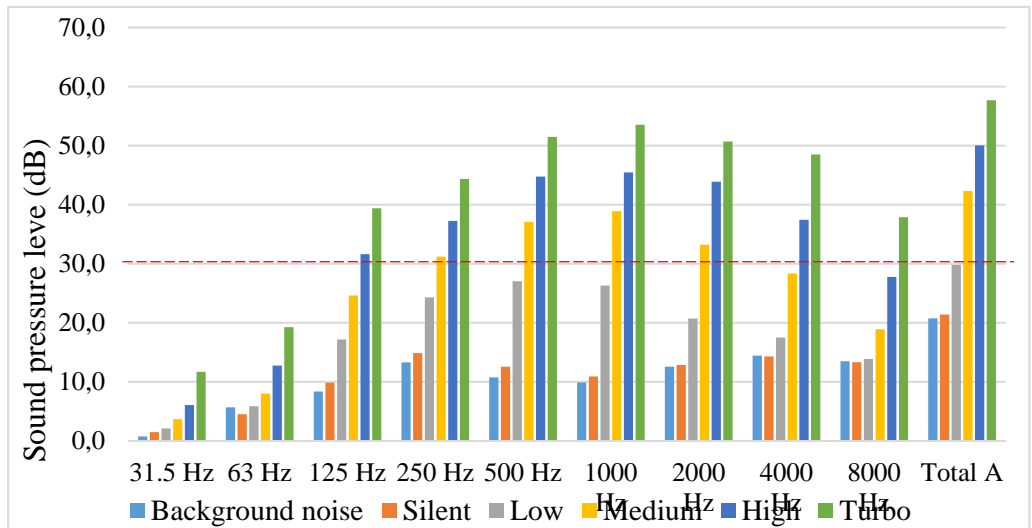


Fig. 4 – Sound pressure levels measured.

4. Conclusions

Taking into consideration that tests were made in-situ, with a commercial air purifier, measurements showed that in the living room, the air purifier reduced considerably the amount of present dust particles PM_{2.5} within 1 hour of system functioning. PM₁₀ was also reduced, proofing its capacity to filter small or large particles. For the humidification process it was found that the system can rapidly increase humidity of up to 10% in maximum 1 hour, therefore it is safe to state that has a good capability of moisturizing the air. One remarkable conclusion of the measurements conducted in the bedroom, is that for smaller volume spaces, the air purifier performs best, as the PM_{2.5} and PM₁₀ reached lowest possible values ($<0.1 \mu\text{g}/\text{m}^3$). As acoustic comfort is an important parameter when dealing with HVAC (Heating Ventilation Air Conditioning) systems, a series of sound pressure measurements were conducted for different air flows streams.

REFERENCES

- [1] V.K. Vijayan, H. Paramesh, S.S. Salvi, A. A. K. Dalal, “Enhancing indoor air quality –The air filter advantage”, Lung India, vol. 32, Oct. 2015
- [2] Z. Deng, Z. Zhang, *Performance Test and Structural Analysis of Indoor Air Purifier*, Chemical Engineering Transactions, Vol. 71, 2018
- [3] L. Jia-ying, C. Zhao, G. Jia-jun, F. Zi-jun, L. Xiao, S. Bao-quig, *Efficacy of air purifier therapy in allergic rhinitis*, Asian Pacific Journal of Allergy and Immunology, Vol. 36, Dec.2018
- [4] A.Pacitto, F. Amato, T.Moreno, M. Pandolfi, A.Fonseca, M. Mazaheri, L. Stabile, G. Buonnanno, X. Querol, “Effect of ventilation strategies and air purifiers on the children’s exposure to airborne particles and gaseous pollutants in school gyms,” Science of the Total Environment, vol. 712, Apr. 2020.
- [5] E.E.. Reisman, P.M. Mauriello, G.B. Davis, J.W. Georgitis, J.M. DeMasi, “A Double-Blind Study of the Effectiveness of a High-Efficiency Particulate Air (HEPA) Filter in the Treatment of Patients With Perennial Allergic Rhinitis and Asthma,” J Allergy Clin Immunol., vol. 85, Jun.1990
- [6] Y. Wang, H. Wang, C. Zhao, Y. Zhang, *Research Progress of Air Purifier Principles and Material Technologies*, Advanced Materials Research, Vol. 1092-1093, pp. 1025-1028, 2015
- [7] A. Smythe, *Effectiveness of Particle Air Purifiers in Improving the Air Quality in Classrooms in Three Urban Public Schools in the Northeastern United States*, Harvard, 2018.
- [8] Malays J Med Sci, *Effects of Dust Exposure on the Respiratory Health Symptoms and Pulmonary Functions of Street Sweepers*, Zahedan University of Medical Sciences,2018.
- [9] M Kotsyfakis, S G. Zarogainnis, E Patelarou, *The health impact of Saharan dust exposure*, Czech Academy of Sciences , Hellenic Mediterranean University , University of Thessaly, 2019.

BUILDING ENERGY MODELING OF A STUDENTS' RESIDENCE IN TIMIȘOARA

Ioan Silviu DOBOȘI^{1*}, Ștefan DUNĂ¹ and Cristina TĂNASĂ¹

¹Politehnica University Timisoara

Abstract. *It is well known by now that buildings have a key role towards the reduction of energy consumption from fossil fuels and decarbonization of EU. However, currently there is little knowledge about energy demand from the higher education sector. Addressing energy efficiency in buildings of higher education institutions emissions is particularly important. This paper presents the case study of a student residence, which is currently under construction in Timisoara, Romania. The building has highly energy efficient envelope and ventilation with heat recovery. The study is focused on assessing the energy consumption and indoor environmental conditions of the building by means of energy modelling and hourly simulation. The building consumes in total 132.55 kWh/m²year, which is below the maximum limit for class A of energy efficiency in Romania.*

Keywords: energy efficiency, building energy modelling, hourly simulation, interior comfort.

1. Introduction

It is well known already that buildings account for approximately 36% of the greenhouse gas emissions in the European Union. Therefore, the concern related to the energy consumption of buildings has become widespread and resulted in all kind of measures to reduce building's impact on the environment. Various studies show that the highest potential for reducing energy consumption from fossil fuels and the related greenhouse gas emission (GHG) lies in the building sector [1]. Therefore, improving buildings from the energy performance perspective is crucial towards achieving the European Union long term goal of reducing greenhouse gas emissions with 80-95% by 2050 compared the levels in 1990 [2]. New buildings designed and constructed in the present have a great energy efficiency and optimisation potential. Addressing energy efficiency in buildings of higher education institutions emissions is particularly important. In a study made by Petidis et al [3], several scenarios for reducing the energy consumption of a students' residence were investigated and led to energy savings of about 36%. The study concluded that energy saving measures should be focused on the thermal insulation of the building envelope, use of efficient lighting and appliances and

reduce energy waste [3]. The use of simulation models for building energy is suitable for both the design of energy-efficient buildings and the design of renovation solutions for existing building stocks and allows a precise and detailed calculation of the building energy requirements for providing a comfortable and healthy indoor environment under the influence of external factors. This paper presents the energy modeling and simulation results for a students' residence. The main goal of this study is to assess the energy use of the students' residence and validate the energy performance of the building envelope in combination with the designed HVAC system.

2. Case study building

2.1. Architectural and functional characteristics

The building subjected to analysis is a new student residence, currently under construction, located in the city of Timisoara, south-west Romania. From architectural perspective, we can see the building has quite an interesting layout, with the horizontal plan presented in the situation plan in Fig.1.



Fig. 1 – Site location and orientation of the building



Fig. 2 – Architectural renderings

In Fig.2 are presented the architectural renderings of the building. The building has a total of 9 levels, including the basement and top withdrawn floor. From a functional point of view, in the basement there are technical spaces and parking lots. The ground floor contains administrative offices, technical spaces and spaces for commercial activities. On floors from 1 to 6, there are 222 student accommodation rooms, each equipped with 3 beds, except one room per each floor, which is equipped with only 2 beds and arranged for students with disabilities. The top floor is composed of a study room and a gym, which provide optimum conditions to the students for individual learning and recreation. Also, on the top floor there are technical spaces where the building equipment are placed. The building facades are composed of two main types of exterior walls, presented in Fig .3. The walls of the top floor consist in masonry walls with 10 cm layer of insulation. The floors that are in contact with the outdoor environment (terraces, floor above ground level) are also insulated with at least 20 cm thickness of thermal insulation. Table 1 presents the thermal transfer resistance of the envelope elements, as they were used in the simulation.

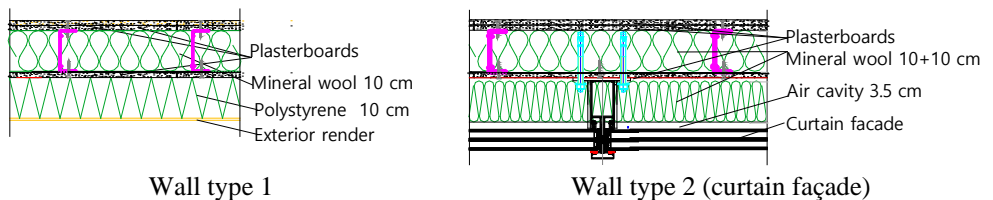


Fig. 3 – Main types of exterior walls

Table 1

Thermal transfer characteristics of the envelope elements

Envelope element	Thermal transfer resistance [$\text{m}^2\text{K/W}$]
<i>Exterior walls type 1</i>	<i>5.94</i>
<i>Exterior walls type 2</i>	<i>6.16</i>
<i>Exterior walls top floor</i>	<i>4.63</i>
<i>6th Floor Terrace</i>	<i>5.23</i>
<i>Top floor terrace</i>	<i>5.65</i>
<i>Floor above ground level</i>	<i>5.77</i>
<i>Windows (triple glazed and aluminium frame)</i>	<i>1.25</i>

2.2. HVAC system

The building is equipped with a complex system for heating, cooling and ventilation. The heating plant consists in a 1440 kW boiler, while the cooling plant is a chiller that has a thermal power of 1200 kW. The building is heated/cooled by using 4 pipe fan coil

units installed in the ceiling. Fresh air is provided by means of mechanical ventilation with the help of an air handling unit, equipped with heating and cooling coils and heat recovery with a minimum efficiency of 50%. The air handling unit only serves the spaces from 1st Floor to the top floor. The distribution of fresh air is developed horizontally for each level. The connection between the air handling unit and the horizontal distribution on each floor is made by means of two air columns. Each room is connected independently to the main distribution channels. The fresh air is supplied in rooms and the exhaust air is extracted from bathrooms. The air transfer between bedrooms and bathrooms will be made through transfer grids preferably placed in doors. The mechanical ventilation system assures a slight pressurization of the entire buildings. Domestic hot water is provided with the help of the heating boiler and solar collectors placed on the roof terrace. The solar collectors are with vacuum tubes, mounted with an angle of inclination of minimum 25° between horizontal and panel.

3. Building energy modelling using VABI Elements

Building energy modelling is the computational simulation, performed to estimate and evaluate the energy consumption of a building. A building energy model is created in a simulation tool and represents the most effective way of predicting consumption of energy of a building in the design phase [4]. The energy performance of a building can be analyzed by means of steady-state or dynamic simulation. Depending on the type of simulation and used software, the volume of input data and complexity and accuracy of the results might vary significantly. The process of whole building energy modelling (BEM) for dynamic energy simulations is a complex activity that requires detailed information related to the building envelope, systems and operation. The study presented in this paper is based on a complex energy modelling of the students' residence by using Vabi Elements tool. The building simulation module in Vabi Elements simulates hourly energy flows and temperatures for a whole year, presenting results and visualizations of the building's performance. The calculation is based on the selected building characteristics such as climate, HVAC systems, internal heat gains and the properties of the building materials. The software calculates hourly temperatures and the heating and cooling energy use of the building.

3.1. Modelling building envelope and thermal zones

This study aims at determining the energy use associated to student accommodation and facilities, therefore the basement and the ground floors were not considered in the calculation. However, the ground floor was introduced in the building energy model in order to properly assess the heat transfer between the first floor and ground floor. To create the building energy model, division of the building into thermal zones was the first step. Not to confuse a thermal zone with a geometrical zone. A thermal zone is the space inside the building that is characterized by the same set-point temperature and ventilation requirements and has negligible temperature variation between rooms. A

thermal zone can be composed from multiple rooms of the building. The studied building was divided into several types of thermal zones on each floor as follows: bedrooms, bathrooms, kitchen, laundry room and corridors. In Figure 4 is presented the thermal zoning pattern of floors from 1 to 6. Each zone is coloured differently, depending on the type of thermal zones. For rooms, there are thermal zones that include 14 rooms, 4 rooms, 6 rooms and 3 rooms. Similarly for bathrooms. The whole corridor area was considered as a single thermal zone, as well as the kitchen and dressing room. The top floor is divided into four thermal zones: study room, gym, corridors and technical spaces. Figure 5 presents a perspective of the building energy model geometry.

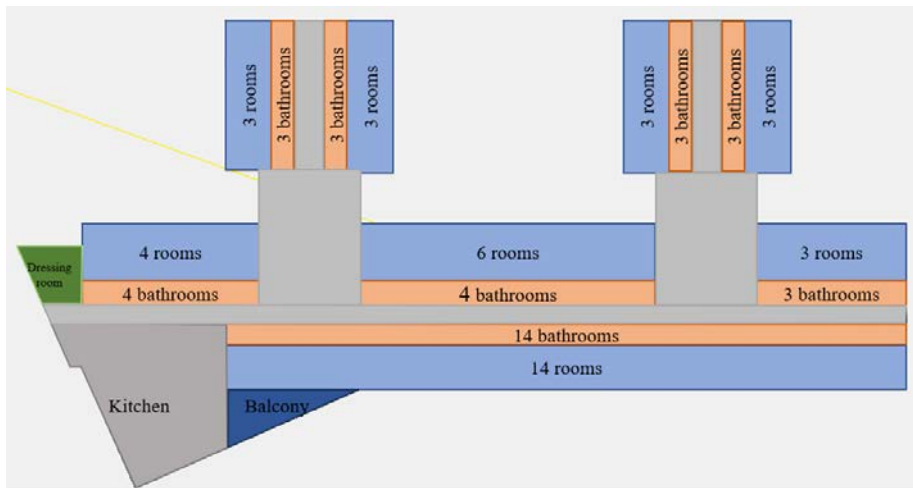


Fig. 4 – Thermal zoning of the building

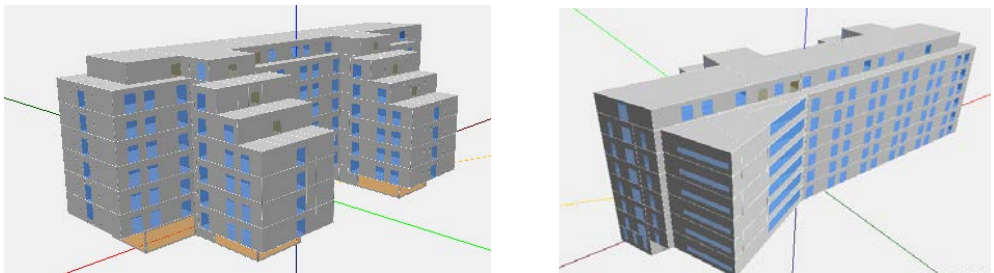


Fig. 5 – Energy model – geometry

3.2. Occupancy and lighting schedules

Internal heat gain is divided into gains associated to the building occupants and heat gains coming from the lighting system. Schedules of use are linked to the internal heat production of people and lighting. The building has a total of 222 rooms, out of which 216 rooms have 3 beds and 6 rooms have 2 beds, accommodating a total number of 658

students. Thus, for each thermal zone, depending on the number of rooms included, the corresponding number of people was defined. The rooms' occupancy schedules were defined hourly, as fraction of the total number of inhabitants and is presented in Fig. 6. Similarly, the schedules were defined for the other thermal zones: kitchen, corridors, study room and gym.

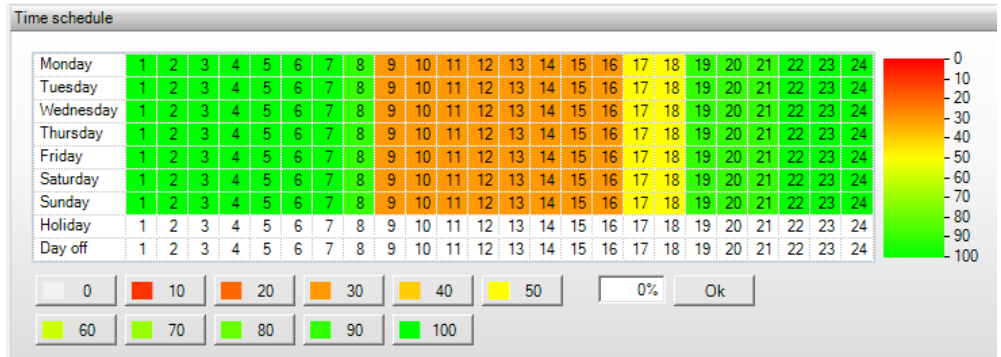


Fig. 6 – Rooms occupancy schedules

A major part of the energy consumed by the interior lighting in the building becomes a heat gain and influences the building energy balance. In order to define as accurate as possible the internal loads associated to interior lighting, hourly use schedules were defined for each thermal zone, as fraction of the maximum lighting power. The data for lighting was defined separately for each thermal zone, depending on the lighting requirement established based on the room activity [5]. The rooms lighting schedules used in the building energy simulation are presented in Figure 7.

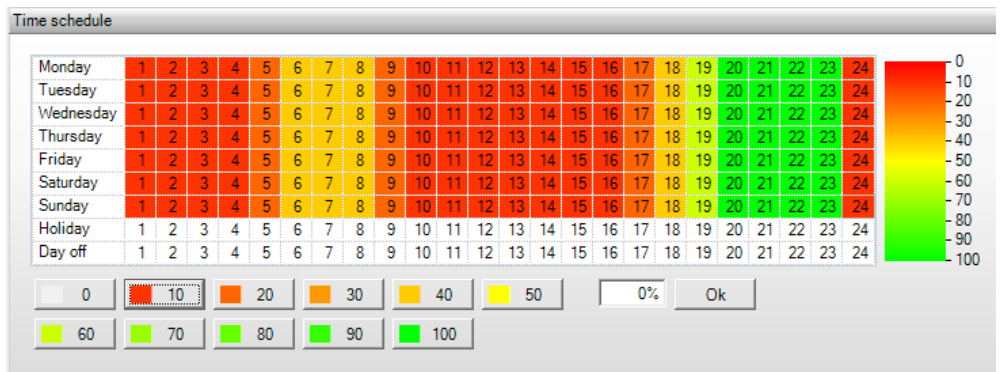


Fig. 7 – Rooms lighting schedules

In the occupancy and lighting schedules, we distinguish the days of the week, and the holidays. Being a students' residence, the holidays include the summer vacation and the

winter holiday. Thus, the simulation does not include the period from July until the end of September and the last two weeks of December.

3.3. Heating, cooling and ventilation

In order to assess the energy consumption of the building, interior air temperature was defined as control parameter for each thermal zone. The design temperature differs depending on the room destination and were defined in accordance with the Romanian standards [6]. Table 2 presents the heating and cooling temperature set-points for each type of thermal zone and the ventilation flow rate, extracted from the design project. The simulation was performed considering continuous operation of the HVAC system.

Table 2
Use requirements for heating, cooling and ventilation

Room type	Heating temperature [°C]	Cooling temperature [°C]	Ventilation flow rate [m ³ /h]
<i>Bedroom</i>	22	25	90
<i>Bathroom</i>	24	25	90
<i>Laundry</i>	20	25	160
<i>Study room</i>	22	25	1800
<i>Gym</i>	18	25	560
<i>Corridors</i>	20	25	1000

The building energy model accounts for air infiltration of exterior building enclosure area. The number of air changes due to infiltration rate was set to 0.20 h⁻¹ for thermal zones in contact with outdoor air. The air handling unit, boiler and chiller characteristics were defined using the parameters from the technical documents of each equipment.

3.4. Weather data

In addition to data relating to the building operating state, accurate weather data is required to suit the response of the building to external simulation conditions. The building is located in Timișoara and corresponds to climate zone II in accordance with Romanian regulations [7]. The weather data used in this study was provided by ASHRAE IWEC2 (International Weather for Energy Calculations). The IWEC2 weather files contain 'typical' year hourly weather data for Timișoara which can be used in building energy simulation programs [8]. Figure Fig. 8 show the graphs for air temperature hourly variation, with a maximum of 34°C and a minimum of -12°C.

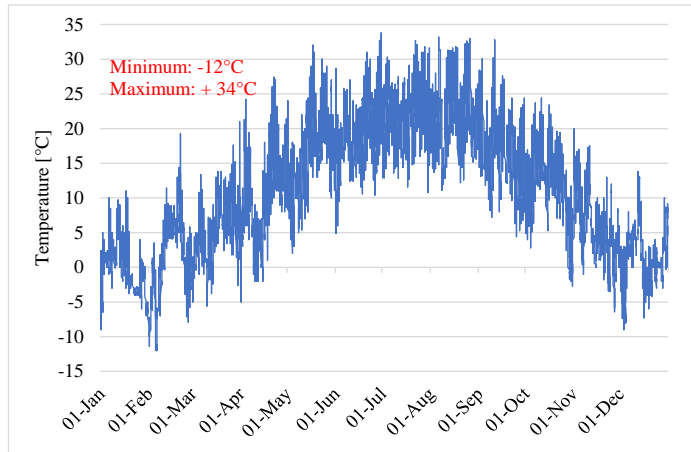


Fig. 8 – Hourly exterior air temperature in Timișoara – typical year

4. Results and discussion

4.1. Energy consumption

Table 3 shows the simulation results related to annual energy consumption on categories of consumption. The highest energy consumption is related to domestic hot water preparation, representing approximately 35% of the total annual energy consumption of the building, followed by heating with a percentage of 33% (Fig. 9). The building consumes in total 132.55 kWh/m²year, which is below the maximum limit for class A of energy efficiency in Romania. The solar contribution is not so high because the building is not in use during summer, when the solar hot water production is maximum.

Table 3

Table Name

Consumption category	Simulation results [kWh/m ² year]
<i>Heating</i>	<i>43.3</i>
<i>Domestic hot water (natural gas)</i>	<i>43.2</i>
<i>Domestic hot water (solar)</i>	<i>3.67</i>
<i>Cooling</i>	<i>3.00</i>
<i>Ventilation and pumps</i>	<i>26.02</i>
<i>Lighting</i>	<i>14.07</i>

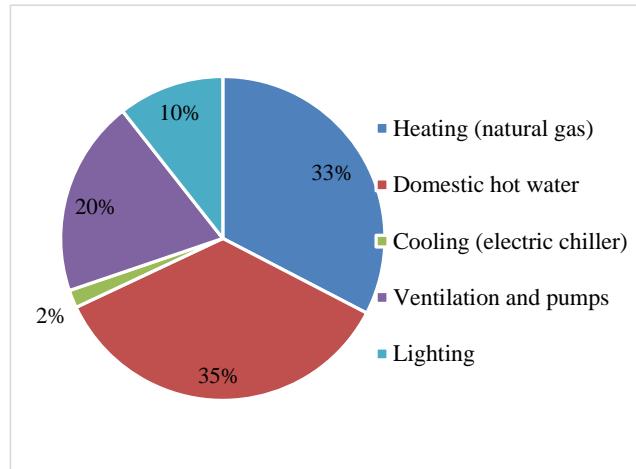


Fig. 9 – Percentage by usage type of total energy consumption

As we can see in Fig. 10, the consumption for ventilation and pumps has similar values for all the months of the calculation period. The highest consumption for heating energy is reported in January and a very low heating energy consumption can be observed in May. It is noticeable the energy consumption for cooling, which has a very small value due to the fact that the building is not in user for most of the summer, when buildings require cooling.

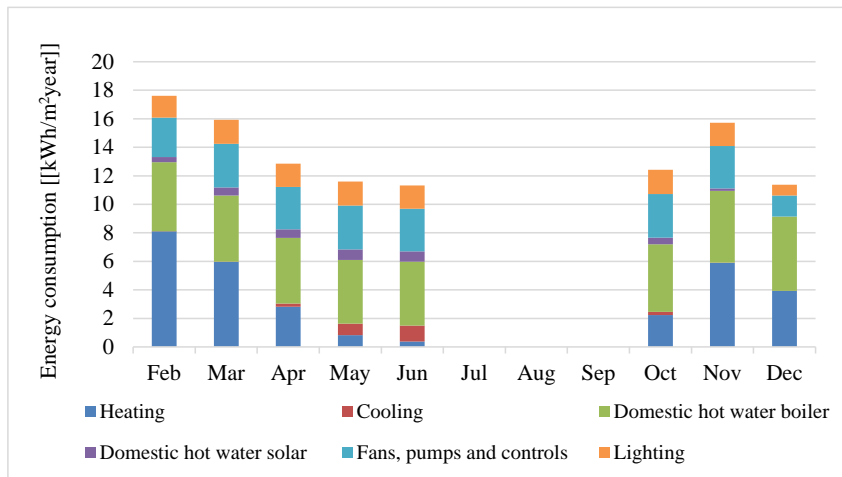


Fig. 10 – Monthly energy use by usage type

4.2. Indoor air quality and thermal comfort

Besides energy consumption calculation, the software also calculates hourly temperatures in the thermal zones of the building, as well as comfort temperature. Comfort temperature is the average comfort temperature in the room, calculated as the average of air temperature and radiant temperature. Fig. 11 and Fig. 12 shows temperature analysis for a randomly chosen room, for a day in February (with the lowest outside temperature) and a day in June (with the highest outside temperature during the calculation period). It is noticeable that the air temperature closely follows the comfort temperature, independently of the outside temperature variation.

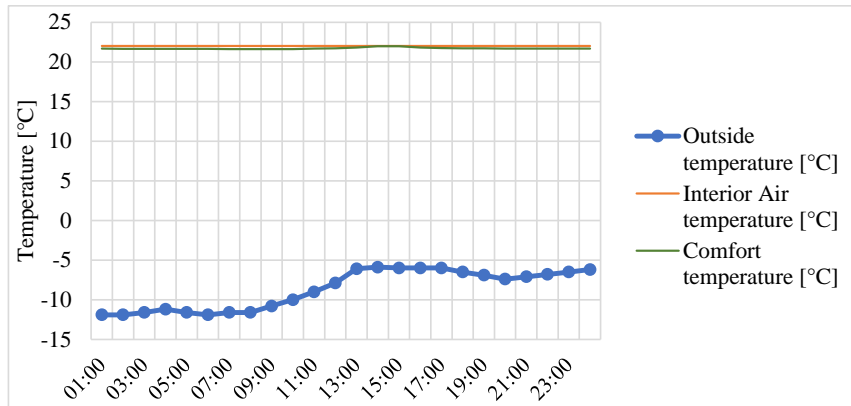


Fig. 11 – Daily temperature variation during heating season in a thermal zone which includes bedrooms – day with the lowest outside temperature (JUNE)

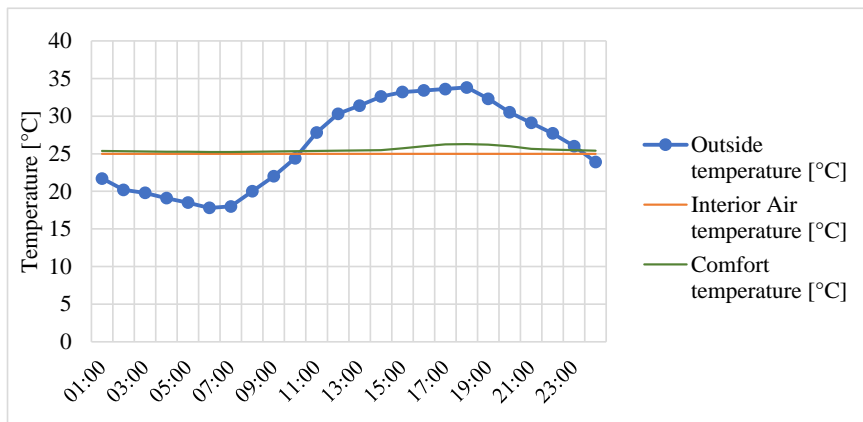


Fig. 12 – Daily temperature variation during cooling season in a thermal zone which includes bedrooms – day with the highest outside temperature

5. Conclusions

This paper presents the process of energy modeling and simulation results of a student's residence currently under construction, located in Timișoara, Romania. In terms of energy efficiency, the case study buildings combines highly insulated envelope with efficient HVAC, ventilation with heat recovery and also integrates renewable energy as a secondary source for domestic hot water. The energy evaluation results show that the highest energy consumption is related to domestic hot water and for space heating, followed by ventilation, lighting and cooling. The building can be classified in class A of energy consumption, having a total energy consumption below 150 kWh/m²year (maximum for class A buildings in Romania). The HVAC systems manages to maintain proper indoor conditions, providing comfortable air temperature. The student residence in Timișoara is one of the few documented new buildings for student accommodation in the higher education system. The results of this study aim at providing some indicators in terms of energy efficiency for new buildings in this category.

REFERENCES

- [1] Energy efficiency drivers in Europe - Regulations and other instruments open new horizons for Energy Management in buildings, Schneider Electric, 2009.
- [2] Directive 2012/27/EU of the European Parliament and of the Council of 25 October 2012 on energy efficiency, amending Directives 2009/125/EC and 2010/30/EU and repealing Directive 2004/8/EC and 2006/32/EC., European Commission, 2012.
- [3] I. Petidis, M. Aryblia, T. Daras and T. Tsoutsos, "Energy saving and thermal comfort interventions based on occupants' needs: A students' residence building case," *Energy and Buildings*, vol. 174, pp. 347-364, 2019.
- [4] M. E. Ryan and F. T. Sanquist, "Validation of building energy modeling tools under idealized and realistic conditions," *Energy and Buildings*, vol. 47, pp. 375-382, 2012.
- [5] Indicativ: NP 061 - 02. *Normativ pentru proiectarea și executarea sistemelor de iluminat artificial din clădiri*, 2002.
- [6] EN ISO 13790 - *Energy performance of buildings — Calculation of energy use for space heating and cooling*, 2008.
- [7] Ordin 386/2016 pentru modificare și completare indicativ C 107 - 2005.
- [8] <https://energyplus.net/weather>.

INTEGRATED HEALTH MONITORING & DISINFECTING SYSTEM FOR ORGANIZATIONS AND SOCIETIES

Sheeja NAIR^{1,*}, Ionuț Cristian SCURTU² and Sebastian Valeriu HUDIȘTEANU³

¹Dwarkadas J Sanghvi College of engineering, Mumbai, Maharashtra, India

²Mircea cel Batran Naval Academy, Constanta, Romania

³Gheorghe Asachi Technical University of Iasi, Iasi, Romania

Abstract. *In the wake of the current pandemic. The outbreak of COVID-19 across the world has headed researchers, healthcare department and government authorities to work together and find an optimum solution to get rid of the disease and restrict its spread. The purpose of this research work is to create awareness about public safety and solutions by ways of health monitoring system, which will measure successfully the body temperature along with heart rate of a person and hence create a safer environment around. Primarily for this sensor (MLX90614) is used to measure the temperature as well as pulse sensor to monitor the heart rate, which is then interfaced with controller to control and monitor the data for smart communication. Also touchless sanitizing device can be used to take precautionary measures which helps to sanitize the hands to decrease and till some extent kill the harmful virus. The paper basically focuses on the safety measures to be incorporated post lockdown. So, it's very effective to place the health monitoring system along with touchless sanitizer device at the entrance of any building.*

Keywords: Health monitoring system, touchless sanitizer device, sensor.

1. Introduction

In the 20th century the three deadly pandemic diseases which shook the world were identified as SARS-CoV, MERS-CoV and Covid-19. SARS-CoV was first detected in China on November 2002 and subsequently spread to 30 countries. In this outbreak, 8096 cases were reported worldwide, with 774 deaths [1]. The second pandemic disease MERS coronavirus was the MERS-CoV which is a severe acute respiratory condition [2]. Though in 2019, there were 2494 cases of MERS-CoV reported worldwide with 858 related deaths from 27 countries [3]. The world witnessed the third deadliest pandemic disease COVID-19 of the genus beta coronavirus and is related to MERS and SARS was reported in Wuhan- China and later spread extensively worldwide. As per World health organisation, the coronavirus positive

confirmed cases as of now across the world is 9 473 214 and death tolls to 484 249 across 216 countries and still rising. [4]. Fig.1- Overall situation in numbers by WHO regions.

Countries Affected	Total cases	Death cases
Globally	9 473 214	4 84 249
Africa	258 752	5 564
Americas	4 709 927	233 628
Eastern Mediterranean	987 534	22 464
Europe	2 619 753	195 535
South-East Asia	686 1922	19 651
Western Pacific	210 315	7 394

Fig.1. Overall situation in numbers (by WHO Region)

One-third of the global population has been on coronavirus lockdown, the World health organization, which has officially confirmed the outbreak as pandemic has called on “all countries to proceed with endeavours in order to limit the number of cases and slow down the spread of the virus”.

After effects of Lockdown

Scientists are exploring ways to exit out of this pandemic and get life back to normalcy. It is now very important to kick-start the economy and start with the business activities as before. In any case, we have to get back to normal and resume the activities as we did before. As William Sutherland, of the University of Cambridge, said “There will be a second wave of the virus”. Hence social distancing, care and precautions are highly recommended. The focus of this research paper is to find some necessary steps to safeguard the employees and for that every organization would require taking necessary steps to curtail the spread of virus. The paper proposes precautionary measures by installing smart health monitoring system [5] along with non-contact hand sanitizer for employees joining after long period of lockdown.

Workers or employees ought to be entirely permitted to enter the gateway by screening their identity card at the entrance, such that the data monitoring can be directly linked to the employee database. The purpose is to contain the spread of the virus in a simple, fast, economical and efficient manner with certain necessary measures using sensors, hardware design, wireless networks and low-cost microcontrollers can pave way for new and innovative solutions. The serious issues in the ongoing juncture is to screen numerous patients whose wellbeing must be checked often as a piece of indicative method, the need for a financially savvy and advanced brisk response instruments have become intensely required when there is a flare-up of

pandemic malady. Appropriate execution of such frameworks can give convenient alerts to doctors and their service can be activated in case of medical emergencies. Thus, this paper explores an innovative solution for a prototype with low cost and scalable health monitoring system along with a disinfectant system.

The purpose of the whole research revolves around the mechanism to detect fever, using non-contact temperature sensor and in the process if any individual is detected with high fever, a set alarm will alert the security systems and the individual would be sent to the infirmary for further test [6]. The individual's heart rate will also be monitored using the heart monitoring system which works on the principle of photoplethysmography. The change in flow of blood through any organ impacts the change in the light intensity through that organ. If the individual clears the screening, he will be allowed to use non-contact hand sanitizer where the ultrasonic sensor is enacted with advance controller to give signal to the sanitizer valve to open. With the current scenario and situation around, alcohol-based hand sanitizers are increasingly being used as disinfectants over standard hand wash. This has resulted in improvement of hand hygiene with a reduction of infections/virus. Utilizing alcohol based sanitizer, have proven to stop spreading the virus [7].

The design is essentially ordered into two main classifications: Design a health monitoring system & a non-contact sanitizing system. Both the design techniques are mentioned below in 2 & 3 sections.

2. Design a health monitoring system

Health monitoring system will measure body temperature and heart rate of a person. Raised body temperature is considered the most widely recognized indications of any sort of body infections [8]. Continuous monitoring of such changing parameter is challenging considering the burden of rehashed estimation of a person's internal heat levels, particularly when the individual may appear doing well [9]. Generally, the body temperature ranges from 36°C to 37°C . Any range from 38°C up to 39°C is considered as the beginning of fever. A lethal temperature of 39°C and above where medical treatment is an unquestionable requirement [10].

Along with fever detection heart rate monitoring is also essential. As people who have heart disease have less of cardiac reserve to be able to withstand the stress and fear which increased tremendously post pandemic spread [11]. Also if a person is infected with virus then the heart muscle can become inflamed and it can increase clotting and decrease flow of oxygen. Hence heart rate monitoring is also required.

2.1. System Architecture

The interconnections between various segments are explained using the design of frameworks. The patient interface is mapped by the temperature, pulse sensor and further processed by the controller. The information is then captured, and then appears

on human machine interfacing (HMI) which is displayed on LCD and simultaneously if the temperature and heart rate exceeds the set range, the alarm triggers. The operation of the system is divided into four segments: Sense, monitor control and data transfer. Sensors are used to detect fever and heart rating of a person entering the building. The output signal from the sensor is controlled by the controllers which work on analog as well as digital signal. The control incorporates interfacing the sensors with the controllers and transmitting them wirelessly to the monitoring equipment using wifi module. WiFi module is used which transmit data wirelessly to health care expert. Lcd display is used to monitor the output obtained. Fig.2- Health monitoring system.

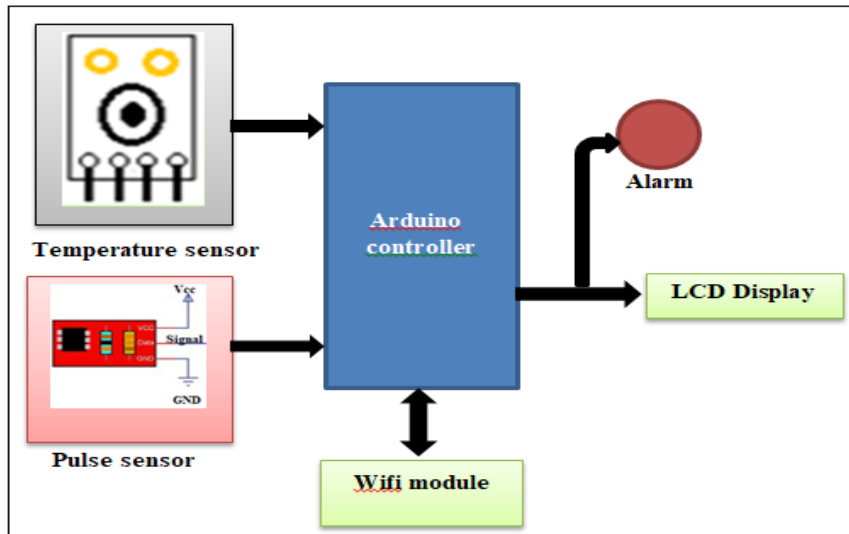


Fig. 2 – Health monitoring system

2.2. System Components

Temperature Sensor: The MLX90614 temperature sensor is an infra-red thermometer for non-contact temperature measurement and a signal conditioning processor [12].

As per the Stefan- Boltzmann law, any object that isn't beneath total zero (0^0 K) emits (non-human eye visible) light in the infrared spectrum that is directly proportional to its temperature. The infrared thermopile in the temperature sensor (MLX90614) senses how much infrared energy is being emitted by the subject and then produces an electrical signal proportional to it. It is a small size easy to integrate device with temperature variation range from -400^0 C to $+850^0$ C for sensor temperature.

Pulse sensor: The pulse sensor consists of three ports: Vcc supply, ground and signal. Fig.3- Pulse sensor with arduino.

Pulse sensor	Arduino Uno	Description of pulse sensor
Vcc Power	5V	Connected to 5V dc supply
GND	GND	Connected to arduino ground
Signal	Analog A0	Pulsating analog signal

Fig.3- Pulse sensor with arduino

Pulse sensor works on the principle of optical method also known as photoplethysmography. On one side of the pulse sensor, led is placed along with an ambient light sensor and on the other side is an electronic integrated circuit which is responsible for amplifying the signal. To calculate the heart rate, the individual's fingertip is placed on the LED and accordingly the flow rate of the blood impacts the light emitting from the led. The heart rate can be calculated based upon the led display that blinks with each heartbeat per minute [13].

Arduino: The sensor output is connected to the analog pins of arduino controller. It converts the analog signal into digital signal. The digital signal is then interfaced with the lcd to display the output [14]. Controller is also connected with wifi module. The output from the controller can be wirelessly transmitted using ESP8266 wifi module to smart phones/devices.

HMI, LCD Display/Alarm: The human machine interface (HMI) is the interface between the machine and user to translate complex process variables into usable and actionable data. The reason for the HMI is to show effectively justifiable, real time, ongoing operational data. It is then interfaced with LCD and alarm. The liquid crystal display is an electronic device widely used to display digital output. If the temperature is greater than set value i.e. 37°C or heart rate exceeds 100bpm or goes below 60bpm then alarm gets activated and alerts the guard.

WiFi module

ESP8266 is a wifi enabled system on chip [15]. For wireless communication wifi module is used which can connect with Arduino board transmitter Tx and receiver Rx. Table describe the connectivity between WiFi module with Arduino uno board. Fig.4- Wifi module with Arduino uno.

Wifi module	Resistor	Arduino Uno
Vcc Power	10K	3.3V
CH_EN/Enable	10K	3.3V
Tx/Transmitter	-	Pin 3
Rx/Receiver	1k	Pin2
GND	-	GND

Fig.4- Wifi module with arduino uno

It consists of two general purpose input and output port GPIO-0 and GPIO-2, transmitter/receiver, supply, ground, channel enable pin CH_EN and reset to start. Fig.5-Wifi module.

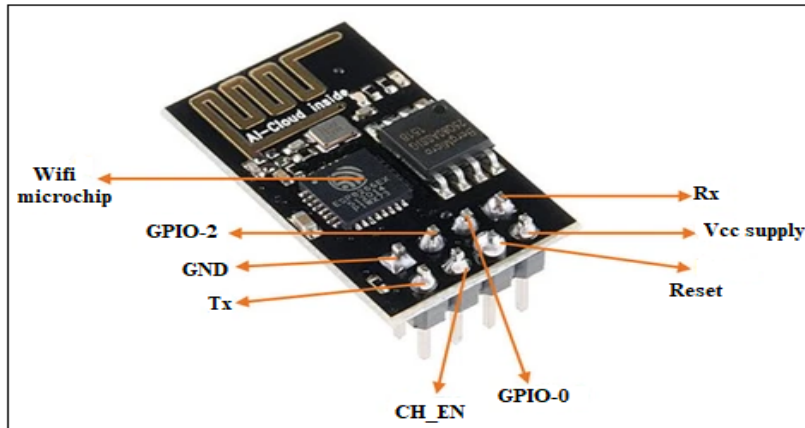


Fig.5. Wifi module

The wifi module is used to send signal to the health expert if the health monitoring system detects abnormality. ESP8266 is a microcontroller which has the ability to function wifi related activities. Fig.6- Alert to health expert.

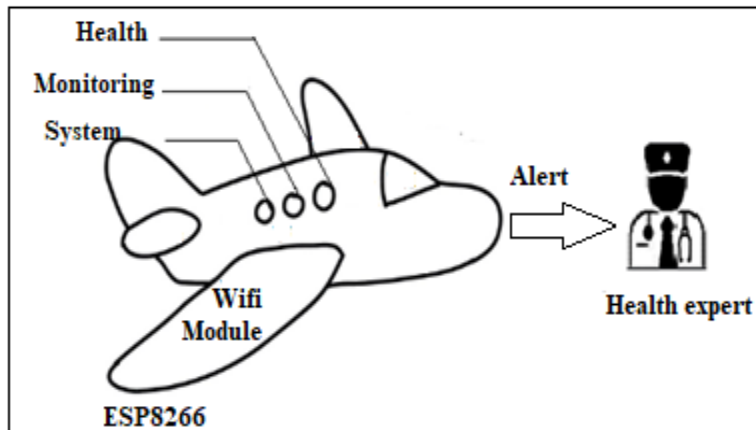


Fig.6 – Alert to health expert

Non-contact sanitizer system

Alcohol-based water free hand sanitizer dispensers (HSD) are an inexorably well-known strategy for hand cleanliness and help prevent hospital-acquired infection

(HAI). Subsequently in order to eradicate the spread of such dangerous virus sanitizer is useful [16].

4.1. System Architecture

A model of the proposed non-contact hand sanitizer dispensers can be given by the framework demonstrated. This portrayal of the framework introduced gives an understanding of how the proposed framework is being made. It mainly consists of ultrasonic sensor, Arduino uno board, relay, servomotor, water reservoir, hand sanitizer valve. An ultrasonic sensor is utilized to check the presence of hands beneath the sanitizer dispenser and also calculates the distance between the dispenser and hands. Then it passes the information to Arduino uno board which turns on the servomotor with the assistance of the relay and hand sanitizer dispenser valve gets opened. Reservoir is used to store the sanitizer. Fig.7- Non-contact hand sanitizer dispensers.

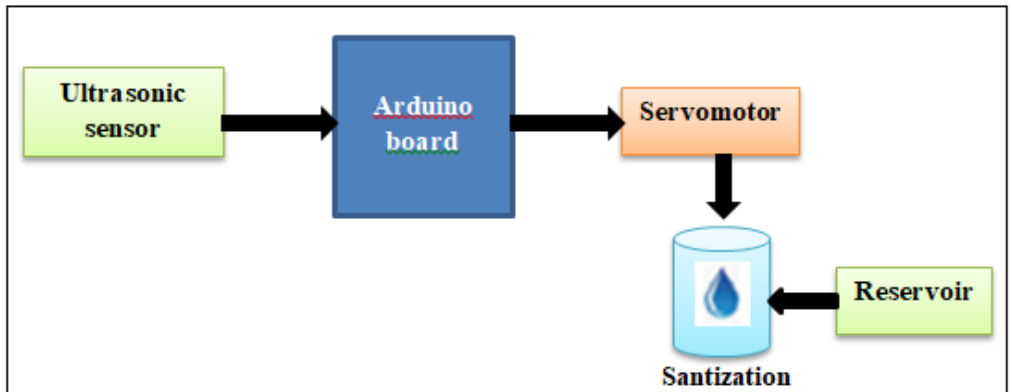


Fig. 7 - Non-contact hand sanitizer dispensers

4.2. System components

Ultrasonic sensor: An ultrasonic sensor is a device that estimates distance to an object using sound waves. It works by sending out a sound wave at ultrasonic frequency and bounce back if meets article. Fig.8- Ultrasonic sensor. To calculate the distance the time delay between transmission and receiving of the sound given:

$$\text{Distance} = (\text{Speed of the sound} \times \text{Time delay}) / 2$$

Ultrasonic sensor used here to detect the article by sending sound waves which hit the article and reflect the sound waves back to the receiving echo end [17]. Ultrasonic sensor detects frequency normally between the range 100 KHz to 50MHz. Any article coming ahead of the ultrasonic sensor is detected and also calculates the distance from sending the signal to receiving the signal which then passed to the arduino controller.

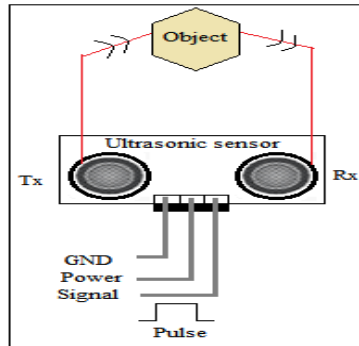


Fig. 8 - Ultrasonic sensor

Servomotor: Arduino gives signal to servomotor to rotate from 0 to 180° as per requirement. If there is no or low signal from the controller then servomotor doesn't rotate and valve remains closed and when high signal is transmitted from the controller the servomotor rotates thus can open the dispenser valve.

5. Results

5.1. Design a Health monitoring system

Pulse sensor is used to detect the heartbeat in beats per minute of any individual. It consists of Vcc (5V supply), ground (GND), potentiometer (POT) and oscilloscope. The simulation is executed using simulation. Thus potentiometer is used as the input and the obtained waveform is observed in the oscilloscope. Fig.9- Pulse sensor

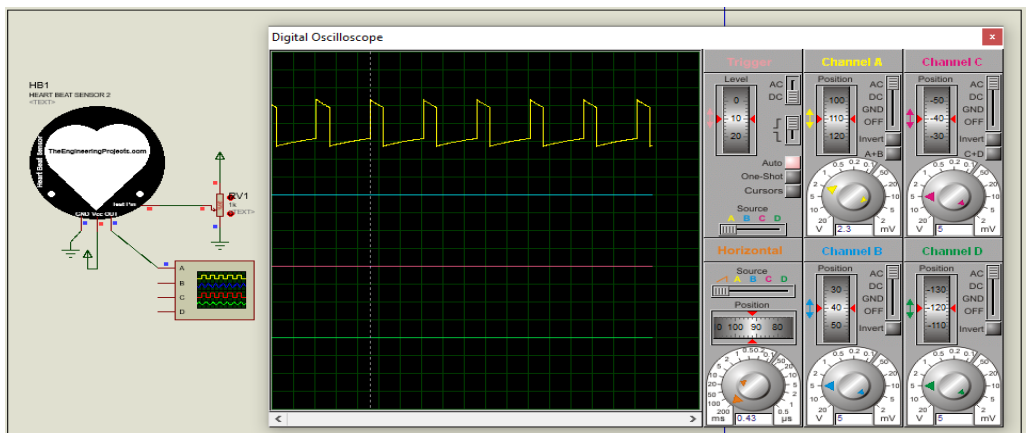


Fig.9- Pulse sensor

The pulse sensor output signal when connected to the arduino controller gives the output obtained and is then displayed. It indicates the heart beat per minutes. The output executed can be displayed online. Hence health expert can monitor the data of any individual for particular time and day monitored. Necessary measures can be taken at the earliest if any serious fluctuation occurs. Fig.10 - Heart rate monitor. The information is constantly varying with respect to time which helps the health care expert to understand the situation comprehensively.

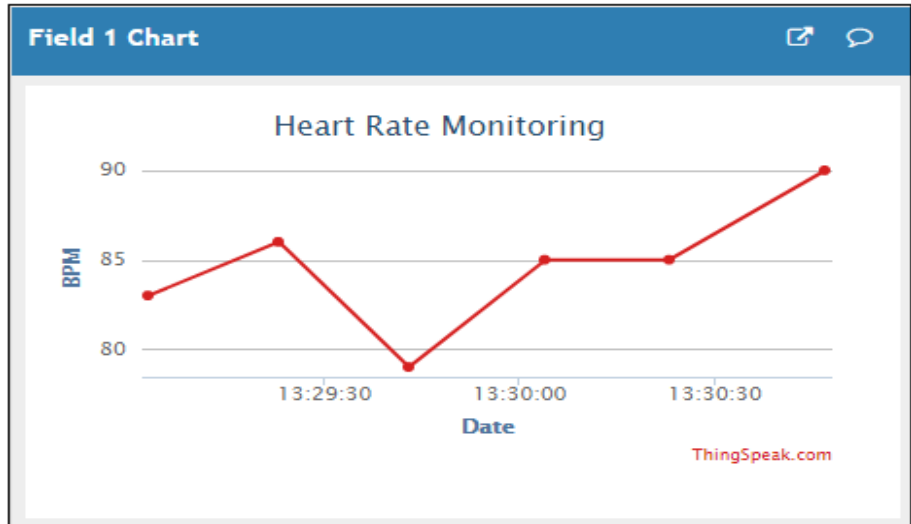


Fig.10- Heart rate monitor

Temperature sensor MLX90614 consists of four pins VDD, GND, SCL and SDA which is connected to arduino controller and output is displayed on LCD and alarm triggers if temperature and heart rate detects more or less value than normal range. Power is connected to 5V, ground is connected to GND whereas SCL and SDA are connected to analog. All of those components are connected and controlled mainly by arduino controller. Pushbutton is used which is reset when human being/object is detected. Fig.11- Non-contact fever detection device.

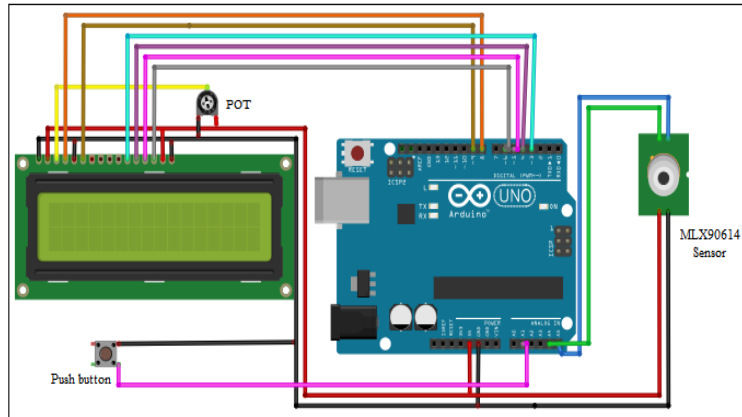


Fig.11. Non-contact fever detection device

For wireless communication wifi module is used which is connected with arduino board controller along with temperature sensor and resistors. Resistors are mainly used to restrict the flow of high currents in the circuit. Fig.12- Wifi module interfacing with arduino controller.

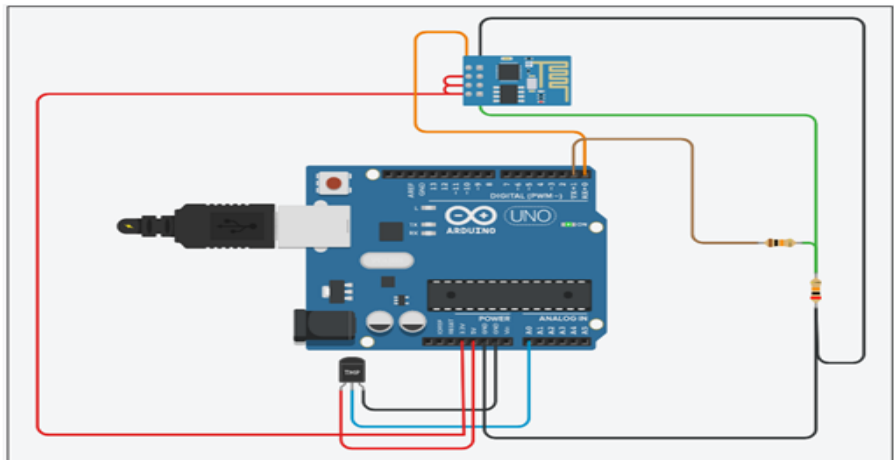


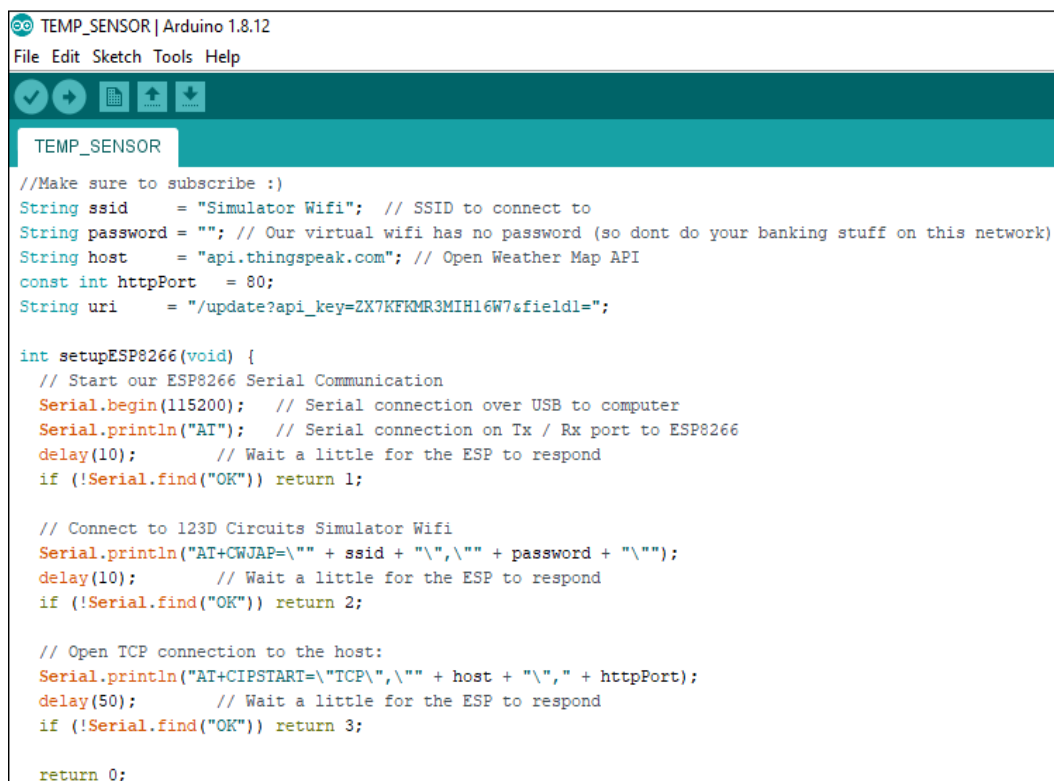
Fig.12 - Wifi module interfacing with arduino controller

Temperature sensor consists of three pins: Vcc supply connected to 5V, Ground connected to GND and signal connected to analog Ao of the Arduino controller. Table below mentions the overall relation between wifi module, Arduino controller along with resistor values. Fig.13- Wifi-module connected to Arduino controller.

Wifi module	Arduino	Resistor values
Transmitter,Tx	Receiver	30K
-	Transmitter	10K
Vcc supply	3.3V	-
Reset	3.3V	-
Channel enable	3.3V	-
Ground	GND	20K

Fig.13- Wifi-module connected to arduino controller

The code for the Arduino is mentioned to monitor the temperature. The output is monitored online through any smart devices. The code is written in Arduino 1.8.12 board and monitored the data online. Fig.14 a and b- Temperature sensor monitored along with Arduino controller.



```

TEMP_SENSOR | Arduino 1.8.12
File Edit Sketch Tools Help

TEMP_SENSOR

//Make sure to subscribe :)
String ssid = "Simulator Wifi"; // SSID to connect to
String password = ""; // Our virtual wifi has no password (so dont do your banking stuff on this network)
String host = "api.thingspeak.com"; // Open Weather Map API
const int httpPort = 80;
String uri = "/update?api_key=ZX7KFKMR3MIH16W7&field1=";

int setupESP8266(void) {
  // Start our ESP8266 Serial Communication
  Serial.begin(115200); // Serial connection over USB to computer
  Serial.println("AT"); // Serial connection on Tx / Rx port to ESP8266
  delay(10); // Wait a little for the ESP to respond
  if (!Serial.find("OK")) return 1;

  // Connect to 123D Circuits Simulator Wifi
  Serial.println("AT+CWJAP=\"" + ssid + "\",\"" + password + "\"");
  delay(10); // Wait a little for the ESP to respond
  if (!Serial.find("OK")) return 2;

  // Open TCP connection to the host:
  Serial.println("AT+CIPSTART=\"TCP\", \"" + host + "\", " + httpPort);
  delay(50); // Wait a little for the ESP to respond
  if (!Serial.find("OK")) return 3;

  return 0;
}

```

Fig.14 a) Temperature sensor monitored along with Arduino controller


```

File Edit Sketch Tools Help
TEMP_SENSOR §

void anydata(void) {
  int temp = map(analogRead(A0), 20, 358, -40, 125);
  // Construct our HTTP call
  String httpPacket = "GET " + uri + String(temp) + " HTTP/1.1\r\nHost: " + host + "\r\n\r\n";
  int length = httpPacket.length();

  // Send our message length
  Serial.print("AT+CIPSEND=");
  Serial.println(length);
  delay(10); // Wait a little for the ESP to respond if (!Serial.find(">")) return -1;

  // Send our http request
  Serial.print(httpPacket);
  delay(10); // Wait a little for the ESP to respond
  if (!Serial.find("SEND OK\r\n")) return;
}

void setup() {
  setupESP8266();
}

void loop() {
  anydata();
  delay(10000);
}

```

Fig.14 b) Temperature sensor monitored along with Arduino controller

The flowchart visualizes the process of detecting human body temperature (without contacting) with the help of MLX90614 sensor. If the human temperature is above the set temperature in the logic, then the individual is routed to the hospital for further process and if it's less than the set temperature limit then he would be granted entry.

Fig. 15- Flow chart.

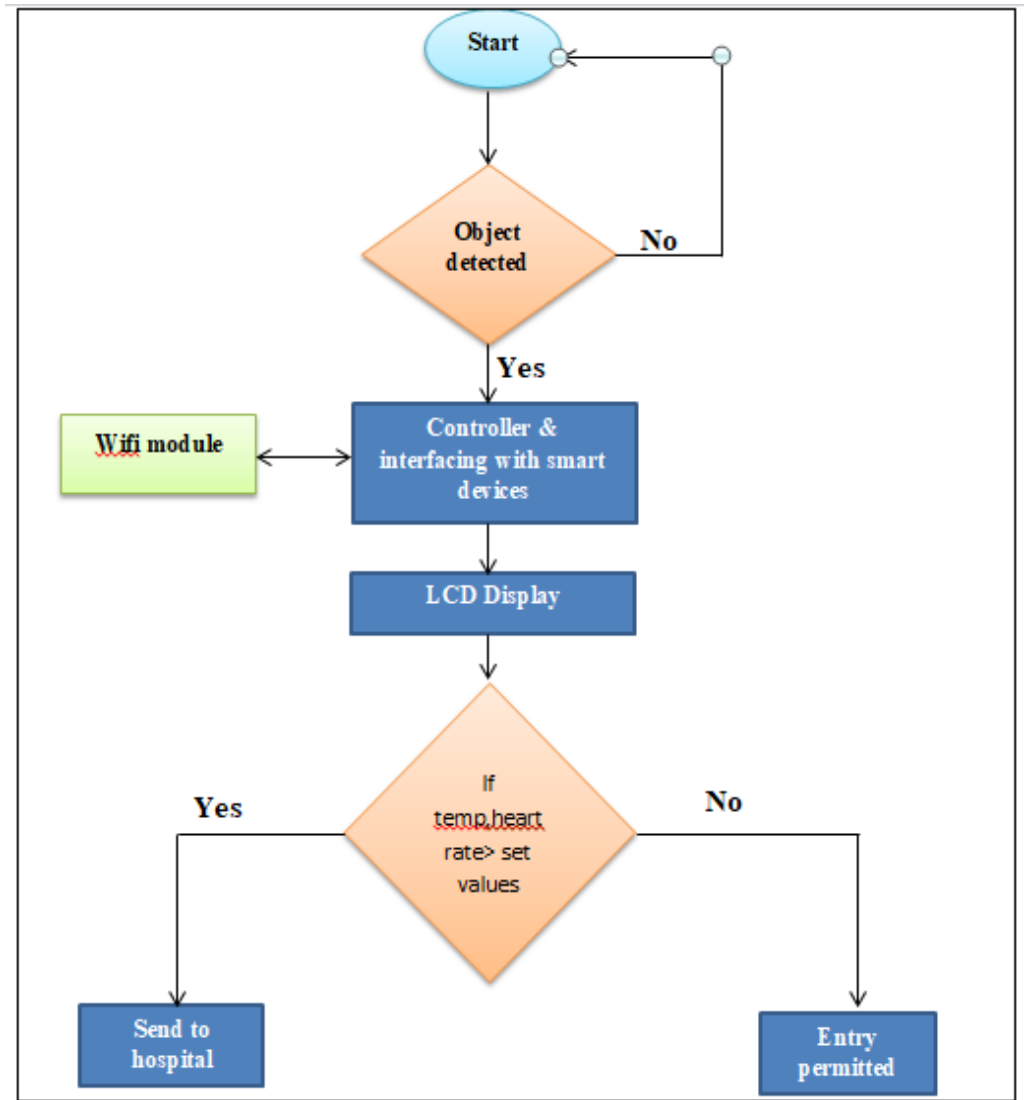


Fig. 15- Flow chart

5.2. Non-contact sanitizer

Ultrasonic sensor consists of three pins power, ground and signal which are connected to Arduino uno board. Power is connected to 5V supply; ground to GND pin and the signal is connected to digital pin D7 of Arduino board. The signal is passed to the servomotor through controller. The servomotor comprises of three pins: Power, signal and ground. Power and ground are connected to Arduino board 5V supply and ground pin and signal is connected to digital pin 12. When the object is detected a pulse is

generated shown in the oscilloscope which then allows servomotor to rotate and thus opens the valve and sanitizer comes out of the valve. Fig.16- Non-contact sanitizer simulation

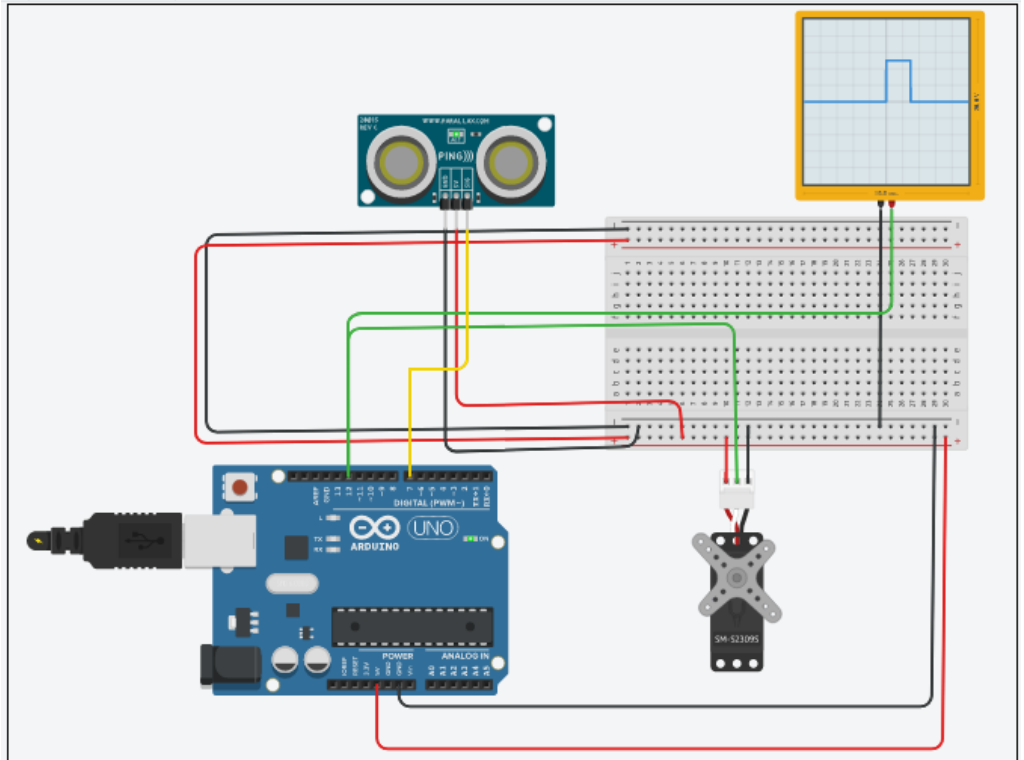


Fig.16- Non-contact sanitizer simulation

Flowchart shows if an object is placed below the ultrasonic sensor then it passes the signal to the Arduino which rotates the servomotor and thus open valve to allow sanitizer to come out from the dispenser by avoiding direct contact. Fig.17- Flow chart non-contact hand sanitizer dispenser

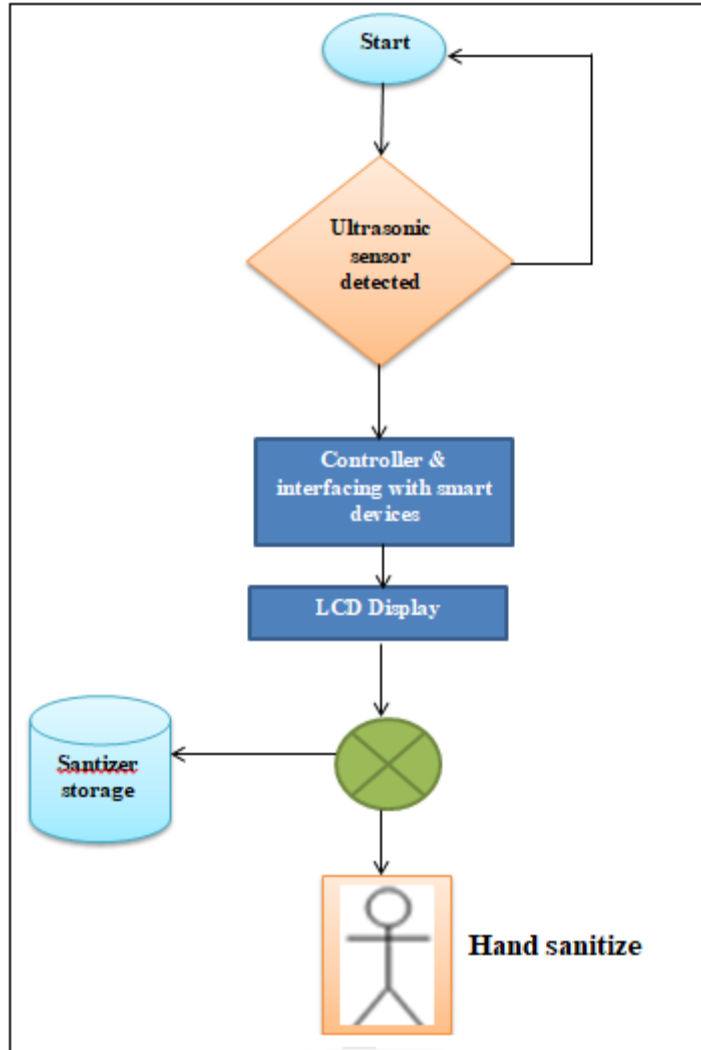


Fig.17- Flow chart non-contact hand sanitizer dispenser

6. Conclusion

Regarding the overall research paper. The message is to bring a model based framework focusing at micro level aspects, wherein emphasis is given to technologically advanced systems to be adapted by various organizations, Society and even individuals to contain the spread of virus thereby integrating technology in the day today activity by ways of implementation of the proposed system. This would surely help to focus on the aspects of dealing with the Virus post Lockdown, this also

revolves around the precautionary measures on limiting the spread of the Virus. Further emphasizing on this model, it would also additionally benefit individuals to monitor their health status online for individual and suggestive purpose.

REFERENCES

- [1]WORLD Health Organization (WHO). 31st Dec 2003. <https://www.biorxiv.org/content/10.1101/2020.01.31.929547v1.full.pdf>
- [2]WORLD Health Organization (WHO). 10th June 2013. https://www.who.int/mediacentre/news/releases/2013/mers_cov_20130610/en/
- [3]WORLD Health Organization (WHO). Nov 2019. <https://www.who.int/emergencies/mers-cov/en/>
- [4]WORLD Health Organization (WHO).Coronavirus 2020. https://www.who.int/docs/default-source/coronaviruse/situation-reports/20200626-covid-19-sitrep-158.pdf?sfvrsn=1d1aae8a_2
- [5]Anushka Patil, Chetana Pawar,Neha Patil ,Rohini Tambe, “Smart health monitoring system for animals”,Conference: 2015International Conference on Green Computing and Internet of Things (ICGCIoT),10.1109/ ICGCIoT .2015.73807 15.
- [6] Neuman, Michael. R. (2010). Measurement of Vital Signs: Temperature. IEEE Pulse, Sept/Oct, 40-49.
- [7]Nina A. Gold1; Usha Avva2, book on “Alcohol sanitizer” by statpearls. <https://www.ncbi.nlm.nih.gov/books/NBK513254/>
- [8] Radchenko, N. A concept of the design and operation of heat exchangers with change of phase. Archives of Thermodynamics: Polish Academy of Sciences. 2004, no.4, vol.25, pp. 3–19.
DOI absent
- [9] Ross B Kaplan, Timothy M Johnson, Ralf O Schneider, Shankar M Krishnan, “A DESIGN FOR LOW COST AND SCALABLE NON-CONTACT FEVER SCREENING SYSTEM.” 2011-2830.
- [10]Mayo Clinic Family Health Book, 4th edition and normal temperature Available: <https://www.pregnancybirthbaby.org.au/fever-in-babies>
- [11] Christopher Schmitz¹, Lindsey Drake², Megan Laake³, Peng Yin⁴, and Rachel Pradarelli⁵, “Physiological Response to Fear in Expected and Unexpected Situations on Heart Rate, Respiration Rate and Horizontal Eye Movements”. Physiological Response of Fear in Expected and Unexpected Situations
- [12] MLX90614 sensor. <https://www.digchip.com/datasheets/1110594-mlx90614.html>
- [13] Working of heartbeat sensor. <https://www.elprocus.com/heartbeat-sensor-circuit-daigram-working-with-8051/>
- [14] Arduino board. <https://www.arduino.cc/en/Guide/ArduinoUno>
- [15] Wifi module. <https://quartzcomponents.com/products/esp8266-01-wifi-module>
- [16]Touch less hand sanitizer. <https://circuitdigest.com/microcontroller-projects/automatic-hand-sanitizer-dispenser-with-covid19-live-updates>
- [17] Ultrasonic sensor. <https://www.electroschematics.com/ultrasonic-sensor-circuit/>

SETTING AN INNOVATIVE MASTER DEGREE ON ENERGY SUPPLY FOCUSING ON ISOLATED AREAS – THE MESfIA ERASMUS+ PROJECT

Antonios TSIKALAKIS¹, Georges ZISSIS², Laurent CANALE², Yiannis KATSIGIANNIS¹, Sarintip TANTANEE³, Deny HAMDANI⁴, Shobhakar DHAKAL⁵, Sivanappan KUMAR⁵, Hoang Nam Kha NGUYEN⁶, Trung Hung VO⁷, Sarjiya SARJIY⁸, Salvador Suarez GARCIA⁹

¹ Hellenic Mediterranean University, Greece

² Univesrité de Toulouse, LAPLACE, UMR5213 CNRS-INPT-UT3, France

³ Naresuan University, Thailand

⁴ Institut Teknologi Bandung, Inonesia

⁵ Asian Institute of Technology, Thailand

⁶ Nong Lam University, Vietnam

⁷ University of Technology and Education, The University of Danang, Vietnam

⁸ Universitas Gadjah Mada, Indonesia

⁹ Instituto Tecnológico de Canarias, Spain

Abstract. *Mastering Energy Supply focusing on Isolated Areas (MESfIA) Erasmus+ Capacity Building project, aims to provide high quality postgraduate education on energy supply systems for engineers and graduates from science departments, aiming to have activity or to be employed in projects in countries with many isolated areas and insular systems. It is a transnational co-operation activity between Europe and South-East Asian Countries (namely in our case Thailand, Vietnam and Indonesia) to improve capacity of Postgraduate Students in S.E. Asian Universities. Energy efficiency is among the items to be addressed in this training.*

Keywords: Power Systems, Electrical Grids, Island Networks, Postgraduate Training curricula, Transnational collaboration.

1. Introduction

Access to affordable and reliable energy supply is a necessary prerequisite to the economic development and poverty alleviation [1]. It seems awkward to realize that about 840 million people (11% of the world population) do not have access to electricity [2], 95% of them in sub-Saharan Africa and developing countries in Asia. In Southeast Asia alone, 125 million out of 625 million residents lack access to stable electricity [3]. These people quite often reside in either physical islands, mostly in Indonesia, or isolated areas that electrically can be considered as islands. Taking into

account, that electricity leads to a number of quality-of-life improvements, such as improved communications, educational attainment, improved health services and easier access to potable water, access to electricity services has been explicitly identified by the World Summit on Sustainable Development (WSSD) as an essential for achieving the UN Millennium Development Goals for halving poverty by 2015 in the world's poorest countries [4]. Additionally, the UN sustainable Development Goal n°7 [5] aims to "Ensure access to affordable, reliable, sustainable and modern energy for all". Clearly, improving access to energy for all should be considered as a key target for the realization of this Goal.

This is further important for remote or/and island areas and rural electrification campaigns clearly serve this purpose. Such areas may include villages away from the grid, in forest or mountainous areas but mostly island areas. These areas share a few common characteristics that induce difficulties in satisfying energy demand at best at similar cost with people residing in large metropolitan areas or even for with similar reliability indices. These areas may have more frequent and longer electricity cuts, even though some of these may be even interconnected to stronger grids, with rather weak interconnections, though. Sometimes a single fault that in an interconnected power system would remain unnoticed, in such areas may even lead to black out of the power system.

At the same time, limited fuel resources and less efficient operating points of operation increase the energy cost in these areas which can be significantly higher compared to the mainland [6]. Moreover, high electricity demand usually appears during the touristic periods with even more increased peaks in specific times of the day. This notable seasonality and periodically requires an advanced and adaptive approach including both energy management and efficiency but also flexible energy production. To increase complexity, these areas are usually located in fragile environment areas. Thus, transportation and use of fuel harms such an environment especially in islands where sea environment is also linked. Potential accidents like oil spills, vessel sinking, fires, chemical accidents, etc. are the causes of severe damages to what are the two main income capital chapters, fishing and tourism, the major activities of the population as confirmed by the questionnaires developed within the MESfIA project. An additional issue is that oil has not only high transportation cost, but also significant environmental footprint inducing air pollution, water quality issues.

The declining cost of Renewable Energy Resources (RES) is opening new opportunities to achieve access and reduce reliance on costly diesel generators in isolated areas [7]. Clearly RES, especially combined with storage, has provided significant boost to rural electrification in various areas of the world and in bibliography there is a number of exceptional cases where local or regional cooperation has improved electrification [8]. The most successful example is the use of Solar Home Systems (SHS) to provide minimum lighting and use of small

appliances [9]. One can distinguish technical and non-technical barriers, requiring special and creative techniques to be followed for the exploitation of RES to be increased [10].

However, beyond these barriers, a main issue is still lying on the availability of skilled engineers and technicians in the immediate neighbourhood. In all these areas difficulty of specialized assistance to access rapidly the place require highly qualified personnel to be available on site. Understanding these peculiarities, barriers and understanding the potential solutions is one of the cornerstones for improving energy supply focusing on isolated areas. In fact, it is commonly accepted that the more skilled technicians and engineers available, the lower the danger of prolonged power cut is. Erasmus+ Capacity building MESfIA (Mastering Energy Supply focusing on Isolated Areas) project is ambitious to hedge this gap.

The objective of the project is presented in Section 2 while in Section 3 the preparation phase along with the major training axes are presented.

2. The MESfIA Project-Scope and Objectives

The aim of the MESfIA project is to provide high quality postgraduate education on energy supply systems for engineers and graduates from science departments, aiming to have activity or to be employed in projects in countries with many isolated areas and insular systems. Education on various aspects of Intelligent Energy Systems, which have also become a reality in the partner countries, should cover Energy Management, Renewable Energy Sources (RES) utilization, Energy conservation, intelligent materials application to energy sector and Demand Side management. However, there is need for more systematic training on the aforementioned issues for application on the fragile environment of isolated areas taking into account the peculiarities of the island power systems. This is where MESfIA emphasizes and the innovative character is to provide via existing or new MSc programs of the Partner countries the capability to apply specific skills to help in the more efficient energy supply of isolated areas. It has been observed that the establishment of a master program that targets in satisfying needs linked to specific geographic conditions tends to make their students more willing to move to areas where their specialization will be better adapted, promising and needed.

In that way, MESfIA combines all of the above elements, by suggesting the establishment of a number of Master Courses, combining the existing experience of the EU and Asian countries in these issues. The MESfIA Master, aiming to start in late 2020 in Asian Universities has a clear ambition to transfer the knowledge to countries of South-East Asian regions where the renewable energy potential is huge, and explore novel approaches in educating high quality specialists in RES, intelligent energy management and consumption reduction.

2.1 The MESfIA consortium

European and South East Asian Universities co-operate in order to develop the necessary adaptations to existing MSc programs in South East Asia Universities or develop a new stream of Courses focusing on Energy issues especially of isolated areas. Additionally, existing courses will be adapted to serve these specific needs by suitable examples.

As the project has a broad scope of targeting academic, industrial and civilian sectors, the consortium partners have been selected on the basis of their know-how and the target group they can approach. The members of MESfIA consortium come in great part from island Areas, i.e. Crete, Canary Islands, Indonesia or have islands or remote areas still un-electrified like Vietnam and Thailand. Four of the academic institutions are based on island areas. All institutions, but mainly island ones, have had close collaboration for a long time with their local Electrical Distribution Network Operators for the more efficient operation of the autonomous power systems of Crete, Canary Islands and Indonesia, respectively.

In Table 1 the list of the 11 MESfIA's Consortium members is provided along with a map showing the global Dimension of the consortium in Figure 1.

Table 1

The Consortium members

European Partners	Asian Partners
Hellenic Mediterranean University, Greece (Coordinator)	Asian Institute of Technology, Thailand
Eurotraining Educational Organization, Greece	Naresuan University, Thailand
Université Toulouse 3 – Paul Sabatier, France	Institut Teknologi Bandung, Indonesia
Instituto Tecnológico de Canarias (ITC), Spain	Universitas Gadjah Mada, Indonesia
Canary Wharf Consulting Ltd, UK	Nong Lam University, Vietnam
	University of Danang, Vietnam



Fig. 1 – The global Dimension of the MESfIA project.

3. MESfIA activities and expected impacts

To achieve its objectives, MESfIA consortium is developing a large range of activities; some of them are listed below.

- Surveys on related national and international programs and on needs for intelligent energy systems, emphasising on the needs of electrical and/or geographically isolated inland and island areas, following an itinerary that secures the validity and quality of the project based on the mature research of partners. This will help to avoid replications and pinpoint the potential needs mainly of Asia students on such systems. Additionally, will help students and participants prepare state-of-the art and ready to apply methodologies for more efficient and intelligent solutions, for meeting energy demand.
- Formulation of recommendations, based on the results of the survey and the expertise of all participants, regarding both academical aspects and potential technological solutions that better match global and mainly local industry demands. The requirements' identification will point out all the specific areas where the whole system can be "weaved" together achieving smooth integration. The identification of the exact framework, the required tools and the necessary prerequisites will also identify the best educational approach required for each session. Finally, these proposals will result in new courses and proposals for adapting existing ones.
- Capacities building through intense collaboration among all participants staff will be strongly promoted, aiming at enhancing Asian partners capacities, promoting the bonds among European industrial and academic bodies and their Asian counterparts and supporting the generation of innovative solutions to common problems.

- Promotion and advertising campaigns for making programmes activities known to special and wider audiences.

The project focus in the wider South-East Asian countries sharing common culture, making unification of such approaches more effective. Traditional in-class lectures will be applied, in order to maintain the bonding between students and teachers, and this will be enhanced by the participation of teaching staff and experts from European participants. Live Streaming will be utilized for experiments that should take place at site-specific areas like the TALOS infrastructure, a unique installation site for testing insulators [11]

3.1 Preparation phase

The preparation phase included a literature review of the needs of the local communities in South East Asia, Good practices from other regions of the planet. Feedback from industrial partners and the society was deemed essential in this stage to tailor the program and courses according to the market needs For this reason, two questionnaires were set up to identify the potential issues of interest for the stakeholders of South East Asia. These questionnaires refer to the social needs and the technical skills that should be available to the trainees of the MESfIA project.

By the response in the social needs it can be identified that the major issues that the people residing in autonomous power systems have to face are Health anxiety and then the energy issues. When discussing the energy issues from the social perspective:

- Among Energy issues, reduced power quality and expensive prices are the issues that worry more the people residing in such areas
- People believe that lack of funding and unclear legislation framework is one of the reasons that impede RES penetration in these areas
- Cooking is not very often based on electricity while for areas not interconnected to the grid, PVs and Diesel gensets are the major sources for providing electricity.

As far as training needs in the energy sector these have been identified as follows:

- Training should focus more on PVs and Energy Storage
- There should be significant emphasis on more practical aspects of training
- Funding and regulatory framework should be explicitly examined.

3.2 Education Material and Curricula development

The consortium has prepared at a first step a detailed planning of training cycles including scheduling and effort management for implementation of training courses in each country, in order to provide postgraduate training mostly on Electrical, mechanical engineers focusing on:

- Realizing the difficulties in Isolated Environments and the associated peculiarities with energy management on such systems

- Training of Engineers at Post Graduate Level so that they can cope with the aforementioned peculiarities and become ready for applying intelligent solutions to energy supply of isolated areas. Some of these solutions could be applied in stronger power systems as well.

Lectures and laboratory exercises will help students understand these topics, adopt them for improving Energy Supply and help in the adaptation of various European Norms in their local environment. Regarding the Pedagogical Approach, suitable modern and well-established methodologies will be adopted, adjusted to the needs and special characteristics of the areas of interest.

Based on the discussions among the partners, bibliographical reviews and the results from the questionnaires, the education material under development in the frame of the project will cover:

- Use of Renewable Energy Sources (RES) has been proven vital for electrification especially in remote areas. Exchange of knowledge of good practices for exploiting RES, adapting to the special characteristics of each environment, such as salinity for islands, will be addressed. There is significant expertise in the consortium regarding management of RES in such areas (e.g. Crete; Indonesia and Canary Islands). Significant focus will be provided to Solar Energy. More interesting on Wind Power exists in Vietnam, the country with the highest wind potential in the area.
- Energy Storage is a key issue for improving energy supply, mainly via more efficient integration of RES into isolated power networks. The students, after the corresponding MSc cycles will be able to understand the value of Energy Storage for energy management and identify potential business models for Energy storage integration based on the legislation. Energy storage is one of the key subjects for which material will be developed.
- Managing of Energy Resources for promoting energy security, emphasizing in power systems of isolated areas. Students will acquire sufficient expertise to combining local knowledge with techniques for analysing energy resources. Students following MESfIA MSc programs will gain the capacity to pinpoint suitable solutions for rural development satisfying local stakeholders.
- Demand Side Management as many isolated areas share as common characteristic low average to peak demand ratio. Meeting Increased peak demand may require significantly more sophisticated solutions. In order to utilize efficiently power generation facilities in such areas, demand side management can be more essential compared to stronger interconnected power systems. Students will be able to propose methods for controlling peak energy demand of isolated areas based on the special characteristics of each area.
- Increasing energy efficiency may be much more important for isolated areas as the energy cost per unit of energy is expected to be higher. In order to address such issues, educational material on the following sections is under development:

- Improved lighting performance.
 - More efficient control drives and electrical machines
 - Building Automation ranging from simple automation schemes to Intelligent Buildings
 - More efficient devices including also alternative ways of cooking.
 - More intelligent materials for the building envelope
- Grid Infrastructure demonstrates a critical role for electricity supply, especially insulation materials in coastal and tropical areas. Within the course the fundamental knowledge and methodology for the design, operation and maintenance of Grid is going to be presented. Testing of insulators under various environments will be performed via live streaming in the TALOS test Station [11].
- Protection and automation systems in power grid: Power system protection and automation systems constitute the operation intelligence of a smart grid and ensure its safe, efficient and reliable operation. Within the course, advanced protection and automation schemes will be taught, emphasising in substations and distribution networks.
- Investment environment for Energy Systems: This group of lectures will address the channels for funding Energy Supply and Saving Systems. Additionally, will provide the trainees with the qualification for more efficient sales of Energy Systems in both National and International level. In the beginning of the project this item was not considered as required, the response of the questionnaires however, revealed the need for increased focus on these items. Special focus should be given on the capability of finding resources for extending the grid.

4. Conclusions

MESfIA will impact a variety of target groups like teaching staff, trainees, technical staff, graduate students and professional groups dealing with power systems. The expected impacts are ranging from local to international level:

- Local level and Regional Level: As the partner Universities are not at the same city for the same country, regional centres of excellence will be created at each country.
- National Level: Each one of the three countries will have the ability to have well-defined paths for providing the knowledge for mastering in energy supply in their isolated areas. This is in line with their needs. Additionally, via the training of trainees and the strong collaboration of EU and Partner countries universities two major areas of the planet will converge in terms of education in power systems.
- International Level: The collaboration among universities will help mutual understanding among EU countries and South East Asia organizations. Workshops and Conferences in the greater area of South East Asia will make EU and especially academic activities widespread known to this area. The

organization of lectures will also help EU universities realize potential adaptation of their MSc in their continuous assessment of their own curricula.

By the end of the project, graduates from the MSc program in the Partner Countries Higher Education Institutions (HEIs) should be able to claim their expertise on improving energy supply conditions in isolated areas. An ambition of the project is to attract students from areas with problems in energy supply and prepare them to have activity in the energy sector in their own homeland. As South-East Asia is a bridge between Asia and multi-island Pacific Area, students from these areas could be reached as well as a follow-up of this project.

All partner universities are ready to adapt the new MSc degrees and training programs they offer so that their graduates can claim they have masters focusing on Supplying Isolated Areas. Their role includes preparation of the learning outcomes, course contents and assessment tools. Further, partners from Europe may replicate the methodology to other island countries themselves or on their own islands and enhance their training material.

Some of these solutions could be applied in stronger power systems as well.

Acknowledgements. This work is supported by Erasmus+ Program of the European Union, Project No. 598716-EPP-1-2018-1-EL-EPPKA2-CBHE-JP. www.mesfia.eu

REFERENCES

- [1] Renewable Energy Policy Network. *Energy for Development: The Potential Role of Renewable Energy in Meeting the Millennium Development Goals*, World watch Institute, Washington DC, 2005
- [2] United Nations Economic and Social Council. 2019. “*Special Edition: progress towards the Sustainable Development Goals.*” E/2019/68, May 8. Accessed December 15, 2019. <https://undocs.org/E/2019/68>.
- [3] Brasington, Louis. 2018. “*Power to the People: Remote Microgrids Across Southeast Asia.*” Accessed December 15, 2019. <https://www.cleantech.com/power-to-the-people-remote-microgrids-across-southeast-asia/>.
- [4] V.S. Modi, D. McDade, C. Lallement, and J. Saghir, *Energy and the Millennium Development Goals*, World Bank, New York, 2006
- [5] UN General Assembly. 2015. “*Sustainable Development goals. SDGs, Transforming our world: the, 2030 Agenda for Sustainable Development Response of the Stakeholder Group of Ageing.*” <https://sustainabledevelopment.un.org/content/documents/7945ageing.pdf>
- [6] N. D. Hatziaargyriou, A. Tsikalakis, A. Androutsos, “*Status Of Distributed Generation In The Greek Islands*”, In proc of the 2006 IEEE PES General Meeting 18-22 June 2006, Montreal, Canada, PESGM2006-00368.
- [7] Southeast Asia Energy Outlook, International Energy Agency, 2017
- [8] Bangladesh Rural Electrification Board, <http://www.reb.gov.bd/> Accessed December 28, 2019.
- [9] Antonios Tsikalakis and Terpsihori Tzouliadaki, “*Chapter 9. Electrification of Rural Areas using Renewable Energy Sources: Review of Best Practices Around the World*” In *Renewable Energy: Economics, Emerging Technologies and Global Practices*, Edited by Andreas Poullikkas, in Nova Publishers, 2013. ISBN: 978-1-62618-264-6, pp 197-246.
- [10] Electricity beyond the grid, Cooper global power & utilities, 2016
- [11] <http://talos-ts.com/index.php/the-station/location>

NUMERICAL SIMULATION OF A HYBRID SOLAR GEOTHERMAL ENERGY SYSTEM USED FOR AN ENERGY POSITIVE BUILDING

Tiberiu CATALINA^{1,2,*}, Robert GAVRILIUC^{1,2} and Corina GHERASIM¹

¹Technical University of Civil Engineering, Faculty of Building Services Bucharest Romania

² Romanian GEOEXCHANGE SOCIETY Romania (www.geoexchange.ro)

Abstract. *This article is intended to be a clear demonstration of the benefits of implementation of multiple renewable energy sources to cover the energy needs of a residential building. The simulated building in this article is the EFDeN Signature building and represented Romania at SolarDecathlon Dubai 2018 competition. By using a double U heat exchanger inside a 100 m borehole and connected to a 5kW heat pump, the total CO₂ emission reduction was calculated to be 3786 kg/year, while the 62.1 m² solar photovoltaic panels produced 11522 kWh/year covering entirely the building energy demands.*

Keywords: geothermal heat pump, nZEB building, EFdeN Signature, SolarDecathlon competition.

1. Introduction

According to the latest reports, the energy consumption in the European Union (EU) continued to increase for the third consecutive year, thus moving away from energy efficiency targets. Among the main energy consumers, buildings' operation represents one of the most important ones with a share of almost 40%. It is clear that EU policies and directives are focused on this particular field that can make a huge difference for the coming years. Multiple guidelines and standards were elaborated to promote the use of renewable energy resources (RES) or to build constructions with nearly zero energy consumptions and entitled nZEBs (Nearly Zero Energy Buildings) or even energy positive ones. The main energy consumption of a building is needed to ensure a comfortable indoor environment, thus heating & cooling represents almost 50%, while the rest is divided between appliances (11-13%), lighting (10-12%), domestic water heating (12-14%), computers and electronics (3-4%) and other (10-11%). To reach the goal of nZEB the need to better insulate the building or to use RES is no longer optional but mandatory. The use of numerical simulations or accurate measurements are needed when converting or better said upgrading an existing building to the nZEB standards [1]. Not only the purpose is to reduce the energy consumption but finally to reduce the carbon emissions and the need of dynamic life cycle assessment is one of the best options

to have a global view on the nZEB solutions [2]. During a study [3] made in Hong Kong, the authors proposed the use of building integrated photovoltaics, wind turbines and thermal energy storage to reach the nZEB goal. Paduos and Corrado [4] analysed 107 retrofit solutions for existing buildings suitable for the nZEB target and found out that there are buildings that cannot respect the minimum use of RES requirements imposed by the standards. An interesting evaluation of different solutions to improve the energy efficiency was made for a Greek residential building [5] using energy simulations. It was found that correct insulation, windows, and shading devices can decrease the energy consumption by 30% and enable the reduction of the annual energy demand to less than 50 kWh/m²/year. The use of RES plays a major role in achieving the nZEB standard and among the most used RES geothermal and solar energy are mentioned. Shallow geothermal energy is one of the promising solutions that will attract funding for the next decade [6]. The use of simulations to predict the performances of geothermal heat pumps is preferred by many researchers including the one mentioned in [7] where the authors found out that a geothermal solution can reduce up to 43% the energy consumption of an office building and also reduce the CO₂ emission by 7 kg/m²/year.

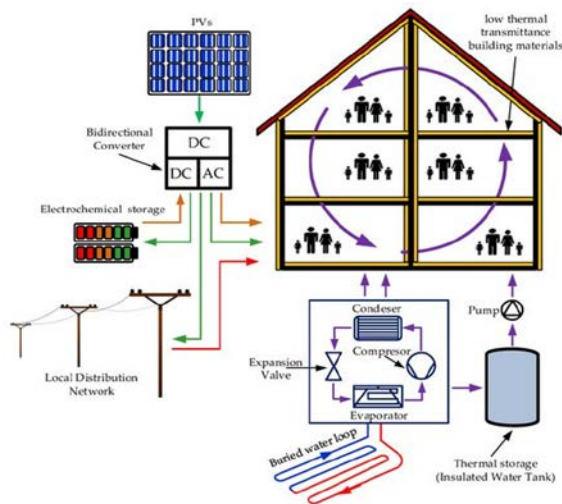


Fig. 1 – Schematic illustration of a HVAC system for a nZEB building [8]

The use of a geothermal source heat pump (GSHP) combined with solar thermal or photovoltaic panels is one of the combinations which allows reaching the nZEB standard. Figure 1 presents the proposed system [8] for a multi-family building located in Athens and it was found out that this is an efficient RES combination.

2. Study case presentation

The evaluated building in this paper is the EFDeN Signature building and it represented Romania during the largest competition of solar houses SolarDecathlon in Dubai, UAE in 2018. The building structural system combines prefabricated modules for slabs, load-bearing walls, and beams for added resistance. It was specially tailored to an open and continuous architectural space. The solution was to use a mix of three structural systems: Cross Laminated Timber, Timber Frame and Glued Laminated Wood. The house was constructed as a cell structure, designed as a multi-layered skin envelope which acts as a protective barrier from the harsh environment. The building respects all the nZEB standards in terms of thermal insulation, as all opaque envelope elements were insulated with top quality mineral wool with a thermal conductivity of 0.035 W/mK. Avoiding thermal bridging was also a key-point of the structure and building insulation as Passive House certified joineries system were used. The wooden structure - unlike concrete or steel ones - was found to be an excellent solution for thermal insulation, and it helped reducing thermal bridging.

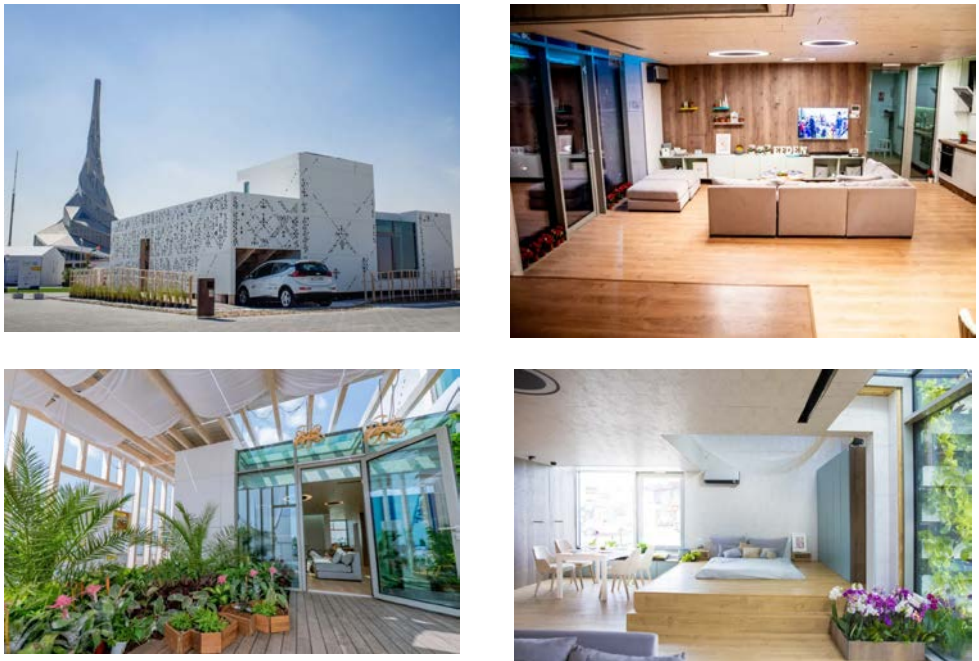


Fig. 2 – EFDeN Signature photos (www.efden.org).

As windows are in most cases the weak thermal points of a building, special focus was needed and finally the EFDeN Signature project was equipped with triple glazing panels Cool-lite Xtreme 60-28 II with 90% Argon buffers, a “g” solar factor of 0.28 and a U-value of 1.0 W/m²K. As indoor air quality is also an important criterion in nZEB

buildings, fresh air is supplied through a heat and humidity recovery unit. The mechanical ventilation is monitored and controlled by air quality sensors, to ensure that the CO₂ concentration is below 800 ppm and that humidity is between 30% and 60%. Unlike typical enthalpic recovery units, the model used in the EFDeN Signature house is a plate heat exchanger made of desiccant fibbers, thus the sound power is considerably reduced. The use of Renewable Energy Sources (RES) - like solar energy - is another key point of the building. The solar-powered photovoltaic system is designed to meet the consumption requirements of the house to reach a positive energy balance. This target is achieved by planning the energy strategies and by thoroughly using passive and active systems. The house system consists of 4 photovoltaic strings with 8 polycrystalline solar modules of 280 Wp each, which makes a total peak power of 8.96 [kWp]. These four strings enter 2 by 2 into the string inverters. During daytime, when solar production reaches the highest levels, the produced electricity is used on-site to fuel the heat-pump, the house appliances and other smaller electric consumers (e.g. laptop or building management system). The over production of electricity is not injected in the network but stored in batteries using LiFePO₄ as technology with highest discharge capacity (almost 100%), so that the storage capacity (13.8 kWh) can be used almost entirely. Logically, the main strategy adopted is self-consumption, which is the act of consuming only the energy you have produced. This strategy works best when one has a positive balance and, in general, for the whole year, the energy balance is positive, which is in line with the project strategy. Based on numerical simulations the main energy consumptions of the house are represented by the heating energy - 4195 kWh/ year, the pumping energy - 1711 kWh/year and the mechanical ventilation energy - 65 kWh/year.

3. The Hybrid solar geothermal system

While during the SolarDecathlon competition the main solution for air-conditioning was the use of a classic air-to-air heat pump, for the new improved version the proposed heating/cooling system for the EFDeN Signature house is composed of a 5 kW geothermal heat pump and a single 100 m borehole with an estimated thermal production of 50 W/m. The system was defined for 4 people in a 150 m² built area and 74 m² usable area, with a daily consumption of 200 litres/day of domestic hot water in a house with low energy consumption, located in Bucharest Pache Protopopescu Street no. 66. The total energy requirement, excluding domestic hot water, is 4195 kWh, and the room temperature is set at 20°C during winter period and 26°C during summer. The 5 kW heat pump is mounted inside the heated area, with a heat loss of approximately 5% and a nominal seasonal coefficient of performance (COP) of 4.3. As concerns the shallow geothermal heat exchanger, this one is composed of a 32 mm double U heat exchanger in a single borehole drilled at a depth of 100 m. The ground heating potential is 0.08°C and a temperature gradient of 0.03 K/m. The borehole is filled with bentonite to allow better heat transmission between the ground heat exchangers and the ground,

but also to maintain temperature uniformity and structural resistance of the borehole. The heat pump is connected to a buffer tank of 700 litres. The heating&/cooling terminals are air fan coils with a heating power of 1700 W and a cooling power of 1100 W.

4. Numerical simulations

Nowadays the building is in the construction phase in the courtyard of the Faculty of Building Services Bucharest and the assembly process will reach its final stages during October 2020. As numerical simulations are excellent solutions to predict the potential of energy production and system design, the research team decided to use the well-known Swiss energy modelling software called PolySun. For this project, the numerical tool was found to be a reliable and professional platform for simulating renewable energy systems like geothermal or solar. The system was configured and assembled using predefined elements like the heat pump, borehole, buffer tank or solar PV panels. Figure 2 presents a schematic view from the PolySun simulation platform for the proposed system of the EFdeN Signature house.

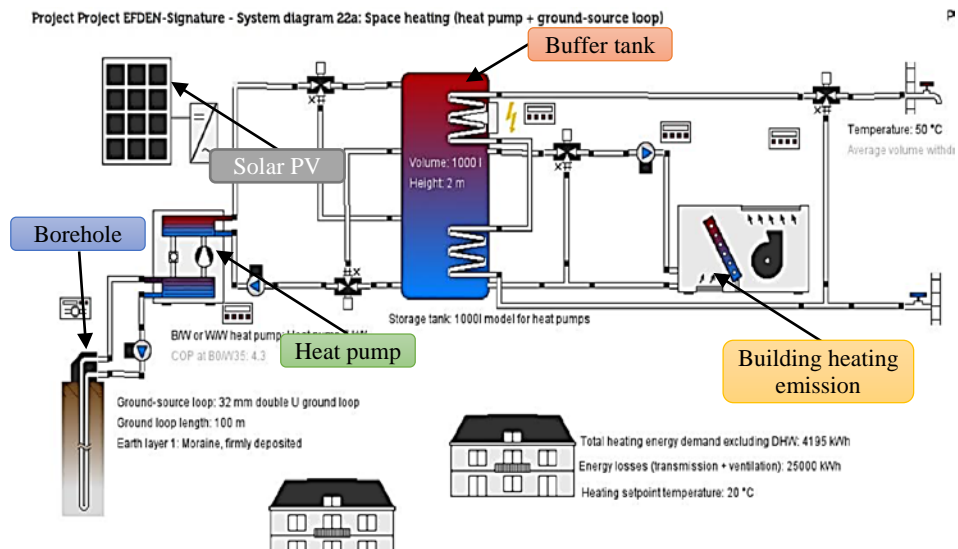


Fig. 3 – Schematic view of the main systems elements in PolySun Simulation Tool.

The energy reduction has a clear impact on the CO₂ savings and these ones were calculated based on the Romanian standards (conversion factor 2.62 from final energy to primary energy for the electricity and afterwards multiplied by the emission factor 0.299 kg CO₂/kWh). From Table 1 it can be concluded that the solar PV panels have a

net production of 11522.5 kWh and thus the CO₂ emissions reduction are near to 9 tonnes CO₂/year. As concerns the geothermal heat pump the calculated seasonal factor was found to be 3.7, with an electricity consumption of 1797 kWh and a total reduction of CO₂ of almost 4 tonnes CO₂/year.

Table 1
Overview photovoltaics (annual values)

Characteristic	Results
<i>Total gross area</i>	<i>62.1 m²</i>
<i>Energy production DC</i>	<i>12388.5 kWh</i>
<i>Energy production AC</i>	<i>11522.5 kWh</i>
<i>Total nominal power DC</i>	<i>8.96 kW</i>
<i>Performance ratio</i>	<i>79.6%</i>
<i>Specific annual yield</i>	<i>1.286 kWh/kWp</i>
<i>Total reduction in CO₂ emissions</i>	<i>9026 kg</i>

The double U ground source heat exchanger, as mentioned previously, has a length of 100 m, an inlet temperature during operation of 2.7°C and an outlet temperature during operation of 5°C. It is responsible for an energy withdrawal from the ground-source loop of 4844 kWh, thus completely ensuring the building heating energy demand of 4195 kWh.

Table 2
Overview heat pump (annual values)

Characteristic	Results
<i>Seasonal performance factor (without pump energy)</i>	<i>3.7</i>
<i>Total electricity consumption when heating</i>	<i>1797 kWh</i>
<i>Ground loop length</i>	<i>100 m</i>
<i>Energy withdrawal of the ground-source loop</i>	<i>4844 kWh</i>
<i>Total energy savings</i>	<i>4833 kWh</i>
<i>Total reduction in CO₂ emissions</i>	<i>3786 kg</i>

The pump for the space heating loop has a flow rate of 321 l/h and a final electricity consumption of 73.5 kWh. On the other hand, the pump of the heat source has an energy consumption of 61.4 kWh. The storage tank buffer is made of steel and insulated with 80 mm rigid PU foam and thus the heat losses are 330 kWh. As concerns the monthly distribution of the energy production (see Figure 3) it can be noticed that the highest energy production is supplied in August with a value of 1246 kWh while the minimum in December with 501 kWh. The total energy consumption of the building in terms of HVAC system (heat pump, circulation pump, BMS) without appliances are covered 100% for the whole year. In fact, the PV system produces more energy than needed with a value of 9566 kWh/year and hence the building not only reached the nZEB standard but even the energy positive standard.

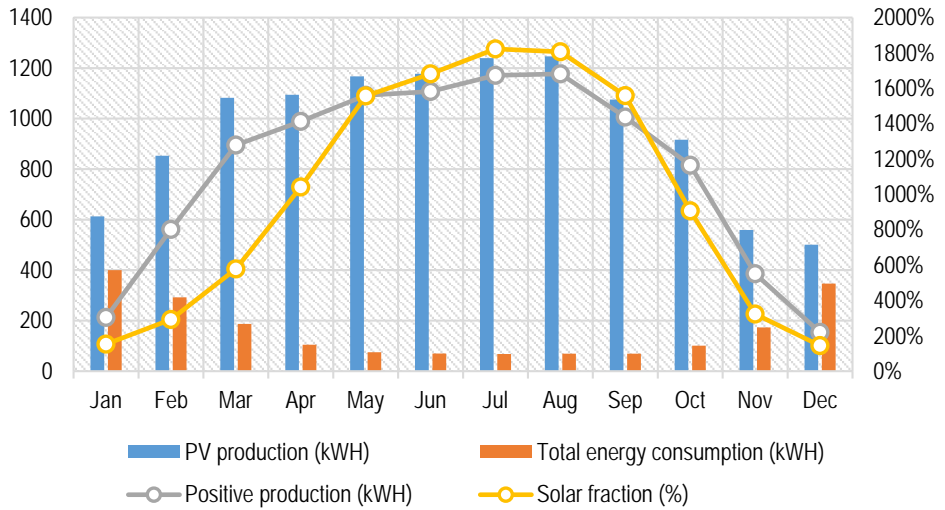


Fig. 4 – Photovoltaic solar energy production versus total energy consumption

As the main energy consumption of the building is needed for heating the building, the GSHP supplies the demanded energy for heating and DHW purposes. It can be seen from Figure 4 that the maximum heating demand is found for January with 1408 kWh.

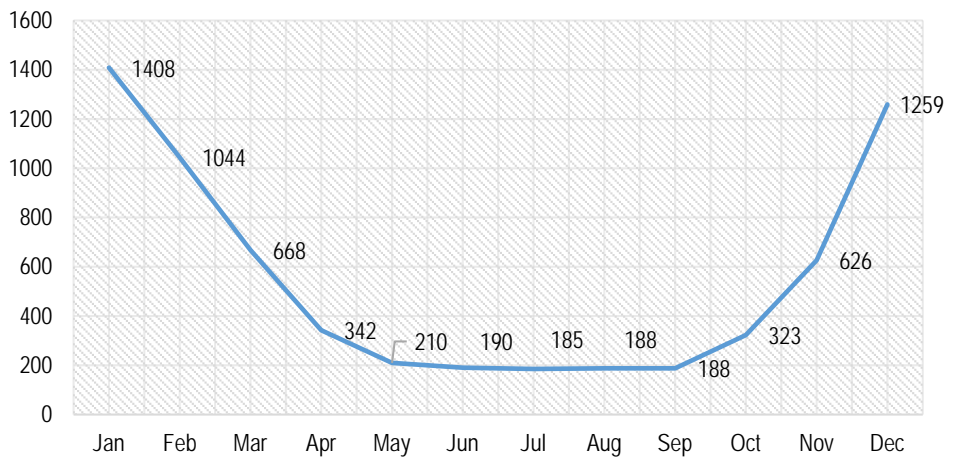


Fig. 5 – Energy to the system provided by the GSHP (kWh)

4. Conclusions

In this paper it was presented a solar house called EfDeN Signature supplied with a geothermal heat pump to cover the heating/DHW energy demand of the building. The 5kW heat pump and a 100 m double U ground source heat exchanger were found out to be the right combination to ensure full coverage of the energy demand. The numerical simulations proved that the solar house has an energy production from the solar photovoltaic panels of 11522 kWh/year, thus not only covering the total energy consumption of the building, but moreover over-producing by 9566 kWh/year. The total CO₂ emission reduction obtained from the use of the two RES systems (geothermal heat pump and solar photovoltaic panels) is almost 13 tonnes CO₂/year classifying this building as one of the best in Romania in terms of environment protection. The building itself is currently under construction and in October 2020 it will be monitored and the experimental results will serve as validation for the numerical simulations.

Acknowledgements. The authors would like to acknowledge the work performed by the team of students who participated with the EFdeN Signature project at SolarDecathlon Dubai 2018, but also the work done by the students who are currently assembling for the 3rd and final time the building in Bucharest, Romania.

REFERENCES

- [1] S. Charisi, *The Role of the Building Envelope in Achieving Nearly-zero Energy Buildings (nZEBs)*, Procedia Environmental Sciences, Volume 38, 2017, Pages 115-120
- [2] F. Asdrubali, P. Baggio, A. Prada, G. Grazieschi, C. Guattari, *Dynamic life cycle assessment modelling of a NZEB building*, Energy, Volume 191, 2020, 116489
- [3] Y. Zhou, S. Cao, *Investigation of the flexibility of a residential net-zero energy building (NZEB) integrated with an electric vehicle in Hong Kong*, Energy Procedia, Volume 158, 2019, Pages 2567-2579
- [4] S. Paduos, V. Corrado, *Cost-optimal approach to transform the public buildings into nZEBs: an European cross-country comparison*, Energy Procedia, Volume 140, 2017, Pages 314-324,
- [5] S. Charisi, *The Role of the Building Envelope in Achieving Nearly-zero Energy Buildings (nZEBs)*, Procedia Environmental Sciences, Volume 38, 2017, Pages 115-120
- [6] S. Chen, Q. Zhang, H. Li, B. Mclellan, T. Zhang, Z. Tan, *Investment decision on shallow geothermal heating & cooling based on compound options model: A case study of China*, Applied Energy, Volume 254, 2019, 113655
- [7] W. Lyu, X. Li, S. Yan, S. Jiang, *Utilizing shallow geothermal energy to develop an energy efficient HVAC system*, Renewable Energy, Volume 147, Part 1, 2020, Pages 672-682
- [8] F. Kotarella, A. Kyritsis, N. Papanikolaou, *On the Implementation of the Nearly Zero Energy Building Concept for Jointly Acting Renewables Self-Consumers in Mediterranean Climate Conditions*, Energies, Volume 13, Issue 5, 2020, 1032

ANALYSIS OF THE COOLING EFFECT ON THE EFFICIENCY OF THE PHOTOVOLTAIC PANELS

Sebastian Valeriu HUDIȘTEANU^{1,*}, Nelu-Cristian CHERECHEȘ¹, Cătălin-George POPOVICI¹, Marina VERDEȘ¹, Vasilică CIOCAN¹, Marius-Costel BALAN¹ and Florin-Emilian ȚURCANU¹

¹Gheorghe Asachi Technical University of Iași, Faculty of Civil Engineering and Building Services, Iași, Romania

Abstract. *The paper presents the analysis of the cooling of a photovoltaic (PV) panel integrated on the facade of buildings, in vertical position, for different orientations: South, South-East and South-West. The effect of the cooling of PV panel is presented comparatively for the basic case, the case of the PV location apparently on the building facade, without the possibility of ventilation on its rear area and also for the integration in the ventilated facade of the building. Finally, the optimal solutions for obtaining passive cooling by using air and heat sinks or active cooling by using water film exchanger are evaluated. The study aims to evaluate the efficiency of PV panels according to climatic conditions and does not concern the operation of the entire photovoltaic system.*

Keywords: BIPV, passive cooling, active cooling, conversion efficiency.

1. Introduction

Photovoltaic conversion has important advantages, considering that the energy source is renewable and free, and the processes of electricity production do not have a negative impact on the environment (CO₂ and NO_x emissions, waste, noise etc.). The generation of electricity is done without the use of moving parts, determining reduced maintenance costs. The energy produced is consumed locally, which results in low power losses [1].

The Building Integrated Photovoltaics (BIPV) concept consists in placing PV panels on the roof or facades of buildings [2]. The integration is justified if the main advantages of the local production and consumption of electricity are analysed, which imply reduced energy losses and the possibility of complex use of electricity and heat. By increasing energy generation and reducing consumer losses, a reduction in CO₂ and NO_x emissions and environmental protection are achieved, maintaining the same comfort conditions for occupants.

One of the main problems concerning the operation of photovoltaic panels is the significant increase of their operating temperature which causes an important drop of

conversion efficiency [3-5]. The decrease of the efficiency and of the produced power related to the increase of the temperature have values between -0,46...-0,50%/°C and -0,47...-0,50%/°C, respectively [6, 7].

As the power of a photovoltaic cell is influenced by the temperature and radiation levels, the standard test conditions (STC) parameters were defined: $t_{cell} = 25^{\circ}\text{C}$, $G = 1000 \text{ W/m}^2$, AM1.5. In STC the PV panels produce the Watt-peak power [Wp], but a real concern is that in regular operation, at 1000 W/m^2 , the photovoltaic panels can reach temperatures of $80...90^{\circ}\text{C}$ [8], leading to a significant decrease of the efficiency.

Experimental tests on monocrystalline or polycrystalline photovoltaic panels, that show the decrease of the efficiency as the operating temperature increases and the necessity of cooling solutions are current concerns in the literature [6, 7]. Most of the studies on the cooling of photovoltaic panels [9-11] are also focused on the usage of the thermal energy extracted as a result of this process, so that the recovery time of the investment is less than of the stand-alone photovoltaic systems.

The simultaneous conversion of solar energy into electric and thermal energy using photovoltaic-thermal panels is known in the literature as PVT (Photovoltaic-Thermal System) [9]. A particular feature of this solution is the BIPVT concept, which implies the integration of photovoltaic-thermal panels into buildings [10, 11]. The generation of two of the most used types of energy is performed in such conditions in which the operation of each of the two systems is beneficial to the other, with priority to the production of electricity and ensuring the efficiency of photovoltaic conversion. The PVT concept is commercialized as hybrid photovoltaic solar panels, passive cooling solutions with polymeric films or ventilated cooling systems [12].

This study presents the performance analysis of a photovoltaic panel integrated in the facade of a building, for different locations in Romania: Bucharest, Cluj-Napoca, Iasi and Timisoara. The four large cities have different climatic conditions, in a national context, being located on variable latitudes and longitudes. The study aims to evaluate the performance of photovoltaic panels according to climatic conditions and does not concern the operation of the entire photovoltaic system.

2. Numerical modelling

The numerical simulation was performed in the TRNSYS modelling environment, and the purpose of the study is to determine the energy efficiency of the photovoltaic panel under the conditions of integration in double skin façade (DSF) and its temperature reduction. The model is created by using the following blocks: climatic data, photovoltaic panel model, conversion elements of the units of measurement and units for calculating and displaying the output quantities.

There are analysed the operating parameters of a photovoltaic (PV) panel, integrated on the facade of a building, at a height of 10 m above the ground, while the results are

reported to the surface area [W/m^2] and [kWh/m^2]. The photovoltaic panel consists of 36 solar cells connected in series.

The PV panel is modelled using Type 94 of TRNSYS software, recommended in modelling monocrystalline or polycrystalline silicon modules. For a more realistic analysis, the four parameters model is used [13, 14], which takes into account both series and shunt resistances, R_s and R_{sh} .

The value for the output current of the PV cell is determined with the following expression, Eq. 1:

$$I = I_{ph} - I_D \left(\exp \frac{q(V + R_s I)}{nKT_{cell}} - 1 \right) - \frac{(V + R_s I)}{R_{sh}} \quad (A) \quad (1)$$

For the same hypothesis, the open circuit voltage of the cell can be determined using Eq. 2:

$$V_{oc} \cong \frac{nKT_{cell}}{q} \ln \left(\frac{I_{ph}}{I_D} + 1 \right) \quad (V) \quad (2)$$

Where, I - current produced by PV cell [A];

I_{ph} - photocurrent produced by PV cell [A];

I_D - reverse saturation current of diode [A];

q - electric charge of electron [C];

V - voltage on diode terminal [V];

R_s - series resistance [Ω];

n - ideality factor;

K - Boltzmann constant, $K = 1.38 \cdot 10^{-23} [\text{J} \cdot \text{K}^{-1}]$;

T_{cell} - operating temperature of PV cell [$^{\circ}\text{C}$];

R_{sh} - shunt resistance [Ω];

V_{oc} - open circuit voltage [V].

The PV panel cooling is achieved by using some of the most widespread solutions in the literature: heat sink [8] and water film changer [15], attached to the back of the panel. The efficiency is determined in the conditions of cooling the photovoltaic panel to a temperature as close as possible to the nominal one, of 25°C . In order to obtain more intuitive results, a standard PV panel of 100 Wp is analysed. Table 1 shows the dimensional characteristics and parameters of the analysed photovoltaic panel [16].

Table 1
Photovoltaic panel parameters, input data and output data from the model

PV panel parameters	Input data	Output data
Surface of PV: $S_{PV} = 0,89 \text{ m}^2$;	- PV orientation:	- PV panel efficiency;
Short-circuit current: $I_{sc} = 6,5 \text{ A}$;	- S, S-E, S-W;	
Open-circuit voltage: $V_{oc} = 21,6 \text{ V}$;	- PV position: -	- maximum power, current and voltage generated;
Maximum power: $P_{mp} = 100,3 \text{ W}$	horizontal, vertical;	
Current at P_{mp} : $I_{mp} = 5,9 \text{ A}$;		
Voltage at P_{mp} : $V_{mp} = 17,0 \text{ V}$;	- climatic conditions:	- operating temperature of PV panel;
$t_{NOCT} = 47 \text{ }^\circ\text{C}$;	Bucharest, Cluj-Napoca, Iasi and Timisoara (TMY);	
Temperature coefficient of V_{oc} : -0,045;		
Reference temperature: $t_{ref} = 25 \text{ }^\circ\text{C}$;	- interval: annual, monthly and daily.	- power generated by PV panel.
Reference solar radiation: $G = 1000 \text{ W/m}^2$.		

Studied cases

The four locations analysed in the study represent the biggest cities of Romania and have slightly different climatic conditions according to the following coordinates:

- Bucharest (44°26'10.1"N, 26°06'03.4"E);
- Cluj-Napoca (46°46'16.6"N, 23°35'24.1"E);
- Iasi (47°09'06.9"N, 27°35'13.1"E);
- Timisoara (45°45'23.9"N, 21°13'43.2"E).

The study analysed the power produced by the photovoltaic panel for each of the four locations, for three different orientations in vertical position (South, South-East and South-West), for annual, monthly and daily study intervals.

The cooling effect of the photovoltaic panel is presented comparatively for the basic case (when the PV panel is positioned apparently on the building façade, without the possibility of ventilation in its rear area) and for the solution of integration in the ventilated facade of the building. In the end, the optimal passive cooling (air and heat sink) and active cooling (water film exchanger) are analysed.

3. Results

The influence of cooling is shown in Figure 1. The annual variation of the average operating temperature of the photovoltaic panel is presented, in a vertical-South position, for Bucharest climatic conditions. The climatic conditions used in modelling are according to the typical meteorological year, according to TRNSYS database [16]. Each simulation is realized by using a time step of 1 hour.

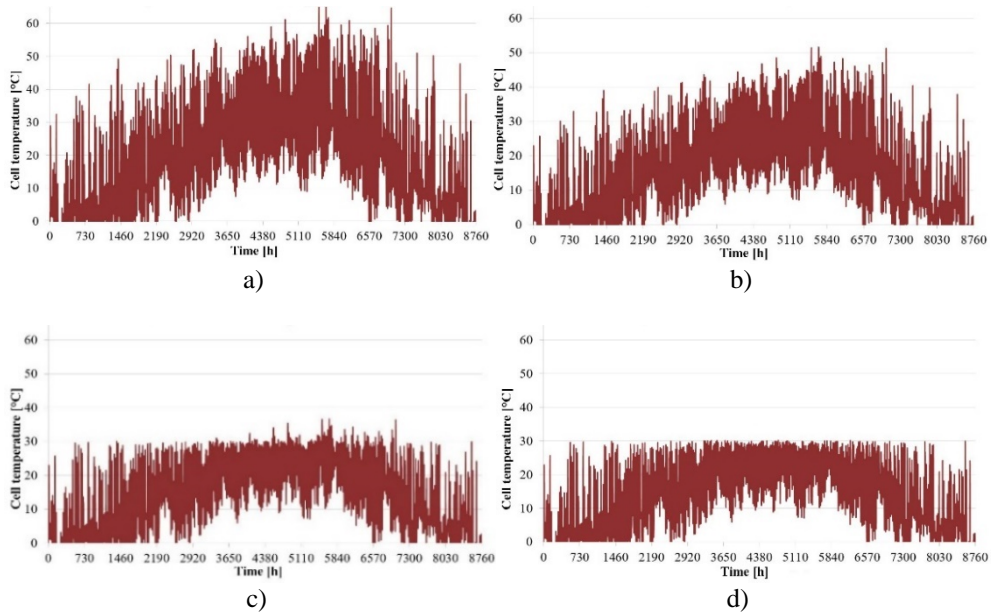


Fig. 1 - Evolution of the operating temperature of the photovoltaic panel during the year, vertical-South position, Bucharest: a) without ventilated facade; b) integrated in ventilated facade c) with heat sink; d) with water film heat exchanger.

Case 1 – Bucharest

The cooling effect of the photovoltaic panel is presented in Figure 2, which shows the electricity production obtained for one given year for each of the integration solutions proposed for Bucharest. Figure 3 shows the increase of the percentage of annual energy produced, compared to the base case.

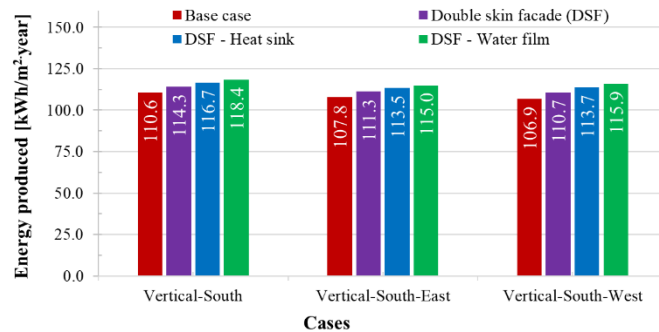


Fig. 2 - Bucharest – Energy produced one given year per surface unit according to orientation and cooling solution.

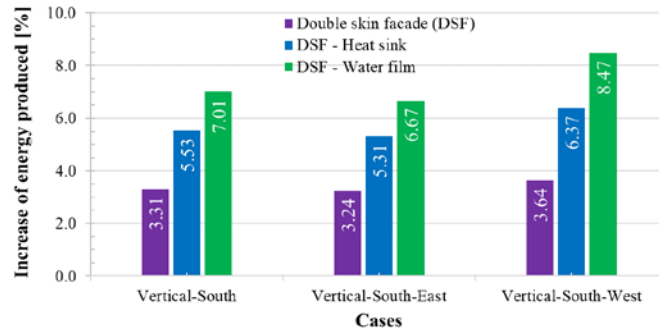


Fig. 3 - Bucharest – Additional energy produced one given year depending on the orientation and cooling solution, relative to the base case.

The cooling effect of the solutions proposed during the year, for Bucharest in the vertical position of the photovoltaic panel, can be tracked in Figure 4.

For Bucharest case, it is found that for the vertical integration of the photovoltaic panel, significant amounts of additional energy are obtained, if cooling is achieved between May and September.

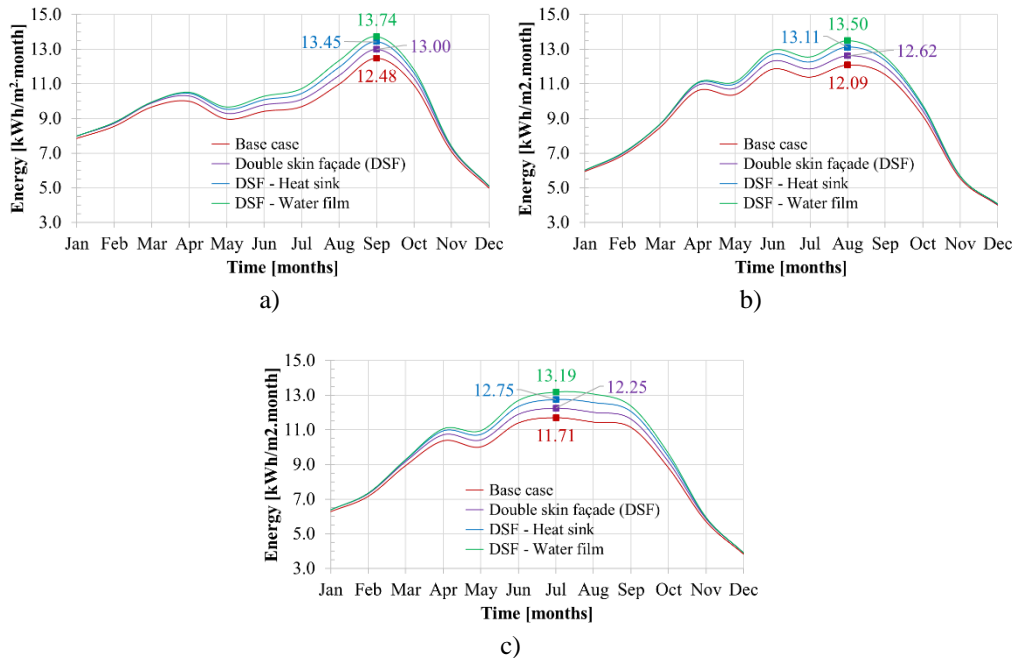


Fig. 4 - Bucharest – The effect of cooling solutions on the monthly electricity production for the vertical position of the PV: a) South; b) South-East; c) South-West.

Case 2 – Cluj-Napoca

Figure 5 shows the electricity production obtained annually for each of the integration solutions proposed for Cluj-Napoca. Figure 6 shows the increase of the percentage of annual energy produced, compared to the base case.

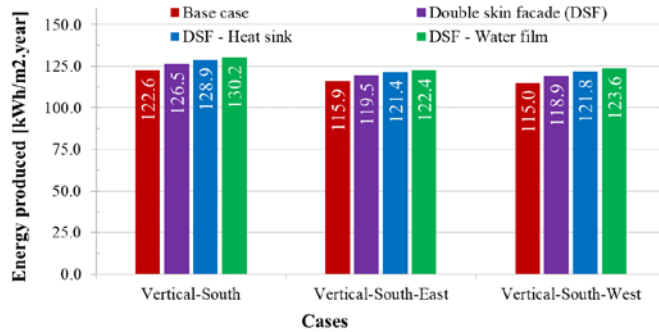


Fig. 5 - Cluj-Napoca – Energy produced one given year per surface unit according to orientation and cooling solution.

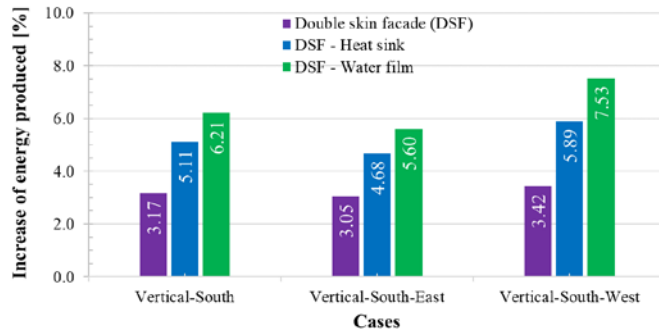


Fig. 6 - Cluj-Napoca – Additional energy produced one given year depending on the orientation and cooling solution, relative to the base case.

The cooling effect of the solutions proposed during the year, for Cluj-Napoca in the vertical position of the photovoltaic panel are presented in Figure 7.

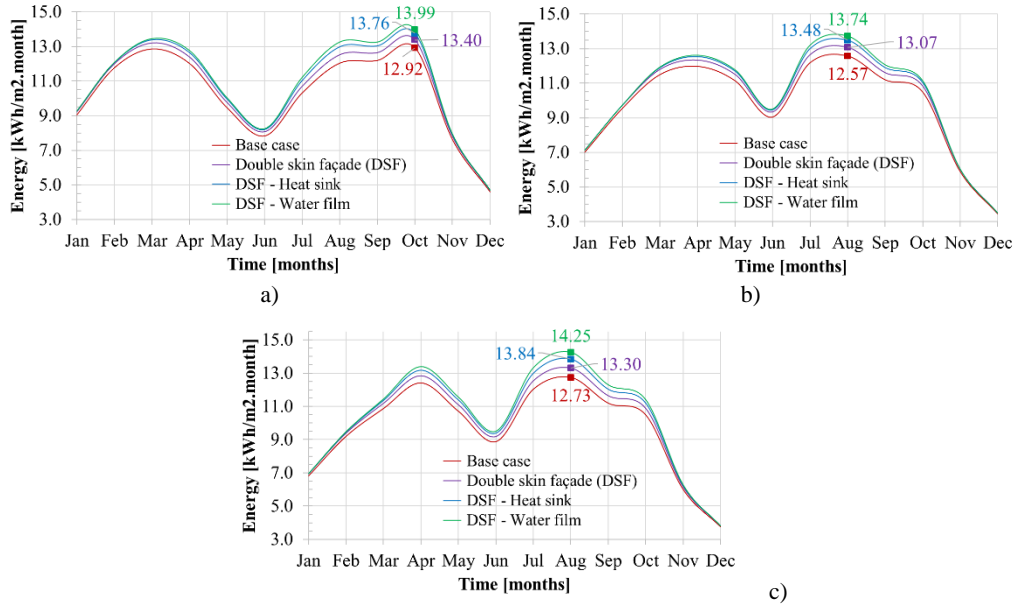


Fig. 7 - Cluj-Napoca – The effect of cooling solutions on the monthly electricity production for the vertical position of the PV: a) South; b) South-East; c) South-West.

In the case of Cluj-Napoca, it is found that for the vertical integration of the photovoltaic panel, significant amounts of additional energy are obtained if cooling is performed between July and October.

Case 3 – Iasi

Figure 8 shows the electricity production obtained annually for each of the integration solutions proposed for Iași. Figure 9 shows the increase of the percentage of annual energy produced, compared to the base case.

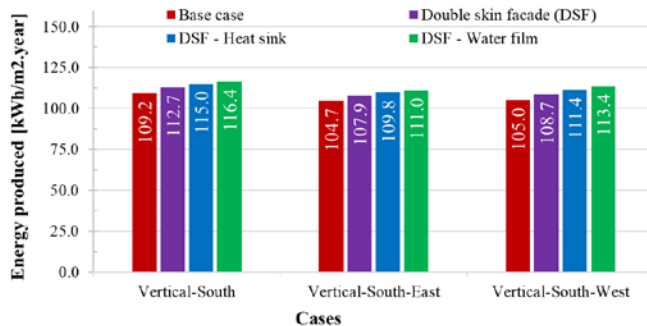


Fig. 8 - Iasi – Energy produced one given year per surface unit according to orientation and cooling solution.

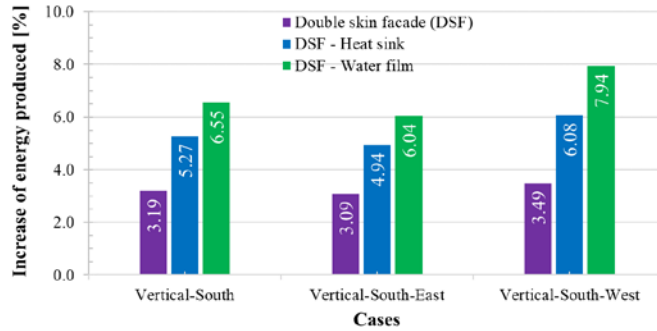


Fig. 9 - Iasi – Additional energy produced one given year depending on the orientation and cooling solution, relative to the base case.

The cooling effect of the solutions proposed during the year, for Iasi in the vertical position of the photovoltaic panel, can be observed in Figure 10.

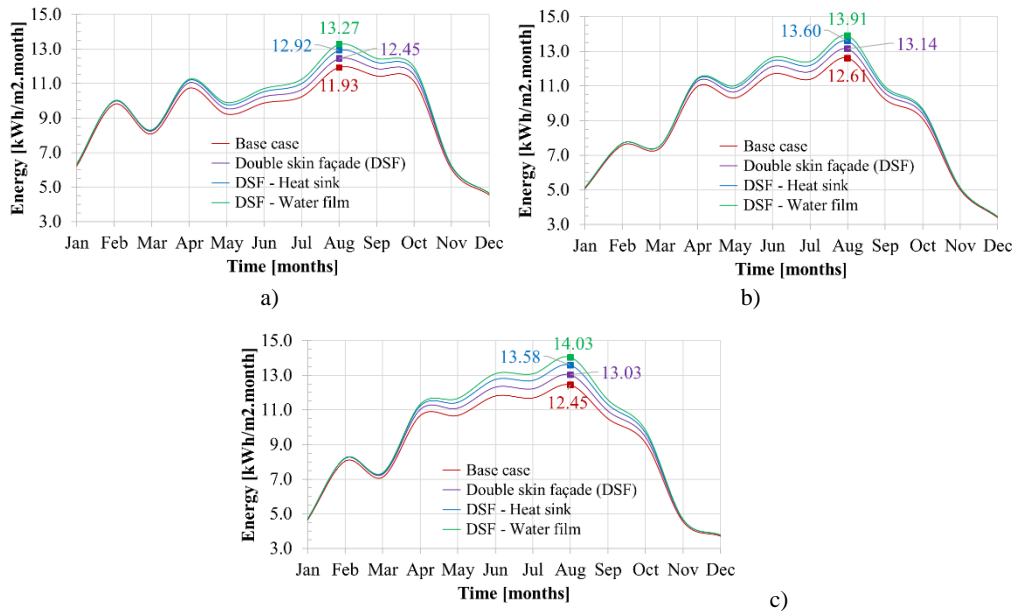


Fig. 10 - Iasi – The effect of cooling solutions on the monthly electricity production for the vertical position of the PV: a) South; b) South-East; c) South-West.

In the case of Iasi, it is found that for the vertical position of the photovoltaic panel in buildings, significant amounts of additional energy are obtained if cooling is performed between April and September.

Case 4 – Timisoara

Figure 11 shows the electricity production obtained annually for each of the integration solutions proposed for Timisoara. Figure 12 shows the increase of the percentage of annual energy produced, compared to the base case.

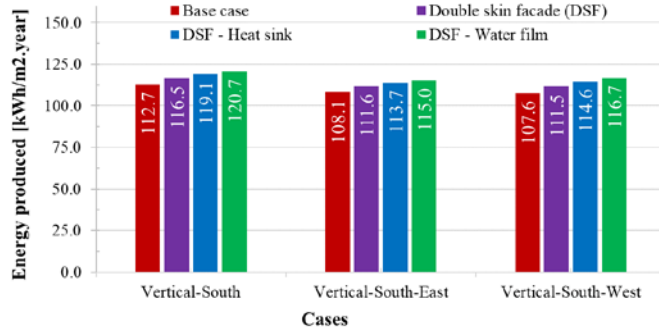


Fig. 11 - Timisoara – Energy produced one given year per surface unit according to orientation and cooling solution.

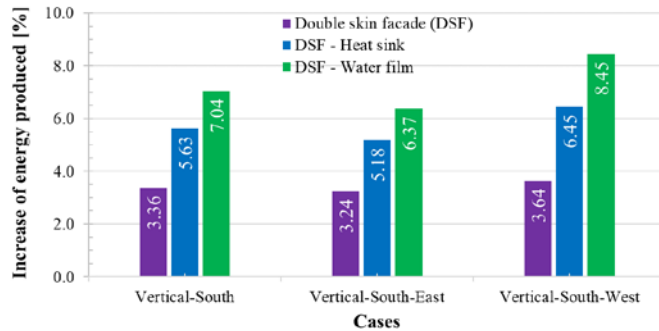


Fig. 12 - Timisoara – Additional energy produced one given year depending on the orientation and cooling solution, relative to the base case.

The cooling effect of the solutions proposed during the year, for the locality of Timisoara and the vertical position of the photovoltaic panel, can be observed in Figure 13.

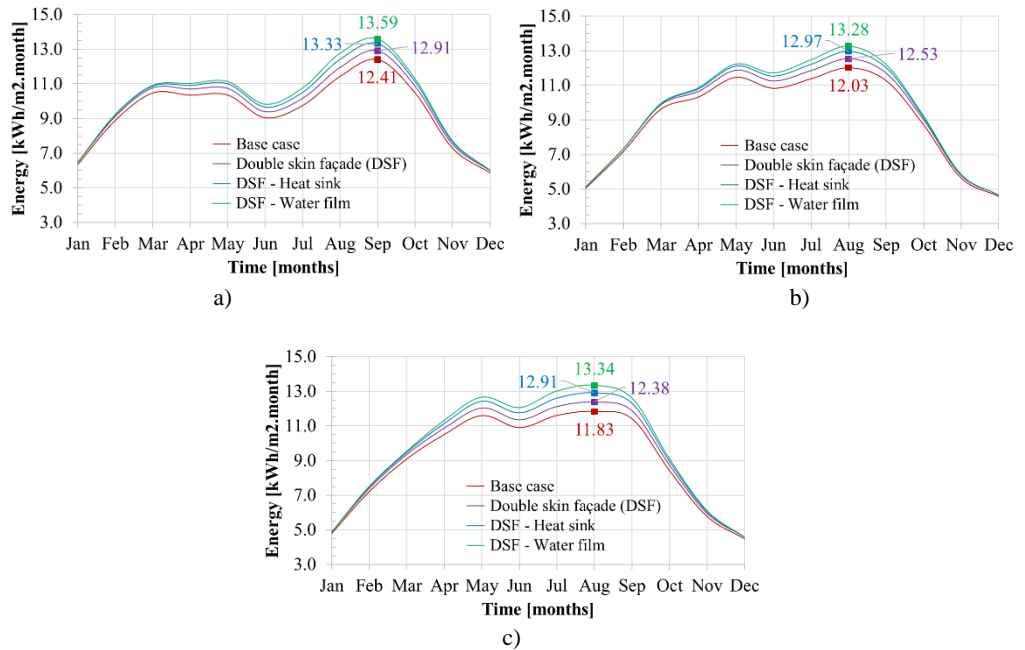


Fig. 13 - Timisoara – The effect of cooling solutions on the monthly electricity production for the vertical position of the PV: a) South; b) South-East; c) South-West.

In the case of Timisoara, it is observed that for the vertical position of the photovoltaic panel in the buildings, important amounts of additional energy are obtained if the cooling is carried out between May and September.

Highlighting the effect of cooling on the day with maximum production

The maximum daily power produced when the cooling is achieved by water film heat exchanger is presented for the case of Iasi, Vertical-South-East, August. For the day with maximum energy production, the parameters of the photovoltaic panel in the basic case are comparatively presented, Figure 14.a, in the situation of simple integration in the ventilated facade of the building, Figure 14.b, and in the situation of using the optimal variant of water film heat exchanger, Figure 14.c.

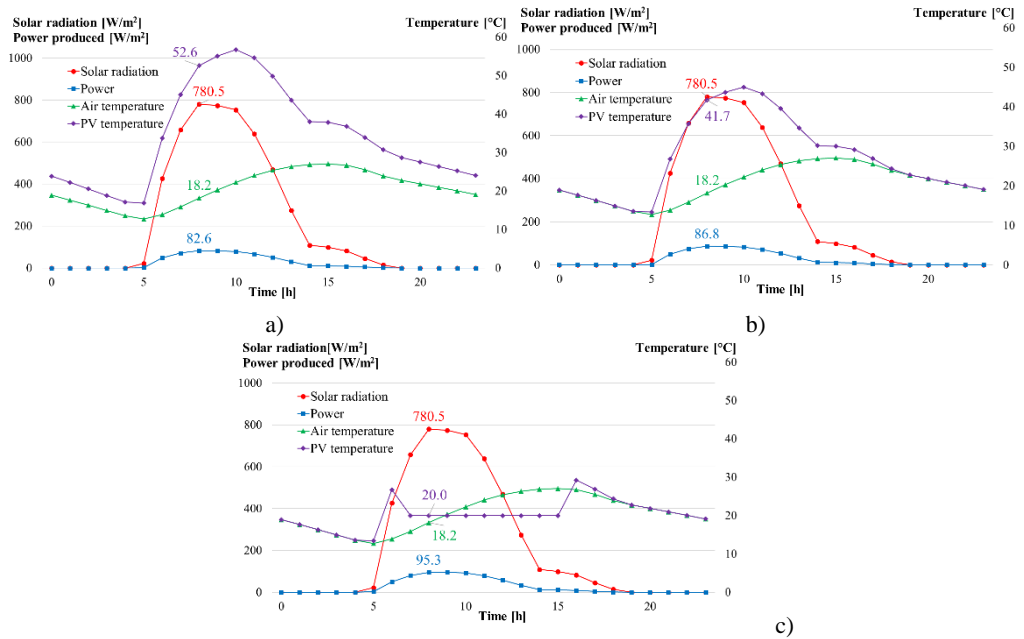


Fig. 14 - The evolution of the temperature and power produced by PV panel during the maximum day, for the vertical-South-East position in Iasi: a) basic case; b) integration in DSF; c) water film heat exchanger.

It is observed that the integration of the photovoltaic panel in the ventilated facade and the use of the water film heat exchanger determines the reduction of the operating temperature and the increase of the produced power, in the same external conditions, Figure 15.

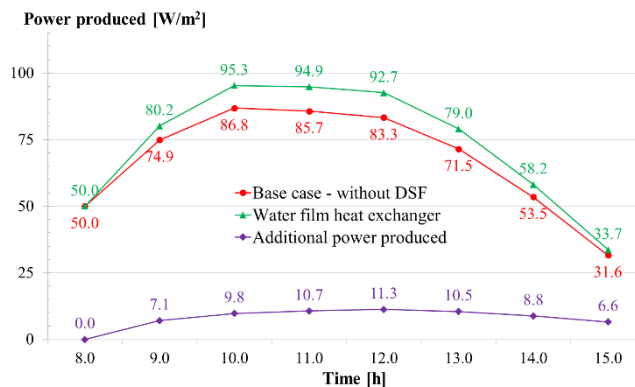


Fig. 15 - Daily analysis of PV electricity production - comparison between the optimal water film heat exchanger solution and simple integration in the ventilated façade.

For a decrease in efficiency of $-0.45\%/^{\circ}\text{C}$, according to [8], cooling may result in an increase of generated power according to Figure 15 and Figure 16.

According to Figure 15 and Table 2, if the temperature reduction of the photovoltaic panel is applied by using the water film heat exchanger between 08:00 and 15:00, the efficiency of the panel is increased, up to values of 12.38%. Consequently, the electrical power produced by the photovoltaic panel in similar sunny conditions is higher than that obtained under normal operating conditions. The energy increase over the cooling interval is approximately 47.7 Wh/m^2 , which represents an increase of 8.2% compared to the conditions of its integration in the ventilated facade.

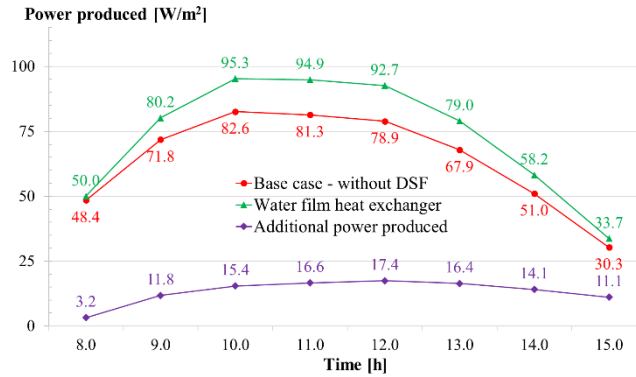


Fig. 16 - Daily analysis of PV panel electricity production - comparison between the optimal water film heat exchanger solution and the base case.

Table 2

The parameters of the PV panel in optimized conditions for Iasi - August

Interval	G_{med} [W/m ²]	T_{base} [°C]	P_{base} [W/m ²]	η_{base} [%]	T_{DSF} [°C]	P_{DSF} [W/m ²]	η_{DSF} [%]	T_{opt} [°C]	P_{opt} [W/m ²]	η_{opt} [%]
06-07	22,1	16,9	2,4	10,73	13,4	2,4	10,90	16,88	2,4	10,90
07-08	426,0	33,7	48,4	11,37	26,7	50,0	11,73	20,00	50,0	11,73
08-09	657,6	45,0	71,8	10,92	35,7	74,9	11,39	20,00	80,2	12,20
09-10	780,5	52,6	82,6	10,58	41,7	86,8	11,13	21,56	95,3	12,21
10-11	774,0	55,0	81,3	10,51	43,7	85,7	11,08	22,57	94,9	12,26
11-12	753,3	56,7	78,9	10,48	45,0	83,3	11,06	23,25	92,7	12,30
12-13	638,3	54,6	67,9	10,64	43,3	71,5	11,20	22,39	79,0	12,38
13-14	469,1	49,8	51,0	10,88	39,6	53,5	11,41	20,44	58,2	12,41
14-15	274,4	43,6	30,3	11,06	34,6	31,6	11,52	20,00	33,7	12,28
15-16	108,9	38,0	11,9	10,92	30,2	12,3	11,32	20,00	12,9	11,84
16-17	98,9	37,9	10,8	10,88	30,0	11,2	11,28	20,00	11,7	11,79
17-18	82,3	36,8	8,9	10,82	29,2	9,2	11,21	20,00	9,2	11,21
18-19	45,5	33,9	4,8	10,60	26,9	5,0	10,95	20,00	5,0	10,95
TOTAL	-	-	551	-	-	577	-	-	625	-

where, G_{med} - average intensity of solar radiation in the time interval [W/m^2];
 T_{opt} - average cell temperature under cooling conditions [$^{\circ}C$];
 η_{base} – effective conversion yield (simple integration in façade) [%];
 η_{base} – effective conversion yield (integration in DSF) [%];
 η_{opt} - optimized conversion yield (integration in DSF and water cooling) [%];
 P_{add} - the electrical power produced additionally by PV panel after cooling [W/m^2].

Table 2 presents the values of the parameters of the photovoltaic panel in the cooling conditions, for Iasi, August and the vertical-South-East position of PV panel. The determined quantities represent the averages calculated on the study time intervals. Table 3 shows the raise of power generated and efficiency of the PV panel when water cooling is achieved compared to the basic case or simple integration into the DSF.

Table 3
The effect of the water cooling of the PV panel for Iasi - August

P_{add} [W/m^2]		$\Delta\eta$ [%]	
compared to		compared to	
base	DSF	base	DSF
1,56	-	3,23	-
8,44	5,31	11,75	7,08
12,73	8,49	15,41	9,78
13,52	9,14	16,62	10,66
13,76	9,37	17,43	11,25
11,13	7,51	16,40	10,50
7,19	4,71	14,08	8,80
3,36	2,08	11,09	6,59
1,00	0,56	8,41	4,58
0,90	0,50	8,33	4,52
74,1	47,7	13,28	8,2

Comparative analysis of the cooling effect for the four locations

The productivity of photovoltaic panels depending on location and orientation is presented in Tables 4-6.

Table 4
The energy produced annually by PV panel integrated in the double-glazed ventilated façade

Orientation	Vertical-S	Vertical-SE	Vertical-SW
Bucharest	90 %	87,9 %	87,5 %
Cluj-Napoca	100 % (126,5 kWh/m²-year)	94,4 %	94 %
Iasi	89 %	85,2 %	85,9 %
Timisoara	92,1 %	88,2 %	88,1 %

Table 5*The energy produced annually by the PV panel integrated in the DSF and heat sink*

Orientation	Vertical-S	Vertical-SE	Vertical-SW
Bucharest	90,5 %	88,1 %	88,2 %
Cluj-Napoca	100 % (128,9 kWh/m ² ·year)	94,2 %	94,5 %
Iasi	89,2 %	85,2 %	86,4 %
Timisoara	92,4 %	88,2 %	88,9 %

Table 6*The energy produced annually by the PV panel integrated in DSF and water film heat exchanger*

Orientation	Vertical-S	Vertical-SE	Vertical-SW
Bucharest	90,9 %	88,3 %	89 %
Cluj-Napoca	100 % (130,2 kWh/m ² ·year)	94 %	94,9 %
Iasi	89,4 %	85,3 %	87,1 %
Timisoara	92,7 %	88,3 %	89,6 %

4. Conclusions

Taking into account that in large urban centres, the available horizontal area is limited, both at the level of buildings and on the ground, it is considered appropriate to place the vertical photovoltaic systems in the facades of buildings. For this position, the influence of the orientation of the photovoltaic panels on the energy produced annually, monthly and daily was determined. The analysis of the results regarding the integration of photovoltaic panels in buildings, for the four locations, highlighted a series of relevant data. The maximum energy output is obtained for the South orientation of the photovoltaic panel. Under these conditions, the maximum energy production is recorded for the building integration of the PV panels in Cluj-Napoca.

The annual analysis shows that the influence of the PV panel orientation has the same tendency for all the studied locations. The values range from 107.9...126.5 kWh/m²·year, with maximums recorded for Cluj-Napoca for all orientations (118.9....126.5 kWh/m²·year) and minimums for Iasi (107.9...112.7 kWh/m²·year).

Regarding the average efficiency of the photovoltaic panel, it varies between 11.54% and 11.66% for the annual analysis interval. The average efficiency, for the months of maximum production, is lower than the annual one, being located in the range 11.17...11.47%, while the values for the maximum day is even lower, of 10.82%...11,66%. These values are directly dependent on the intensity of solar radiation and negatively influenced by the operating temperatures of the photovoltaic panel.

One way to improve the efficiency of PV panel, during hot days and with increased input of solar radiation, is to reduce its operating temperature. Water cooling has the advantage of obtaining the best efficiency, the performance increase being between 5.60

... 8.47%, compared to the case of apparent integration on the building facade. However, the energy used to make the liquid flow needs to be accounted and it will be studied in further researches. This solution can be capitalized on by producing hot water for consumption. There is the possibility of using water from the cold-water supply system, being a cheap energy source with optimal parameters for an efficient heat exchange with the photovoltaic panel. Thus, the so-called hybrid PV/T (photovoltaic/thermal) systems can be obtained, using the excess heat extracted from the PV panel to preheat the domestic hot water. In the case of hybrid systems, the aim must always be to obtain the optimum efficiency for the photovoltaic panel, and to extract the excess heat by achieving the lowest possible energy consumption.

REFERENCES

- [1] S. V. Hudisteanu, T. D. Mateescu, C. G. Popovici, C. N. Chereches, “*The influence of the building integrated photovoltaic panels position on the conversion efficiency*”, Bulletin of the Polytechnic Institute of Jassy, Construction. Architecture Section, vol. 62 (66), no. 2, 2016, pp. 93-104.
- [2] S. V. Hudişteanu, C. G. Popovici, T. D. Mateescu, NC Cherecheş, “*Efficiency analysis of BIPV systems for different locations in Romania*”, Energy Procedia, vol. 112, 2017, pp. 404-411.
- [3] S. Dubey, J. N. Sarvaiya, B.Seshadri, “*Temperature Dependent Photovoltaic (PV) Efficiency and Its Effect on PV Production in the World A Review*”, Energy Procedia, vol. 33, 2013, pp. 311–321.
- [4] E. Skoplaki, J. A. Palyvos, “*On the temperature dependence of photovoltaic module electrical performance: A review of efficiency/power correlations*”, Solar Energy, vol. 83, 2009, pp. 614–624.
- [5] N. Hamrouni, M. Jraidi, A. Chérif, “*Solar radiation and ambient temperature effects on the performances of a PV pumping system*”, Revue des E Renouvelables, vol. 11, 2008, pp. 95-106.
- [6] C. Berthod, R. Strandberg, J. O. Odden, “*Temperature coefficients of compensated silicon solar cells – influence of ingot position and blend-in-ratio*”, Energy Procedia, vol. 77, 2015, pp. 15-20.
- [7] J. G. Hernandez-Perez, J. G. Carrillo, A. Bassam, M. Flota-Banuelos, L. D. Patino-Lopez, “*A new passive PV heatsink design to reduce efficiency losses: A computational and experimental evaluation*”, Renewable Energy, vol. 147, 2020, pp. 1209-1220.
- [8] C. G. Popovici, Hudişteanu S. V., Mateescu T. D., Cherecheş N. C., “*Efficiency improvement of photovoltaic panels by using air cooled heat sinks*”, Energy Procedia, vol. 85, 2016, pp. 425-432.
- [9] M. Herrando, A. M. Pantaleo, K. Wang, C. N. Markides, “*Solar combined cooling, heating and power systems based on hybrid PVT, PV or solar-thermal collectors for building applications*”, Renewable Energy, vol. 143, 2019, pp. 637-647.
- [10] A. Ibrahim, A. Fudholi, K. Sopian, M. Y. Othman, M. H. Ruslan, “*Efficiencies and improvement potential of building integrated photovoltaic thermal (BIPVT) system*”, E Conv and Manag, vol. 77, 2014, pp. 527-534.
- [11] C. Lamnatou, G.Notton, D.Chemisana, C. Cristofari, “*Storage systems for (BIPV) and building-integrated photovoltaic/thermal (BIPVT) installations: Environmental profile and other aspects*”, Science of The Total Environment, 2019, 60 pag.
- [12] <https://www.solar-depot.ro/106/Panou-solar-fotovoltaic-HIBRID>, last accessed on 03.10.2019.
- [13] Z. Wang, F. Qiu, W. Yang, X. Zhao, S. Mei, “*Experimental investigation of the thermal and electrical performance of the heat pipe BIPV/T system with metal wires*”, Applied Energy, vol. 170, 2016, pp. 314–323.
- [14] R. A. Agathokleous, S. Kalogirou, “*Double skin facades (DSF) and building integrated photovoltaics (BIPV): A review of configurations and heat transfer characteristics*”, Renewable Energy, vol. 89, 2016, pp.743-756.

- [15] V. S. Hudisteanu, T. D. Mateescu, C. G. Popovici, “*Comparative study of water film heat exchangers for cooling photovoltaic panels*”, Proceedings of The International Scientific Conference CIBv, 2015, pp. 386-392.
- [16] TRNSYS Documentation

EXPERIMENTAL INVESTIGATION ON THE OPTIMUM FILLING RATIO OF HEAT PIPES USED FOR HEAT RECOVERY SYSTEMS

Robert Ștefan VIZITIU^{1,*}, Andrei BURLACU¹, Chérifa ABID – DAVID², Alexandru ȘERBAN³, Marina VERDEȘ¹, Vasilică CIOCAN¹ and Marius BRĂNOAEA¹

¹Faculty of Civil Engineering and Building Services of Iasi

²Aix-Marseille Université, IUSTI UMR 7343, Marseille

³Faculty of Mechanical Engineering and Mechatronics of Bucharest

Abstract. Thermal energy recovery plays an important part when it comes to increasing the energy efficiency of an industrial processes or of a building. The equipment used for heat recovery has undergone gradual improvements over time, one of the most significant being the introduction of heat pipes as part of their components. In order to optimize the functioning of heat recovery systems, it is important to use heat pipes suitable for the temperature and the nature of the heat source. This study consists of an experimental analysis of the filling ratios of copper heat pipes which are going to be used in the design of a heat recovery system. Distilled water is used as working fluid and the vacuum inside was made using a vacuum pump. A number of 20 heat pipes were designed and manufactured with 5 different filling ratios: 15 ml, 20 ml, 36 ml, 48 ml and 72 ml, the last one representing 50% of the internal volume of the shell. The evaporator of the heat pipes was introduced in hot water and the temperature variation on the adiabatic and the condenser zone was measured on different heights for one hour. The results showed that the tested thermosyphons have the best efficiency when the fill ratio is 25%.

Keywords: Heat pipe, Thermosyphon, Working fluid, Fill ratio, Optimization

1. Introduction

Heat pipes are a very efficient mean for transferring significant quantities of heat at high rates. The main components of a heat pipe are the external shell, the working fluid and the wick. The material used for the shell usually has a high thermal conductivity and the working fluid is chosen based on the applications of the heat pipes. Inside the shell the pressure is very low so that the working fluid can evaporate at lower temperatures than usual. When the evaporator is heated, the working fluid turns into vapours and transfer the heat to the condenser. The vapours will turn into liquid droplets and return to the initial zone either through a wick or gravitationally. The gravitational heat pipe is also known as thermosiphon and it is widely used mainly because of its low costs of production. Figure 1 presents the working principle of a thermosiphon

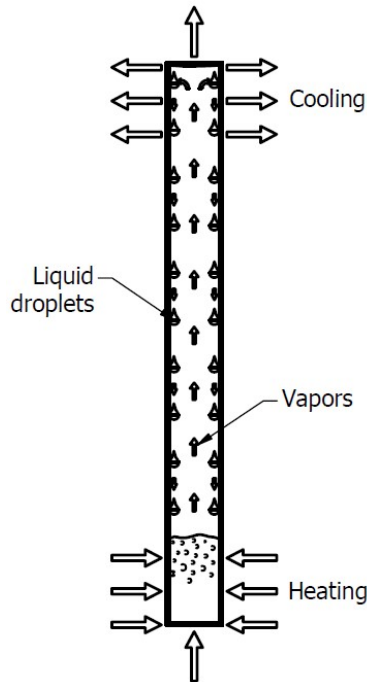


Fig. 1 – Thermosiphon

In order to have an efficient heat pipe, the filling ratio must be optimized. There are certain studies that analyse this aspect either numerically or experimentally, but most of them are focused on wicked heat pipes.

A research made in 2018 [1] studied how the filling ratio affects the thermal performance of a neon cryogenic oscillating heat pipe which is 480 mm long and has an external diameter of 2 mm. The thermal conductivity was higher at lower filling ratios such as 15.3%, 22.1%, 28.9% and 35.9% but when the heat input was higher, the heat pipes with filling ratios of 43.1% and 51.5% had better efficiencies.

Another study [2] investigated a 200 mm pulsating heat pipe which uses helium as working fluid with different filling ratios and orientations. The results of the investigation revealed that the optimum filling ratio is depending on the heat input and is somewhere between 48.8% and 66.1%.

A miniature loop heat pipe which uses distilled water as working fluid was tested with several filling ratios and the experiments proved that the optimum percentage is 30% [3]. Aly et al. [4] tested a helically-micro-grooved heat pipe filled with either water or and Al₂O₃ nanofluid under several inclination angles and with diverse fill ratios. When the filling ratio increases, the thermal resistance decreases and better performances were obtained using the nanofluid.

A study from 2018 [5] concluded that the best fill ratio for a cryogenic nitrogen heat pipe is around 20%. A heat pipe which uses R-134a as working fluid had the best efficiency at a fill ratio of 15% at a heat flux of 5.92kW/m² [6].

There are also several studies aimed to find the optimum filling ratio for different types of thermosiphons [7, 8, 9]. A team of researchers [10] investigated how the fill ratio and inclination angle is affecting the thermal performance of a thermosiphon. When the evaporator was filled to 65%, the thermal resistance of the gravitational heat pipe recorder the lowest value. Another study regarding thermosiphons [11] revealed that higher fill ratios are limiting the ability to transfer heat but is advantaging in avoiding the evaporator dryout.

The range of applications where heat pipes are used is very diverse. The most common and well known use of these devices is at solar collectors [12], but they are also an important part of different types of heat recovery systems [13] [14].

This study consists of an experimental analysis of the filling ratios of heat pipes which are going to be used in the design of a heat recovery system.

2. Experimental setup

The equipment used in the experiment consists of a box filled with 18 liters of water which are heated by an electric resistance of 1800W. There were designed and manufactured 20 heat pipes with a length of 1m and an external diameter of 0.015m, filled with distilled water at different percentages as shown in Table 1. The material used for creating the thermosiphons was copper with a thickness of 1mm.

Table 1
Heat pipes used in the experiments

No. of heat pipes	Volume of working fluid [ml]	Fill ratio [%]
4	15	10
4	20	15
4	36	25
4	48	33
4	72	50

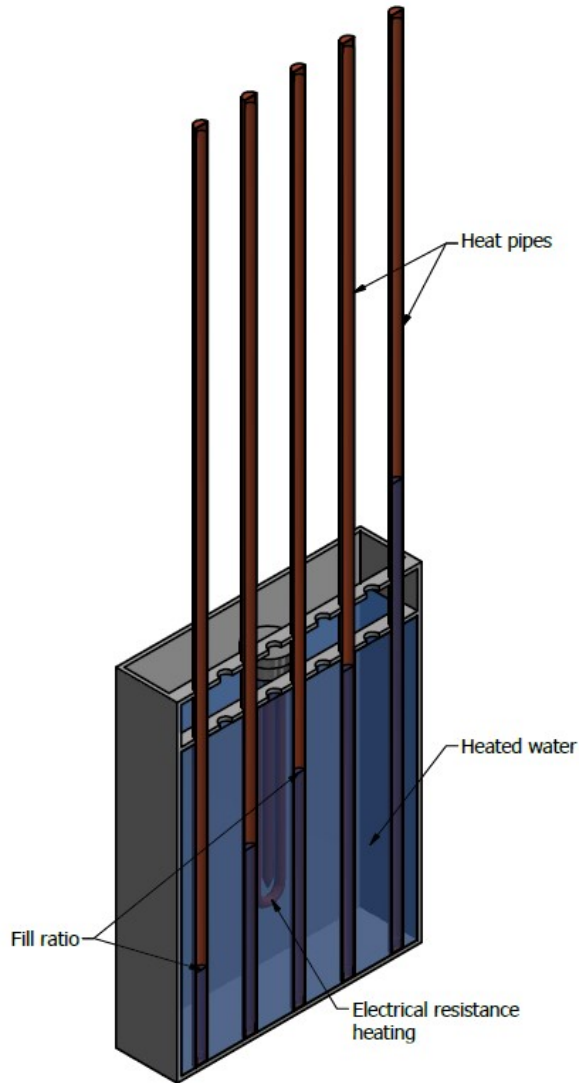


Fig. 2 – The experimental setup in 3D

Figure 2 presents a mid-plane section of a 3D geometry of the experimental setup.

On each heat pipe there are 4 temperature sensors at 0.60m, 0.70m, 0.80m and 0.90m, connected to an electronic thermometer model LT BTM-4208SD which has a precision of $\pm 0.4\%$. Since there are tested 4 heat pipes at a time and a thermometer only has 12 channels, there were used two devices.

The temperature of the water that is heated is measured with a thermal probe connected to one of the electronic thermometer. Since there are 4 heat pipes from each category of filling ratio, 5 tests were done using the same parameters. First the temperature sensors were sink in a thermo-conductive paste and then they were attached to the heat pipes at the mentioned heights (Figure 3).

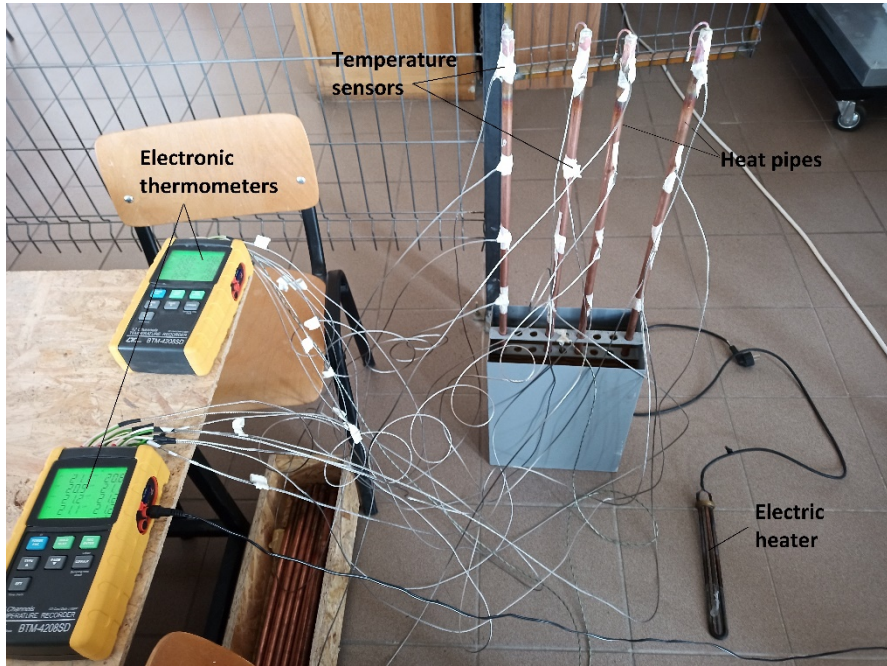


Fig. 3 – The experimental setup in the laboratory

The measurements recording began when the electric heater started heating the water. The initial value of the temperature of the fluid was about 20°C. When it reached 80°C, the heat source was removed and the water started cooling. The thermometer kept recording every 1 minute for 1 hour.

3. Discussions and conclusions

3.1. Discussions

For the first case when the filling ratios was 15ml, the highest temperature recorded on the heat pipes was 63.3°C. The peak temperature was recorded after 26 minutes. As we can observe in Figure 4, at the temperature at the top of the heat pipes is lower than the one recorded by the other 3 sensors. The results were similar for the other 3 heat pipes with the same fill ratio.

For the heat pipes filled with 20ml of distilled water, the results were similar to the ones filled with 15ml. The temperature peak was 65°C after 27 minutes. The main difference between these two cases is the longitudinal temperature variation. There can be observed for case 2 that there is a slight difference between the sensors applied at 0.8m, 0.7m and 0.6m, compared to case 1 when the temperature is almost constant in those 3 points.

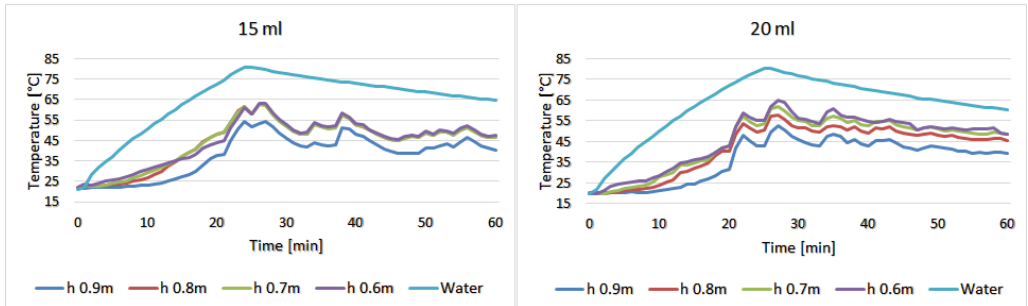


Fig. 4 – The heat pipes with filling ratios of 15ml and 20ml

The optimum filling ratio proved to be the one with 36ml. The peak temperature was 71.6°C after 23 minutes and except for the sensor place at 0.90m, the other 3 sensors recorded almost the same temperature. In figure 5 there can be observed an almost linear heating and cooling of the heat pipe, with very few sudden variations of temperature and very small, compared to the other cases.

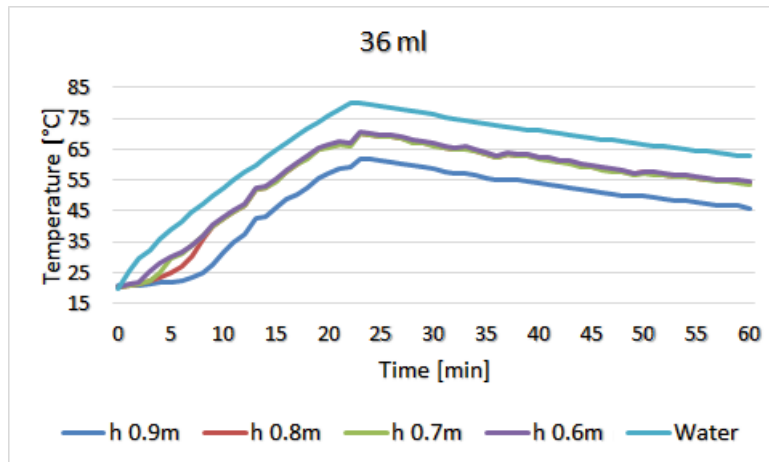


Fig. 5 – The heat pipe with a filling ratio of 36ml

The heat pipe filled with 48ml was the least efficient. The peak temperature was only 56.3°C, and the difference of temperature between all 4 sensors was small. The heat

pipe filled with 72ml had a pea temperature of 66.9°C but the temperature variations recorded by the sensors were very high, which means the heat pipe is not able to maintain a constant pace during the charging or discharging process (Figure 6).

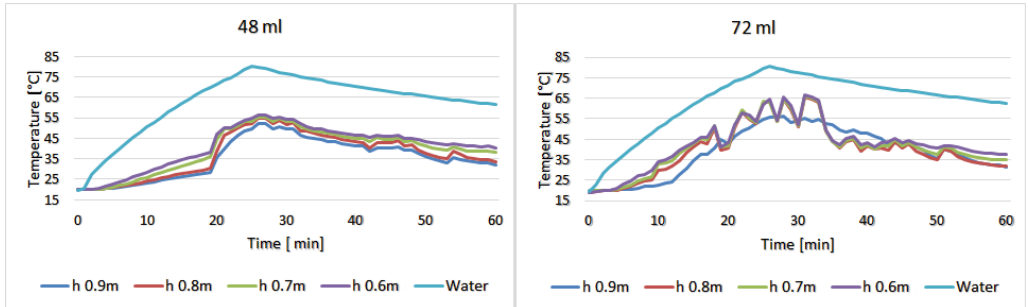


Fig. 6 – The heat pipes with filling ratios of 48ml and 72ml

3.2. Conclusions

Heat pipe technology is used in many heat recovery systems to improve the efficiency of the equipment. The purpose of this research was to find the optimum fill ratio of a 1m long copper thermosyphon which uses distilled water as working fluid by experimental testing. The filling ratios chosen for the experiment were 10%, 15%, 25%, 33%, 50. It is concluded that the best fill ratio for the tested heat pipe is 25%.

The results will be used for choosing the suitable heat pipes for a heat recovery system which recovers waste thermal energy from hot fluids.

Further researches may be done by varying the material used for the shell of the heat pipe or by varying the dimensions and the working fluid.

REFERENCES

- [1] Q. Liang, Y. Li and Q. Wang, "Effects of filling ratio and condenser temperature on the thermal performance of a neon cryogenic oscillating heat pipe," *Cryogenics*, vol. 89, pp. 102-106, 2018.
- [2] D. Xu, L. Li and M. Li, "Effect of filling ratio and orientation on the performance of a multiple turns helium pulsating heat pipes," *Cryogenics*, vol. 100, pp. 62-68, 2019.
- [3] T. Tharayil, L. G. Asirvatham, V. Ravindran and S. Wongwises, "Effect of filling ratio on the performance of a novel miniature loop heat pipe having different diameter transport lines," *Applied Thermal Engineering*, vol. 106, pp. 588-600, 2016.
- [4] W. I. Aly, M. A. Elbalshouny, H. A. El-Hameed and M. Fatouh, "Thermal performance evaluation of a helically-micro-grooved heat pipe working with water and aqueous Al₂O₃ nanofluid at different inclination angle and filling ratio," *Applied Thermal Engineering*, vol. 110, pp. 1294-1304, 2017.
- [5] L. D. Fonseca, F. Miller and J. Pfothner, "Experimental heat transfer analysis of a cryogenic nitrogen pulsating heat pipe at various liquid fill ratios," *Applied Thermal Engineering*, vol. 130, pp. 343-353, 2018.
- [6] T. Sukchana and C. Jaiboonma, "Effect of Filling Ratios and Adiabatic Length on Thermal Efficiency of Long Heat Pipe Filled with R-134a," *Energy Procedia*, vol. 34, pp. 298-306, 2013.

- [7] Z. Q. Long and P. Zhang, "Impact of cooling condition and filling ratio on heat transfer limit of cryogenic thermosyphon," *Cryogenics*, vol. 52, pp. 66-76, 2012.
- [8] M. K. Kim and C. I. Bang, "Comparison of flooding limit and thermal performance of annular and concentric thermosyphons at different fill ratios," *Applied Thermal Engineering*, vol. 99, pp. 179-188, 2016.
- [9] Z. Tong, X.-H. Liu, Z. Li and Y. Jiang, "*Experimental study on the effect of fill ratio on an R744 two-phase thermosyphon loop*," *Applied Thermal Engineering*, vol. 99, pp. 302-312, 2016.
- [10] A. A. Alammam, R. K. Al-Dadah and S. M. Mahmoud, "Numerical investigation of effect of fill ratio and inclination angle on a thermosiphon heat pipe thermal performance," *Applied Thermal Engineering*, vol. 108, pp. 1055-1065, 2016.
- [11] Y. Liu, Z. Li, Y. Li, Y. Jiang and D. Tang, "*Heat transfer and instability characteristics of a loop thermosyphon with wide range of filling ratios*," *Applied Thermal Engineering*, vol. 151, pp. 262-271, 2019.
- [12] A. Shafieian, M. Khiadani and A. Nosrati, "*A review of latest developments, progress, and applications of heat pipe solar collectors*," *Renewable and Sustainable Energy Reviews*, vol. 95, pp. 273-304, 2018.
- [13] J. Zhao, W. Jiang and Z. Rao, "*Thermal performance investigation of an oscillating heat pipe with external expansion structure used for thermal energy recovery and storage*," *International Journal of Heat and Mass Transfer*, vol. 132, pp. 920-928, 2019.
- [14] H. Yang and J. Wang, "Experimental study on a pulsating heat pipe heat exchanger for energy saving in air-conditioning system in summer," *Energy & Buildings*, vol. 196, pp. 1-6, 2019.

ENERGY EFFICIENCY MONITORING OF AN EARTH-SHELTERED HOUSE AFTER 4 YEARS OF USE

George TARANU^{1,*}, Ligia Mihaela MOGA² and
 Ionut Ovidiu TOMA¹

¹Department of Structural Mechanics, Faculty of Civil Engineering and Building Services, Technical University „Gheorghe Asachi” of Iasi, Romania

²Department of Civil Engineering and Management, Faculty of Civil Engineering, Technical University of Cluj-Napoca, Romania

Abstract. *The paper presents the results of monitoring the behavior of a house protected from the ground in terms of energy efficiency after four years of use. The building was built between 2012-2015, being made of ceramic blocks walls confined with reinforced concrete elements, and as a top closing building envelope component, a green roof system is implemented. It is situated near Iasi, in the North East of Romania. Starting with the summer of 2015 the house was inhabited by a family having four members. Wood was used as fuel for heating during the cold season. Thus, the average amount of four seasons consumption is compared with the one of a traditional/ conventional house.*

Keywords: earth-sheltered house, energy efficiency, living comfort

1. Introduction

An earth-shelter building is a structure (usually a house) with earth (soil) in direct contact with the walls, on the roof, or that is entirely buried underground. Earth acts as thermal mass, making it easier to maintain a steady indoor air temperature and therefore reduces energy costs for heating or cooling. Earth sheltering became relatively popular after the mid 1970's, especially among environmentalists. However, the practice has been around for nearly as long as humans have been constructing their own shelters. [1], [2], [3], [4].

The hovel is a type of semi-buried house, known in Romania as “bordei” and in neighboring countries under the name borrowed from Romanians. It is the oldest known permanent dwelling in Romania, identified in archaeological sites from prehistory to the present day. It coexisted from antiquity until after the First World War with the surface house, dominating the Danube plain. [5]

According to standard STAS 6054/85, in Romania the frost depth is between 0.70 m and 1.10 m below ground level. Because below the freezing depth of the soil, the earth's

temperature is relatively constant, around 8-12° C, substantial savings are made in the energy demand for heating this type of house in winter, or cooling during summer.

In 2012, the author, as the beneficiary of a new home, decided to build a modern hovel in Romania, near the city of Iasi, thus being among the first constructions of this type in the area. The town of Iasi is situated in the III-rd climatic zone which is defined by an exterior temperature of -18°C as defined by the Romanian climatic map [5] After three years the construction was ready to be inhabited by a family of 4 members.

2. Building layout, used construction materials, heating and air ventilation systems

The house has a footprint on the ground around 222 square meters, as shown in figure 1, and a height regime of two floors. The basement, as presented in figure 2, has the function of a garage having one exterior wall on the North side with a large door with 3,00 mx 2,20 m. The building envelope is described by the green roof, the walls in contact with the ground, the walls in contact with the exterior, and the slab on the ground. At the basement the walls in contact with the ground and the floors are made of reinforced concrete.

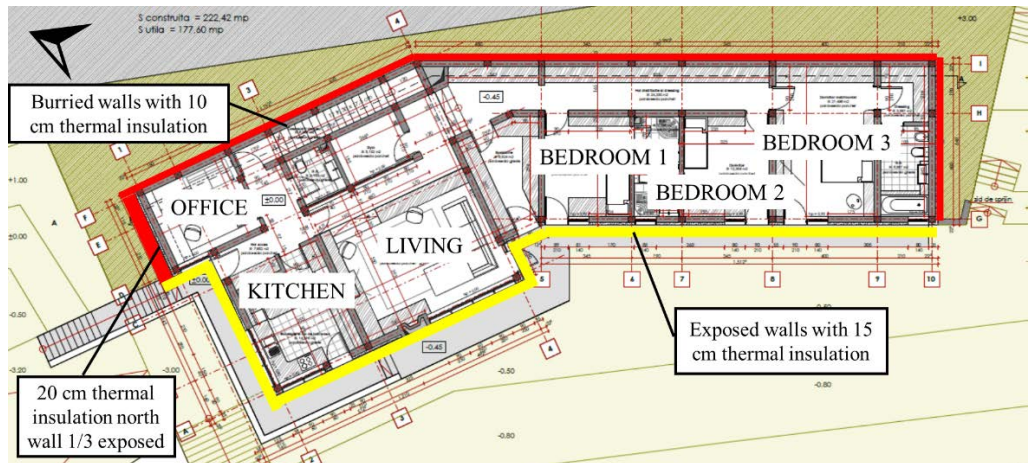


Fig. 1 - Ground level of the earth-sheltered house

A thermal insulation of 10 cm thickness is placed on the exterior side of the walls and under the bottom floor. Additionally, a waterproofing system is also mounted on the exterior side. The ground level has two lateral facades in contact with exterior. The longitudinal façade with windows and doors is oriented on South-West. The other lateral is in contact with the exterior on 30% on the North direction. [6]



Fig. 3 Structural ceramic walls



Fig. 4 Pipe system for natural ventilation

For the fresh air demand a piping system was mounted, as presented in figure 4. There are 3 pipes with 110 mm diameter with the length between 30 m to 50 m. The pipe system has a 3 meters' level difference between the ends.

The heating system was based on a wood stove of a 24 kW nominal power. For increased autonomy and less time in the wood supply for the stove, it was mounted a 1000 l tank puffer. During the winter season from October close to May, the hot water was provided by the heating boiler which has one coil and one electric resistance of 3 kW. The heating system is presented in figure 5.

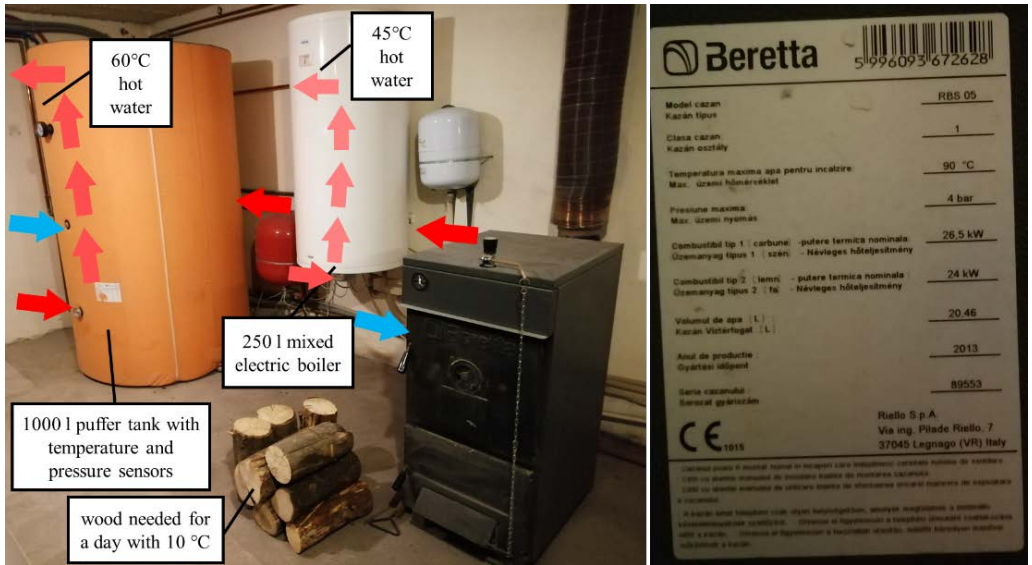


Fig. 5 Heating system mounted in the garage

Table 2
List of radiators

Room	Dimensions (h x l mm)	Power (w)	Surface (m ²)
Basement Office	600 x 600	840	10.53
Upper Office	900 x 900	1260	10.53
Kitchen	600 x 600	840	14.31
Living	800 x 800 + 600 x 800	2520*	38.20
Bedroom 1	600 x 900	1260	12.30
Bedroom 2	600 x 900	1260	12.35
Bedroom 3	800 x 1200	2700	21.46
Bathroom 1	300 x 500	300	3.16
Bathroom 2	300 x 500	300	3.16
Bathroom 3	300 x 500	300	3.16
Bathroom 4	600 x 900	600	6.38
Hall 1	600 x 200	300	7.85
Hall 2	600 x 900	1260	24.23
TOTAL		12480	167.62

**used only when the outside temperature under - 15°C*

The radiators are made of aluminum as it can be seen in figure 6, having the characteristics mentioned in table 1. The chimney for smoke evacuation of the stove was mounted in a combined system of two stainless steel pipes with 200 mm diameters.

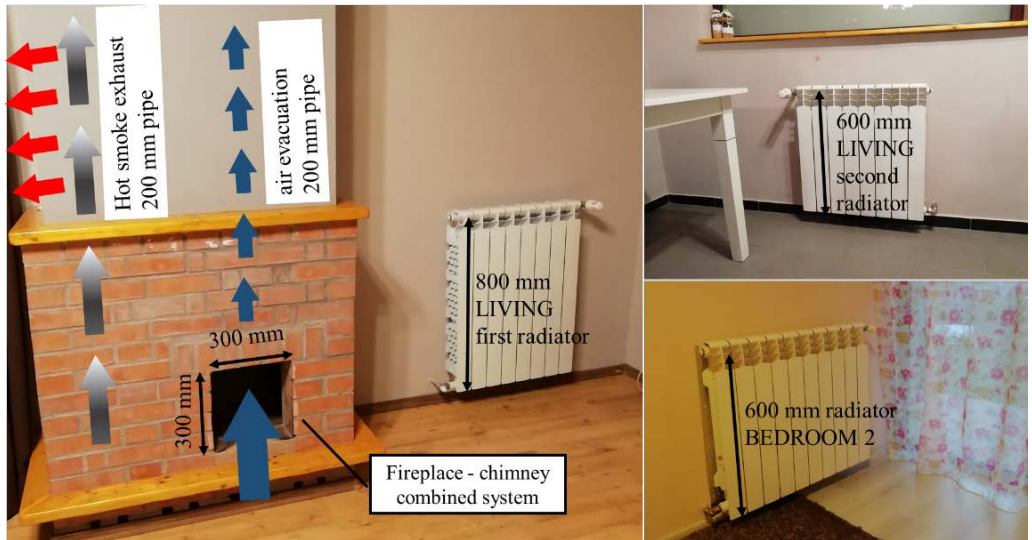


Fig. 6 Chimney included in fireplace system and aluminum radiators

The exterior of the house is presented in figure 7. The vegetation is completely indigenous and natural. There is no irrigation system. On the facade exposed to the sun (South-West) there are trees that are offering shading in the evening for the facades directly exposed to solar radiation.



Fig. 7 Exterior of the house in 2019

2. Measurement recordings during operation

Starting from the first year of operation, i.e. the summer of 2015, it was observed that the initial humidity value was around 70%...80% caused by the building materials, like mortar and finishing materials moisture. For monitoring purposes, were mounted five sensors for the interior and exterior temperature and humidity measurements. These were monitored for four years from summer of 2015 to winter of 2019, during 4 winters

and 4 summers. Some examples of recordings are presented in fig. 8 indicating at the same moment an increased exterior temperature on the exposed façade of 52.8°C and a temperature of 27.3°C on the interior living room. The black thermometer shows similar reading during winter time. These temperatures were measured in the exterior environment and the living room in 2016, during summer and winter.



Fig. 8 - Thermometer sensors

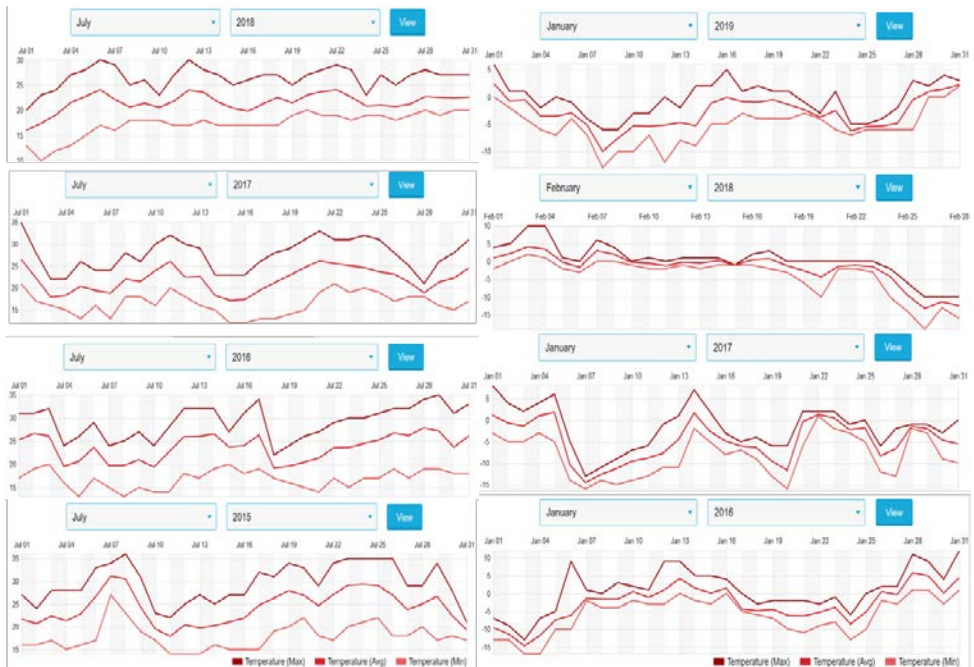


Fig. 9 Temperature history in July and January 2015 – 2019 [8]

3. Results and Discussion

Every year during summertime, quantities varying from 14 m³ to 18 m³ of wood were bought. The total amount and the monthly wood consumption on each season are presented in figure 10. For the interior temperature values of 22 up to 23°C, the wood consumption depended on the outdoor weather which has been presented in figure 9 which represent de outside temperature variation in July an January/ February from 2015 to 2019.

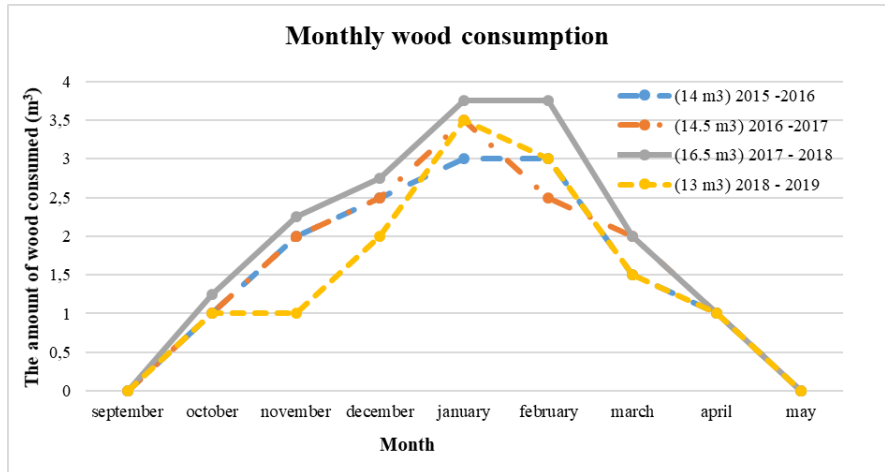


Fig. 10- Monthly wood consumption data

For an average of 14,5 m³ amount of wood in 4 years, the total heating energy was 30450 kW/year. Considering the heating system efficiency at 80% the annual heating consumption for 267 m² of usable area is presented in figure 11 [9].

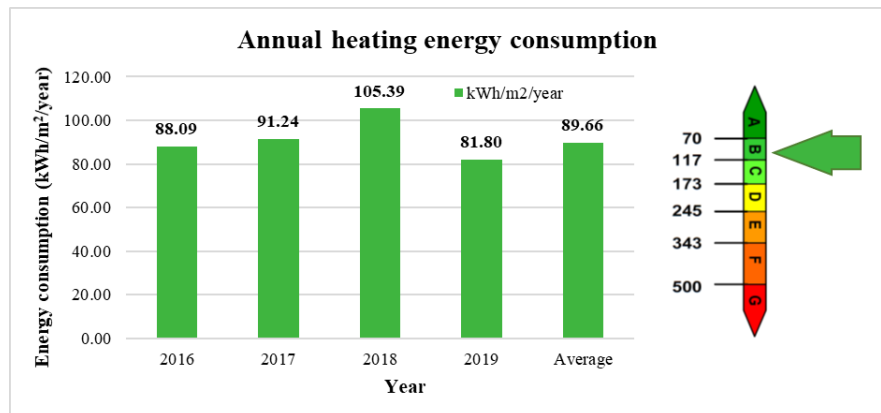


Fig. 11 - Annual heating energy consumption

A conventional house of a neighbor with 80 m² usable area, based on the owner's statement, consumed in the 2017 – 2018 season around 10 m³ having the annual heating energy consumption of 210 kWh/m²/year. At EU level, the average annual specific consumption per m² for all types of buildings was around 180 kWh/m² in 2013. It differs among countries: from 55 kWh/m² in Malta and 70 kWh/m² for Portugal or Cyprus, to 300 kWh/m² in Romania (or 285 kWh/m² in Latvia and Estonia) which is significantly higher than the EU average. However, even for countries with a similar climate, significant discrepancies exist (e.g. 200 kWh/m² in Sweden, 18% lower than Finland). Such differences are partly explained by climatic conditions, type of buildings and statistical definitions. [10]

The average price for 16 cubic meters of wood (e.g. beech, oak, hornbeam) was around 1500 € So the medium annual cost for 267 m² was around 5,62 €/m²/season (year) for heating.

In terms of cooling the living area the effort is zero. The maximum temperature at a humidity value of 65% on the hottest day was 27 °C in Living room, with a high level of indoor comfort. In the rest of time the temperature is around 23°C up to 24°C in during summer. At the basement level the temperature is almost constant during summer and winter, varying from 18°C ... 20°C.

For the domestic hot water consumption during summer, the electric boiler is set to work with a timer on hourly intervals around 4 hours / day (1 hour in the morning, 1 hour at noon and two hours in the evening) which means 25% of total amount of electric energy in a month.

The main aspect which can substantially change the comfort is humidity, if this is greater than 70%. In order to maintain the humidity level under 70%, it was very important to monitor this value and to assure the air circulation through the natural ventilation pipe system.

The system of house semi-buried and the roof covered with 15 cm of soil showed to be efficient having a big thermal mass. From September until December the heat stored in the surrounding massive earth reduced the heat losses of the house which translated in 30% less wood used for heating. During January and February of almost every year the exterior temperature was below -10°C. To have an average indoor temperature of 22 °C, the amount of wood consumed was double. The annual average per square meter in terms of heating energy consumption is 90 kW/m²/year placing the building in energy efficiency class B.

4. Conclusions

In this paper are presented some observations and data recorded during a period of 4 years of building usage of an earth sheltered house built near Iasi, in North-East of Romania.

The system has been proven to be affordable to heat almost 267 m² of usable area resulting an average of 90 kW/m²/year, a B class of heating energy efficiency. The advantages of thermal inertia are obvious for all types of weather. During summers, the interior comfort is natural within the optimal limits without any additional effort to cool the air or dehumidify it.

Some of the main disadvantages observed can be mentioned: the additional effort regarding a proper waterproofing of the buried surfaces, and the addition of all the layers of the green roof system. Regarding the use of wood as a fuel for heating, although the system is automated and the energy consumption is very low, there are some inconveniences such as the supply of wood, the processing, the storage but also the removal of ash. One of the alternatives which can be implemented is a combination of heat pumps, natural gas and solar energy which is considered to be implemented in the following years.

REFERENCES

- [1] [Online]. Available: https://en.wikipedia.org/wiki/Earth_shelter.
- [2] D. S. Heba Hassan, "Earth-sheltered buildings in hot-arid climates: Design guidelines," Beni-Suef University Journal of Basic and Applied Sciences, vol. 7, pp. 397-406, 2018.
- [3] H. Hassan, T. Arima, A. Ahmed, D. Sumiyoshi and Y. Akashi, "Testing the Basements Thermal Performance as an Approach to the Earth-Sheltered Buildings Application at Hot Climates," in ASIM, Tokyo, Japan, 2014.
- [4] N. K. F. Aleksandar, R. Milanović, "Earth-Sheltered Housing Buildings in the Energy Efficient Structures Context," Building Materials and Structures, vol. 60, no. 3, pp. 47-60, 2017.
- [5] [Online]. Available: <https://ro.wikipedia.org/wiki/Bordei>.
- [6] H. Tundrea, Energy efficiency of green homes, Ph.D. dissertation, TUIASI, 2014.
- [7] "International Standard EN-ISO 10456:2007 'Building materials and products - Hygrothermal properties - Tabulated design values and procedures for determining declared and design thermal values'," ISO, 2007.
- [8] [Online]. Available: <https://www.wunderground.com/history/daily/LRIA>.
- [9] "Ordinul 386/2016 pentru modificarea si completarea Reglementarii Tehnice "Normativ privind calculul termotehnic al elementelor de construcție ale clădirilor, C107-2005"," O.M. nr. 2055/2005, 2016.
- [10] "Energy use in buildings," [Online]. Available: https://ec.europa.eu/energy/eu-buildings-factsheets-topics-tree/energy-use-buildings_en.

A NUMERICAL ANALYSIS ON RADIANT FLOOR HEATING SYSTEMS WITH INTEGRATED PHASE CHANGE MATERIALS

Marius BRĂNOAEA^{1,*}, Andrei BURLACU¹, Vasilică CIOCAN¹, Marina VERDEȘ¹, Florin Emilian ȚURCANU¹ and Robert Ștefan VIZITIU¹

¹ Gheorghe Asachi" Technical University of Iasi-Romania, Faculty of Civil Engineering and Building Services,

Abstract. *Recently, the modern society has gained an increased interest in the concept of buildings energy consumption and diverse studies regarding methods to reduce the buildings energy demand have been published in order to mitigate the impact buildings pose to the society, economy and environment. With their properties of being able to accumulate and release increased amounts of thermal energy, phase change materials (PCMs) present great potential. The implementation of a PCM into the heating system of a building can provide a substantial reduction in the energy demand for heating. Through CFD simulations this paper highlights that a reduction in the daily energy consumption for heating buildings can be achieved with the integration of PCMs through reducing the number of daily heating cycles and by increasing the discharge phase time the heating phase can be set during off peak periods taking advantage of the reduced energy price.*

Keywords: Phase Change Material, CFD, Energy efficiency, Floor heating

1. Introduction

Currently the energy consumption of buildings amounts to over 40% of the worldwide energy demand, and the emissions of CO₂ amount to over 30% of the global net greenhouse gas emissions, this being a major result of the rapidly increase in urbanization, global climate change, chaotic deforestation and the growth of indoor residence time that led to a rise in the demand for indoor thermal environments [1].

In the residential sector, a big portion of the demand for electric energy is consumed with heating and cooling. PCMs can be a good link in the supply and demand chain due to them having the property of storing high quantities of heat over time [2].

Phase changing materials are very advanced materials, being able to accumulate energy in the form of latent heat during the phase change process without an increase in

temperature. Afterwards through the phase transition process from liquid to solid, the material releases the stored thermal energy over an extended period of time, thus reducing the number of heating cycles [3].

Through their properties of storing high quantities of thermal energy with the purpose of reducing buildings energy requirement, thermal energy accumulation with the use of PCMs has gained interest in the scientific community in recent years, being a key study field for researchers around the globe in different fields.

Studies show that energy demand represent a substantial contribution regarding the GDP growth in a country. European energy demand in both the industrial sector and the services/household sector is elastic and, in this region, natural gas and electricity serve as substitutes in terms of energy demand [4, 5].

The EU adopted in 2012 a legislation with the target to reduce the emissions of greenhouse gases until 2020 by 20% compared to the values of 1990. Studies performed in 2017 showed that these conditions would not be met, and as a result the restrictions were increased, the targets for 2030 demanded a decrease of 27% in energy consumption and diminishing the emissions of greenhouse gases by 40% [6].

For the purpose of increasing the energy performance of buildings, thermal energy accumulation can provide a pertinent method to achieve this. In terms of classification there are two forms in which thermal energy can be stored: as sensible heat and latent heat [7].

Studies show that among the numerous methods of harnessing heat, the most favourable option is the use of PCMs due to their advantages in comparison to other methods. PCMs can accumulate and release increased quantities of heat throughout the phase transition phase [8].

In terms of the type of transition phase, the most commonly used are solid-liquid PCMs, being able to so store high quantities of thermal energy as latent heat without significant change in terms of volume in comparison to the other categories [9].

Another classification for phase change materials presents 3 main categories: organic PCMs, that can be furthermore classified into paraffin compounds and non-paraffin compounds, inorganic PCMs, that can be classified as hydrated salts and metallic salts, and eutectic PCMs that are formed by combining multiple phase change materials, a combination of either organic or inorganic PCMs, in order to achieve a specially designed material for the needed purpose [10].

With the primary purpose being thermal energy accumulation, PCMs can be integrated in various applications for active or passive systems.

The scientific community has shown a great interest towards the applications of PCMs, integrating them in multiple building elements: floors [11, 12, 13, 14, 15, 16], ceilings [17, 18], walls [19, 20, 21] and windows [22, 23].

2. Research methodology

To achieve the objective of the research paper, the studies were performed using the ANSYS Fluent CFD software to simulate the correct operation of both underfloor heating systems, a classic dry underfloor heating system and a dry underfloor heating installation with an integrated PCM.

For the study an electrical dry floor heating mat was considered due to it having superior advantages in comparison to a water based radiant floor heating system, it is implementable on a larger scale in every room and the only drawback of a higher operation cost can be reduced by using green energy sources such as photovoltaic panels both in small residential and large scale industrial applications. Another advantage of the electric floor heating system is an increased reduction in costs with the use of PCMs through the use of electricity during off peak load in order to heat the floor and with the thermal properties of the PCM the discharge phase continues well into the peak load period during a day, when the cost of electrical energy is higher [15].

The research addresses multiple numerical simulations performed using ANSYS Fluent CFD as a means to study the heat distribution of both systems during the heating cycle in order to demonstrate the viability of the system in the energy performance improvement of buildings.

The numerical 3D modelling was completed using software 2019 R3 with the same conditions for both models. A section of the models is presented in Fig.1, the key difference between the first and second model is that in the first one, layer number 2 is representing a PCM that is placed between two layers of concrete in order for it to have shape stabilization during the phase transition process, while in the second model there is no PCM layer.

The analysed models are 1 meter in length and 1 meter wide, the height of the models is 35mm as follows: first concrete layer 10 mm, PCM layer 10 mm, second concrete layer 5 mm, floor heating 10 mm.

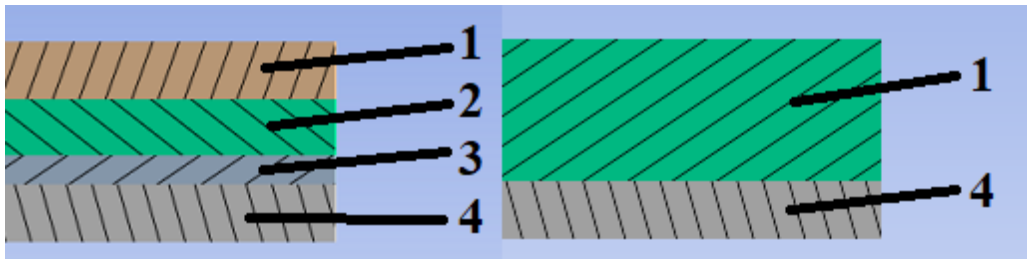


Fig. 1 – A section of the models
1. Concrete layer 1 2. PCM 3. Concrete layer 2 4. Electrical heating mat

In terms of mesh initialization and sizing, linear element order and the element size of 5 mm were imposed, resulting a 280.000 element mesh (Fig. 2).

To have an accurate representation CFD simulation for the models in the case of the PCM model apart from the energy equation, the solidification/melting model was used.

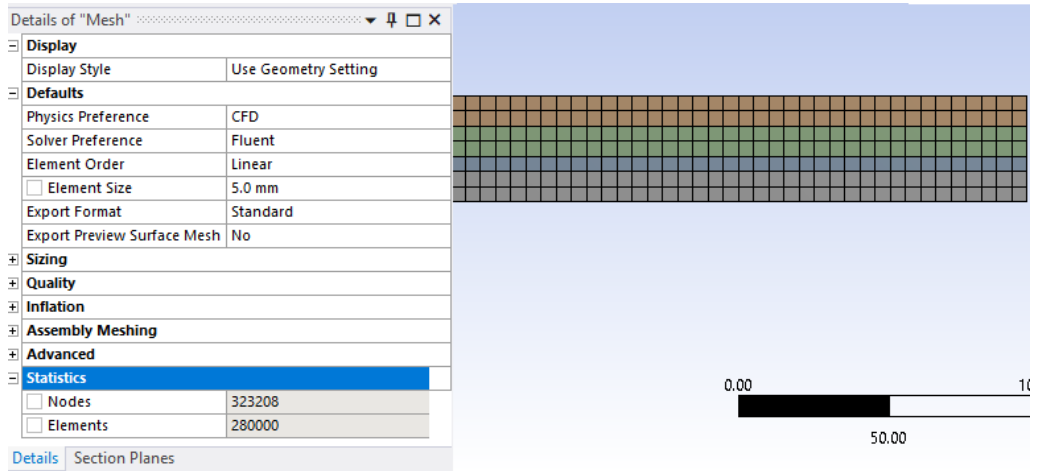


Fig. 2 – Model mesh sizing and initialization

For the phase change material, RT 21 HC produced by Rubitherm Technologies GmbH was considered with the properties shown in Fig. 3.

Characteristics	Value	Units
<i>Melting area</i>	20-23	[°C]
<i>Solidification area</i>	21-19	[°C]
<i>Heat storage capacity</i>	190	[kJ/kg]
<i>Specific heat capacity</i>	2	[kJ/kg·K]
<i>Density solid (at 15°C)</i>	0.88	[kg/l]
<i>Density liquid (at 25°C)</i>	0.77	[kg/l]
<i>Heat conductivity</i>	0.2	[W/(m·K)]
<i>Max. operation temperature</i>	45	[°C]

Fig. 3 – RT 21 HC Material properties

The reference temperature for the electric heating mat was considered to be 35 °C, this being a recommended operating temperature for the heating source in a floor heating system.

The initial room temperature for the system was considered 10°C.

For both cases the heating and cooling time was recorded in order to have an accurate representation in time of the charge/discharge cycle.

3. Results and Discussion

The numerical simulation highlighted that in the case when a layer of PCM was introduced in the floor heating system the heating phase require more time in comparison to the regular system but during the discharge phase the properties of the phase change material are harnessed, the floor retaining the thermal energy for much higher quantities of time.

A first analysis can be performed considering a complete charging and discharging cycle in order to analyse the thermal storage capabilities of both systems.

The numerical simulations highlight that the PCM starts melting after 5 minutes and it reaches almost fully liquid state after 70 min with a liquid fraction factor of 99.66%. (Fig.4)

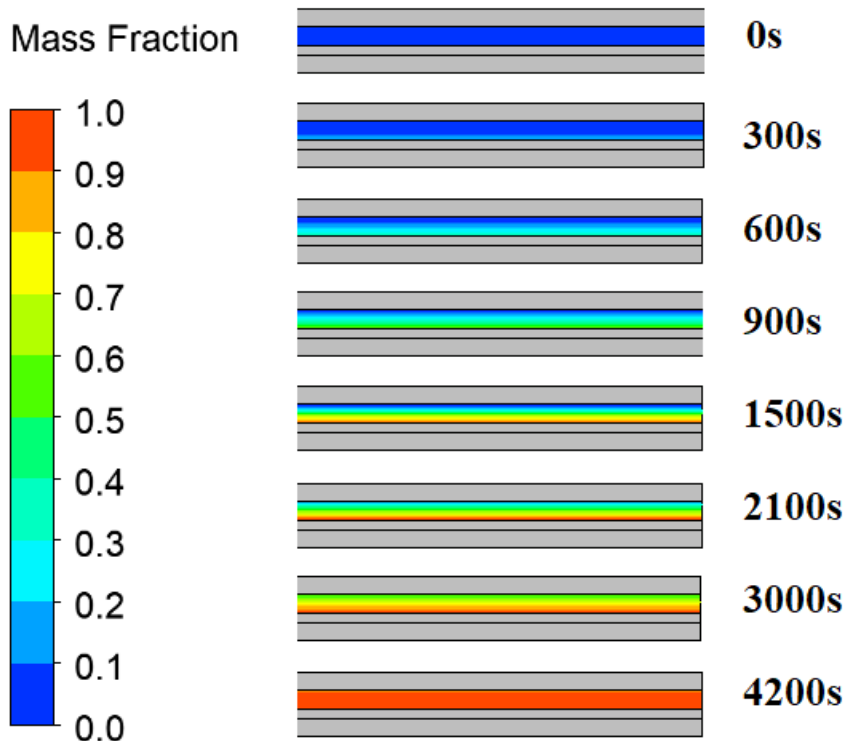


Fig. 4 – PCM integrated floor mass fraction throughout the heating phase

The numerical analysis of the temperature of the PCM integrated floor heating system during the heating phase (Fig. 5) highlights that in the first minutes of operation, the temperature of the PCM rises rapidly until it reaches the melting temperature, afterwards while it melts the increase in temperature is reduced up to the point when the material is fully melted, after 70 min as emphasised by the mass fraction, than it starts to rapidly rise again until the radiant floor is fully heated, at 98 min.

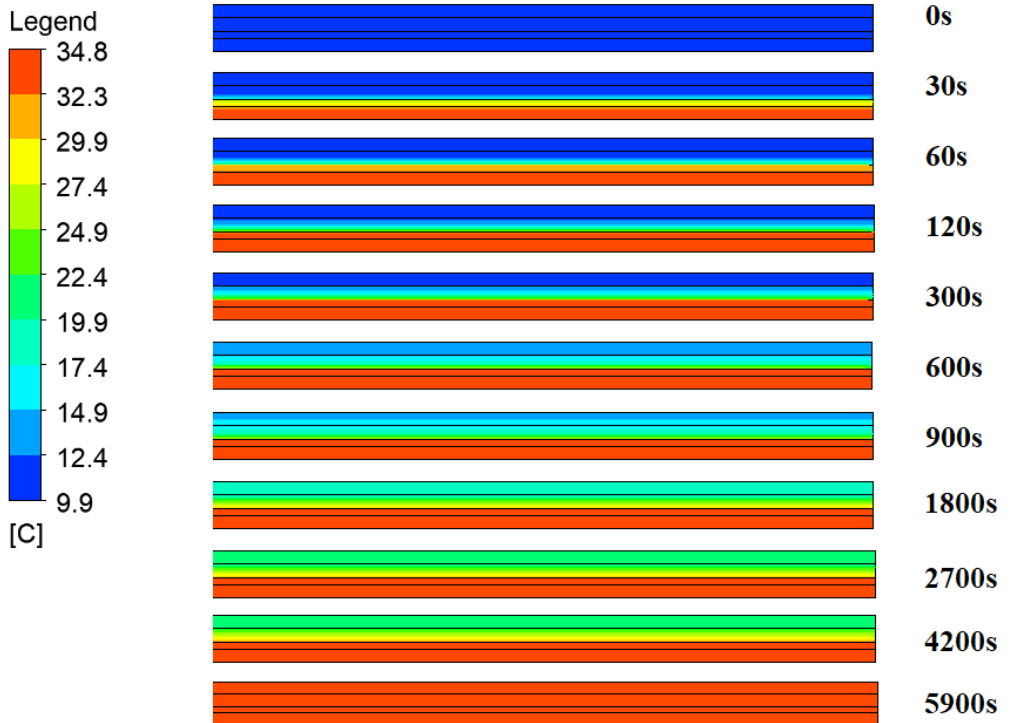


Fig. 5 – PCM integrated floor temperature profile throughout the heating phase

During the cooling process, the noteworthy moments are when the PCM starts solidifying, after 10 min, and when it reaches a fully solid state after 125 min as expressed in Fig. 6

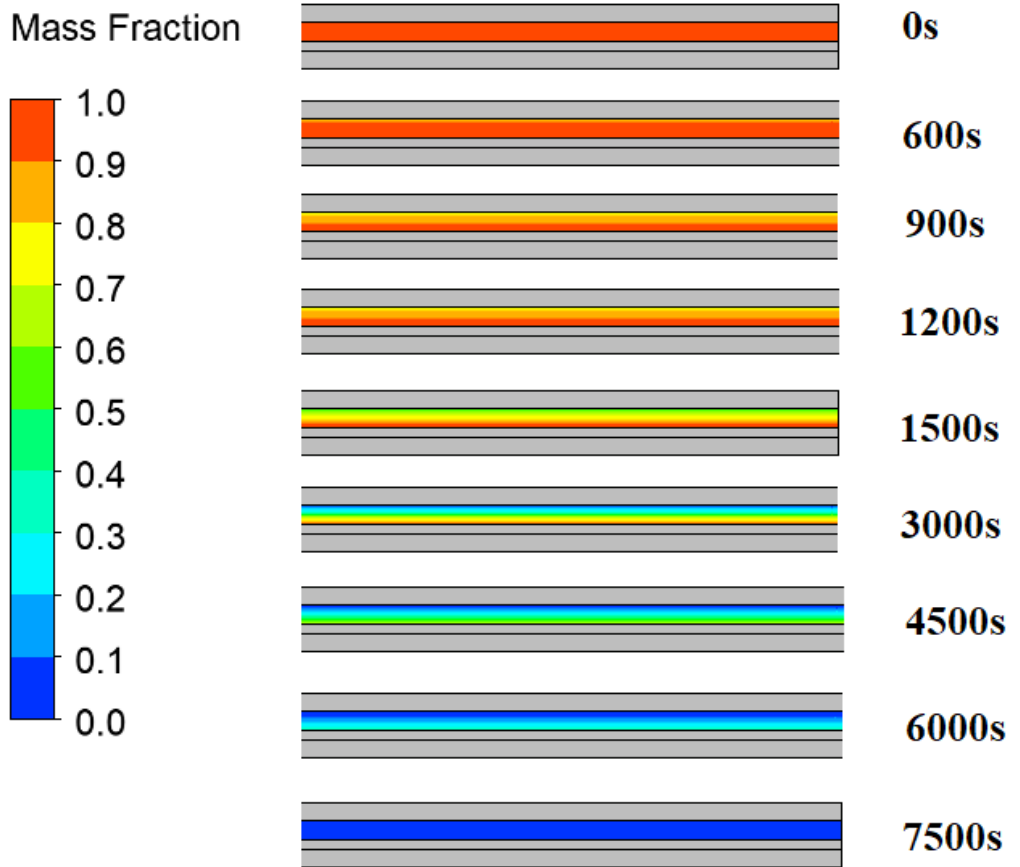


Fig. 6 – PCM integrated floor mass fraction throughout the cooling phase

The cooling process of the PCM integrated floor heating system at various moments in time (Fig. 7) shows that as was the case of the heating phase, the temperature decreases quicker before the PCM starts solidifying and it slows down considerably during the solidification process. The system is fully cooled after 215 minutes proving the increased thermal storage capacity of the PCM.

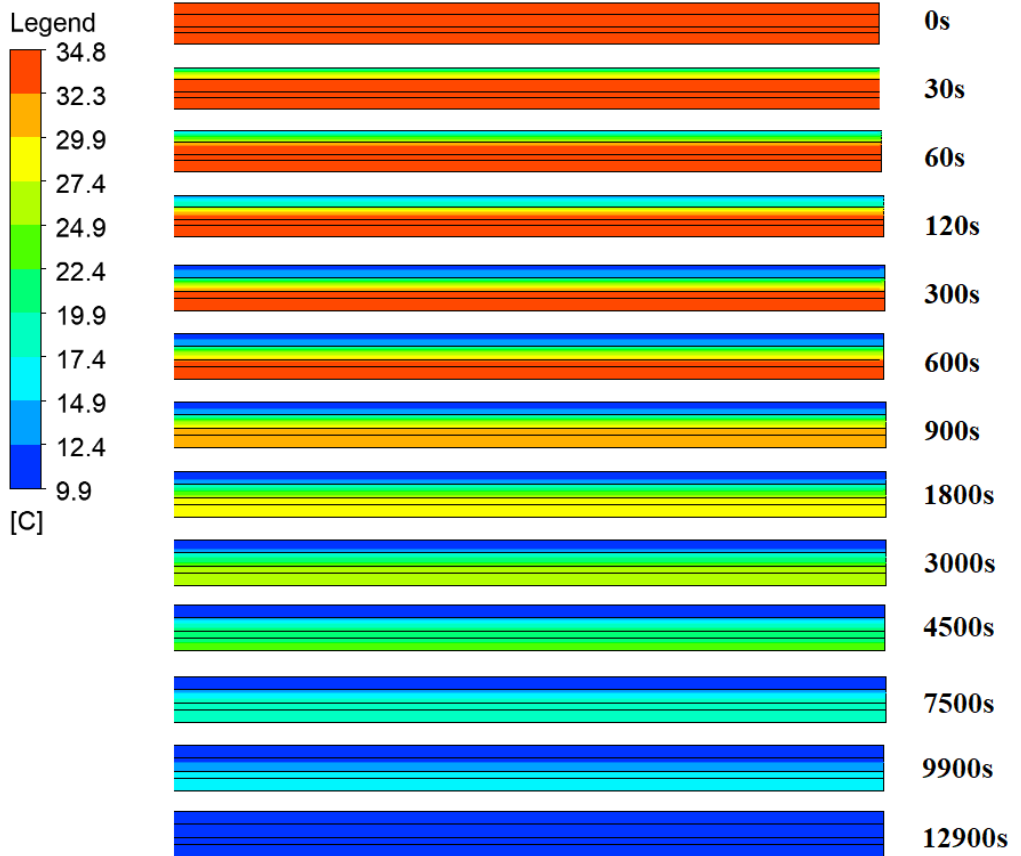


Fig. 7 – PCM integrated floor temperature profile throughout the discharge phase

The temperature profile of the classic floor heating system during the heating/ cooling phases shows that it requires around 20 min for the floor to be fully heated (Fig. 8) and 45 min for the floor to cool after the heating source was turned off (Fig.8)

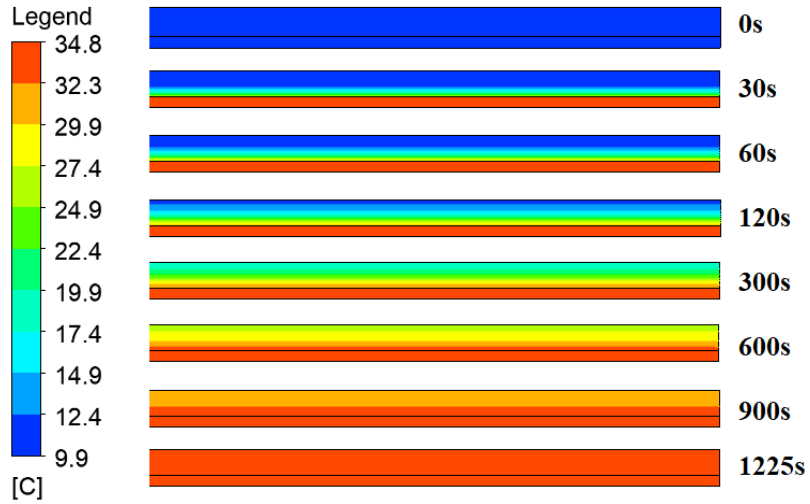


Fig. 8 – Classic floor temperature profile throughout the heating phase

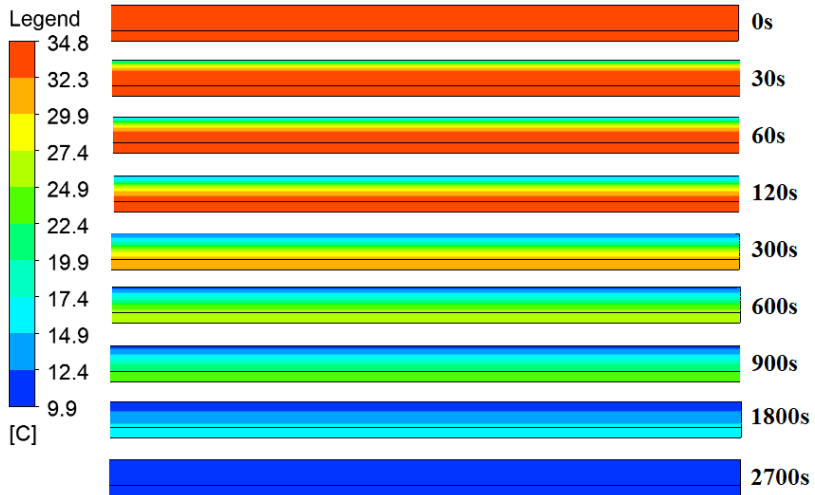


Fig. 9 – Classic floor temperature profile throughout the discharge phase

Considering the charging and release times for the thermal energy for both cases, the number of uninterrupted cycles during a period of 24h in the case with the PCM integrated floor is 4.6 and 23.19 in the case without the PCM.

Knowing the number of cycles/day and the time the electric heating mat spends energy heating for each cycle, it results a number of required hours of heating for the PCM integrated floor heating system of 7.53/day and 7.89 without the PCM resulting in an important reduction in the energy consumption.

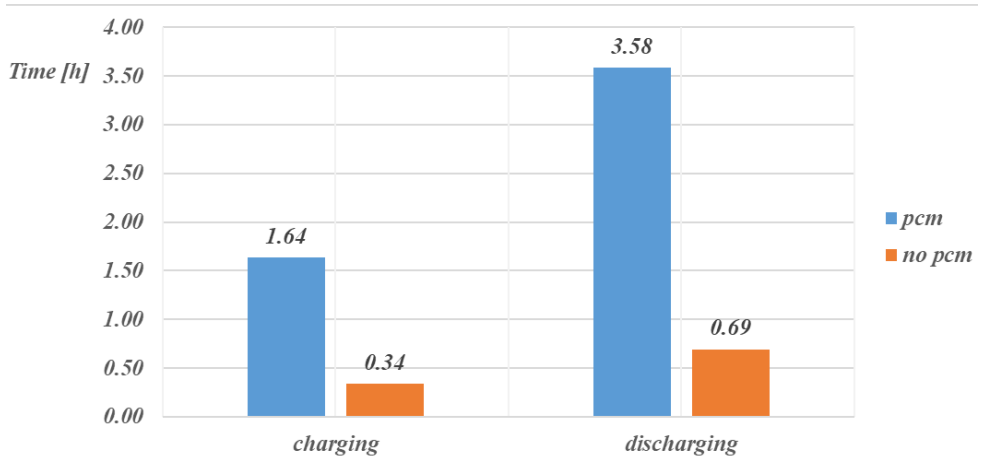


Fig. 10 – Results of a complete charge/discharge cycle

Furthermore, due to the longer discharge cycles the PCM floor heating system can benefit from the reduced price in electricity during the off-peak load times, resulting in further reduction in the heating cost.

These results highlight that the considered PCM integrated radiant floor manages to achieve a diminishment in the consumption of energy even with an intermittent operation.

In order to verify the validity of the results further research will be conducted on other types of phase changing materials and an analytical study on a real scale model will be conducted in the future.

4. Conclusions

With their properties of being able to accumulate and release increased amounts of thermal energy, PCMs present great potential in the residential sector. The implementation of a PCM into the heating system of a building can provide a substantial diminishment in the requisite energy for heating.

The numerical analysis shows that through the incorporation of a PCM in a dry floor electrical heating system a substantial reduction in costs can be achieved through both the reduction of the operating time of the electrical hearing mat during a day from 7.89 hours in the case of a classic system to 7.53 hours for the PCM floor and due to the longer heating/cooling cycles which can be programmed to consume energy during off-peak periods taking advantage of the reduced prices in electrical energy.

REFERENCES

- [1] X. Cao, X. Dai and J. Liu, "Building energy-consumption status worldwide and the state-of-the-art technologies for zero-energy buildings during the past decade," *Energy and Buildings*, vol. 128, p. 198–213, 2016.
- [2] F. Guarino, A. Athienitis, M. Cellura and D. Bastien, "PCM thermal storage design in buildings: Experimental studies and applications to solar in cold climates," *Applied Energy*, vol. 185, pp. 95–106, 2017.
- [3] S. S. Magendran, F. S. A. Khan, N. M. Mubarak, M. Khalid, R. Walvekar, E. C. Abdullah, S. Nizamuddin and R. R. Karri, "Synthesis of organic phase change materials by using carbon nanotubes as filler material," *Nano-Structures & Nano-Objects*, vol. 19, p. 100361, 2019.
- [4] E. Akalpler and M. E. Shingil, "Statistical reasoning the link between energy demand, CO₂ emissions and growth: Evidence from China," *Procedia Computer Science*, vol. 120, p. 182–188, 2017.
- [5] P. Fotis, S. Karkalakos and D. Asteriou, "The relationship between energy demand and real GDP growth rate: The role of price asymmetries and spatial externalities within 34 countries across the globe," *Energy Economics*, vol. 66, pp. 69–84, 2017.
- [6] F. P. Cambeiro, J. Armesto, G. Bastos, J. I. P. López and F. P. Barbeito, "Economic appraisal of energy efficiency renovations in tertiary buildings," *Sustainable Cities and Society*, vol. 47, p. 101503, 2019.
- [7] K. Belz, F. Kuznik, K. F. Werner, T. Schmidt and W. Ruck, "Thermal energy storage systems for heating and hot water in residential buildings," in *Advances in Thermal Energy Storage Systems*, Woodhead Publishing Series in Energy, 2015, pp. 441–465.
- [8] S. S. Magendran, F. S. A. Khan, N. M. Mubarak, M. Vaka, R. Walvekar, M. Khalid, E. C. Abdullah, S. Nizamuddin and R. R. Karri, "Synthesis of organic phase change materials (PCM) for energy storage applications: A review," *Nano-Structures & Nano-Objects*, vol. 20, p. 100399, 2019.
- [9] Y. Lin, Y. Jia, G. Alva and G. Fang, "Review on thermal conductivity enhancement, thermal properties and applications of phase change materials in thermal energy storage," *Renewable and Sustainable Energy Reviews*, vol. 82, no. 3, pp. 2730–2742, 2018.
- [10] S. R. L. Cunha and J. L. B. Aguiar, "Phase change materials and energy efficiency of buildings: A review of knowledge," *Journal of Energy Storage*, vol. 27, p. 101083, 2020.
- [11] B. Y. Yun, S. Yang, H. M. Cho, S. J. Chang and S. Kim, "Design and analysis of phase change material based floor heating system for thermal energy storage," *Environmental Research*, vol. 173, pp. 480–488, 2019.
- [12] S. Lu, B. Xu and X. Tang, "Experimental study on double pipe PCM floor heating system under different operation strategies," *Renewable Energy*, vol. 145, pp. 1280–1291, 2020.
- [13] K. Faraj, J. Faraj, F. Hachem, H. Bazzi, M. Khaled and C. Castelain, "Analysis of underfloor electrical heating system integrated with coconut oil-PCM plates," *Applied Thermal Engineering*, vol. 158, p. 113778, 2019.
- [14] J. Guo, Y. Jiang, Y. Wang and B. Zou, "Thermal storage and thermal management properties of a novel ventilated mortar block integrated with phase change material for floor heating: an experimental study," *Energy Conversion and Management*, vol. 205, p. 112288, 2020.
- [15] A. E. Mays, R. Ammar, H. Mahamad, M. A. Akroush, F. Hachem, M. Khaled and M. Ramadan, "Using phase change material in under floor heating," *Energy Procedia*, vol. 119, pp. 806–811, 2017.
- [16] P. Devaux and M. M. Farid, "Benefits of PCM underfloor heating with PCM wallboards for space heating in winter," *Applied Energy*, no. 191, p. 593–602, 2017.
- [17] H. Weinläder, F. Klinker and M. Yasin, "PCM cooling ceilings in the Energy Efficiency Center – Regeneration behaviour of two different system designs," *Energy and Buildings*, vol. 156, pp. 70–77, 2017.
- [18] M. Yasin, E. Scheidemantel, F. Klinker, H. Weinläder and S. Weismann, "Generation of a simulation model for chilled PCM ceilings in TRNSYS and validation with real scale building data," *Journal of Building Engineering*, vol. 22, pp. 372–382, 2019.

- [19] X. Kong, L. Wang, H. Li, G. Yuan and C. Yao, "*Experimental study on a novel hybrid system of active composite PCM wall and solar thermal system for clean heating supply in winter*," Solar Energy, vol. 195, p. 259–270, 2020.
- [20] H. Wang, W. Lu, Z. Wu and G. Zhang, "*Parametric analysis of applying PCM wallboards for energy saving in high-rise lightweight buildings in Shanghai*," Renewable Energy, vol. 145, pp. 52-64, 2020.
- [21] P. K. S. Rathore and S. K. Shukla, "*Potential of macroencapsulated pcm for thermal energy storage in buildings: A comprehensive review*," Construction and Building Materials, vol. 225, p. 723–744, 2019.
- [22] S. Li, K. Zou, G. Sun and X. Zhang, "*Simulation research on the dynamic thermal performance of a novel triple-glazed window filled with PCM*," Sustainable Cities and Society, vol. 40, pp. 266-273, 2018.
- [23] Y. Hu and P. K. Heiselberg, "*A new ventilated window with PCM heat exchanger—Performance analysis and design optimization*," Energy and Buildings, vol. 169, pp. 185-194, 2018.

INCREASING THE ENERGY PERFORMANCE OF NON-RESIDENTIAL BUILDINGS BY THERMAL INSULATION OF WALLS ON THE INTERIOR SURFACE

Laura DUMITRESCU¹, Radu-Aurel PESCARU¹, Irina BARAN¹ and Irina BLIUC¹

¹"Gheorghe Asachi" Technical University from Iasi, Romania

Abstract. *Increasing the energy efficiency of buildings is one of the most important goals of today. In this context, the category of buildings with historical and architectural values is a special one, because the method consisting in adding an insulation layer on the outside is not an option, the only one is insulation on the inside of the walls. However, this solution does present certain risks of interstitial condensation and degradation due to frost or expansion of the masonry. The paper presents a study of a particular case of a building where only a façade cannot be thermally renovated from the outside because it has a mosaic surface. Thermal field simulations performed for a characteristic area emphasised the hygrothermal behaviour of the wall.*

Keywords: interior insulation, thermal bridge, linear thermal transmittance, temperature factor, energy efficiency

1. Introduction

Sustainability and energy efficiency are key concepts of the present. According to the Buildings Performance Institute Europe [1], the buildings sector is responsible for 40% of total energy consumption and 36% of Greenhouse Gas Emissions (GHG). However, statistics show that about 35% of buildings are older than 50 years and 75% of the building stock is energy inefficient. Estimates suggest that there is potential for reducing the EU's overall energy consumption by 5-6% through measures to improve the energy efficiency of buildings and a corresponding reduction in total GHG emissions of around 5% [2].

In Romania, it is estimated that the stock of public buildings represents about 25% of the total number of buildings [3]. However, many of them (education, health, public administration) are very old, about 60% were built between 1950 and 1990. In addition, they have low thermal insulation, according to the standards of the time when they were built, and in many cases the thermal insulation is damaged due to climatic conditions. Several public buildings have a special status due to their historical value and architectural appearance, as many of them constitute the identity

of the city. This category of buildings requires special types of measures to increase energy efficiency. Usually these are measures to insulate building envelope elements, to increase the tightness, to replace glazing surfaces and to improve building equipment. However, in the case of this particular type of building, retrofitting is a complex act of intervention that poses particular challenges.

The category of buildings of architectural value is a special one, as they require special approaches, the essential element being the need to preserve the appearance of the façades. This is the case for old buildings (education, health, culture, commerce, tourism), many of which having brick structures (Figure 1), but also for some public buildings from the 1980s, with a monumental appearance, peculiar solutions for façade finishing that give the buildings their individuality (Figure 2).



Fig. 1 – National College from Jassy
a. Main façade; b. Architectural details

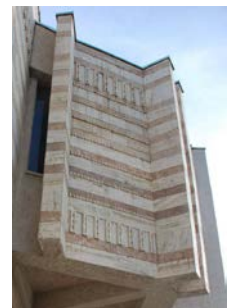


Fig. 2 – “Luceafărul” Theater for children and youth from Jassy
a. Main façade; b. Architectural details

Heat losses through the external walls account for the largest share of the overall energy balance of a building, namely 35% for ground floor buildings and 65% for multi-storey buildings. This justifies the constant effort to improve systems and solutions to ensure adequate thermal insulation for the opaque part of the façades, both in new buildings and in buildings undergoing renovation. The solution adopted in Romania after 1990 was to apply a layer of thermal insulation on the external surface of the wall, a layer protected with a thin plaster - ETICS system - or with a waterproof covering over a layer of air in contact with the outside air - Double-Skin system (ventilated façade). The solution is recommended first of all by adequate hygrothermal behaviour, as it eliminates the risk of progressive accumulation of condensed water vapour inside the structure, but also by other characteristics related to thermal inertia, simple technology, etc.

The extension of thermal energy rehabilitation action in the area of public buildings whose façades must be preserved, as well as the tendency to carry out partial thermal retrofitting works at the level of an apartment (which significantly affects the appearance of the façades), have drawn the attention of the parties involved to the solution of increasing the level of thermal insulation by applying an additional layer of thermal insulation material on the inner surface of the walls. This solution has a number of advantages, but it also involves certain risks that must be analysed in detail in order to avoid further negative consequences that are more difficult to resolve.

Moreover, in the case of buildings to be rehabilitated in this way, the assessment of energy performance requires knowledge of the value of the linear heat transfer coefficients corresponding to the solution of thermal insulation on the internal surface, different from those contained in the thermal bridge catalogues, which refer only to the situation of external thermal insulation.

2. Specificity of additional thermal insulation on inside part of walls

2.1. Exterior versus interior thermal insulation

In the retrofitting process, the reduction of transmission losses through walls plays an important role, as this element makes up a large part of the building envelope. There are two approaches to increasing the thermal insulation level of walls: on the outside and on the inside. The first solution is by far the most efficient (Figure 3).

However, for buildings of historical value or with façades that must be preserved, additional insulation on the inside remain the only option.

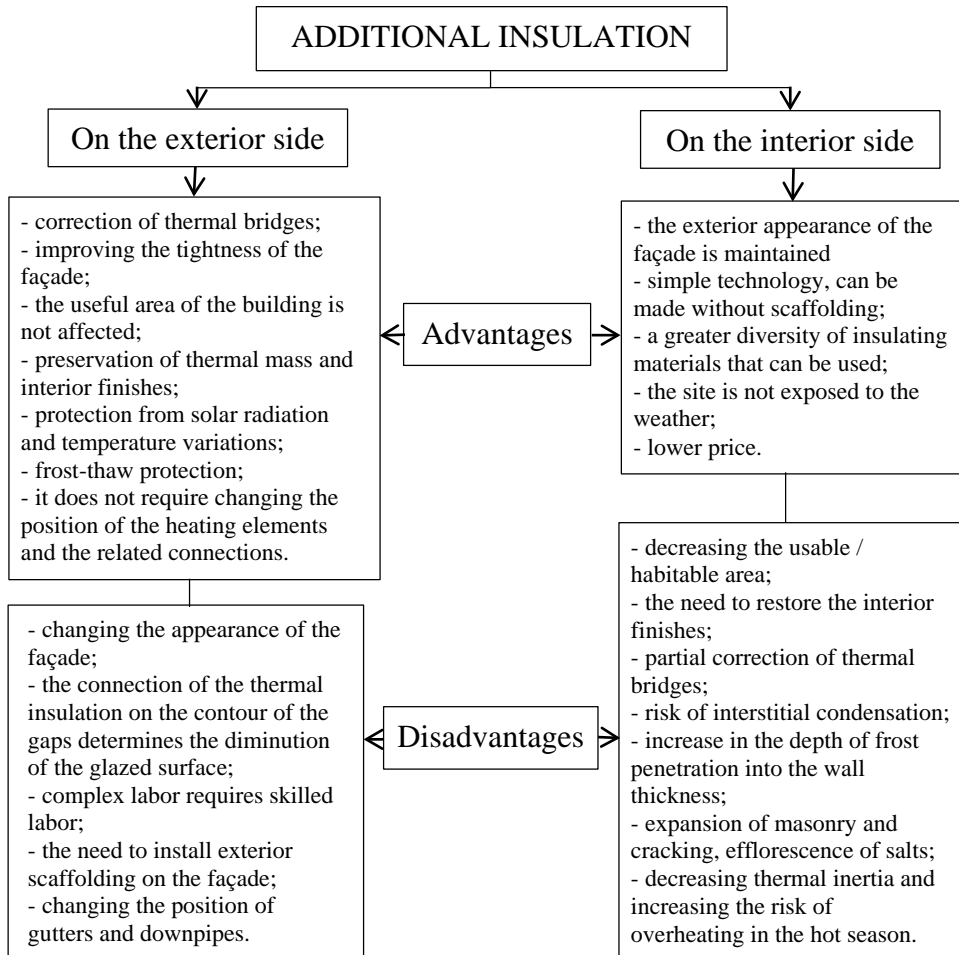


Fig. 3 – Comparison between exterior and interior thermal insulation

2.2 Risks associated with the additional insulation applied on the interior side of the building envelope elements

The thermal insulation on the inside can cause various hygrothermal and mechanical phenomena that affect the durability of existing walls. These are the alteration of the hygrothermal properties of the wall, and as a consequence, certain risks of interstitial condensation, frost damage, mould growth and other damage can occur. Today, however, there are some innovative systems that reduce moisture retention in the wall structure, but allow internal drying [4]. There are three types of insulation materials that are specifically suited for interior applications: capillary-active and vapour-open insulation materials that have the ability to buffer moisture, vapour-open insulation

materials that allow vapour to be transported into the wall, and vapour-tight systems that prevent moisture transport through the insulation [5].

The main risks that have been identified are:

- - interstitial condensation by diffusion;
- - degradation due to frost or expansion of masonry;
- - decrease of thermal inertia and risk of overheating.

A detailed analysis of these risks allows the identification of the aspects that must be taken into account in choosing the optimal strategies in order to avoid them.

a. The risk of interstitial condensation due to vapour diffusion

Vapour condensation occurs when the actual pressure reaches the saturation value. In case of application of the thermal insulation layer on the inside, this phenomenon most likely occurs on the cold surface of the thermal insulation or on the interface between the thermal insulation and the existing structure. Moisture accumulated in the materials in this way can cause their degradation and, in particular, a significant decrease in the insulating capacity of the material.

b. Freezing and deformability of masonry walls

The fact that the wall structure is generally colder and wetter causes the penetration of the moisture front inwards, causing degradation, especially when freezing-thaw phenomena are associated, which increase/reduce the volume of water contained in the pores of the masonry blocks.

Therefore, the application of thermal insulation on the inside of the elements of the building envelope may aggravate an existing situation if no measures are taken to limit rainwater ingress and to maintain the drying potential of the wall. A waterproof cladding that closes off a layer of ventilated air could be a solution to reduce the negative effects mentioned above.

3. Case study

A particular case of an educational building was chosen as case study. The building has four floors and an amphitheatre at the upper level. Its bearing structure is made of reinforced concrete diaphragm walls with pillars in the façades plans. The building belongs to the Technical University “Gheorghe Asachi” from Iasi, has been built in 1973, and in 2007 has undergone thermal rehabilitation in order to ensure the requirements of energy efficiency and indoor comfort. The applied thermal rehabilitation measures were: adding a 5 cm layer of expanded polystyrene on the external face of the envelope walls, 10 cm of extruded polystyrene on the roof and top amphitheatre floor and changing the old wooden windows with new ones of aluminium frames and insulated glazing. A particular element of this building is the presence of a mosaic on a part of the northern façade, which make impossible the

application of external insulation system (Figure 4). It is a special situation when the external insulation must be coupled with the interior one.



Fig. 4 – Building northern façade and mosaic detail

The constructive details of the external walls are presented in Figure 5, both for the wall without mosaic and the wall with mosaic.

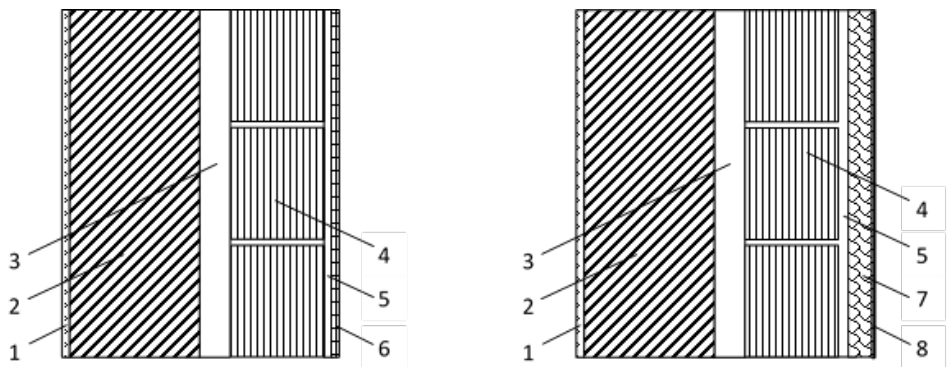


Fig. 5 – External wall details: 1- internal plaster; 2 – reinforced concrete; 3 – unventilated air layer; 4 - masonry units with vertical holes; 5 – cement mortar; 6 – marble mosaic; 7 - expanded polystyrene (EPS) insulation; 8 – external plaster

The external corner between the wall without mosaic and the wall with mosaic will be further analysed in detail in terms of energy efficiency and surface condensation risk.

3.1. Method

The thermal field in this building zone was numerically modelled using the THERM 7.6 software [6], developed at Lawrence Berkeley National Laboratory (LBNL). Based on the finite-element method, THERM allows for two-dimensional conduction and radiation heat-transfer analysis in building components. The input data are the geometric and thermal characteristics of material layers, and boundary conditions. The results can be viewed as U-factors (R-values), heat flows, isotherms, flux vectors, constant flux lines, temperature values, and surface condensation potential.

The material properties used in simulation are presented in Table 1.

Table 1
Geometric and thermal characteristics of material layers

No.	Material	Thickness [cm]	Density [kg/m ³]	Thermal conductivity [W/(mK)]
1	<i>Lime-cement interior plaster</i>	2	1,700	0.87
2	<i>Reinforced concrete</i>	20	2,500	1.74
3	<i>Air layer (R = 0.18 m²K/W)</i>	6	-	-
4	<i>Masonry units with vertical holes</i>	14	1,450	0.64
5	<i>Cement mortar</i>	2	1,800	0.93
6	<i>Mosaic</i>	2	2,400	2.03
7	<i>EPS insulation</i>	5	20	0.04
8	<i>Exterior plaster</i>	0.7	1,750	0.90
9	<i>Plasterboard</i>	1.3	700	0.23

The boundary conditions are: indoor air temperature $\theta_i = 20^\circ\text{C}$, interior surface heat transfer coefficient $h_i = 8 \text{ W/m}^2\text{K}$, outdoor air temperature $\theta_e = -15^\circ\text{C}$, exterior surface heat transfer coefficient $h_e = 24 \text{ W/m}^2\text{K}$. The relative humidity of the indoor air is $\text{RH}_i = 60\%$ and the relative humidity of the outdoor air for winter conditions is $\text{RH}_e = 85\%$.

By thermal field modelling with THERM, the influence of thermal bridging can be studied and the construction details can be optimized.

The influence of linear thermal bridges is taken into account by using linear thermal transmittances values, ψ [W/(mK)], which can be found in thermal bridge atlases, i.e. the Romanian C107-3 P1-P6 [7] for the typical thermal bridges or must be determined using numerical calculation software.

The equation for ψ -value calculation is:

$$\psi = \frac{\Phi}{\Delta\theta} - \frac{B}{R} = U_{\text{therm}} \cdot l_{\text{therm}} - \frac{B}{R} \quad (1)$$

where: Φ is the thermal flow resulted from 2D numerical calculation for a surface having the width B and the length 1 m, [W/m];

$\Delta\theta = \theta_i - \theta_e$ is the temperature difference between the indoor and outdoor environment, [K];

U_{therm} is the thermal transmittance calculated by THERM for area (length) corresponding to the thermal bridge, [W/(m²K)];

l_{therm} is the length of the contour of the heat transfer surface, [m];

B is the length corresponding to the thermal bridge, measured on the inner face of the exterior construction elements, in accordance with C107-2005, Part 3, Annex J, [m];

R is the thermal resistance of the construction element without thermal bridge (in current field), [m²K/W].

According to [8], it was introduced a criterion, the surface temperature factor, f_{Rsi} , that is defined as the difference between the temperature on inner surface θ_{si} , calculated with a surface resistance R_{si} and outside air temperature θ_e , relative to the difference between the indoor air temperature θ_i and the outside air temperature θ_e , and is expressed by the relation:

$$f_{Rsi} = \frac{\theta_{si} - \theta_e}{\theta_i - \theta_e} = \frac{R - R_{si}}{R} \quad (2)$$

This parameter, which can also be defined as an indicator of the level of thermal insulation, can be calculated at any point of the building envelope, including the thermal bridge zones. Minimum values of the temperature factor, $f_{Rsi, \text{crit}}$, were established and are specified in national regulation as design factors in order to avoid the mould growth risk or surface condensation risk.

For Romania, critical values of the temperature factor f_{Rsi} are given in [7], depending on the relative humidity of the indoor air and outdoor air temperature. For example, for $\theta_i = 20$ °C, $\theta_e = -15$ °C and $RH_i = 60\%$, the surface temperature factor $f_{Rsi} \geq 0.78$ to avoid the superficial condensation risk. The temperature factor $f_{0.25}$ is calculated with a value of the interior surface thermal resistance $R_{si} = 0.25$ m²K/W.

3.2. Results and Discussion

The thermal field was numerically modelled for the thermal bridge resulted at the external corner between the mosaic external wall and the regular external wall, which can be thermal insulated on the exterior surface.

To evaluate the thermal behaviour of this building area, 19 different configurations obtained by varying the thicknesses of thermal insulation layers have been studied, as presented in Table 2, in which:

- d_1 – thickness of the EPS layer applied on the exterior surface of the regular wall;

- d_2 – thickness of the EPS layer applied on the interior side of the mosaic wall and protected with a plasterboard of 1.3 cm thickness;
- d_3 – extension length of the EPS layer on the adjacent wall in order to minimise the thermal bridge effect.

Table 2

Values of linear thermal transmittances and surface temperature factors for the analysed thermal bridges configurations

Case No.	Thermal bridge configuration			Thermal bridge coefficient, ψ [W/(mK)]		Temperature factor, f [-]	
	d_1 [cm]	d_2 [cm]	d_3 [cm]	1-regular wall	2-mosaic wall	1-regular wall	2-mosaic wall
1	0	0	0	0.300	0.305	0.592	0.595
2	0	5	0	0.375	0.054	0.571	0.866
3	0	5	50	-0.192	0.04	0.714	0.870
4	5	0	0	0.454	0.212	0.777	0.615
5	5	5	0	0.539	0.023	0.753	0.873
6	5	5	10	0.490	-0.032	0.776	0.878
7	5	5	20	0.405	-0.026	0.794	0.876
8	5	5	30	0.337	-0.021	0.809	0.875
9	5	5	40	0.279	-0.017	0.821	0.874
10	5	5	50	0.230	-0.015	0.832	0.874
11	10	0	0	0.507	0.197	0.815	0.618
12	10	5	0	0.591	0.018	0.790	0.874
13	10	5	50	0.325	-0.019	0.858	0.875
14	15	0	0	0.532	0.191	0.831	0.619
15	15	5	0	0.615	0.016	0.807	0.874
16	15	5	50	0.367	-0.020	0.869	0.875
17	20	0	0	0.547	0.187	0.840	0.620
18	20	5	0	0.629	0.014	0.816	0.874
19	20	5	50	0.391	-0.021	0.876	0.875

For all studied alternatives, using the output data resulted from THERM, the following results have been determined:

- values of the linear thermal transmittances of the thermal bridge, ψ_1 for the regular wall, and ψ_2 for the mosaic wall;
- surface temperature factors $f_{0.25}$, f_1 for the regular wall, and f_2 for the mosaic wall;

Examples of the results obtained are given in Figure 6, in two cases:

- a) exterior insulation of 5 cm thickness;

b) 5 cm exterior insulation and 5 cm interior insulation with 50 cm extension on the adjacent wall.

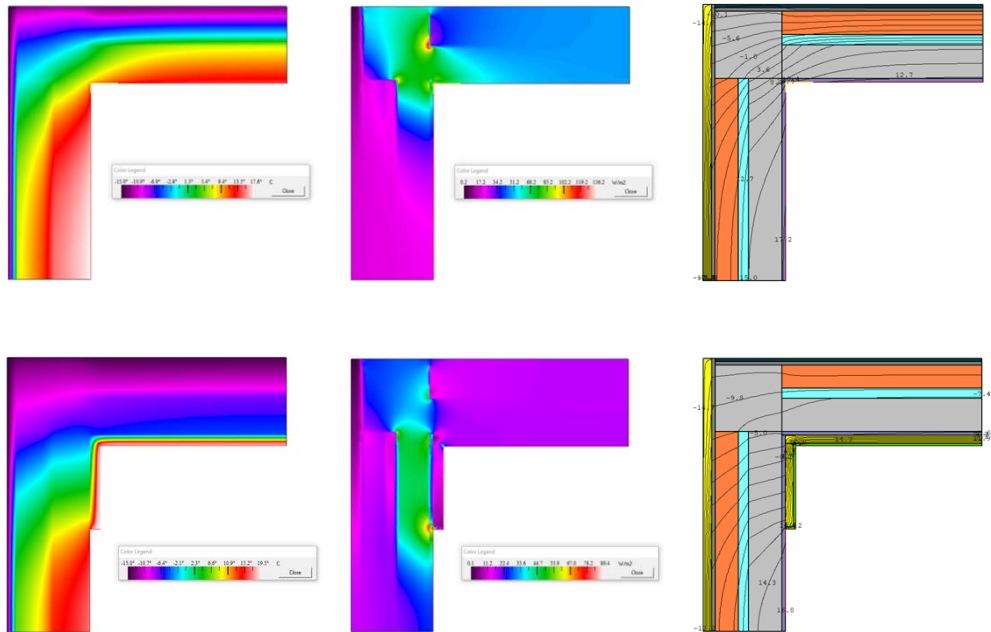


Fig. 6 – THERM results for cases a) and b): thermal field, flux magnitude, isotherms

As can be observed in Figure 6, the exterior insulation only diminish the thermal flow through the regular wall, but the superficial condensation may occur on the internal surface of the corner. Through applying interior thermal insulation with an extension on the adjacent wall, the superficial condensation risk is eliminated.

Even if a 5 cm thickness of exterior insulation ensured the minimum energy efficiency requirements at the time when the thermal rehabilitation of the building has been accomplished, in present these conditions became more demanding, this is the reason for this paper analysed the increasing of the exterior insulation thickness until 20 cm.

The ψ -values variation according to the thickness of the exterior thermal insulation is presented in Figure 7, for three cases.

It can be observed that ψ_1 -value is increasing in all cases comparative with the value for the uninsulated wall, which means an increase of the thermal bridge effect for the regular wall, with 82.3% in case A, 67.6% in case B. Even in case C, when effort has been made to correct the thermal bridging by extending the thermal insulation layer on the adjacent wall, $\psi_{1-C} = 0.391$ W/mK for 20 cm thickness of exterior insulation layer, which means an important thermal bridge effect. Contrary, the thermal bridge effect

for the mosaic wall (ψ_2 -values) is decreasing with the increase of the thickness of the exterior thermal insulation layer.

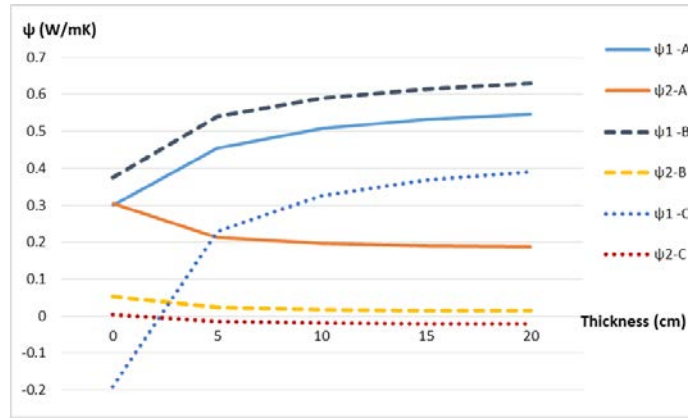


Fig. 7 – ψ coefficients variation according to the thermal insulation alternative.

Case A – mosaic wall without interior thermal insulation; Case B – mosaic wall with 5 cm interior thermal insulation; Case C – mosaic wall with 5 cm interior insulation extended 50 cm on the adjacent wall.

For the same cases, in Figure 8 is presented the surface temperature factors variation, in comparison with the critical value, $f_{crit} = 0.78$.

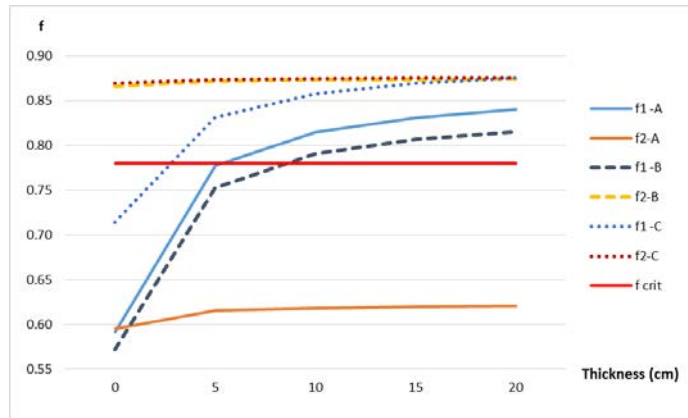


Fig. 8 – Temperature factors variation according to the thermal insulation alternative.

Case A – mosaic wall without interior thermal insulation; Case B – mosaic wall with 5 cm interior thermal insulation; Case C – mosaic wall with 5 cm interior insulation extended 50 cm on the adjacent wall.

Regarding the surface temperature factors variation presented in Figure 8, it can be observed that, for the exterior thermal insulation layer thicker than 10 cm, all temperature factors have values greater than the critical value ($f_{crit} = 0.78$), except for the f_{2-A} values, which assess the surface condensation risk on the uninsulated mosaic wall. It is found that an increase in the thickness of the external thermal insulation over the value of 10 cm does not significantly affect the value of the linear thermal transmittance nor of the temperature factor.

In Figure 9, the ψ coefficients variation according to the length of the thermal insulation extension on the adjacent wall is presented, for 5 cm thickness of the thermal insulation layer, both on the exterior of the regular wall and the interior of the mosaic wall.

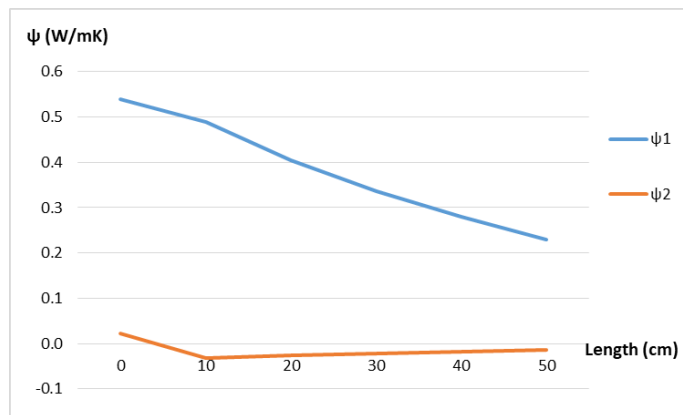


Fig. 9 – ψ coefficients variation according to the length of thermal insulation

Regarding the variation of ψ -values with the length of thermal insulation extension, it is obvious that the thermal bridge effect is decreasing with the increase of the length, but the decision about the length value should also take into consideration economic and technological considerations.

4. Conclusions

In order to increase the thermal energy efficiency of buildings with historical or architectural values, the method consisting in applying an insulation layer on the outside of the walls is not a suitable solution.

The application of an insulation layer on the inside contributes significantly to the reduction of energy consumption, but carries some risks regarding interstitial condensation and degradation due to frost or expansion of the masonry.

The case study refers to a particular situation, respectively the case of a building where only one façade cannot be thermal rehabilitated from outside.

Thermal field simulations performed for a characteristic area (the jointing between the insulated wall on the outside and another one on the interior) revealed the following:

- applying the interior insulation leads to a decrease in linear thermal transmittance of this wall and an increase for the wall with exterior thermal insulation;
- increasing the thickness of the exterior thermal insulation layer over 10 cm does not significantly influence the value of linear thermal transmittance, and therefore nor the thermal bridging effect on the heat losses;
- the risk of surface condensation is present when the mosaic wall is not insulated and decreases with the application of the insulation, disappearing at 40 cm extending on the adjacent wall.

The analysis of the other thermal bridges presents in the Northern façade of the building (that with mosaic) as well as the risks associated with the proposed interior insulation will be the subject of a study, which besides stationary temperature field simulations, will also include simulations of the humidity regime and in situ measurements.

Based on this study, it will be possible to adopt the optimal system of thermal interior insulation, which will ensure a balance between the value of energy saved and the risks related to the hygrothermal behaviour and the depth of frost penetration.

REFERENCES

- [1] F. Bean & all, *A guide to implement the energy performance of buildings directive (2018/844)*, Buildings Performance Institute Europe (BPIE), 2019.
- [2] R. Dudău, *Creșterea eficienței energetice în clădiri în România: provocări, oportunități și recomandări de politici*, Energy Policy Group, 2018.
- [3] *Romanian National Institute of Statistics*, <https://insse.ro/cms/en>.
- [4] E. Vereecken, L. Van Gelder, H. Janssen, S. Roels, “*Interior insulation for wall retrofitting – A probabilistic analysis of energy savings and hygrothermal risks*”, *Energy and Buildings* 89 (2015) 231–244.
- [5] T.K. Heusen, S.P. Bjarlov, R.H. Peuhkuri, M. Harrestrup, “*Long term in situ measurements of hygrothermal conditions at critical points in four cases of internally insulated historic solid masonry walls*”, *Energy & Buildings* 172 (2018) 235–248.
- [6] Two-Dimensional Building Heat-Transfer Modeling THERM version 7.6, Lawrence Berkeley National Laboratory, <https://windows.lbl.gov/software/therm>.
- [7] *Catalogue with thermal bridges specific to buildings*, C107-3 P1-P6, 2012 (in Romanian).
- [8] *Hygrothermal performance of building components and building elements - Internal surface temperature to avoid critical surface humidity and interstitial condensation - Calculation methods*, SR EN ISO 13788, 2013 (in Romanian).

DESIGN STRATEGIES FOR "nZEB" TYPE BUILDINGS

Victoria COTOROBAI¹, Theodor MATEESCU¹, Mihai PROFIRE¹, Ioan Cristian COTOROBAI¹ and Sebastian Valeriu HUDIȘTEANU¹

¹Gheorghe Asachi Technical University of Iași, Romania

Abstract. *Imposing new energy exigency for the future buildings (nZEB and other buildings) requires the reviewing of all the rules related to design elements and identifying a method for selecting the most appropriate passive strategies to ensure comfort in these buildings. These tasks must be carefully analysed and the effect of each must be quantified correctly within the regulations regarding the inner climate, hygro-thermal comfort, building performance, user requirements and their behaviour (physical activity, clothing). In this paper it is presented a numerical analysis of the impact of the different passive strategies used for insurance of hygro-thermal comfort, by assessing the contribution of each strategy in providing the indoor comfort indicators of establishing them as models of static dynamic or adaptive comfort. The analysis aims at identifying the best strategies passive acquiring comfort for different types of buildings and locations.*

Keywords: nZEB, passive strategies, adaptive comfort.

1. Introduction

The main cause responsible for the depreciation of the environment consists in CO₂ resulting from the combustion process of conventional fuels and their accumulation in the atmosphere [1, 2]. To identify the causes of this phenomenon, numerous studies and researches have been initiated around the world [3]. The first measures to correct the CO₂ concentration in the atmosphere were correlated with the energy consumption produced by burning conventional fuels in buildings, these measures being gradually implemented. Measures to reduce CO₂ emissions in the atmosphere have been found to have a positive impact in improving the ozone layer of the Earth's atmosphere [4-6].

More than a quarter of the construction found to be operated in Romania in 2050 will be built in the near future, which opens a promising horizon for reducing CO₂ emissions by controlling their design process [2]. Currently, several new concepts of energy efficient buildings have been promoted that have a minimum energy consumption from conventional resources for heating / cooling and the rest of the energy used in buildings to be obtained, almost entirely by capitalizing on renewable resources.

Thus, at EU level, ambitious CO₂ reduction targets have been set, by reducing the energy consumption produced by burning conventional fuels, by reducing the greenhouse gas emissions by 2050 by approx. 80% compared to 1990 levels and increasing security of energy supply by constantly reducing domestic consumption. Important steps have been taken to establish a definition and instructions for the implementation of "buildings with almost zero annual energy consumption" (nZEB) [7].

The "Energy Performance of Buildings Directive" (EPBD), revised in 2010, introduced the requirement to bring the energy performance of buildings to the level of "buildings with annual energy consumption for almost zero heating / cooling" (nZEB), starting in 2019 for residential buildings and from 2021 for all newly built buildings.

Recently, other major causes of affecting the ecological balance on Earth have been identified, such as the change in the water cycle in nature due to the intensification of solar activity, which is considered by far the most important one. Explosions and increased electromagnetic and proton emissions / solar electromagnetic field / solar winds have a major impact on the absorption capacity of CO₂ from the atmosphere at the surface level of the sea and of the ocean. According to some researchers [7-10], these factors would be responsible for a double amount of CO₂ accumulated in the atmosphere compared to that of anthropogenic origin.

The "International Initiative for a Sustainable Built Environment" (iiSBE) focuses on reducing the consumption (energy, water etc.) of a building, while reducing the amount of waste and pollutants generated over its lifetime. The application of any initiative to reduce consumption and CO₂ emissions must also include a requirement of the building, namely ensuring a healthy indoor environment, ensuring hygrothermal, visual or acoustic comfort in indoor spaces, respectively. Therefore, the requirements and parameters to be ensured for the indoor climate are regulated by norms / standards. In order to obtain an nZEB building, ensuring a zero balance of annual energy consumption for heating / cooling, requires hyper-insulation and hyper-sealing of the building and ensuring the ventilation for fresh air, which in turn must also be heated. In Romania, the design process of the heating / cooling building services is based on seasonal average values of outdoor air temperature. The variation of all external climatic parameters (temperature; direct, diffuse, global, reflected solar radiation) can substantially influence the behaviour of a building designed on the basis of average values during the (heating) season and does not allow the selection of the best equipment and heating / cooling strategies and control.

2. Interior comfort criteria suitable for nZEB buildings

The relation of the occupants with the interior environment is complex and it is characterized by the notion of comfort, which is defined by the sense of good / satisfaction that the human body feels in relation to its external environment [11]. In the last 50 years, comfort problems have been the subject of numerous studies and researches aimed at establishing the comfort parameters necessary for the design of

buildings [7] and their performances (especially energy), as well as their control strategies. The quality criteria related to the indoor environments concern the hygrothermal, visual, acoustic and sanitary comfort. The parameters that characterize the interior environment are relatively numerous and extremely variable over time [12]. The occupant (the user of the interior space) is influenced by the nature and dynamics of these parameters and he can contribute to changing the characteristics and dynamics of the environment in which he operates. Thus, the need arises to predict the parameters that will ensure an optimal indoor climate from a hygro-thermal and healthy point of view for the human being and its activities and implicitly the need to select / design the most suitable strategies to ensure comfort. It is necessary to reconsider the concept of habitat as well as the mandatory limit values for the defining parameters of the different levels of hygrothermal comfort corresponding to energy efficient buildings. Some of the energy-efficient buildings are characterized by hyper-tightness and insulation. Other energy efficient buildings (some of the NZBE buildings, passive buildings, passive solar buildings, passive bio-climatic buildings) rely on the human factor in the effort to ensure indoor comfort conditions, which is why the comfort should be analysed differently than standard buildings.

The buildings of the future will be mostly intelligent buildings, with intelligent envelope, dynamic-adaptable to the characteristics of the external climate and the variable requirements of the users. In these buildings, comfort is itself characterized by dynamism and the criteria for establishing its parameters are different than in the cases listed above. Through the criteria set out above, thermal criteria is of major importance in terms of the design and evaluation of the performance of heating / cooling / ventilation / air conditioning installations. Parameters that influence hygrothermal comfort can be grouped into three main categories [13]:

- a. physical parameters (air temperature, average radiant temperature of the enclosure walls, relative humidity of the air, relative air velocity inside the enclosure, atmospheric pressure, light intensity, noise level);
- b. organic parameters (age, sex, national characteristics of the occupants);
- c. external parameters (level of human activity, type of clothing, social conditions).

The positive or negative effect of one parameter can be enhanced or counterbalance by another parameter. For the design of NZBE buildings, it is important to set the parameters of thermal comfort so that they are obtained with minimum energy consumption. For this purpose, different models of hygrothermal comfort have been proposed, each of them being correlated with the requirements imposed on the buildings of that time. These are very important for designing energy efficient buildings. They describe quantitatively, the limiting climatic conditions for which people feel good from a thermal point of view. These conditions are used to ensure a comfortable thermal environment, with minimum energy consumption, regardless of the external climatic conditions.

In case of nZEB buildings, the specialists [2], propose the use of the “adaptive comfort” model, respectively the use of strategies for the acquisition of comfort parameters by natural ventilation. The use of only this strategy for the buildings located in geographical areas with high winter / summer or day / night variability, does not provide the comfort for the entire operating period. There is a need for a broader analysis of the possible passive strategies for providing comfort in NZBE buildings and their selection methods. The importance of achieving a comfortable indoor climate, given that the parameters of the outdoor climate vary over time, simultaneously with "avoiding unnecessary energy consumption", are among the stated objectives of the "European Directive on the Energy Performance of Buildings". A relevant analysis to a correct design of the buildings, in the context of comfort conditions, must be mainly ensured by passive strategies.

In this paper, an analysis tool developed in US (Climate Consultant) was used [14]. It addresses several comfort models and consideration of several strategies to obtain them. The comfort models considered are: *Adaptive Comfort Model*, *Predictive Mean Vote Model* [5]. This analysis is useful in establishing the best design strategies for energy efficient buildings, under different climatic conditions. The authors highlight the wide variation of each climate parameter, in order to identify a mechanism for selecting passive heating/cooling strategies of nZEB buildings.

3. Methods

3.1. Net Zero concept - a criterion of global performance of buildings, useful in the construction of a sustainable environment

In the effort to define the most comprehensive actions for a sustainable built environment, the “*Net Zero Concept*” was promoted, with the significance of a strategy for setting performance objectives for the built environment based on the local availability of renewable energy and water resources. Other concepts, meant to contribute to the definition of a sustainable built environment, have been developed:

- nZEB - “almost Zero-Energy Building” include buildings with more energy produced than consumed, with an of energy produced and with the energy used for household appliances, lighting, ventilation, obtained from local renewable resources [2, 7, 16];
- ZNC – “Zero Net Carbon”, zero carbon dioxide emissions: this sets, for both new and existing buildings, a clear direction: towards a built environment with zero emissions with a negative impact on the environment (carbon/ CO₂ and other). The promotion of ZNC buildings respond to the urgent need to mitigate the impact of CO₂ emissions from burning fossil fuels. A ZNC building is defined as: "a very energy-efficient building, which produces or purchases sufficient renewable energy without carbon emissions to meet the energy consumption of buildings annually" [16]. In a ZNC building, carbon-based energy consumption is reduced first by building design strategies and also by measures to make them more

efficient. This task is achieved by generating on-site energy from renewable resources and by purchasing energy produced at a distance from the building, from renewable resources. By establishing a net zero balance of carbon-free energy consumption, the definition of ZNC can be applied to all types of buildings, new and existing, with a relatively high or limited capacity to generate renewable energy on-site (buildings in dense urban environments). The definition of ZNC will play a significant role in guiding the processes of building design, the development of urban space in general as well as the operations for professional organizations and political decision-makers.

- The 100% renewables energies platform, promoted in 2018, aims to use the most adequate local renewable energy resources for buildings and decentralizing energy production [2, 8].

3.2. Other complementary concepts

Other concepts developed under this umbrella:

- NZWB – “Net Zero Water Building” Strategies: net consumption of water in buildings is zero;
- Net Zero Waste / Zero Waste, consist in reducing the amount of waste generated, selective collection, recycling, reuse, recovery and conditioning almost entirely, as far as possible, in order of priority, locally and then collectively.

In the paper, the authors took into account the possibility of using and integrating all the concepts stated above.

3.3. Analysis tools

In order to assure the requirements for increasing the energy performance of buildings [12], it was necessary to ensure new energy quality requirements, differentiated in relation to the age of the buildings (new or existing) and the time horizon (short term - 2020; long term - 2050). In the short term, new buildings will have to meet the requirements of nZEB buildings, and in the long term it is necessary to bring existing buildings to the same quality requirements as those imposed on new buildings. But the performances for which the building is qualified with the nZEB attribute are determined by each state and consequently, they are different from one country to another. On the other hand, the development strategies proposed by different states, took into account the experience of the respective countries in the field, but this experience consisted of design measures for static comfort criteria. They include solutions which are not adapted to the particularities of the location environment and its dynamics.

This paper presents an analysis of the impact of different passive strategies for the acquisition of comfort, according to different comfort standards, taking into account the real climate data and their impact on the different strategies (temperature of dry / wet thermometer, direct / diffused / reflected solar radiation, normal / inclined solar radiation, soil temperature at different depths, wind speed and direction, nebula and

hours of solar glare). The design strategies considered within the Climate Consultant analysis software are correlated with the comfort models and for each of these there is determined the number of operating hours.

The software also allows partial analyses for other types of strategies useful in achieving the conditions of hygrothermal comfort, respectively: identifying the useful elements in the evaluation of the impact of the phase change materials (PCM) in the process of ensuring the hygrothermal comfort, evaluating the possibilities of ground coupling, identifying the opportunity of harnessing the solar energy carried by the direct / diffuse / global radiation, identifying the opportunity of harnessing the wind energy with the help of turbines with vertical or horizontal axis etc.

The software used for analysis were:

- Opaque, for the study of the behaviour of the construction elements (of those with embedded PCM) under the dynamic climate conditions. This allows the evaluation of thermal losses / contributions by element during the whole year - Figure 1;
- Climate Consultant, an extremely useful software for assessing the impact of strategies used to provide comfort parameters, for different comfort models, in different locations and different neighbourhoods. It allows to determine the number of active hours for each strategy and its weight in the overall process of ensuring the thermal comfort parameters [14, 17];
- The TRNSYS platform, for evaluating the overall behaviour of the building and the related installation systems.

These analysis tools were used because they allow complex analyses, considering all the climate impact parameters from the desired location and highlight the extremely strong dependence on climatic parameters that are not taken into account in the classical design (respectively the structure of solar radiation, wind direction etc.).

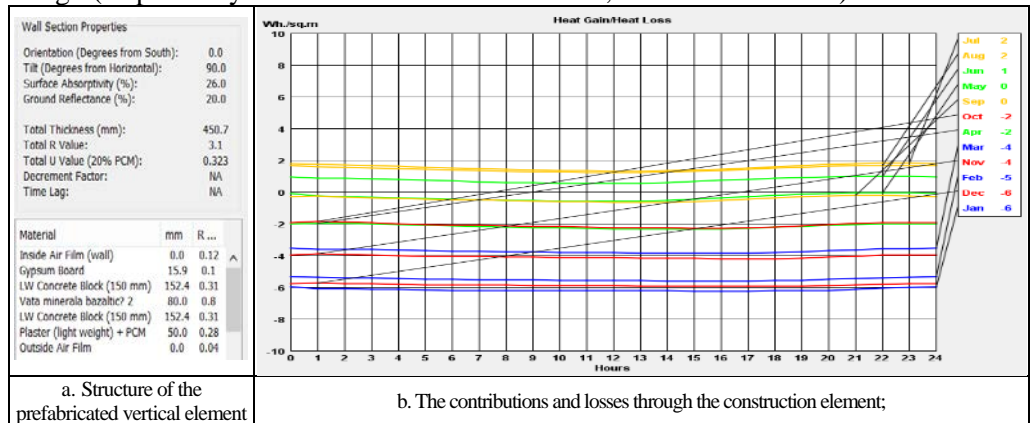


Fig. 1 - Dynamic behaviour of a construction element with PCM located outside

The contributions and losses through the construction element with PCM, are smaller compared to the element without PCM – Figure 1.

3.4. The analysis method used in Climate Consultant software

Human thermal comfort can be defined primarily by dry bulb temperature and humidity, although different sources have slightly different definitions. The Climate Consultant software allows the user to select from one of four comfort definitions. The alternative Comfort Models include the following [11]:

- a) California Energy Code Comfort Model, 2013;
- b) ASHRAE Standard 55, Current Handbook of Fundamentals Comfort Model;
- c) ASHRAE Handbook of Fundamentals Comfort Model through 2005;
- d) Adaptive Comfort Model in ASHRAE Standard 55-2010.

Models of Thermal Comfort. There are two different types of models for assessing thermal comfort: static models and adaptive models [11]. The California Energy Code Comfort Model which is the default in Climate Consultant is a static model. It assumes that the indoor temperature required for thermal comfort does not change with the seasons. The high and low temperatures which define the comfort range are static. At the other extreme is the Adaptive Comfort Model defined in ASHRAE Standard 55. It assumes spaces are naturally ventilated and occupants can open and close windows. Thus, their thermal response will depend in part on outdoor conditions and they will have a wider comfort range than in buildings with centralized HVAC systems. In between these extremes are two other model options in Climate Consultant: ASHRAE Handbook of Fundamentals Comfort Model and the ASHRAE Standard 55 Comfort Model using PMV (Predicted Mean Vote). Both these models assume that people will adapt to climate change by changing their clothing and thus have two comfort zones (one for winter and one for summer) based on a shift in comfort low and comfort high temperatures.

Psychrometric Chart is one of the most powerful design tools in Climate Consultant. It represents the dry bulb temperature and moisture content. The curved line on the far left is the saturation line (100% Relative Humidity line). The full description of this powerful design tool is presented in [17]. On this chart, every hour in the EPW climate data file is shown as a dot. The colour of each dot can represent whether or not the hour is comfortable (green) or uncomfortable (red), according to the inputs defining comfort on the criteria screen.

Design Strategies. The software provides 16 strategies that can be extended by the user: 1 - Comfort; 2 - Shading window; 3 - Thermal mass with high inertia; 4 - Thermal table with high inertia washed at night; 5 - Cooling by direct evaporation; 6 - Two-stage evaporative cooling; 7 - Cooling by natural ventilation; 8 - Cooling by mechanical ventilation; 9 - Internal thermal inputs; 10 - Passive solar contributions from low thermal masses; 11 - Passive solar contributions from high thermal masses; 12 - Wind protection

of outdoor spaces; 13 - Humidification; 14 - Dehumidification; 15 - Cooling and dehumidifying; 16 - Heating and humidification [2, 14].

Certain building design strategies are more suitable for buildings located in specific climates. For example, for buildings where the energy performance of the envelope largely determines the performance of the building (homes, offices, schools, accommodation buildings), the influence of the climate is major. The software allows the evaluation for different locations, the selection of the desired comfort models, the desired heating / cooling strategies and the evaluation of the performances of each model and strategy through the number of hours of participation in ensuring comfort during the year.

The total number of Comfortable Hours using the Selected Strategies is given and write in Psychrometric Chart. This represents a design that is a composite of all the selected strategies where each hour is counted only once, thus the total number of Comfortable Hours will not exceed 100%. These percentages help identify which passive Design Strategies will be most effective in this climate.

Comfort Zone. The comfort zone is represented in the Psychrometric Chart, where it is defined by the Temperature of the dry bulb and in some models also the humidity and "clo" (seasonal clothing). The comfort model adopted has a major impact on the number of comfortable hours. An observation to be made is that for nZEB buildings it is recommended to use adaptive comfort, but our study showed that the number of hours of comfort provided by passive strategies can be increased by optimizing the passive strategies in that location.

Comfortable Hours using Selected Strategies. In the Psychrometric Chart are given the overall percentage and total number of comfortable hours created by all the strategies that are selected (highlighted).

Show Best Set of Design Strategies. The software allows you to highlight the best set of passive design strategies (for example, the smallest set of strategies that maximize the number of comfortable hours without using conventional heating or cooling systems) [8, 18].

4. Results

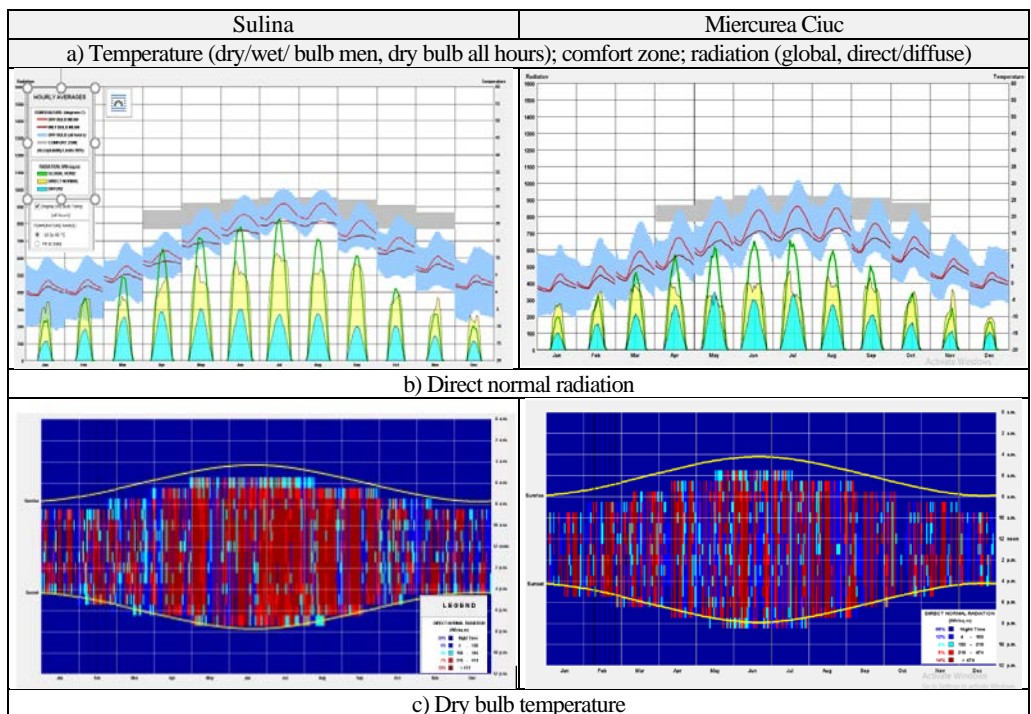
4.1. Hypothesis

The building analysed was a residential one. The comfort criteria considered are those set out in subchapter 3.4. For analysis, the information on different climatic parameters of interest was retained (number of hours with temperature / direct and global radiation / coverage degree etc.).

4.2. Results obtained

The obtained results were represented as graphs with hourly / daily / monthly variations and average values (maximum / minimum averages) and monthly and hourly averages of the main climatic parameters: temperature of dry and humid thermometer; global solar radiation, direct normal, diffused, reflected by the soil with different coverings, on an inclined plane; the degree of sky cover; direct normal lighting; number of hours of solar brightness, soil temperature at different depths, wind speed and direction [4]. An extract of these data is shown in Figure 2.a.-f.

The graphs are presented in parallel, Figure 2, for the city of Sulina and the city Miercurea-Ciuc, representative cities for the territory of Romania (Sulina, located in the Danube Delta, in a very sunny area; Miercurea-Ciuc, in a depression surrounded by mountains, a real pole of cold ("Little Siberia": with very short summers – 2...3 months a year), temperatures between 2°...32° C; with long winters and frosty, with temperatures often below -30°).



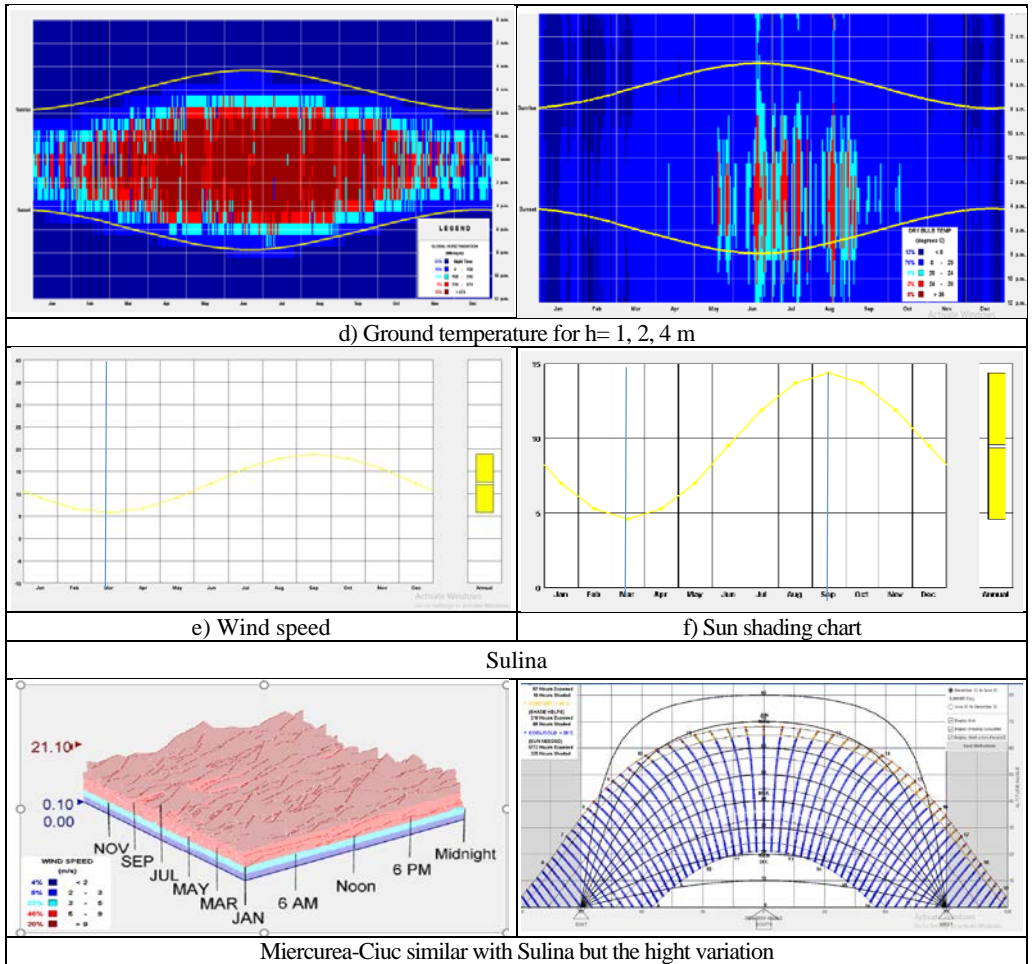


Fig. 2 - Climate data used in the analysis of the passive strategies for achieving comfort in buildings with human activity

Table 1
Interior comfort parameters for different models and locations

	Location	Sulina	Miercurea-Ciuc
Size, limits			
Acceptance limits (%)		90.0	90.0
Average monthly outdoor temperature of the minimum dry glob-thermometer		10.0	10.0
Minimum monthly outdoor temperature of the minimum dry glob-thermometer		22.5	19.8
Low comfort - Minimum operating temperature in this location		18.4	18.4
High comfort - Maximum operating temperature in this location		27.3	26.4

The analysis method used in Climate Consultant. After an initial analysis of the dynamics of climatic parameters and conversion systems, an analysis of storage systems and an analysis of updated global costs over the life of the building is required. The analysis considered the different comfort models, strategies and parameters [5]. The represented parameters allow the selection of the heating/cooling strategies to be analysed, respectively of the appropriate heating/cooling systems - Table 2. The locations for which the analyses were carried out were: Sulina, Miercurea-Ciuc. Climate data were extracted from Meteonorm 7.2 [18].

Table 2

Extract from the research results with the impact of different strategies for achieving a comfortable indoor climate, in different comfort models and locations-continuation

Design Strategies*	Location	Miercurea-Ciuc				Sulina			
	Comfort model	1	2	3	4	1	2	3	4
1	Hours (h)	0	766	126	646	0	639	788	500
	%	0	8.7	14.4	7.4	0	7.3	9.0	5.7
2	Hours (h)	0	549	668	993	0	205	296	552
	%	0	6.3	7.8	11.3	0	2.3	3.4	6.3
3	Hours (h)	0	9	0	0	0	45	129	223
	%	0	0.1	0	0	0	0.5	1.5	2.5
4	Hours (h) / %	0	0	0	0	0	0	0	0
5	Hours (h)	0	0	0	56	0	0	0	0
	%	0	0	0	0.6	0	0	0	0
6	Hours (h) / %	0	0	0	0	0	0	0	0
7	Hours (h)	125	0	0	123	620	0	0	0
	%	14.3	0	0	14.1	7.1	0	0	0
8	Hours (h)	0	0	783	0	0	0	201	382
	%	0	0	8.9	0	0	0	2.3	4.4
9	Hours (h)	0	204	202	2131	0	219	215	219
	%	0	23.0	23.1	24.0	0	25.1	24.0	25.1
10	Hours (h)	0	0	0	0	0	0	0	0
	%	0	0	0	0	0	0	0	0
11	Hours (h)	0	1431	1400	1400	0	1336	1342	1342
	%	0	16.3	16	16	0	15.3	15.3	15.3
12	Hours (h)	0	987	956	956	0	70	66	66
	%	0	11.2	10.9	10.9	0	0.8	0.8	0.8
13	Hours (h) / %	0	0	0	0	0	0	0	0
14	Hours (h)	0	124	459	675	0	243	76	38
	%	0	14.2	5.2	7.4	0	2.8	0.9	0.4
15	Hours (h)	0	226	139	181	0	43	0	0
	%	0	26	1.6	2.1	0	0.5	0	0
16	Hours (h)	0	394	339	393	0	480	479	479
	%	0	45.0	44.0	44.0	0	54.0	54.0	54.0
*Strategies for the acquisition of comfort: number 1-16 **Model confort: 1_Adaptive comfort in ASHRAE 55/2010; 2_ASHRAE Handbook of Fundamentals Comfort Model, Through 2005; 3_Plus ASHRAE Standard 55; 4_California Energy Code Comfort Model, 2013									

The energy requirement for heating is relatively high for most of the analysed localities (over 40% of the year). The cooling requirement is relatively small and can be covered

by local appliances. The natural ventilation strategy (the strategy considered to provide adaptive comfort) can ensure comfort for a period of maximum 14.3% of the year. By combining several passive strategies (1-16), the annual period needed for heating / cooling, respectively the energy consumption can be substantially reduced.

Table 3

The climatic parameters of interest for the analysis of the strategies of ensuring the comfortable environment in buildings nZEB, in Romania area

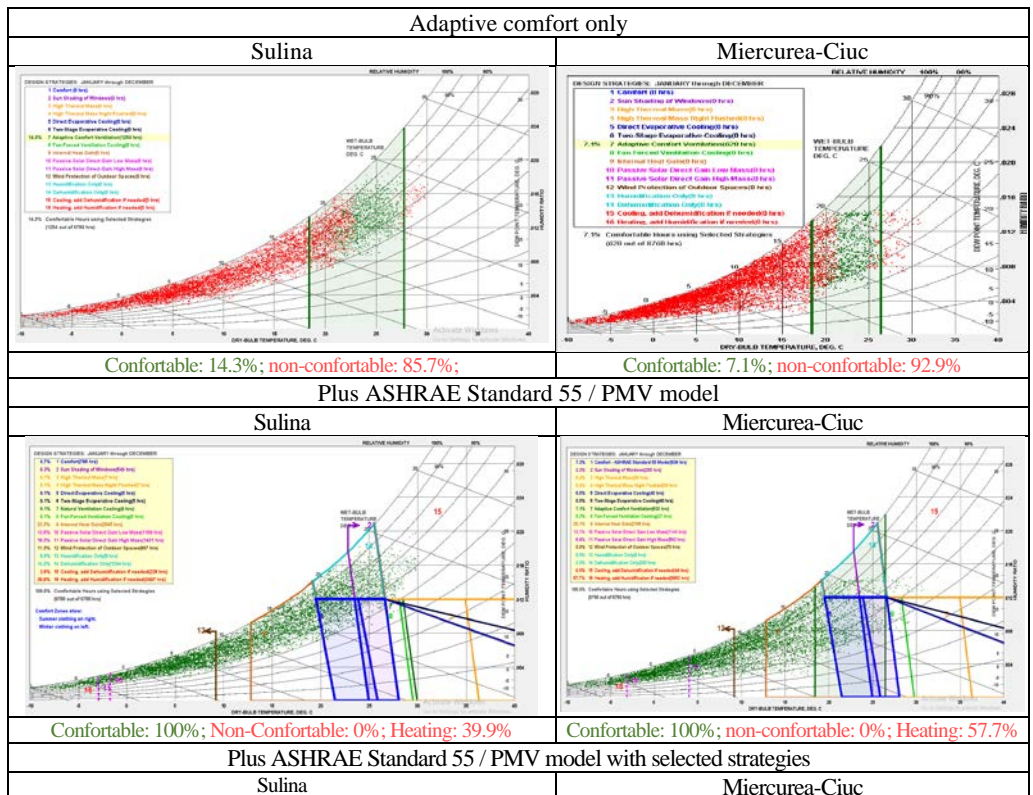
Climatic parameter	Model comfort	Parameter variation inter.	1*	2*	Proposal
Dry Bulb Temperature: interval variation (°C); annual percent %	1,4	<0	9	13	a) PCM can be used in Sulina b) Green roofs/wall are recommended in Sulina.
		[0,20]	67	76	
		(20,24]	15	8	
		(24,38]	10	3	
	2	>38	9	0	
		<0	9	13	
		[0,20]	68	76	
		(20,27]	21	9	
Wind speed (m/s)	1,2,3,4	(27,38]	2	1	Can be used wind turbine: a. with vertical axis in Miercurea-Ciuc, b. with horizontal axis: Sulina; c. with vertical axis and magnetic levitation: both
		>38	0	0	
		<2	4	33	
		[2,3]	6	20	
		(3,5]	23	29	
		(5,9]	46	15	
Horizontal Global Radiation [Wh/m ²]	1,2,3,4	>9	20	3	The global solar radiation in the horizontal plane has a relatively small variation in the area of Romania. It recommended to use roof cooling radiant in Sulina.
		night	51	51	
		[4,158]	15	19	
		(158,316]	11	11	
		(316,474]	9	8	
Direct Normal Radiation [Wh/m ²]	1,2,4	>474	15	11	The thermal solar collector is recommended for Sulina.
		night	58	65	
		[4,158]	9	12	
		(158,316]	6	4	
		(316,474]	7	5	
Vertical surface radiation [Wh/m ²]	1	>474	20	14	Strategies for using smart windows are recommended for Sulina.
		night	57	58	
		[4,158]	17	23	
		(158,316]	10	7	
		(316,474]	9	5	
		>474	8	7	

In Table 3 the characteristic fields of variation of the main climatic parameters are extracted, for the analysed localities by author, in order to identify suitable strategies for ensuring the interior comfort and the optimal condition for use renewables energies systems. Following the analysis of climate data, the following conclusions can be drawn:

- identification of the areas in which the PCM can be used;
- identification of the areas where different wind turbines can be used (with vertical / horizontal axis, magnetic levitation) [4];

- identifying the areas in which the strategies for using smart windows can be used;
- identification of areas with a major impact of cloud cover on the size of the solar radiation reached the ground level;
- identification of the areas where the solar energy systems from the ground can be used efficiently;
- identification of areas with efficient solar shading systems, wind protection systems;
- identification of the favourable areas for the implementation of the different solar systems for the use of solar energy.

The analysis realized by using Climate Consultant software allows the selection of the best strategies for obtaining a comfortable indoor climate. In Figure 3 there are presented, for Sulina and Miercurea-Ciuc, the annual number of active hours for each strategy, given that the comfort model used is only adaptive comfort and the Plus ASHRAE Standard 55 / PMV model.



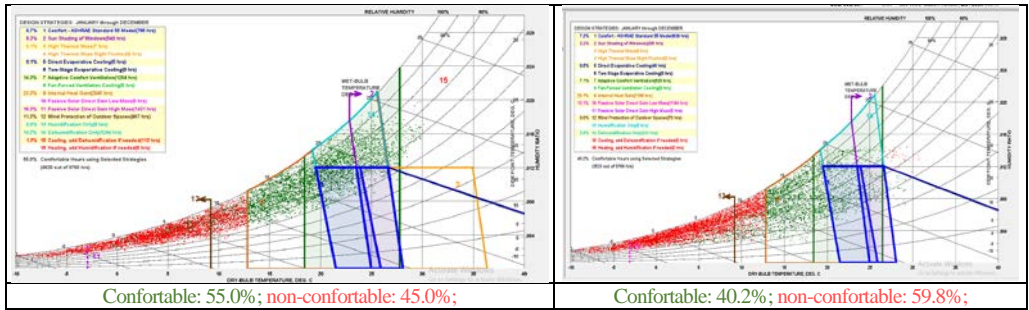


Fig. 3 - The impact of passive strategies to ensure indoor comfort psychrometric charts with comfort zones

It can be noticed that:

- by using the principles of adaptive comfort, the parameters in the indoor space are only partially ensured;
- by using several passive strategies, the interior comfort according to the Plus ASHRAE Standard 55 / PMV model can be ensured for an important period ($\leq 50\%$) [16, 19, 20].

In this study there are included the following passive strategies:

- coupling the construction elements with the PCM panels (with phase change materials - encapsulated micron) to the interior / exterior of the walls and the roof: the construction element with PCM acquires the function of temperature self-regulation, with an impact in reducing the need for energy for cooling;
- the use of intelligent, dynamic, thermochromic, heliotropic windows (the energy required for heating / cooling can be reduced to almost "zero");
- use of Canadian wells;
- the introduction of a strategy of passive cooling of the roof with radiator towards the sky vault;
- adding natural lighting strategies (windows + light wells): allows to reduce energy consumption for lighting; introduction of LED luminaires. Our evaluations also included such strategies.

By applying the adaptive comfort model, respectively by applying the cooling strategy by natural ventilation, the internal comfort requirements cannot be ensured and in addition it cannot be kept constant – Table 4.

Table 4*Increase the duration of comfort by introducing more passive strategies*

Adaptive comfort only. Design strategies: January through December			
Sulina		Miercurea-Ciuc	
7 Adaptive comfort ventilation: 14.3%/649 h		7 Adaptive comfort ventilation: 9.4%/649 h	
Comfortable: 14.3%; non-comfortable: 85.7%		Comfortable: 9.4%; non-comfortable: 91.6%	
Plus ASHRAE Standard 55 with some of the 16 strategies and strategies proposed by the authors			
1	Comfort:	10.4%/766 h	Comfort: 12.4%/639 h
2	Shading window:	10.7%/549 h	Shading window: 4.0%/205 h
3	Thermal mass with high inertia:	0.1%/7 h	Thermal mass with high inertia: 0.7%/38 h
7	Adaptive comfort ventilation:	13.4%/1254	Adaptive comfort ventilation: 0.7% / 38 h
9	Internal thermal inputs:	38.0%/1950 h	Internal thermal inputs: 41.2/2144 h
11	Passive solar with PCM:	22.6%/1160	Passive solar with PCM: 20.8% / 1070 h
12	Wind protection of outdoor spaces:	0.8%/39 h	Wind protection of outdoor spaces: 0.2%/11 h
14	Dehumidification:	24.2/1244 h	Dehumidification: 14.7/243 h
17	Smart/dynamic/thermochoic/heliotropic windows:		Smart/dynamic/thermochoic/heliotropic windows: 3%/263
18	Canadian wells:	8%/701 h	Canadian wells: 9%/788 h
19	Radiant passive cooling roof:	4%/350 h	Radiant passive cooling roof: 1%/88 h
20	Adding natural lighting strategies:	1%/88 h	Adding natural lighting strategies: 1%/88 h
21	Introduction of LED luminaires:	2%/175 h	Introduction of LED luminaires: 2%/176
Comfortable: 98.0% (8633 h); non-comfortable: 2%		Comfortable: 66.1% (5791 h); non-comfortable: 33.9%	

5. Conclusions

In the analysed cases, the adoption of passive heating / cooling strategies proposed in software Climate Consultant, does not ensure the indoor hygrothermal comfort except for approximately 7...15% of the annual period and for the summer period, respectively. For summer, the most appropriate strategy is organized natural ventilation. In this strategy the shading of the windows is no longer necessary to cool the buildings. Active heating of buildings remains necessary and is important (approximative half a year).

For some locations, it is possible to ensure interior comfort only by coupling several passive strategies (adaptive comfort ventilation, passive solar direct gain (low and high), passive solar with PCM and the natural lighting). The appropriate comfort control strategies should be correlated with the specific climatic periods.

Maintaining the functioning of nZEB buildings in the comfort zone is ensured if they are designed after:

- the standard of passive buildings for winter, but with appropriate technologies that favour the reduction of gains solar in the summer period;
- the standard of passive buildings for the summer period, but with strategies of control of the indoor climate for the heatwave period (natural aeration strategies);
- use of renewable energy systems in close correlation with location and availability;
- the standard of passive buildings, but with appropriate technologies that favour the reduction of solar gains in the summer period (with PCM).

REFERENCES

- [1] B. Atanasiu, “Implementarea clădirilor cu consum de energie aproape zero (nZEB) în România – Definiție și foaie de parcurs”, Institutul European pentru Performanța Energetică a Clădirilor (BPIE), august 2012.
- [2] F. Barbolini, P. Cappellacci, L. Guardiglia, “A Design Strategy to Reach nZEB Standards Integrating Energy Efficiency Measures and Passive Energy Use”, *Energy Procedia*, vol. 111, 2017, pp. 205-214.
- [3] H. M. Taleb, “Using passive cooling strategies to improve thermal performance and reduce energy consumption of residential buildings in U.A.E. buildings”, *Frontiers of Architectural Research*, vol. 3(2), 2014, pp. 154-165, <https://doi.org/10.1016/j.foar.2014.01.002>.
- [4] V. Cotorobai, “Systems for the recovery of renewable energy resources”, Vol I and II, Matrixrom publishing house, Bucharest, 2019.
- [5] V. Cotorobai, “Metode de caracterizare a ambianței termice interioare în activitatea de concepere a clădirilor passive”, Conferința Instalații pentru Construcții și Economia de Energie, Iași, 2009, Editura CERMI, ISSN 1843-3510.
- [6] V. Cotorobai, “Instrumente de selectare a celor mai indicate strategii de proiectare pentru clădirile performante energetice”, Conferința internațională Instalații pentru construcții și confortul ambiental, Timișoara, 2017, MATRIXROM, București, 2017.
- [7] L. Antonelli, “Why airtightness is vital for delivering NZEB (part 1)”, <https://blog.siga.swiss/en/why-airtightness-is-vital-for-delivering-nzeb-part-1/>.
- [8] C. Polo López, F. Frontini, “Energy efficiency and renewable solar energy integration in heritage historic buildings”, *Energy Procedia*, vol. 48, 2014, pp. 1493 – 1502.
- [9] A. A. Y. Freewan, “Advances in Passive Cooling Design: An Integrated Design Approach”, 2019, DOI: 10.5772/intechopen.87123.
- [10] A. K. Mohammad, “An overview of passive cooling techniques in buildings: design concepts and architectural interventions”, *Acta Technica Napocensis: Civil Engineering Architecture*, vol. 55(1), 2012, pp. 84-97.
- [11] <https://comfort.cbe.berkeley.edu/>.
- [12] EN 16798-1:2019. “How to assess the energy performance of buildings”, Module M1-6.
- [13] M. C. Ness, “Principles and tools for bioclimatic building design”, PLEA 2017 at: Edinburgh, Vol.: III.
- [14] Software Climate Consultant.
- [15] EN 12665:2019. “Light and lighting - Basic terms and criteria for specifying lighting requirements”.
- [16] G. Baruch, R. Van Nostrand, “Passive and Low Energy Cooling of Buildings”, 1994.
- [17] www.energy-design-tools.aud.ucla.edu.
- [18] <https://meteonorm.com/en/>
- [19] Givoni-Milne, “Architectural Design Based on Climate”, Chapter 6.
- [20] Givoni, “Energy Conservation through Building Design”, Donald Watson, Editor, McGraw-Hill, New York, 1979.

METAMATERIALS FOR "nZEB" BUILDINGS

Victoria COTOROBAI¹, Ioan Cristian COTOROBAI¹, Silvana BRATA², Ionuț-Cristian BRANCA and Ana- Diana ANCAS¹

¹"Gheorghe Asachi" Technical University from Iași

²POLITEHNICA University, Timișoara

Abstract. *Metamaterials are specially designed to interact, in a controlled manner, with various waves. They are very "young" but they have attracted the attention of specialists from the construction area. The buildings have known throughout their existence different approaches in terms of functions, requirements, concepts, materials used, and other, in correlation with the level of civilization, technology, climate characteristics, primary needs, or desire to express the power/the luxury in the different moments and for different people. The concept of the nZEB building was recently promoted. The metamaterials developed so far can also be used in nZEB, such as: for controlling the impact of the different waves with the building; in the equipment of thermal/visual comfort; in the control components; for increasing the performance of power generation equipment. This paper has inventoried some metamaterials that can determine the growth of the building's energetical performances and examples of the growth potential of the thermal and visual performance of glass systems containing metamaterials (static and dynamic).*

Keywords: metamaterials; metamaterials for roof cooling; waves guide for PV cell; thermal & acoustic metamaterials (aerogels).

1. Introduction

1.1. Buildings of the future. Requirements. Insurance possibilities.

The recent climate changes, identified from the studies/measurements/observations made at the level of the planet Earth, have highlighted the need to reduce the concentration of CO₂ in the terrestrial atmosphere, respectively the need to promote the measures of energy efficiency of buildings (reduction emission CO₂, by reduction energy consumption from fossils resources) [1, 2, 3, 4]. Lately, the measures promoted are completely new (results of the newest research & innovation).

These must enable the energy performance of buildings to be increased and in relation to other quality criteria (environmentally friendly, acoustic; ensuring & maintaining human health; be dynamic-adaptable to occupant demands and environmental changes

- interior and exterior; be economical; have a life span correlated with that of the structure; it can be integrated into the structure existing buildings simple and without the significant impact in the occupant's activities [5,6,7].

In existing buildings: it is absolutely necessary to increase the thermal and acoustic protection, by means of interventions, realized in general on the outside of the tire; adaptation of heating/cooling systems to the new requirements imposed on nZEB buildings (reduced loads, uniform energy distribution etc.); the association with systems for generating energy from renewable resources and others [8,9].

1.2. Metamaterials. Definitions. Types of metamaterials. Applications.

Metamaterials know strong development and high worldwide recognition (they are in the top 10 materials that will change the world).

Their definition is not unitary. In the specialized literature, various definitions are given, in relation to the experience in the related field of research and to the experience of the authors. The most common definitions: "*A metamaterial = a material designed to have non-existent properties in natural materials*" [10, 11].

The materials are the structures usually arranged in repeating patterns, at scales that are smaller than the wavelengths of the phenomena they influence. They derive their properties not from the properties of the base materials, but from their newly designed structures (their geometrical properties, precise shape, size, orientation, and arrangement). The new properties obtained give the metamaterial the quality of the smart material [12, 13]. He becomes capable of control electromagnetic waves by blocking, absorbing, enhancing, or bending waves. The metamaterials obtained can have uses that are impossible to achieve with the classical materials. The metamaterials designed for this purpose can affect/control the waves of electromagnetic, acoustic, or seismic radiation. The many and significant research was attracted by the metamaterials with a negative refractive index. This definition, in its most general expression, shows that the concept of metamaterials can cover all areas of physics: in the fields of electromagnetism including optics, acoustics, fluids, seismic etc [14, 15, 16].

In particular, in design composite metamaterials, electromagnetic waves interact with the inclusions that produce electric & magnetic moments, which in turn affect the macroscopic effective permittivity & permeability of the bulk composite medium [17, 18]. So, metamaterials can be synthesized by embedding artificially fabricated inclusions into a specified host medium and, in consequence, this provides the designer with a large collection of independent parameters such as properties of host materials, size, shape, and compositions of inclusions. In the research metamaterials with the characteristic's deliverables, all these properties can play an important role [19]. By manipulating the inclusions, the designer has at its disposal a new possibility for metamaterial processing.

They were designed/studied and even (in some cases) made a variety of metamaterials. A classification of the different types of metamaterials developed so far and a characterization of each category are presented in different publications, [21, 22, 23, 24, 25, 26].

1.3. Applications and research areas of metamaterials in buildings is diverse and multiples.

In the field of buildings, the metamaterials can be used to increase [27]:

- the performances of buildings (thermo-dynamic; acoustic; seismic; absorption / reflection, refraction, transmission, emission; oxidation; thermal/chemical stability) of the opaque/glazed, vertical/horizontal, exterior/interior; performance of heating / cooling systems and their components;
- the performance of indoor lighting systems;
- the performance of thermal/electrical/chemical energy storage systems;
- seismic performance of buildings;
- the performances of the quality control systems of the indoor atmosphere;
- the performance of the thermoregulation systems.

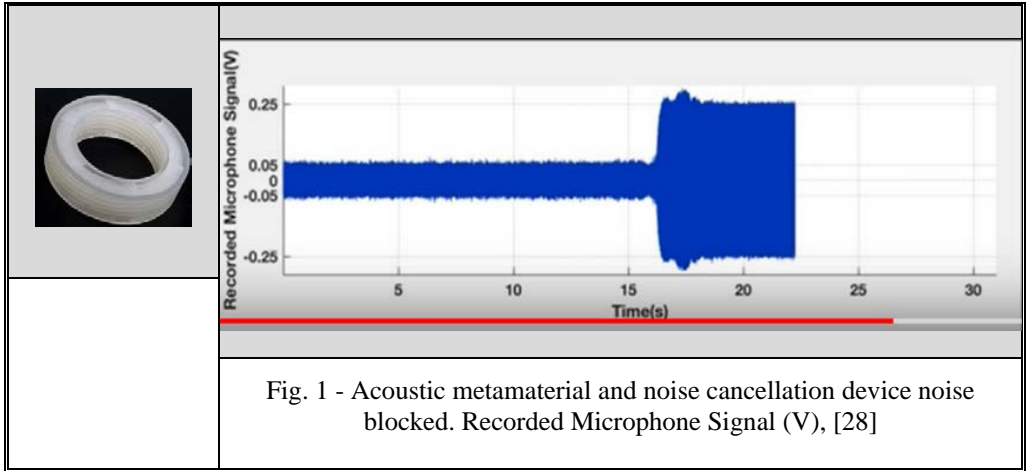
2. Method. Theory. Design. Model

2.1. Theory

2.1.1. *Metamaterials for the protection of buildings against the action of the exterior acoustics waves (noise due to road traffic) and the ventilation/piping installations*

The acoustic performance of the buildings is extremely important for the normal activity of the building. The most difficult issues were those related to: the protection of the building from road noise (which is constantly growing); reduction of noise transmitted by installations (with a positive impact on the location of building ventilation plants par example). The evolution of metamaterial research has provided efficient technological solutions for this purpose: a) *aerogel for acoustical* ant thermic protection building elements structures (presented at the point 2.1.2.); b) *metamaterials structure for acoustical protection of installations*. A solution in this scope:” Synthetic, *sound silencing structures*”. Acoustic metamaterials can block 94% of sounds (but not open-air). This ring of materials will be able to us in vacuum cleaners, air conditioners, fans, and other devices and products much quieter” [28] . The mathematically designed, 3D-printed acoustic metamaterial is shaped in such a way that it sends incoming sounds back to where they came from [28] say. Inside the outer ring, a helical pattern interferes with sounds, blocking them from transmitting through the open centre while preserving air's ability to flow through.

The image of these acoustic metamaterials and the result of the demonstration for their performances is presented in Fig. 1.



2.1.2. Metamaterial for the thermal & acoustical protection of the building

• Metamaterials for thermal and acoustic protection: aerogels

The material is a gel in which the liquid has been completely replaced with air. The actual matrix of the ring can be made of different substances (silica, metal oxides, graphene). The massive presence of air in the aerogel gives it the quality of excellent thermal insulation material and its special structure gives it a very high mechanical strength. The fatal defect of the aerogel is due to fragility, especially when it is made of silica. This disadvantage has been overcome by scientists from NASA who have made and experienced flexible polymer aerogels. Mixing other compounds in even silica-based aerogels could make them more flexible. So, the main qualities of aerogel are good thermal and sound insulation, high mechanical resistance, low density, many types, and high flexibility.

The application of the aerogel in the field of buildings, as thermal and sound insulation, in the form of building blocks for low-density metamaterials is one of the recent initiations. The carbon aerogel is synthesized by sol-gel polymerization of resorcinol with formaldehyde, followed by drying and carbonization of supercritical fluids. The end result is an aero-gel nanostructure, which can be adjusted through the concentrations of reactants and catalysts in the precursor solutions. Negative permittivity and negative permeability are obtained simultaneously in the low-density carbon aerogel. The negative permeability is similar to plasma and can be explained by the low-frequency plasmonic state of the carbon networks. Permissively values have a strong dependence on the frame and carbon aerogel mixers. In Fig.2 is presented the high-frequency magnetic response of the induced circulating currents determines the negative permeability.

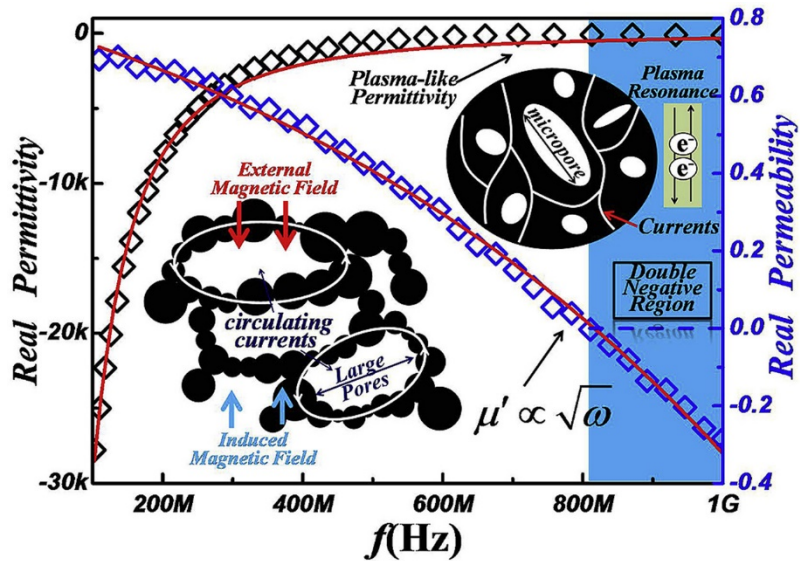


Fig. 2 - The NASA processes to made flexible air-gel (Source: [29])

Following the analytical calculations, the specialists demonstrated that the permeability values have a linear relationship with $(\omega)^{0.5}$. This shows a relaxation spectrum, as opposed to "magnetic plasma" of typical metamaterials. The use of the aerogel is unique and has a high potential for the realization of metamaterials with ultralow density at the nano-scale and also presents the ability to expand the potential applications of metamaterials, for different purposes and under extreme conditions.

Very recently the aerogel has been used in the field of buildings, as thermal and sound insulation and for fuel protection.

• Metamaterial for cooling the roof

He determines radiation to the celestial vault. It is a covering the mirrors for cooling the buildings by pumping the interior heat into space (Fig. 3).

For this action are realized "an air conditioning system for structures" (an engineered material): "it has the ability to cool objects even under direct sunlight with zero energy and water consumption". The metamaterial film, applied to a surface, cools the object underneath: a) it efficiently reflects incoming solar energy back into space while b) simultaneously, it allows the discharge of the energy accumulated by the surface, towards the underside of this film, in the form of infrared thermal radiation.

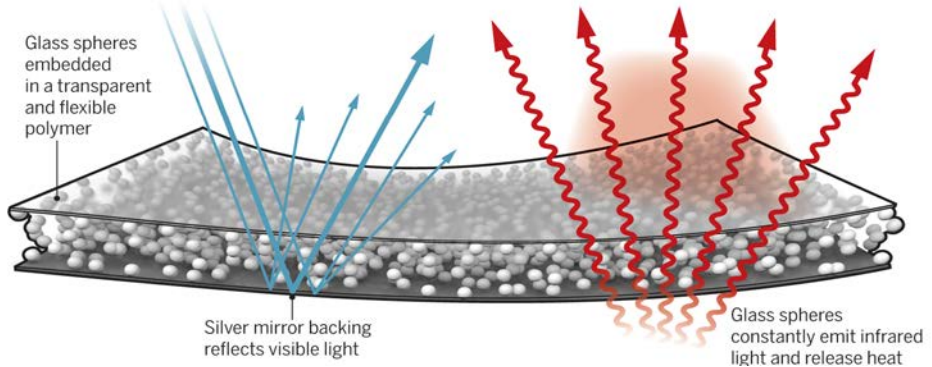


Fig. 3 - Metamaterial radiative-cooling film (Source: [29])

The objective of the inventors of the "Radi-Cool" group consists of ecological cooling technologies with zero energy consumption. The metamaterial system "Optical metamaterials that cool objects underneath (cooling materials)" [29] present diverse properties: a) The system exploits a passive peak cooling technology: it dissipates the heat of objects wrapped on Earth and is covered with radiative cooling film in outer space (the celestial vault is temperature $T = \sim 3$ K), in the form of infrared radiation ($8\text{--}13\text{ }\mu\text{m}$), through the atmospheric transparency window; b) The cooling film was a radiative or hybrid film (glass microscope-metamaterial plastic), completely transparent to radiation from the solar spectrum, with infrared emission greater than 0.93 in the window atmosphere; c) Silver coating of the metamaterial film determined or with average cooling power $P_c > 110$ W in three consecutive days and the night cooling power of 93 W between 11:00 and 14:00; d) The radiative cooling film can have objects below this level with 10 K (below ambient temperature during the day) and 16 K (respectively at night); e) Relatively low cost; f) Production technology: roll-to-roll type; g) By integrating into the silicon photovoltaic cells, it increases the efficiency by 5% and the amount of life (by cell cooling by over 10 K) with 5 years; h) Cooling an nZEB single-family with $S = 50\text{ m}^2$ with a radiative cooling film with the same surface, it can ensure cases where no energy can be brought; This result is possible in South and South-East emplacement from the Romanian area; i) The application of the film directly on the roof leads to a decrease in the cooling necessary energy. This solution with the isolated roof with this film for the large urban area urban eliminates the need to use the "split" cooling peak systems type; j) The application of the film directly on the roof leads to a decrease in the cooling necessary energy. This solution with the isolated roof with this film for the large urban area urban eliminates the need to use the "split" cooling peak systems type.

2.1.3. Metamaterials for increasing the window's performance.

The metamaterials were included in the most important windows from the Middle Ages. But the developments can carry out their research and allow them to create multi-

functionalities and to create a special operation to allow them to be transformed into a multifunctional wall-mounted appliance rather than when it is a single piece of coated glass.

The "window of the future" (according to the emerging concept), it becomes extremely sensitive to change the parameters of the external and internal environment and it is necessary to adapt with regard to the environmental conditions and the requirements of the occupants (processing carried out inside). These include: switchable windows [30] and shading systems [31]. They have variable optical and thermal properties (they can be adapted to the climatic conditions and occupational preferences) [30]. By managing the lighting and cooling activity, a potential intelligent / dynamic adaptive: reducing the peak electric charges [30]; the well-being of the world grows during the day; I can offer comfort and energy production in high temperatures and radiation conditions. An ideal window is needed to be able to propose variable options, with a prompt response to change the climatic conditions and the occupied demands, respectively to adapt to them. To this goal, it is currently: a) passive devices: photochromic and thermochromic; b) active devices: with liquid crystals; with suspended particles; electrochromic. The metamaterials are present in both passive devices and active devices [30]. The spectacular evolution of research in the field of nano, electro, optical allowed the emergence of the most efficient glazed system, by combining electrochromic windows obtained through nano technologies, with thermochromic windows. These are the windows obtained by "heliotrope" technology, which has the following major performances: the transmission of visible light through the window is electronically modulated, from $<3\%$ to $> 50\%$ in a time of $\tau \leq 5$ min; retains the neutral grey appearance, aesthetically pleasing, over the entire range of fading; maintains a neutral grey appearance throughout the fading range; can be electrically connected both wired and wireless; have low power consumption ($<3V$) and controlled state memory functions; can hold comfortably in confined spaces; no installation, maintenance and replacement costs associated with shading systems are required; has a good ability to connect to the HVAC system in buildings; installation costs are lower compared to conventional systems that have associated / integrated shading systems; has an excellent aesthetic; can be controlled on request; they are light; has the best performance compared to other dynamic systems.

2.1.4. *Perovskites — Cheap Solar Cells*

Solar cells made of perovskites. In the global efforts to reduce the costs of PV cells and to increase the efficiency of conversion of perovskite technologies, the evolution of this is important [32]. Since 2009, when the first cells with perovskite products had $\eta = 3.9$, until now, when their efficiency has reached $\eta = 31.3$ for exterior PV and $\eta = 36.3$ to the interior PV (for recovery interior light). Furthermore, the cost of care is much smaller. Perovskites are a class of materials defined by a certain crystalline structure. They can contain any number and type of elements (perovskites and silica, graphene, lead etc). They can be sprayed on glass rather than meticulously assembled in clean

rooms. A special category in this class of metamaterials is perovskite-graphene cells is presented in Fig. 4 [32]. These are very recently developed solar cells, with an excellent quality-efficiency-cost ratio and great flexibility. The perovskite photocells contain in the active layer a natural mineral structure with special properties and it is expected to become a market leader in the field of photoelectric solar energy technologies.

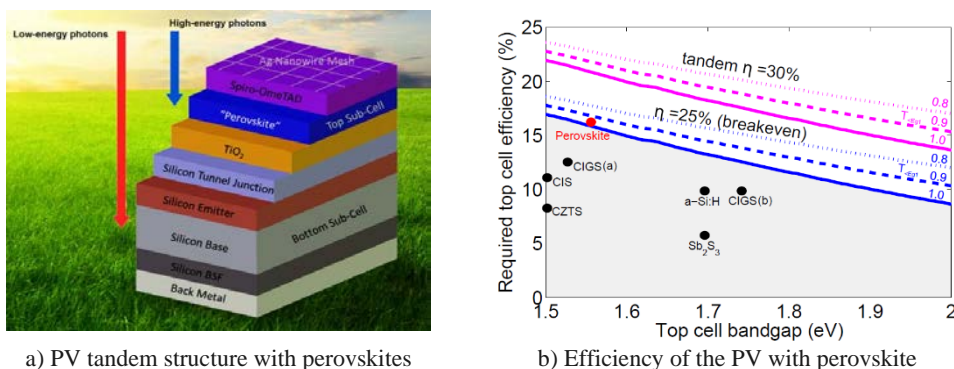


Fig. 4 - PV with perovskite ([23], Image credit: University of Oxford)

Perovskite site presents: a) the possibility of combining several semiconductor materials in order to expand the spectral domain of the solar radiation that can be used with consequences in increasing their efficiency: a cell with perovskite has been recently investigated which has reached the efficiency $\eta = 31\%$ (2018). Considering the much lower price (at least ... times lower than other cells with similar performance), they can become a major option for future technologies in the field; b) ever-increasing efficiency: photovoltaic cells with perovskite increased, from the end of 2009, from $\eta = 3.8\%$, to $\eta = 27\%$ at the beginning of 2017 and 31% at the beginning of 2018. The band structure of the perovskite ore is adjustable: an optimized structure can be designed to allow the exploitation of a proportion of the spectrum of the net solar radiation superior to the cells that use only the visible spectrum. This structure allows the maximum efficiency given by the Shockley - Queisser limit (approximately 31% under the conditions: solar spectrum: AM1.5G; irradiance: $1,000 \text{ W / m}^2$, perovskite bandwidth: 1.55 eV); c) other embedded materials: c1) Initially, lead was used to make them; c2) the technology has advanced and very recently, in 2017, it was proposed to combine perovskite with graphene. They have: eliminated the major disadvantages of lead; added benefits to graphene; c3) the use of graphene has led to multiple innovations and high performances: super-flexible films; increased efficiency; high robustness; low cost price (for portable applications I am a market leader); c4) the possibility of further development / growth.

We are adding another new type of perovskite cell designed especially for the use of light energy from inside in order to power the laptops and other [33,34,35]. These very recently discovered PV cells, together with those integrated in the building envelope to

which dynamic active/passive windows can be added, can ensure the autonomy of the buildings in the south, south-east.

2.1.5. Metamaterials for to increase the performance of the heating/cooling systems

These metamaterials have been developed and diversified very recently. Among these we mention the graphene radiators.

E.g.: Radiator SOLUS (design by KOLEDA) (Fig. 5.) could save you over 80% on your next heating bill due to its clever use of the completely new graphene-based technology.” The nanotech coating has returned test results that are 5x more efficient than conventional radiator” [33].

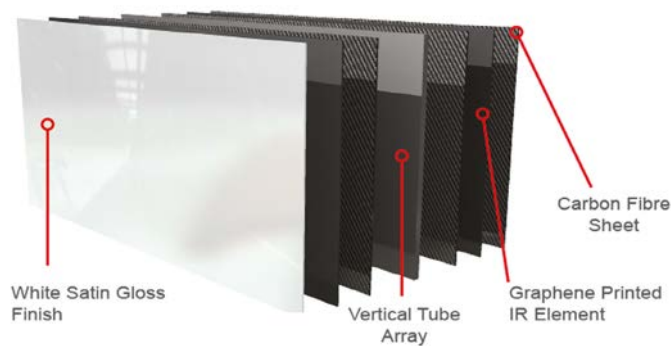


Fig. 5 - Heating radiator with graphene [33], (Source: www.uberdesign.co.uk)

2.1.6. Metamaterials for to increase the performance of power generation systems

The metamaterials have found important use in the field of direct conversion of solar energy into electricity. Is used to increase their efficiency by concentrating solar radiation with the help of so-called waveguides or increasing the performance relative to the absorption of solar energy, respectively radiation in the visible and infrared spectrum (for about 95% of incident solar energy). Researchers in the field have proposed numerous technical solutions, which are becoming more and more efficient [36,37,38]. One of the latest solutions proposed in this field is an ultrafine device (with a thickness of 90 nm) capable of absorbing a large part of the solar radiation from the visible spectrum, in the broadband as well as from the non-polarized light, in a wide range of angles. The technology can be used for photovoltaic conversion but also for photodetectors, thermal transmitters, and optical modulators. So far, it has been difficult to simultaneously meet these requirements, but the discovery and development of graphene research have allowed these desires to be realized.

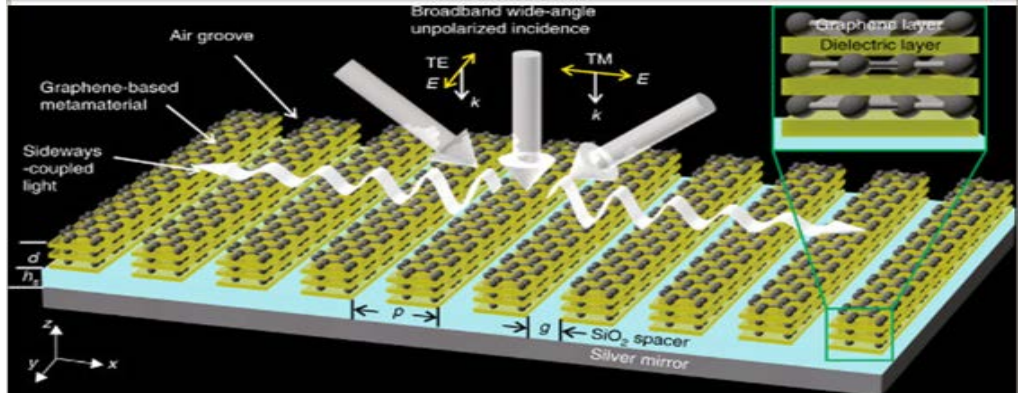


Fig. 6 - Schematic of graphene-based metamaterial absorber [39], (Source: U. Sydney / NPG)

Australian researchers [39] have proposed a metamaterial of "graphene 12.5 cm², 90 nm thick, with approximately 85% absorption of visible polarized light and infrared radiation, covering almost the entire solar spectrum (300-2500 nm)" [40]. The metamaterial is composed of a package made of graphene and dielectric layers, arranged alternately; to achieve broadband absorption over incident angles up to 60 ° used a grating couple the light into waveguide modes. For solar thermal applications, the use of an absorber with very wide spectral and angular responses is ideal (it has been shown that heating at 160 ° C under the influence of natural sunlight is a good solution). So, *"is open a new approach for the applications of the strong absorption of large surface photonic devices based on 2D materials"*.

3. Case study. Metamaterials for increasing the widow's performance.

Results and Discussion

The authors conducted a case study, meant to present a comparison between the performances (visual, solar transmission, coefficient of heat transfer) of the different glass systems to highlight the importance of a preliminary analysis of the performances of some glass systems, in different hypotheses of design and location / irradiation (Table 1.), for the selection of the best performing concepts. The simulations were performed in WINDOW 10 for windows and TRNSYS for simulation comportment of the room / building delimited by glazed surfaces.

The important results obtain after simulation the comportment of glasses systems is:

- **The U-factor of a fenestration assembly** which characterizes the thermal performance of the glazed system separating the indoor environment from the outdoor one between which there is a thermal gap. The thermal transfer processes include the combined effects of conduction, convection, and radiation [41,42].

- **Solar Gain** (by direct or indirect solar radiation), characterized by gain coefficient (SHGC) of the glazing [40]
- **Shading coefficient (SC)** of the window [43,44]
- **Infiltration**, represented by heat loss and gain also occur by infiltration through cracks in the fenestration assembly and measured in terms of the "amount of air (cubic feet or meters per minute) that passes through a unit area of fenestration product (square foot or meter) under given pressure conditions". The infiltration varies with wind-driven and temperature-driven pressure changes.
- **Graph** of the daily & annual variation of luminous variation transmittance/ reflectance flux and energy transmittance/reflectance flux by frontal & dorsal face (Fig. 7).

The *2001 ASHRAE Handbook of Fundamentals* contains the following equation for calculating the energy flow through a fenestration product (assuming no humidity difference and excluding air infiltration) [45,46]:

$$q = U_t \bullet (A_{pf}(t_{out} - t_{in})) + (SHGC_t \bullet A_{pf} \bullet E_t) \quad [1]$$

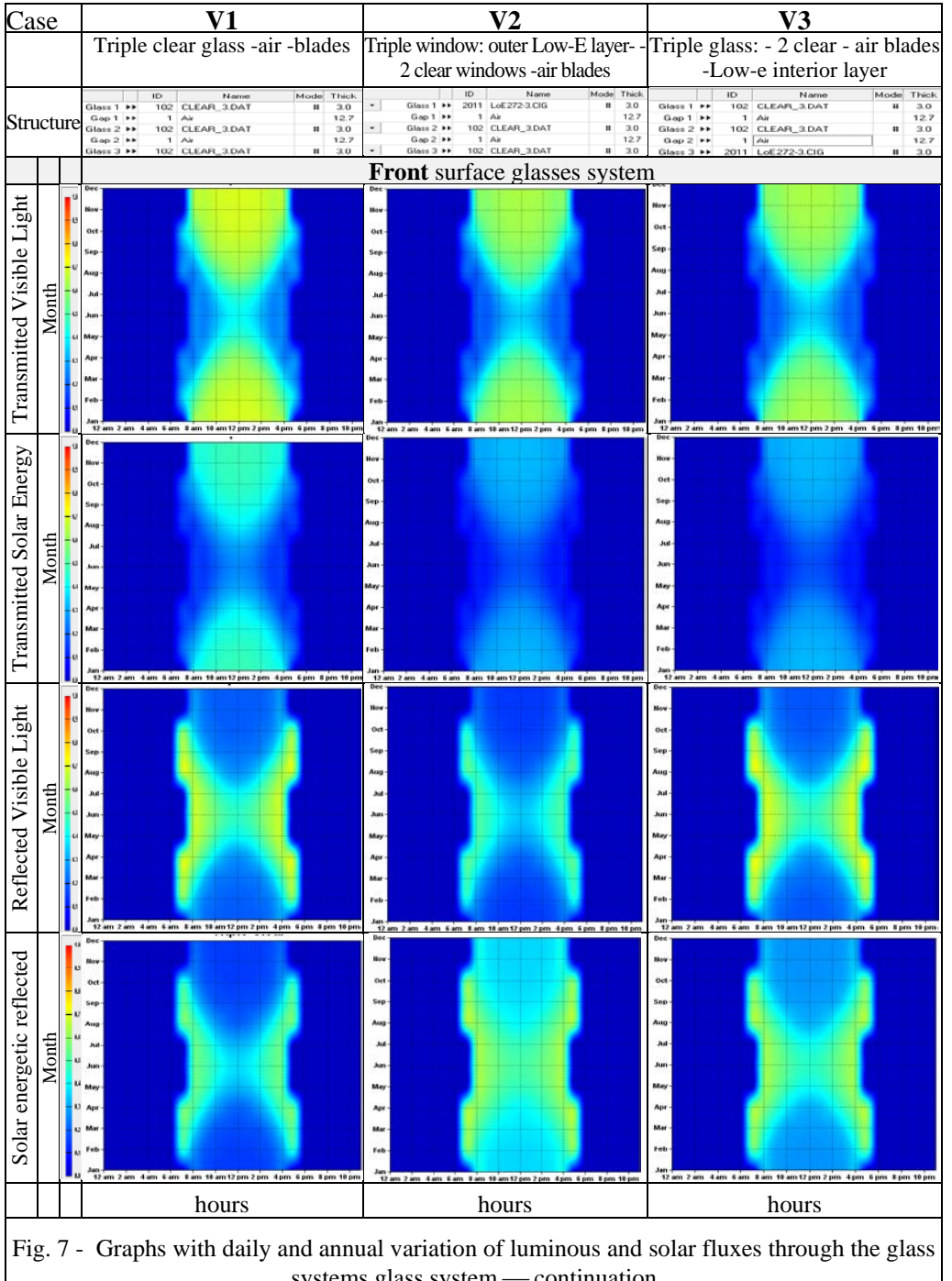
- where: q = instantaneous energy flow in W; U_t = overall coefficient of heat transfer (U-factor), in $W/m^2, K$; t_{in} = interior air temperature, in $^{\circ}C$; t_{out} = exterior air temperature, in $^{\circ}C$; A_{pf} = Total projected area of fenestration, in m^2 ; $SHGC_t$ = overall solar heat gain coefficient, non-dimensional; E_t = incident total irradiance, in W/m^2 .
- the properties U-factor, SHGC, and infiltration determine the energy flow through the system windows [47,48,49].

Our analyses is ample but, for this work I have retained an analysis of the graphs with daily and annual variation of light and solar energy through the glass system (glass system with 2 windows: glass 1, gas layer 1, glass 2; glass system with three windows: glass 1, gas layer 1, glass 2; gas layer 2, glass 3) for the retained variants highlights the following aspects.

There are other factors that determine the performance of windows: window thickness, gas blades; type of gas used; glass configuration-types and position of windows) types and position of shading systems but in the paper, we focused only on the impact of dynamic / intelligent, active or passive glass with metamaterials, on energy performance (solar flux / light).

The resultants of the case study are relevant for demonstrations les performance for the windows with metamaterials. The simulation results are shown in Fig.8, 9,10 and 11.

- V1 is a classic glazed system for the beginning of the third millennium (two windows + air layer in the cavity): much of the sunlight and energy is transmitted through the front but also through the back, without being able to control, in the absence of shading, transmission / reflection process;
- V2, V3, represent classic glazed systems for the 1st decade of the third millennium (two clear windows + a double-glazed window, interior / exterior, air layer in the cavity): solar energy transmitted through the front and back is less transmitted and in the case of Low-e glass -is on the inside, the solar energy is strongly reflected, so the system becomes a solar trap;



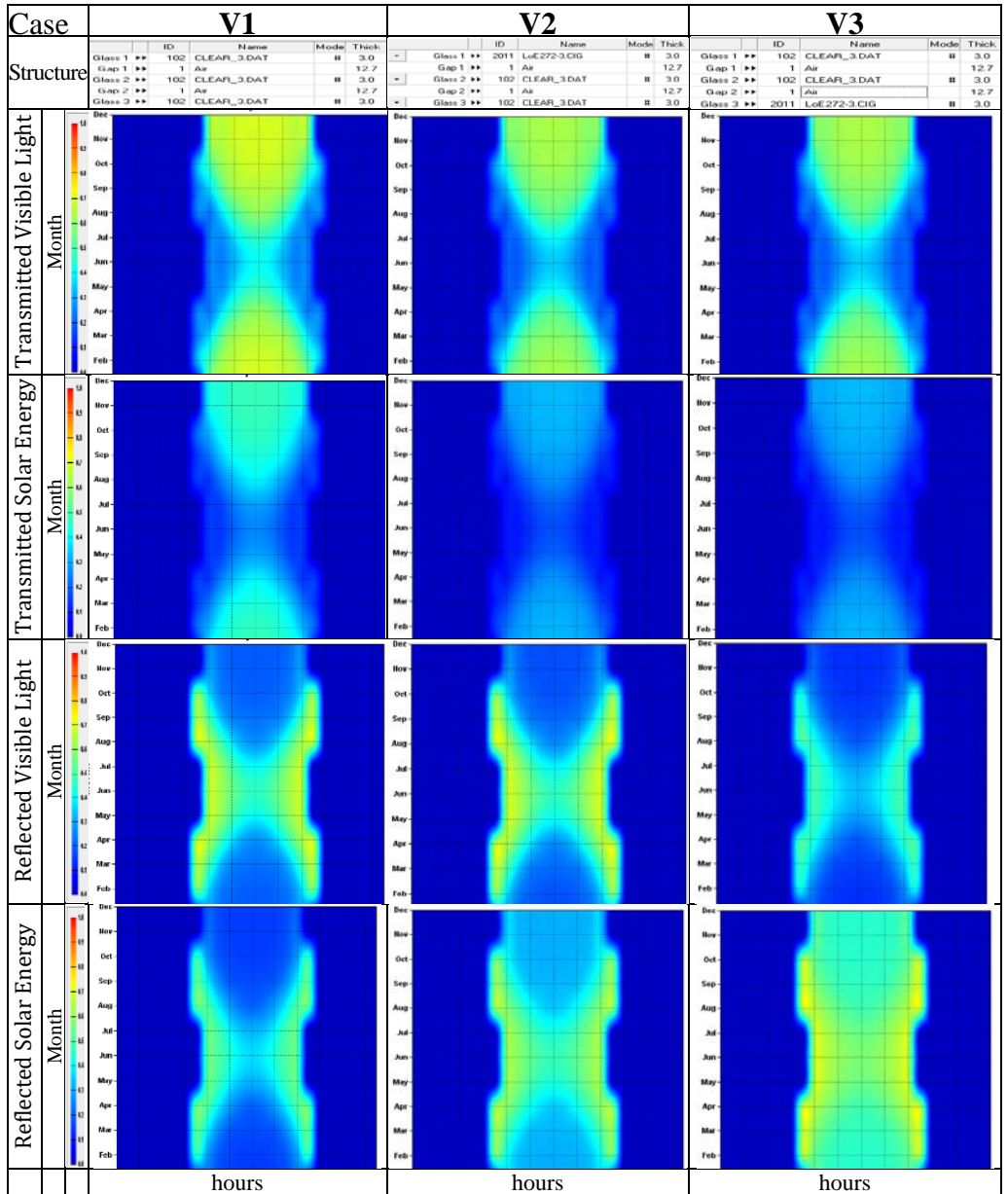
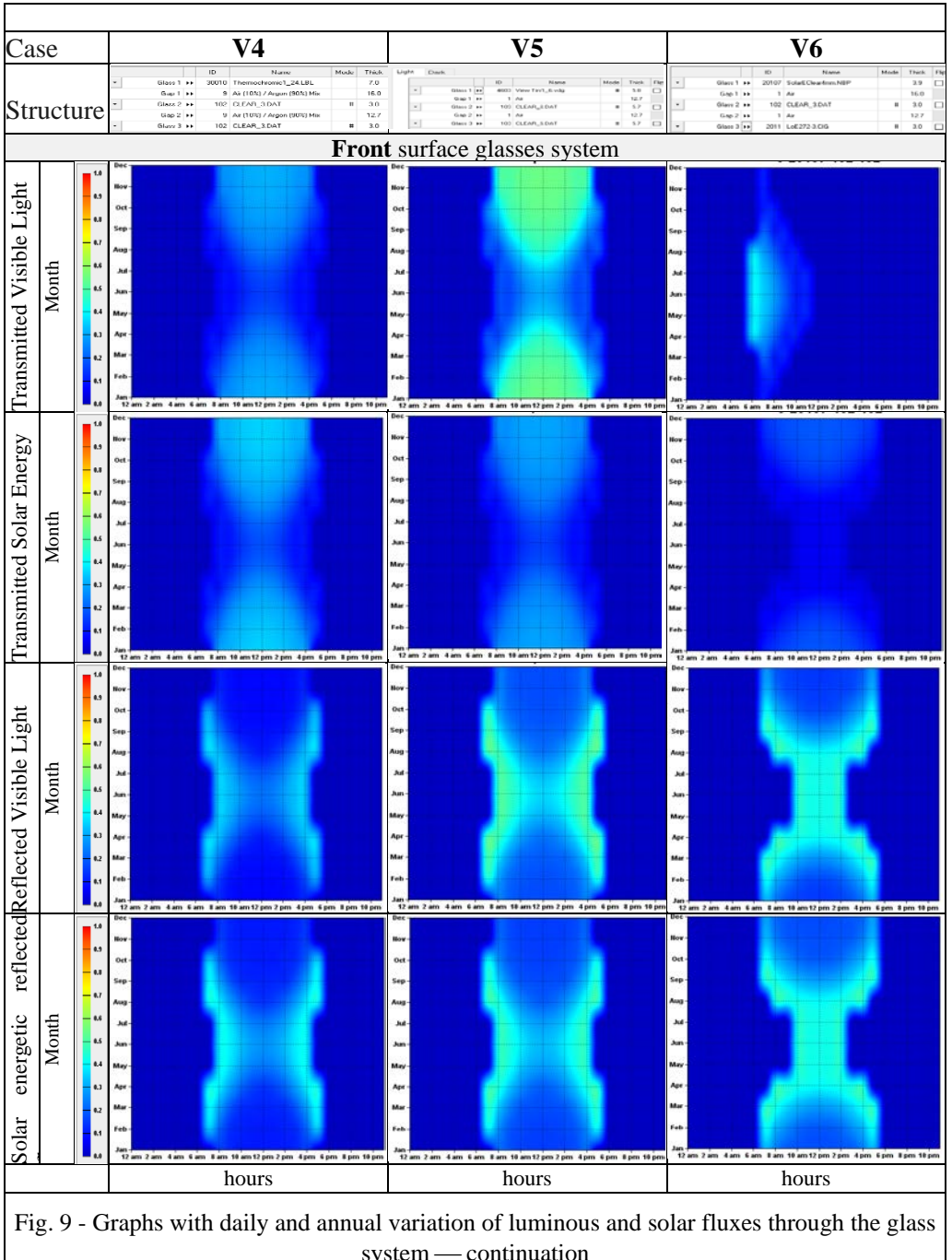
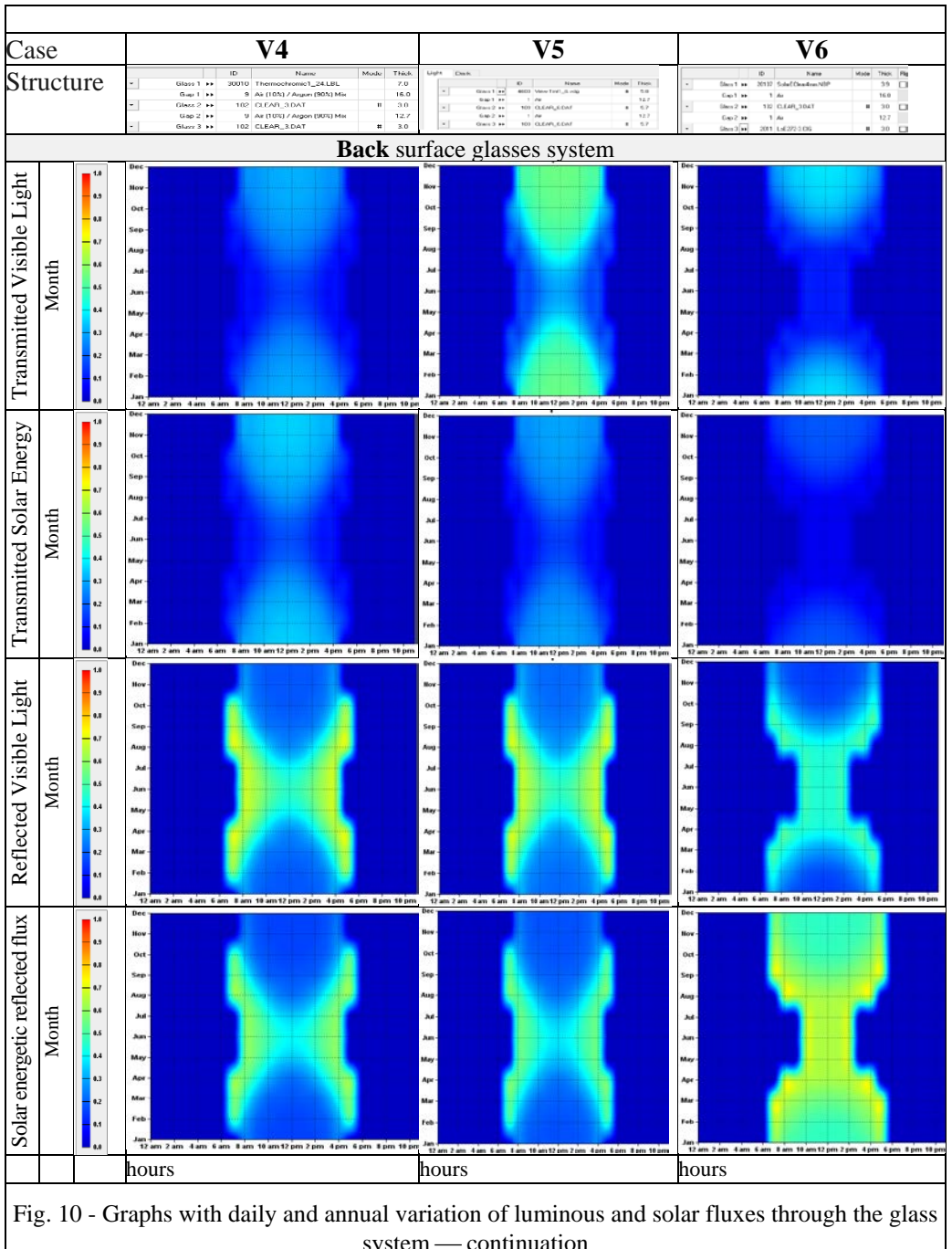
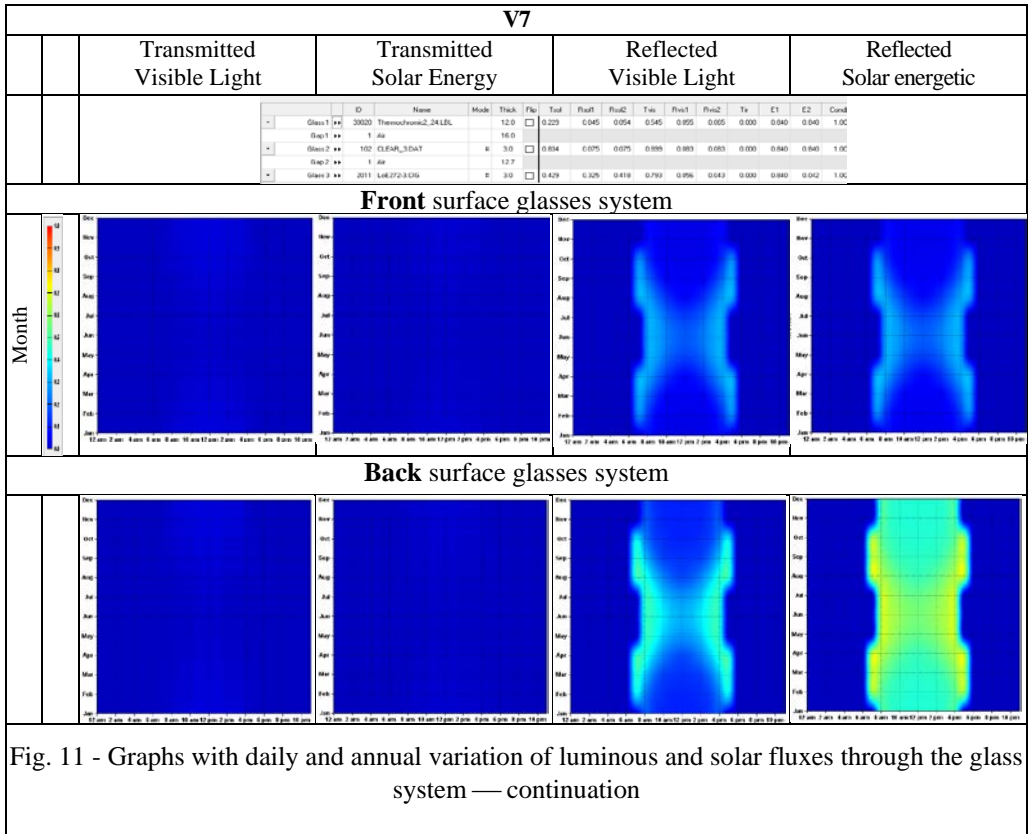


Fig. 8 - Graphs with daily and annual variation of luminous and solar fluxes through the glass system — continuation







- Other simulations, for glasses systems with aerogel, are demonstrated the very good thermal isolation by this system;
- A wrong configuration can turn the glazed system and the room into a solar trap that requires a high amount of cooling energy
- The use of high-performance dynamically adaptive glazed systems can substantially reduce the cooling load (with ca. 50%). The exceeded flux is transformed into energy.
- A favourable behaviour is presented by systems with thermochromic windows (V4, V7): the visible flux transmitted/reflected by electrochromic and thermochromic face glasses is low.

4. Conclusions

- The development of research in the field of metamaterials has opened a huge window to possible applications in the field of buildings.
- Some of these possible uses were exposed within the paper, which could lead to a paradigm shift in the concept of new buildings but especially in increasing the performance of existing buildings (thermal, acoustic, seismic protection measures are

- targeted; heating/cooling equipment; CO₂ collection and recovery equipment; technologies to increase the performance of direct solar energy conversion systems); Example: heliotrope glass, thermochromic glass, nanoelectrochromic glass etc.
- Basically, the Pandora's box was opened, physicists, mathematicians, and theorists respectively know what they have deposited in it but the engineers have to select what is useful today and tomorrow, analysing the performances & risks & evolutions possible over time.

References

- [1] I-C Cotorobai, *Soluții de creștere a performanțelor sistemelor de valorificare multiplă a energiei solare*, Teză doctorat, 2018, Universitatea Tehnică Gheorghe Asachi, Iași.
- [2] I-C Cotorobai, *Sisteme de valorificare a resurselor de energie regenerabilă și recuperabilă*, Ed. MATRIXROM, București, 2019.
- [3] SLAC, Physical Review Letters, Scientific American.
- [4] SRA-E Conference, 16-18 June 2014, Istanbul, Turkey.
- [5] V. Cotorobai, B. Ungureanu, G. Atanasiu, *Possible measures of taking-over/ Dynamic control of seismic actions applicable to urban utility systems. seismic waves deflection/ damping using metamaterials*, Buletinul AGIR, Supliment 2, București, 2015, pag. 184-194.
- [6] V. Cotorobai, B. Ungureanu, G. Atanasiu, *From phononic crystals to seismic metamaterials*, Proceedings of Xth edition of annual Conference of ASTR, 2015.
- [7] Symbiosis in Development, www.except.nl www.except.nl/.../symbiosisindesign.
- [8] Știință, New Scientist, CityLab.
- [9] B. Ungureanu, V. Cotorobai, *Risks associated to the seismic behavior actions of the urban utilities systems during and post-earthquake*, XIII-та МЕЖДУНАРОДНА НАУЧНА КОНФЕРЕНЦИЯ, ЯВСУ'2013, 13th International scientific conference VSU'2013, 6-7 June, Sofia, Bulgaria, Vol. III, ISSN:1314-071X, pp VIII-31 – VIII-36.
- [10] Y. Hao, R. Mittra, *FDTD Modeling of Metamaterials: Theory and Applications*, Technology & Engineering; 2008.
- [11] V. Cotorobai, *Sisteme Vitrate Dinamice Pentru Clădirile nZEB*, Revista Instalatorul, București, 2020.
- [12] P. Xie, W. Sun, Y. Liu, Ai Du, Z. Zhang, G. Wu, R. Fan, *Carbon aerogels towards new candidates for double negative metamaterials of low density*, Carbon, Volume 129, 2018, Pages 598-606, ISSN 0008-6223, <https://doi.org/10.1016/j.carbon.2017.12.009>.
- [13] <http://earthquake.usgs.gov/>.
- [14] <http://www.lefigaro.fr/sciences/2014/04/08/01008-20140408ARTFIG00365> - Une expérience prometteuse d'« invisibilité sismique»
- [15] <https://heliotropetech.com/>
- [16] <https://www.bu.edu/research/articles/>
- [17] https://www.gsa.gov/cdnstatic/GPG_Findings_010-Smart_Windows.pdf
- [18] <https://www.yankodesign.com/2019/03/06/built-with-graphene-based-technology-solus-is-the-most-efficient-radiator/>
- [19] <https://heliotropetech.com/wp-content/uploads/NanoEC-Transp-Data-Sheet-R093019-05-TREU.pdf>.
- [20] S. Brûlé, E. H. Javelaud, S. Enoch, and S. Guenneau, *Experiments on Seismic Metamaterials: Molding*
- [21] C. Chapman, *Fundamentals of Seismic Wave Propagation*, Cambridge University Press, 2004.
- [22] *Les metamateriaux*, www.savoirs.essonne.fr
- [23] Martin Wegener, *Photonic Metamaterials, photonics Cristals*, www.cfn.kit.edu
- [24] O. Speck, T. Speck, *An Overview of Bioinspired and Biomimetic Self-Repairing Materials*. Biomimetics (Basel, Switzerland), 4(1), 26. , 2019. <https://doi.org/10.3390/biomimetics4010026>.
- [25] *Surface Waves*, Physical Review Letters, PRL 112, 133901 ,2014.

- [26] S. R. White, et al., *Restoration of Large Damage Volumes in Polymers*, Science 344, 620, 2014; DOI: 10.1126/science.1251135.
- [27] S. Grozeanu, *Fizică generală*, Editura Academiei Navale” Mircea cel Bătrân”, Constanța, 2008.
- [28] H. Torres-Silva, D. Torres Cabezas, *Chiral Seismic Attenuation with Acoustic Metamaterials*, Buletin AGIR, București, 2015.
- [29] S. Guenneau, *Déformer les ondes pour mieux les contrôler*, La Recherche, dossier 01/02/2012, mensuel, n°461.
- [30] H. Lin et al, A 90-nm-thick graphene metamaterial for strong and extremely broadband absorption of unpolarized light, Nat. Phot. **13**, 270 (2019); DOI: 10.1038/s41566-019-0389-3.
- [31] L’invisibilité, c’est pour bientôt. Le point 2135.
- [32] *Perovskite*, [WSJ, IEEE Spectrum, Chemical & Engineering News, Nature Materials].
- [33] K. Kim and S. Lee, "Detailed balance analysis of plasmonic metamaterial perovskite solar cells," Opt. Express **27**, A1241-A1260, 2019.
- [34] Journal of Electromagnetic Analysis and Applications, 2013, 5, 10-15.
- [35] S.-H. Kim, M.P. Das, *Seismic Waveguide of Metamaterials*. Modern Physics Letters B. doi:10.1142/s0217984912501059, 2012
- [36] Chromogenic Glass Layers | Windows and Daylighting, windows.lbl.gov
- [37] M. Cristea, D. Popov, F. Barvinschi, I. Damian, I. Luminosu, I. Zaharie – “*Fizica. Elemente fundamentale*”, Ed. Politehnica, Timisoara, 2006.
- [38] J. Sun, N.M. Litchinitser, *Metamaterials, Fundamentals and Applications of Nanophotonic*, 2016
- [39] R. Ghaffarivardavagh, and col. Ultra-open acoustic metamaterial silencer based on Fano-like interference, Phys. Rev. B **99**, 024302, 2019
- [40] O. Giorgio, *3D Printed Acoustic Metamaterials: A New Frontier for Suppressors?* Daily News, NFA / Suppressors / Class III
- [41] S. Guenneau, *De la cape d'invisibilité à la protection sismique*. 29 mai 2012, www.gazette-du-sorcier.com]
- [42] J. Yoon, and col., Superflexible, high-efficiency perovskite solar cells utilizing graphene electrodes: towards future foldable power sources, Energy & Environmental Journal, nr. 1, 2017
- [43] Sciences et Avenir /// Azar Khalatbari
- [44] THERM6.3/WINDOW6.3 NFRC Simulation Manual December 2011
- [45] S. Zu, *Bio-inspired multistable metamaterials with reusable large deformation and ultra-high mechanical performance*, Extreme Mechanics Letters, Volume 32, October 2019, 100548
- [46] Chromogenic Glass Layers | Windows and Daylighting, windows.lbl.gov
- [47] <http://radi-cool.com/technologies/>
- [48] <http://waveprojectlewis5.wikispaces.com>
- [49] <http://www.geo.mtu.edu/>

ASSESSING THE SEISMIC PERFORMANCE OF A R.C. FRAME STRUCTURE BY NUMERICAL SIMULATIONS – AN EFFICIENT TOOL FOR A SUSTAINABLE FUTURE

Ana-Maria TOMA¹, George TARANU¹, Takahiro NISHIDA², Aliz Éva MÁTHÉ³, Cristina-Mihaela CÂMPIAN³, Melito BACCAY⁴ and Ionut-Ovidiu TOMA^{1,*}

¹“Gheorghe Asachi” Technical University of Iasi, Faculty of Civil Engineering and Building Services, Iasi, Romania

²Port and Airport Research Institute, Structural Engineering Department, Yokosuka, Kanagawa, Japan

³Technical University of Cluj-Napoca, Faculty of Civil Engineering, Cluj-Napoca, Romania

⁴Technological University of the Philippines, College of Engineering, Manila, The Philippines

Abstract. *The assessment of the seismic performance of RC frame structures after one or more major seismic events is of paramount importance from the point of view of public safety. Numerical simulations by means of FEM proved to be efficient tools in assessing the seismic performance of civil engineering structures. They offer the advantage of varying several parameters in order to obtain the safety margin against structural collapse without the need of expensive experimental tests. The paper proposes a method for assessing the seismic performance of a RC frame structure by means of non-linear time-history analysis (THA). The use of numerical simulations is, in this particular case, the only solution of obtaining the safety margin to seismic actions of an existing building.*

Keywords: safety margin, efficient tool, lateral displacement, storey drift.

1. Introduction

Reinforced concrete (RC) frame structures are one of the most frequently met type of structure in urban areas due to their relatively low cost of construction, compared to other materials, and their high durability. Due to their wide use, such type of structure is bound to be met in highly active seismic areas. Even though initially designed to ensure certain levels of safety in case of earthquakes, the damage accumulated in a RC structure during its lifetime due to seismic events will ultimately require its strengthening or being retrofitted to either comply with the new seismic design regulations [1] or to prevent losses during future earthquakes.

The assessment of the seismic behaviour of RC structures, with particular interest to frame structures, after one or more major seismic events is of paramount importance from the point of view of public safety. A correct estimation of the remaining strength and deformation capacity of a building [2] can be a powerful tool for decision makers in terms of whether repairs were deemed necessary or the demolition of the building would be a more viable solution [3, 4]. Either decision involves temporary shutting down some or all activities in the building and evacuation of inhabitants and providing temporary shelter / accommodation. This could have significant economic consequences, especially in the case that demolition of the building was the only option. There are also secondary effects, such as waste generation, energy consumption for producing new building materials and constructing the new building, all of these with dire consequences upon the environment [5, 6].

Numerical simulations based on the finite-element method (FEM) proved to be efficient tools in assessing the seismic performance of civil engineering structures [7]. They offer the advantage of varying several parameters in order to obtain the safety margin against structural collapse without the need of expensive experimental tests usually conducted on shake tables, in themselves a costly equipment [8]. Another advantage of numerical simulations versus traditional experimental investigations is that they create, virtually, no wastes that need to be disposed and/or recycled. In view of the recent advances in energy efficiency in terms of computational power versus required electrical power of the new computer hardware, the numerical simulations become more attractive even in terms of power consumption and generated heat and CO₂ emissions.

However, there are some drawbacks, too. For instance, in order to generate reliable numerical models, experimental investigations still need to be carried out [8]. Moreover, in case of RC frame structures, there are still some difficulties in generating a reliable numerical model mainly due to the complex nonlinear behaviour of concrete. Consequently, there are numerous research works that attempt at creating more accurate and efficient numerical models in order to grasp this complex phenomenon [9, 10].

The paper presents a method of assessing the seismic performance of a RC frame structure, frequently met in Romanian urban areas, by means of non-linear THA. The use of numerical simulations is, in this particular case, the only solution of obtaining the safety margin to seismic actions of an existing building. The obtained results could be used by competent authorities in their decision-making process in terms of public safety.

2. Numerical Model

As already mentioned, the numerical model was developed based on an existing layout of a building that is frequently met in Romanian urban areas. It is a condominium building having 7 storeys, with a total height of 26.7 meters. The numerical model was generated by means of SAP2000 software.

2.1. Geometry of the structure

The in-plane layout of the structure is shown in Fig. 1, whereas the 3D view is presented in Fig. 2. The ground floor had a height of 4.35 m and the upper floors had a height of 2.75 m. From Fig. 1 it can be observed that even though the rim of the in-plane layout would have an axis of symmetry, in this case Y axis, due to the presence of the staircase and elevator shaft, the geometrical symmetry and the distribution of rigidities would not be ensured. Consequently, it was expected that the fundamental mode of vibration would not be a purely translational one but torsional effects would also be present.

Since the purpose was to conduct a non-linear time-history analysis, the occurrence of plastic hinges is therefore expected and should be modelled into the program. The plastic hinges were allowed to form at the end of both beams and columns. The behaviour of plastic hinges for the beams was considered based on Table 6-7 from FEMA 356 code, whereas the plastic hinges at the end of the columns were defined according to Table 6-8 from FEMA 356 [11]. The formation of the plastic hinges at the ends of beams is generally governed by the bending moment whereas the plastic hinges at the end of columns are governed by the combined effect of the axial force and bi-axial bending. [12].

Although the beams had a constant cross-section along the height of the structure, the columns had different cross-sections. The storeys corresponding to a change in cross-section of the columns as well as changed layouts of the longitudinal reinforcement were 2, 4 and 6.

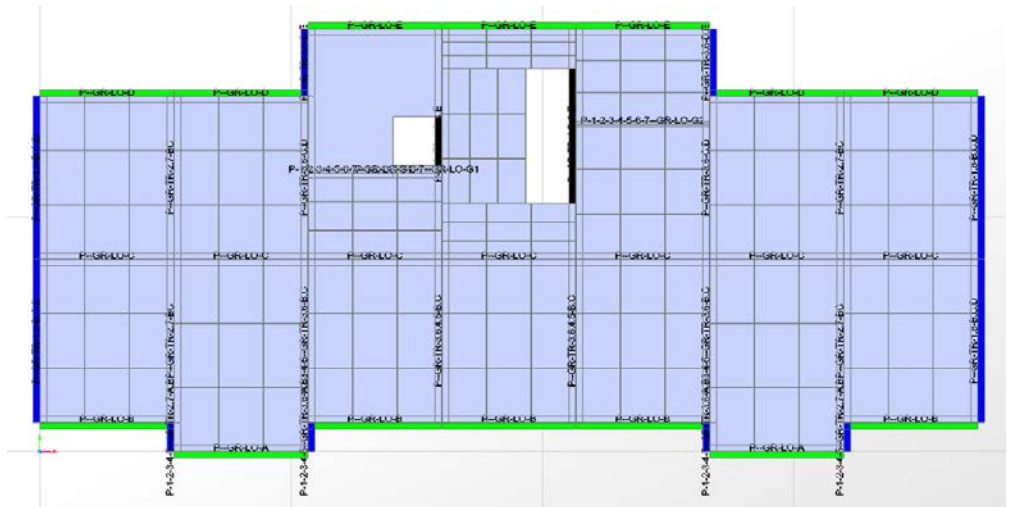


Fig. 1 – In-plane configuration of the building.

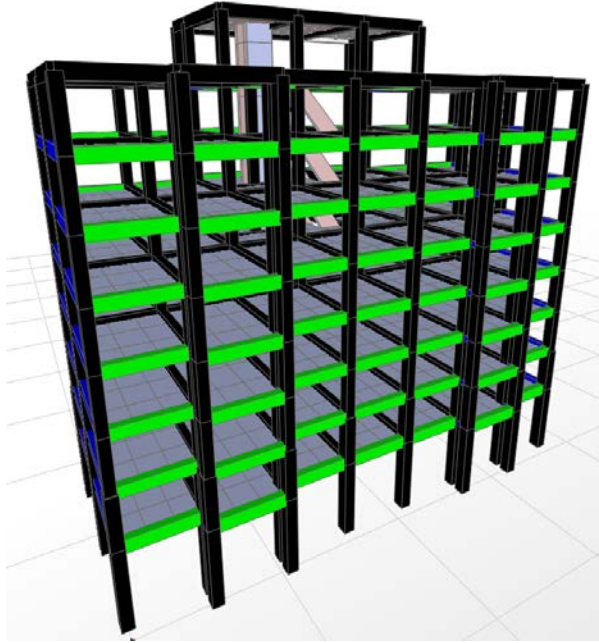


Fig. 2 – 3D view of the building.

2.2. Loading Scenarios

The loading scenarios consist of five earthquakes that occurred during the lifetime of the structure. All earthquakes were produced by the Vrancea fault in 1977, 1986, two earthquakes in 1990 (8 hours apart) and another one in 2004. The defining elements of the seismic motions are presented in Table 1. For the 1977 Vrancea earthquake (analysis code 771) the recordings from Bucharest were used whereas for all other considered earthquakes the recordings from Iasi were considered.

Table 1
Characteristics of the considered earthquakes

Nr. Crt.	Analysis code	Duration [s]	Peak ground accelerations (PGA)			
			Longitudinal component [m/s ²]	Time [s]	Transversal component [m/s ²]	Time [s]
1	771	40.14	1.62	5.58	1.95	6.12
2	861	21.15	0.641	20.385	1.46	19.93
3	901	31.18	1.262	14.33	1.095	14.61
4	902	26.45	0.389	12.025	0.458	0.52
5	041	73.09	0.582	22.72	0.658	22.81

The seismic motions were input into the program as time history functions in the form of time versus acceleration. An example of the time-history functions for the 1977 Vrancea earthquake is shown in Fig. 3.

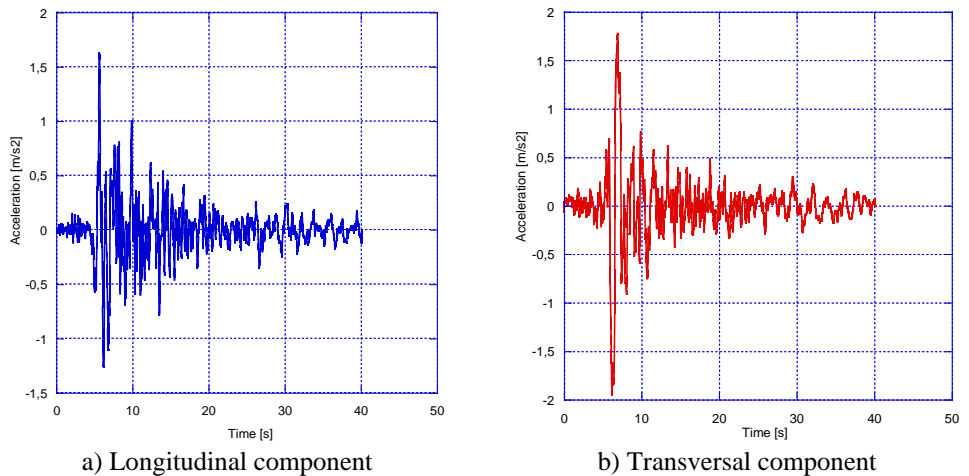


Fig. 3 – Time history functions (1977 Vrancea earthquake).

2.3. Analysis Procedure

The own-weight of the entire structure was partly automatically considered from the geometry of the model (length of the elements, cross-sectional dimensions, thickness of slabs, ramps for stair-case and elevator shaft) and the material characteristics (density) and partly manually input as dead loads (e.g. weight of the exterior walls, partitioning walls, floor finishing). The self-weight was defined as a non-linear static case and served as the starting point for all subsequent non-linear time-history cases. Although no plastic hinges or damages were expected from this initial loading case, by defining it as a non-linear case it offered the possibility of using the stiffness matrix of the numerical model, computed by the program at the end of the analysis step, as input stiffness matrix for the next non-linear analysis case.

Before any non-linear THA case was considered, a modal analysis was performed to obtain the dynamic characteristic of the model in the form of the fundamental period of vibration. It represents a dynamic property of the initial, undamaged, structure and serves as a reference value for the subsequent analysis cases.

Each non-linear THA case used the stiffness matrix of the numerical model computed at the end of the previous non-linear analysis case. In this way, any damage the model might have developed during a certain analysis case, it would be reflected in the stiffness matrix in the form of decreased values of the stiffness for the damaged element or elements.

After each non-linear time-history loading scenario, an additional modal analysis case was considered in order to obtain the new dynamic characteristics of the model. By comparing the newly obtained values for the fundamental periods of vibration with the initial one, it would be possible to assess whether any damage occurred in the model as it would result in increased values for the first period of vibration due to a decreased stiffness.

It would therefore be possible to classify the extent of damage into several intervals based on the degradation coefficient, δ_M , proposed by DiPasquale and Cakmak in 1990 [13]. The degradation coefficient can be assessed by using the following equation:

$$\delta_M = 1 - \frac{T_0}{T_{degr}} \quad (1)$$

where T_0 is the fundamental period of vibration of the initial, undamaged, model and T_{degr} is the fundamental period of vibration of the damaged model. Its usefulness and practical application has been proven by previous research works [14, 15].

In this paper, the relative lateral displacements between storeys is used as an indication of the damage accumulation after each earthquake scenario. The obtained values are compared to the maximum values prescribed by the design codes [16].

3. Results and Discussion

The obtained results are discussed in terms of lateral displacements and storey drifts. These are key parameters when assessing the behaviour of a structure to seismic loads since they can give valuable information with respect to the safety degree of a building.

Fig. 4 presents the maximum lateral displacements obtained for each non-linear time history scenario shown in Table 1. The displacements are along the longitudinal direction represented by X axis in Fig. 1.

From Fig. 4 it can be concluded that the higher the storey number, the larger the lateral displacement. Moreover, there is a certain accumulation of damage, leading to a lower lateral stiffness, with each loading scenario since the maximum lateral displacements tend to increase. The 1986 Vrancea earthquake (analysis code 861) produces smaller lateral displacements compare to the stronger 1977 earthquake.

The relative lateral displacements between storeys, in X direction, are shown in Fig. 5. The relative displacement of the first storey with respect to the ground is larger than the relative displacement between second and first storey. This is due to the fact that the considered building has a higher ground floor height, 4.35 m, compared to the subsequent storey heights, 2.75 m. However, there is an increase in the relative

displacements between lower storeys, especially for the last three earthquake scenarios. This sharp increase corresponds to the storeys where the cross-section of the columns changed along the height of the structures, leading to different lateral stiffness from one storey to another.

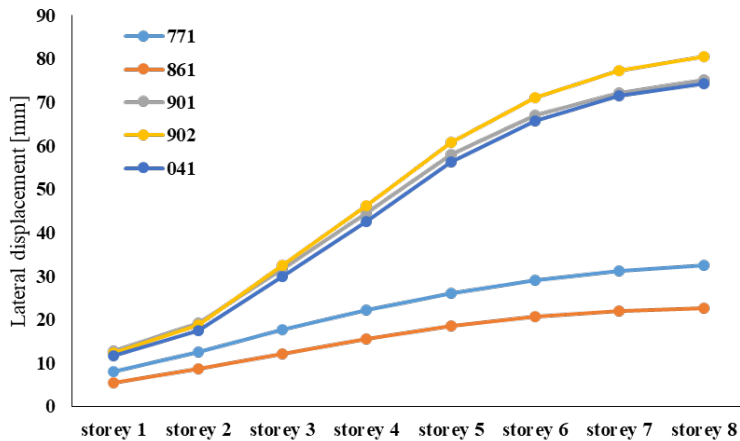


Fig. 4 – Maximum lateral displacements (longitudinal direction).

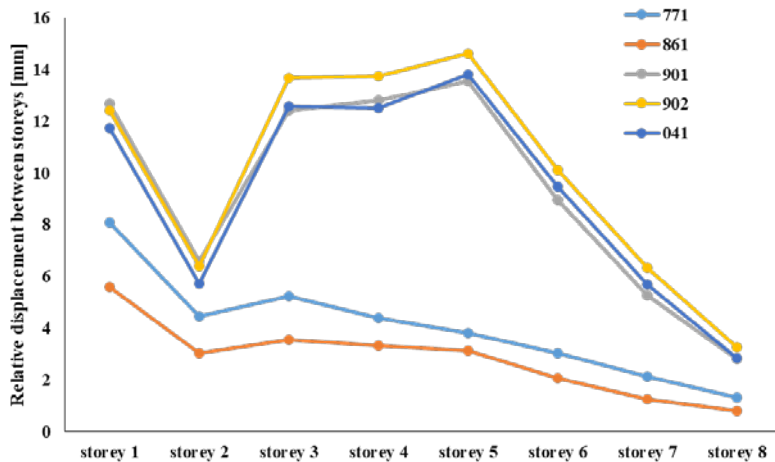


Fig. 5 – Relative displacements between storeys (longitudinal direction).

According to the Romanian seismic design code P100-1/2013 [16] the relative displacement between storeys for the Serviceability Limit State (SLS) is $0.005h$ whereas for the Ultimate Limit State (ULS) is $0.025h$, where h is the storey height, expressed in meters.

It follows that even though the building was subjected to five consecutive earthquakes, the relative displacements between storeys do not exceed the limits prescribed in the design code for either the serviceability or the ultimate limit states.

The inter-storey drifts for each earthquake scenario are presented in Fig. 6. The trend is similar to the one observed for the relative displacements, Fig. 5.

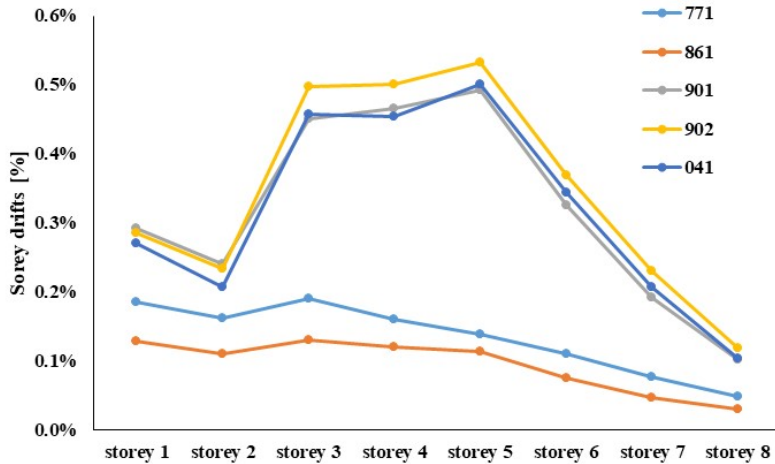


Fig. 6 – Inter-storey drifts (longitudinal direction).

From the obtained results it can be concluded that there is a certain accumulation of damage in the structure due to the seismic events that occurred during its lifetime. However, the degree of degradation, after the fifth earthquake, analysis code 041, is still expressed in terms of relative displacements between storeys or in terms of inter-storey drifts, is well below the limits prescribed in the design codes [16].

Subsequent field investigations by experts confirmed the conclusions of the numerical analyses. The building was found to have sustained minor damages and, therefore, it posed no threat to the safety of its inhabitants. The report mentioned the presence of hairline cracks in non-structural components (e.g. partitioning walls) and beams but without compromising the integrity of the structure. Non-destructive tests and measurements were conducted on the ground-floor columns but no internal damages were detected.

This could offer insightful information for the decision makers when analysing the opportunity for a building to undergo rehabilitation, retrofitting or simply being demolished. Either decision should not be taken lightly in view of the consequences in terms of resulted wastes, relocation of inhabitants and/or equipment, a.s.o. Accurate numerical simulations could represent an efficient tool and could bring a significant contribution to a sustainable future.

4. Conclusions

The paper presents the results of a numerical investigation on the seismic performance of a reinforced concrete frame structure subjected to several earthquake scenarios that occurred during its lifetime. The purpose was to assess whether or not numerical simulations could represent an efficient tool for decision makers and, therefore, contribute to a sustainable future.

Based on the obtained results it can be concluded that the chosen structure, frequently met in Romania urban areas, still offers a sufficiently high degree of safety to its inhabitants against future seismic events.

Even though the obtained results in terms of relative lateral displacements between storeys and the inter-storey drifts shown an accumulation of damage with each analysis case, the values are well below the limits imposed by the design codes. Subsequent field investigations confirmed the findings from the numerical simulations.

Numerical simulations can be an efficient and accurate tool for the decision makers when deciding whether a building needs to undergo rehabilitation, retrofitting to comply with the new codes or needs to be demolished. Each scenario has its own strong points and weak points that have to be assessed and analysed carefully.

REFERENCES

- [1] G. De Martino, M. Di Ludovico, A. Prota, C. Moroni, G. Manfredi and M. Dolce, Estimation of repair costs for RC and masonry residential buildings based on damage data collected by post-earthquake visual inspection, *Bulletin of Earthquake Engineering*, vol. 15, p. 1681–1706, 2017.
- [2] E. Liossatos and M.N. Fardis, Residual displacements of RC structures as SDOF systems, *Earthquake Engineering and Structural Dynamics*, vol. 44, p. 713–734, 2015.
- [3] K. Dai, J. Wang, B. Li and H.P. Hong, “Use of residual drift for post-earthquake damage assessment of RC buildings”, *Engineering Structures*, vol. 147, p. 242–255, 2017.
- [4] M. Polese, M. Di Ludovico and A. Prota, “Post-earthquake reconstruction: A study on the factors influencing demolition decisions after 2009 L’Aquila earthquake”, *Soil Dynamics and Earthquake Engineering*, vol. 105, p. 139–149, 2018.
- [5] C. de Perthuis and R. Trotignon, “Governance of CO₂ markets: Lessons from the EU ETS”, *Energy Policy*, vol. 75, p. 100–106, 2014.
- [6] K. McCormick, S. Anderberg, L. Coenen and L. Neij, “Advancing sustainable urban transformation”, *Journal of Cleaner Production*, vol. 50, p. 1–11, 2013.
- [7] S.E. Abdel Raheem, M.Y.M. Foady, A.G.A. Abdel Shafy, A.M. Taha, Y.A. Abbas and M.M.S. Abdel Latif, “Numerical simulation of potential seismic pounding among adjacent buildings in series”, *Bulletin of Earthquake Engineering*, vol. 17, p. 439–471, 2019.
- [8] B. Richard, S. Cherubini, F. Voldoire, P.E. Charbonnel, T. Chaudat, S. Abouri and N. Bonfils, “SMART 2013: Experimental and numerical assessment of the dynamic behavior by shaking table tests of an asymmetrical reinforced concrete structure subjected to high intensity ground motions”, *Engineering Structures*, vol. 109, p. 99–116, 2016.
- [9] M. Domizio, D. Ambrosini and O. Curadelli, “Nonlinear dynamic numerical analysis of a RC frame subjected to seismic loading”, *Engineering Structures*, vol. 138, p. 410–424, 2017.

- [10] M.R. Azadi Kakavand, M. Neuner, M. Schreter and G. Hofstetter, "A 3D continuum FE-model for predicting the nonlinear response and failure modes of RC frames in pushover analyses", *Bulletin of Earthquake Engineering*, vol. 16, p. 4893–4917, 2018.
- [11] FEMA 356, 'NEHRP – Guidelines for the seismic rehabilitation of buildings', Federal Emergency Management Agency, Washington DC, 2000.
- [12] L. Cedolin, G Cusatis, S Eccheli and M Roveda, "Capacity of rectangular cross-sections under biaxially eccentric loads", *ACI Structural Journal*, vol. 105, no. 2, p. 215-224, 2008.
- [13] E. DiPasquale and A.S. Cakmak, "Seismic damage assessment using linear models", *Soil Dynamics and Earthquake Engineering*, vol. 9, no. 4, p. 194-215, 1990.
- [14] S.R.K. Nielsen, H.U. Koyluoglu and A.S. Cakmak, "On the two dimensional maximum softening damage indicators for reinforced concrete structures under seismic excitation", *Soil Dynamics and Earthquake Engineering*, vol. 11, p. 435-443, 1992.
- [15] A.M. Toma and G.M. Atanasiu, "Seismic risk evaluation based on digital mapping of a Romanian urban area", *Proceedings of 8th International Conference on Urban Earthquake Engineering*, paper ID: 12-124, Tokyo, Japonia, March 7-8, 2011.
- [16] P100-1:2013, 'Cod de proiectare seismică P100 – Partea I – P100-1/2013: Prevederi de proiectare pentru clădiri', *Ministerul Lucrarilor Publice, Dezvoltarii si Administratiei*, 2013.

PERFORMANCE OF VENTILATION AND SMOKE EXHAUST SYSTEMS IN CASE OF FIRE IN UNDERGROUND PARKING LOTS: CASE STUDY

Marius-Costel BALAN^{1,*}, Marina VERDEȘ¹, Vasilică CIOCAN¹, Sebastian Valeriu HUDIȘTEANU¹, Florin-Emilian ȚURCANU¹, Andrei BURLACU¹ and Adrian GROSU¹

¹Gheorghe Asachi Technical University of Iași, Faculty of Civil Engineering and Building Services, Iași, Romania

Abstract. *The purpose of this study was to analyse a ventilation system with impulse fans, which acts to ensure optimal air parameters and to evacuate smoke in case of fire in an underground car park. Given the number of parameters to be taken into account in the spread of smoke, there is a high chance of introducing calculation errors if only conventional methods are used. In this study, CFD simulations were used to compare the various stages of operation of the ventilation system, as well as their effectiveness in the proposed scenarios. In the case of the ventilation scenario, the concentration of carbon monoxide (CO) reached maximum values of 360 PPM, exceeding the maximum allowed value of 100 PPM, this endangering the users of the underground car park. In the second phase, we analysed the operation of the ventilation system simultaneously with that of the impulse fans for the two targeted functions and in this case the maximum concentration reached was 60 PPM, which indicates that this system configuration fulfils the function for which it was designed. The results showed, in the case of the scenarios, that the addition of impulse fans as complementary elements to the ventilation system substantially improved the reduction in the concentration of carbon monoxide (CO) and increased fire visibility in the parking lot.*

Keywords: underground parking, ventilation, jet fan, smoke.

1. Introduction

For modern buildings, the installation of a mechanical ventilation system is essential to ensure the necessary level of air quality and thermal comfort. In addition to ensuring an optimal indoor environment, an important aspect of mechanical ventilation systems is to ensure protection in the event of a fire.

Fires in underground car parks are dangerous due to smoke that can flow quickly through the compartment, almost without any restrictions. These compartments have a large surface area, and their small height reduces the depth of the smoke-free bottom layer. Fire sources can be very difficult to fight, as smoke can easily fill the entire compartment and affect vision.

Combustion products from a fire are the most serious pollutants that can occur in underground parking lots. The knowledge gained by studying the consequences of fire on human beings implies that combustion products can be even more dangerous to human health than other fire-related phenomena. Combustion products from fire reduce the oxygen content of the air, suppress the ability of people to think clearly, reduce the visibility and ability to orient evacuees, and create preconditions for panic. In addition, they directly affect human health in two different ways - through flue gases and toxic gases (CO). [1], [7]

Carbon monoxide (CO) is considered to be the most dangerous combustion product, with a lower poisoning threshold of only 0.01 to 0.02% by volume. At a concentration of over 1% of the volume, man loses consciousness and death occurs in three minutes. Carbon monoxide poisoning is a common cause of fire death. [11], [15], [16]

Over time, the parking lots were ventilated using the traditional method of ventilation with air ducts that took up a lot of space. There is now an innovative new approach, known as impulse ventilation, which eliminates the need to use air ducts and uses special impulse fans, thin, efficient, and powerful, which has made this system very popular in recent years. These fans are positioned in places where smoke or polluted air is expected to stagnate, this being highlighted with the help of CFD simulations.

This system uses the principle of adding momentum to the air to push it to a pre-designated extraction point and to ensure that there are no dead zones for vapor and smoke to stagnate and collect in those areas.

This ventilation system can be used as a normal ventilation system, necessary for the removal of air pollutants, but also as an emergency ventilation system used for the evacuation of flue gases in case of fire.

In the case of underground car parks, the normal ventilation system aims to remove the air polluted by the flue gases generated by the movement of cars, to prevent damage to the health of people inside the car park. The emergency ventilation system is used to fight fires by evacuating excessive heat and flue gases from the fire. Both ventilation systems simultaneously provide fresh air inside the car park to increase the safety of evacuees and emergency crews during evacuation. [4], [8], [9], [18], [19]

From a technical point of view, it is possible that the two ventilation systems, normal ventilation, and emergency ventilation, can be combined into a single physical system, taking into account that such a system must meet the requirements of both types of individual ventilation. This system will have two stages of airflow control, the first stage

serving the normal ventilation system, and the second stage will be used in the event of a fire.

However, in Romania, there is no standard for the design of fire safety systems involving impulse fans, and during the design process, the provisions of standard EN 12101-3 on ventilation systems with impulse fans were observed. [5], [10]

The purpose of this study was to design and analyze a ventilation system with impulse fans for an underground car park. The studied ventilation system has the following functions: ensuring air quality and maintaining optimal comfort parameters by reducing the concentration of carbon monoxide (CO) and the evacuation of flue gases and excessive heat in case of fire.

2. Numerical modelling

The numerical simulation was performed in the (Autodesk CFD, Ansys, SimScale) modelling environment, and the purpose of the study is to determine the behaviour of a ventilation system with impulse fans operating in an underground car park, to identify possible methods of streamlining the system. [2], [3], [6], [13], [17], [19]

For the analysis of the scenarios considered in the present study, a P2 type underground parking lot with a capacity of 250 vehicles was used. The car park has a single level located in the basement of an office building, with an area of 6750 m² and a height of 3.5 m, resulting in a total volume of 23625 m³. The car access to the car park is made from the street level, through a two-way ramp of the following dimensions: 17.6 m x 5.0 m and a slope of 5%. The building is located in an area with low traffic, free from high pollution factors.

The ventilation system designed for underground parking is a ventilation system with impulse fans, which serves two main functions: the first function is to ensure ventilation of the parking lot to reduce the concentration of pollutants, and the second is to evacuate smoke in case of fire. The designed ventilation system has two operating stages, the first stage is used for normal ventilation and the second stage is used for emergency parking ventilation. The two operating stages will convey different airflows according to the regulations of each of the functions.

The introduction, respectively the evacuation of the air necessary for the ventilation is made using three discharge openings and three exhaust outlets, having the dimensions of 2.0 m x 1.0 m. long of the parking lot and the outlets were located in the upper part, opposite the discharge ones. The ventilation system considered in the present study is a vacuum ventilation system, in which the exhaust airflow is higher than the introduced airflow, thus ensuring the circulation of contaminated air to the outside.

To improve the movement of air masses in the parking lot, the technical characteristics of the Flakt Woods Standard 315, 0/7 / 0.09 kW F300 impulse fan, with a diameter of

315 mm and a length of 2.2 m. It has two operating stages that will serve the two functions of the system. To streamline the ventilation system, the CFD simulations from this study will be used, with the help of which we will determine the optimal arrangement of the impulse fans inside the parking lot.

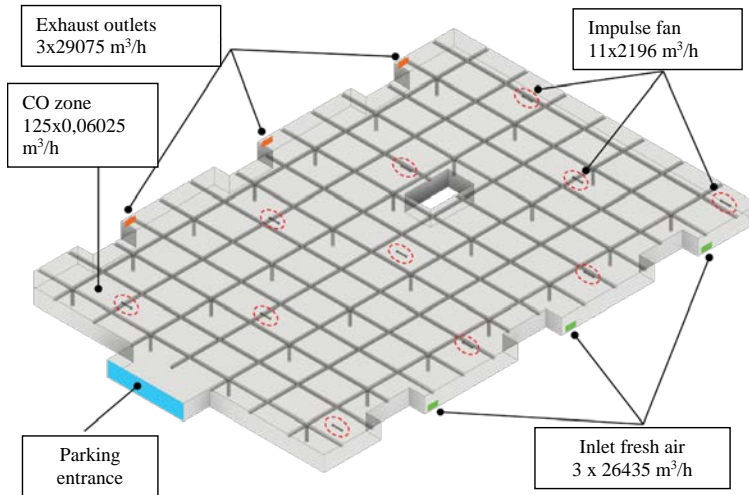


Fig. 1 – Simulation - Ventilation system

Because the ventilation system studied serves two separate functions, this system was dimensioned using the regulations of both individual systems. Considering the aspects mentioned above, four analysis scenarios resulted using CFD simulations as follows:

For the normal ventilation system, designed to ensure optimal air parameters in the parking lot, we considered the following scenarios:

- A. Operation of the ventilation system using the first stage of operation.
- B. Simultaneous operation of the ventilation system and pulse fans also adjusted to the first stage of operation.

For the emergency ventilation system, used for smoke evacuation in case of fire, we considered the following two scenarios:

- C. Operation of the ventilation system using the second operating stage.
- D. Concomitant operation of the ventilation system and the second-stage pulse fans.

Case A and B

To simulate the ventilation system, an airflow of 79300 [m³/h] was considered to be evenly distributed over the three air intake grids, resulting in a flow on each grille of

26435 [m³/h]. The exhaust flow of 87230 [m³/h] is, in turn, evenly distributed over three air exhaust grilles, resulting in a flow of 29075 [m³/h] / grille.

For mixing and directing the air in the parking lot we considered the Flakt Woods Standard impulse fan - with a length of 2.2 m and a diameter of 315 mm. It has two operating stages, and in the case of this scenario the first operating stage with the following characteristics was used: impulse force - 5.7 [N], airflow - 0.61 [m³/s]. The total amount of carbon monoxide (CO) released inside the car park for the situation where 50% of the vehicles are considered to be moving is 7.53 [kg/h]; The computational range used to simulate the ventilation system is Hex-dominant and consisted of 4.9 million cells. As a model of turbulence, we used the k-model model. For the simulation of house B, the same settings of the simulation from the first case were kept, the new calculation field being made up of 6.7 million cells.

Case C and D

To simulate the smoke exhaust system, an airflow of 120,000 [m³/h] was considered to be evenly distributed on the three air intake grids, resulting in a flow on each grid of 40,000 [m³/h]. The exhaust flow of 150,000 [m³/h] is in turn distributed evenly on the three air exhaust grilles, resulting in a flow on each grid of 50,000 [m³/h]. For mixing and directing the air in the parking lot we considered the Flakt Woods Standard impulse fan - 2.2 m long and 315 mm in diameter. It has two operating stages. In the case of this scenario, the second stage of the operation was used, which has the following characteristics: impulse force - 22 [N], airflow - 1.2 [m³/s]. We considered as a smoke source a fire in a car with a length of 5 m and a width of 3 m, resulting in a smoke emission surface of 15 m². It was positioned in the center of the parking lot, at a height of 1 m from the floor. The dimensions of the fire are those recommended in the BS7346 standard for steady-state simulations. According to Table 3.1 of the British standard BS7346, a steady-state car fire has a heat release rate (HRR) equal to 4MW.

Table 1
Recommended values for designing fires in the Steady-State state

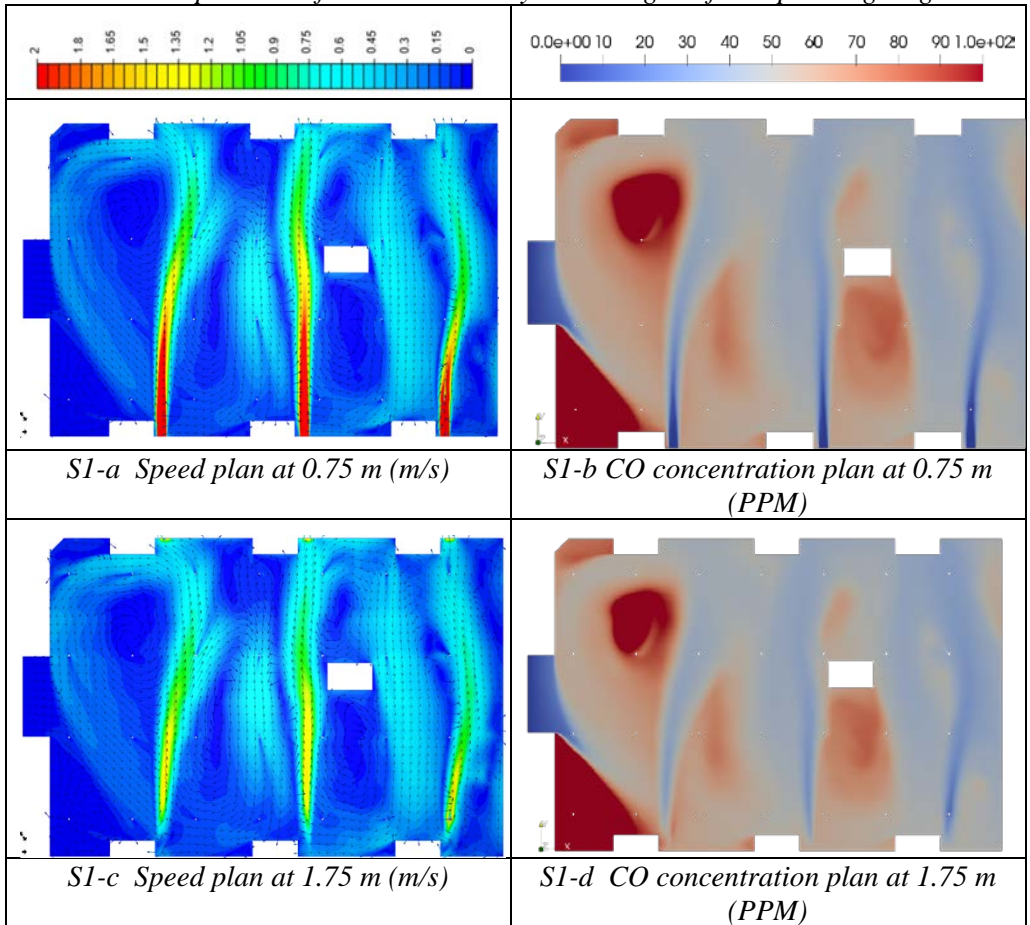
Fire parameters	Parking without sprinkler system	Parking with sprinkler system
Dimensions	5 m x 5 m	3 m x 5 m
Perimeter	20 m	16 m
Heat release rate	8 MW	4 MW

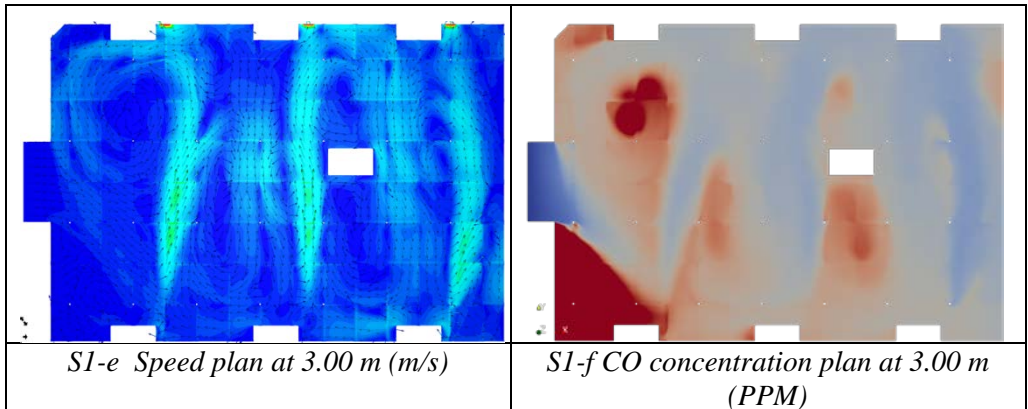
The calculation range used to simulate the smoke exhaust system consisted of 4.9 million cells and is Hex-dominant. As a model of turbulence, we used the k-ε model.

3. Results

In table 2, figures S1-a to S1-f show the movement of air through velocity planes at different heights and how it influences the concentration of carbon monoxide (CO) inside the underground car park.

Table 2
Case A Operation of the ventilation system using the first operating stage





To represent the velocity planes to use a color map distributed in the range 0 - 2 m/s, and for the planes representing the carbon monoxide (CO) concentration to use a colouring in the range 0 - 100 PPM for an obvious problem for areas. In figures S1-a, S1-c, S1-e it is observed until the distribution of air inside our parking lot is uniform, which led to the creation of an air recirculation area. In the area where the air stagnates and, as can be seen in Figures S1-b, S1-d, S1-f, the concentration of carbon monoxide (CO) creates, exceeding a maximum permissible value of 100 PPM in a range of 20 for a minute. In areas in the care of concentration at a deposit of more than 100 PPM, especially in the famous colouring in the intensity of red, can be maximum at 358 PPM.

In view of the above, it follows that the use of a ventilation system without impulse fans does not ensure that the concentrations of pollutants produced by motor vehicles are kept within optimal limits. It is therefore necessary to increase the air mixture in these recirculation zones in order to reduce the risk of developing high concentrations of carbon monoxide (CO). In order to make the ventilation system more efficient, we considered the installation of impulse fans in the parking lot in problematic areas, of air stagnation, to improve its mixture inside and to direct the air currents to the exhaust ports. Figure 2 shows the areas of air stagnation. At the same time, the path of the air movement represented by the velocity vectors can be observed. To improve air movement in problem areas we introduced 11 impulse fans.

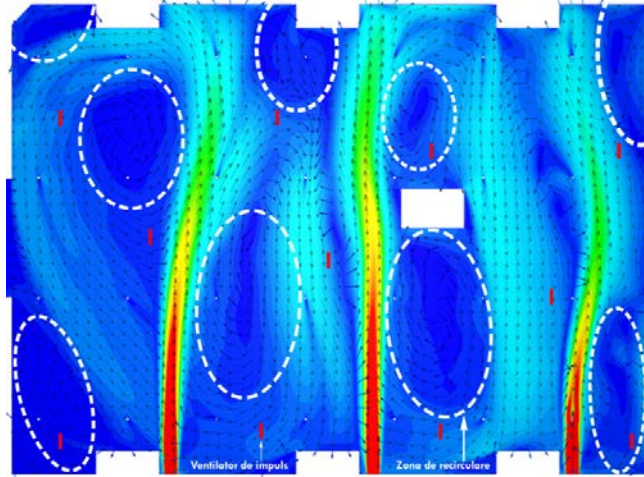


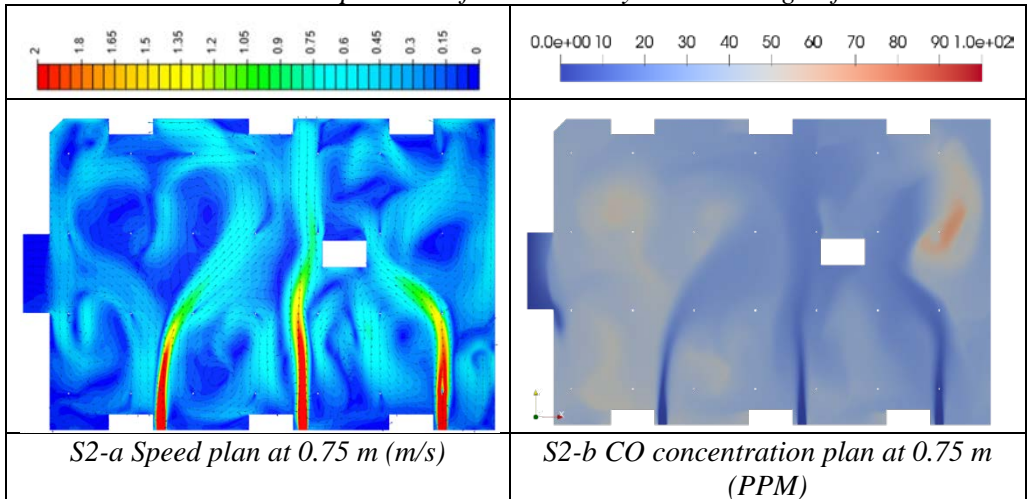
Fig. 2 – Air recirculation areas

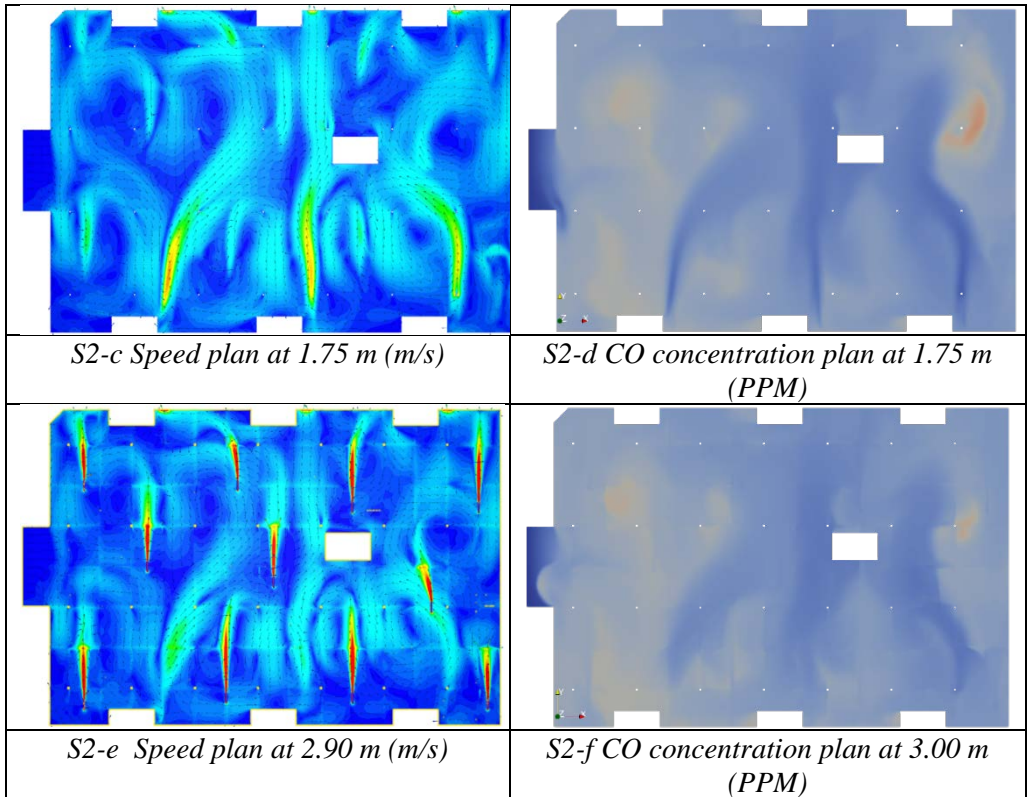
According to Figure 2 we added to the initial geometry the proposed impulse fans and we generated a new calculation field that will be used in the second scenario of this case.

Figures S2-a to S2-f show the movement of air through velocity planes at different heights and how it influences the concentration of carbon monoxide (CO) inside the underground car park.

Table 3

Case B - Concomitant operation of ventilation system and stage I fan blowers





With the improvement of the air movement in the parking lot, it can be observed the decrease of the carbon monoxide (CO) concentration below the maximum allowed values of 100 PPM in an interval of 20 minutes, this showing from figures S1-b, S1-d, S1 f. The maximum value reached in the concentration of carbon monoxide, in this case, was 66 PPM, and the average value inside the car park is 50 PPM.

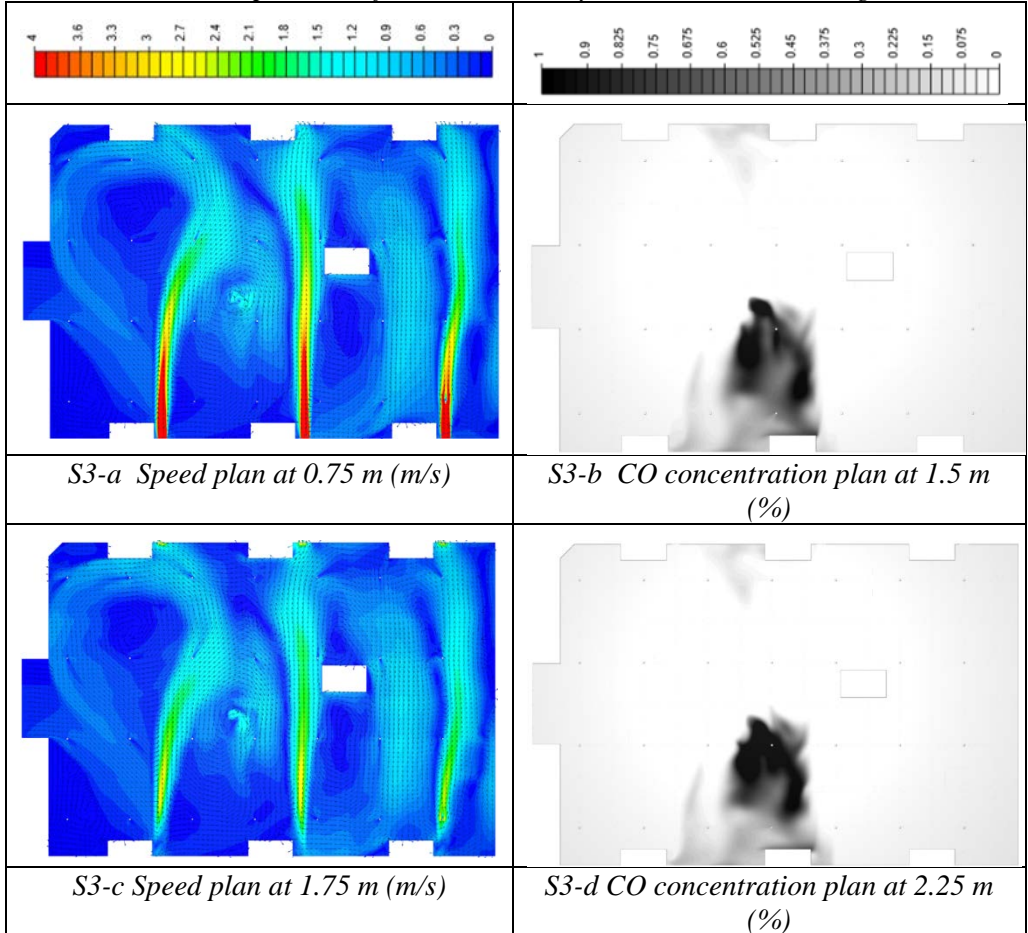
In view of the above, it appears that the solution analyzed in the second scenario of the ventilation installation provided an optimal air flow to reduce the concentrations of pollutants below the maximum allowed level. Therefore, the introduction of impulse fans operating simultaneously with the ventilation system is a valid and efficient solution in order to reduce the concentrations of pollutants released by vehicles when traveling in parking lots.

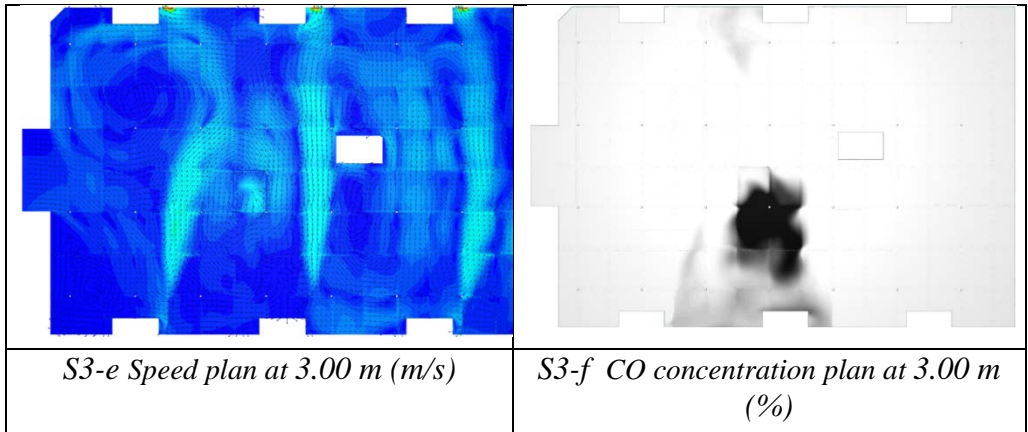
An important aspect for the design of a ventilation system with impulse fans that has a high efficiency in operation is the study through CFD simulations of the positioning of the constructive elements of the installation and the analysis of the air masses produced by these elements, in order to implement the optimal solution.

Figures S3-a to S3-f show the movement of air through the velocity planes at different heights and how it influences the dissipation and concentration of smoke inside the underground car park.

Table 4

Case C - Operation of the ventilation system on the second stage a





Although in this case a much higher air flow was used than in the case of the previously studied ventilation system, in figures S1-a, S1-c, S1-e it is observed that the movement of air inside the parking lot is not uniform, aspect which leads to the creation of air recirculation areas. If in these areas, where the air stagnates, a fire develops, the accumulation and concentration of smoke in that area increases rapidly, which is seen in Figures S1-b, S1-d, S1-f. In this scenario, the area where the smoke concentration reaches a percentage of 100% is 292 m². Figures 3 and 4 show that the clear height under the smoke blanket is quite low (1.4–1.6 m) in areas with high smoke concentration. These issues make it impossible for fire crews to remove the source of the smoke and evacuate people who are near the fire or who are located on the opposite side of the exit.



Fig. 3 – Longitudinal section of fire - smoke concentration



Fig. 4 – Fire cross section - smoke concentration

In view of the above, it follows that, in the present case, the ventilation system without impulse fans does not ensure a reduction in the smoke concentration in order to allow the safe conduct of the activities of the intervention crews and the safe evacuation of parking users.

It is therefore necessary to increase the air mixture in the recirculation areas, in order to reduce the risk of developing high concentrations of smoke and to avoid dangerous situations.

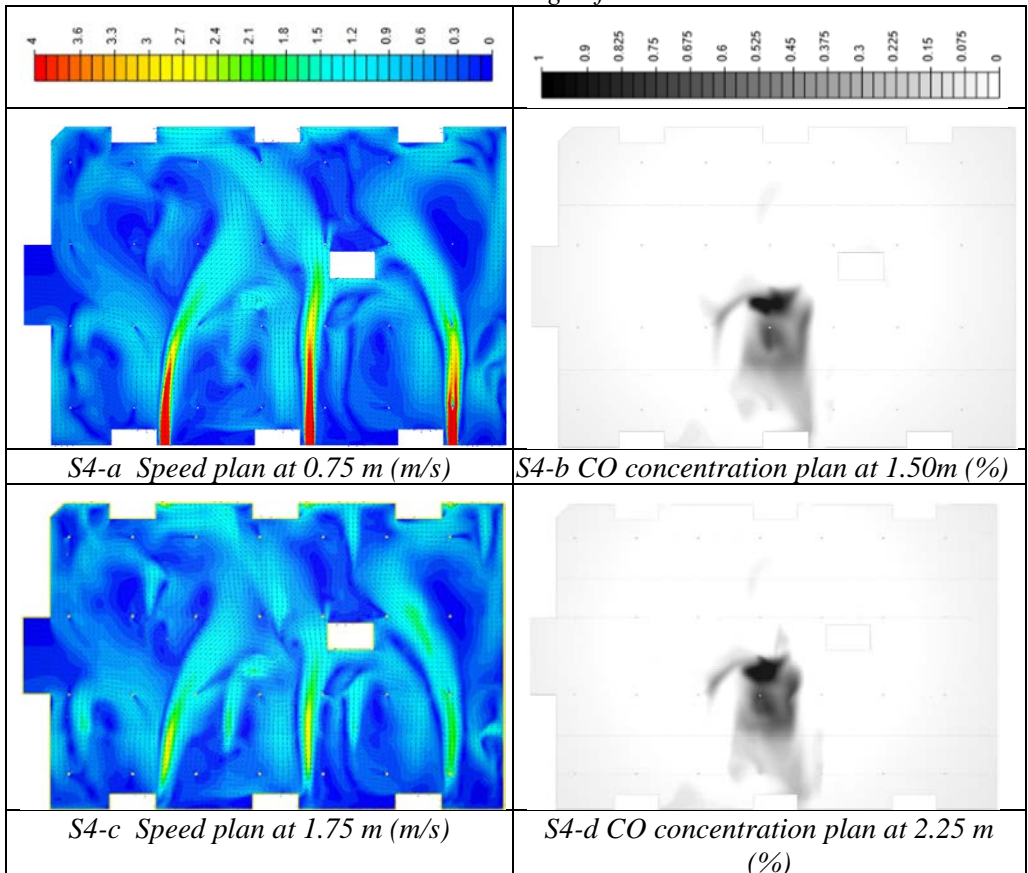
As a consequence, it is recommended to make the ventilation system more efficient by adding impulse fans in problem areas, to stagnate the air, in order to improve its mixture in the car park and to direct the air currents towards the exhaust outlets.

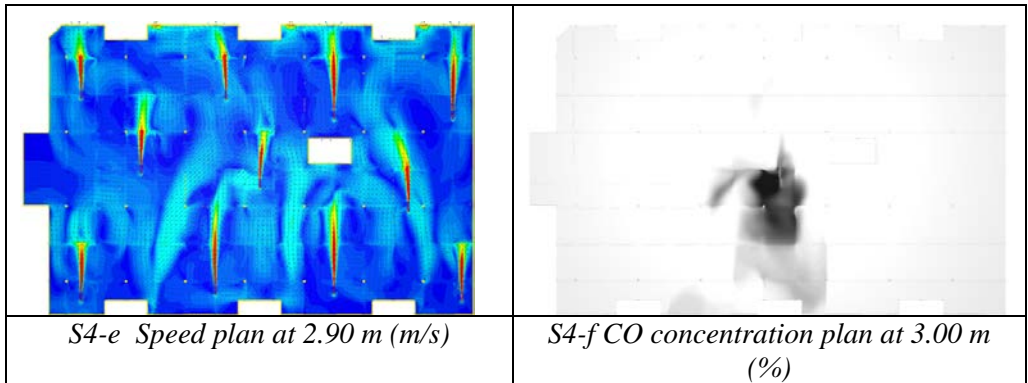
As the air recirculation areas are similar to those identified in the previous simulations, the same arrangement of the impulse fans will be used.

Figures S4-a to S4-f show the movement of air through the velocity planes at different heights and how it influences the dissipation and concentration of smoke inside the underground car park.

Table 5

Case D - Simultaneous operation of the ventilation system and impulse fans on the second stage of





Figures S4-a, S4-c, S4-e shows a considerable improvement in the movement of air inside the parking lot after the placement of the impulse fans. The air flow speed in the parking lot is on average 1.2 m/s, as shown by the figures mentioned.

With the improvement of the air movement in the parking lot, it can be observed the decrease of the smoke concentration and the limitation of the areas where the smoke concentration reaches a maximum percentage, this emerges from figures S4-b, S4-d, -f.

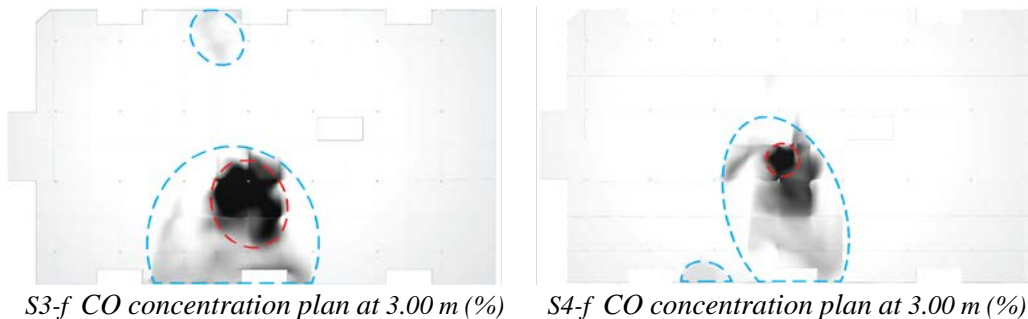


Figure 5 - Comparison between the two scenarios of the Smoke Exhaust System

The area of the areas where the smoke concentration reaches a percentage of 100% decreased considerably reaching 39 m², compared to the previous scenario when the area where the smoke reaches maximum concentrations was 292 m² - this aspect can be seen in Figure 5.

Taking into account the results of the CFD simulation, it results that the solution analysed in this scenario successfully meets the requirements for reducing the smoke concentration, ensuring the necessary visibility conditions for specialised intervention crews and for the safe evacuation of parking users.

For the design of a ventilation system with impulse fans that have a high efficiency in operation, it is very important to analyse through CFD simulations the positioning of

the constructive elements of the installation and the movement of air masses generated by these elements, in order to implement the optimal solution.

4. Conclusions

The CFD simulations provided an in-depth understanding of how the ventilation system works, providing an opportunity to analyse the movement of airflow, velocity fields, pollutant concentration, smoke concentration and the impact of the positioning of ventilation elements in the parking lot. These issues have led to the identification of ways to streamline this system.

In the first phase, we analysed the operation of the system without impulse fans for the two functions concerned. The results of both simulations indicated that the air distribution in the parking lot is not uniform, which implies the appearance of air recirculation areas. In these areas the air stagnates, becoming dangerous areas where the concentrations of pollutants or smoke even exceed the maximum allowed values.

In the case of the ventilation scenario in these areas, the concentration of carbon monoxide (CO) reached maximum values of 360 PPM, exceeding the maximum allowed value of 100 PPM, this endangering the users of the underground car park.

In the case of the smoke evacuation scenario, it was observed that the occurrence of a fire in the perimeter of these areas can lead to rapid accumulation of smoke and, at the same time, rapid increase of smoke concentration to maximum values, which affect visibility inside and prevent crew intervention. Firefighters or evacuating people inside the parking lot.

In conclusion, in the two cases considered of the ventilation system without impulse fans, the operating and safety requirements regulated by the regulations in force were not met.

In order to make the ventilation system more efficient, we considered adding impulse fans to the parking lot in order to improve the air movement and to ensure the requirements regulated by the two functions of this system.

Based on the results of the two initial simulations, the areas where the air stagnates and its better circulation are identified, this aspect allowed the optimal choice of the number of impulse fans and their optimal arrangement for obtaining an increased efficiency. We considered adding a number of 11 impulse fans that work simultaneously with the ventilation system.

In the second phase, we analysed the operation of the ventilation system simultaneously with that of the impulse fans for the two targeted functions. The results of the simulations indicated a considerable improvement of the air movement in the parking lot due to the optimal positioning of the impulse fans. This has led to the removal of air stagnation areas. As a result, pollutant and smoke concentrations have decreased.

In the case of the ventilation scenario, the maximum concentration reached was 60 PPM, which indicates that this system configuration fulfils the function for which it was designed.

In the case of the smoke evacuation scenario, the decrease of the smoke concentration was observed and implicitly of the areas where maximum concentrations are reached, resulting that even in this situation the analysed system fulfils the function for which it was designed.

In conclusion, the use of the impeller fan ventilation system fulfils the functions of normal ventilation and emergency ventilation required in its design, as well as the regulated safety requirements.

REFERENCES

- [1] P. A. Enright, *Impact of jet fan ventilation systems on sprinkler activation* Case Stud. Fire Saf., 2014.
- [2] A. Senveli, T. Dizman, A. Celen, D. Bilge, A. S. Dalkilic, and S. Wongwises, *CFD analysis of smoke and temperature control system of an indoor parking lot with jet fans* J. Therm. Eng., 2015.
- [3] A. Celen, B. Kundu, A. S. Dalkilic, S. O. Atayilmaz, N. Kayaci, and S. Wongwises, *Smoke control of a car park by means of CFD analyses using jet fans* in American Society of Mechanical Engineers, Fluids Engineering Division (Publication) FEDSM, 2014.
- [4] C. H. Su, Y. C. Lin, C. M. Shu, and M. C. Hsu, *Stack effect of smoke for an old-style apartment in Taiwan*, Build. Environ., 2011.
- [5] J. C. F. Teixeira, S. F. C. F. Teixeira, P. Cunha, and A. M. Silva, *Thermal driven dispersion of smoke in a parking space*, in ASME International Mechanical Engineering Congress and Exposition, Proceedings (IMECE), 2016.
- [6] M. A. Santoso, Z. Bey, and Y. S. Nugroho, “*CFD Study on the Ventilation System and Shape Configuration of Underground Car Park in Case of Fire*”, Appl. Mech. Mater., 2015.
- [7] L. Umamaheswararao, *Optimum Design of Impulse Ventilation System in Underground Car Parking Basement by Using CFD Simulation*, Ind. Eng. Manag., 2017.
- [8] M. W. Hsu, S. K. Lee, L. L. Huang, Y. K. Chen, and C. M. Wu, *The simulation of fires in underground parking floors by fire dynamic simulator*, Sensors Mater., 2017.
- [9] B. Alianto, N. Astari, D. Nareshwara, and Y. S. Nugroho, *Modeling of smoke control in underground parking-garage fires*, Int. J. Technol., 2017.
- [10] D. Burlacu, I. Anghel, C. Popa, and I. Cășaru, *Fire Safety Evaluation of an Underground Car Park Using Numerical Simulation*, Math. Model. Civ. Eng., 2018.
- [11] S. Ali, E. E. Khalil, and M. A. Fouad, *Effect of fire locations on the performance of impulse ventilation system in an underground car park*, in 51st AIAA Aerospace Sciences Meeting including the New Horizons Forum and Aerospace Exposition 2013, 2013.
- [12] V. Stoyanov, A. Terziev, and M. Uzunova, *Numerical study of distribution of smoke and hazards in underground parking areas considering the operation of ventilation*, in 3rd International Symposium on Environment Friendly Energies and Applications, EFEA 2014, 2014.
- [13] S. Sultansu and A. Onat, *The CFD Analysis of Ventilation and Smoke Control System with Jet Fan in a Parking Garage*, Int. J. Adv. Eng. Pure Sci., 2020.
- [14] J. C. F. Teixeira, S. F. C. F. Teixeira, P. Cunha, and A. M. Silva, *Thermal Driven Dispersion of Smoke in a Parking Space*, 2016.
- [15] M. R. Carratu et al., *Carbon monoxide*, Environ. Heal. Criteria, 1999.
- [16] B. Nearing, *When General Electric leaves Fort Edward, pollution remains*, Timesunion, 2014.
- [17] M. T. Çakir and Ç. Ün, *CFD Analysis of Smoke and Temperature Control System of Car Park Area with Jet Fans*, J. Eng. Res. Reports, 2020.

- [18] X. Liu, S. Lu, and Y. Huang, *Experimental Study on Smoke Exhaust of Circular Fire Lane in Underground Vehicle Base of Urban Railway*, in IOP Conference Series: Earth and Environmental Science, 2020.
- [19] M. Kmecová, M. Krajčák, Z. Straková, *Designing Jet Fan Ventilation for an Underground Car Park by CFD Simulations*, Periodica Polytechnica Mechanical Engineering, 63(1), pp. 39-43, 2019. <https://doi.org/10.3311/PPme.12529>

IoT CONTRIBUTORS FOR BUILDINGS ENERGY EFFICIENCY

Gabriela COVATARIU and Daniel COVATARIU

*“Gheorghe Asachi” Technical University of Iasi,
Faculty of Civil Engineering and Building Services, Romania*

Abstract. *The paper presents the framework of implementing IoT paradigm in buildings construction and management in order to have a higher energy efficiency at the lowest costs and maintaining/increasing the inhabitant's comfort. Starting from the construction stage, going through the housing and continuing with management, IoT reorganizes every aspect of a building. The data provided by IoT are used to make informed decisions in order to optimize the comfort of the inhabitants. In order to extend the profits and to optimise the buildings processes, the “smart buildings” have to efficiently manage the existing facilities and inhabitant's safety.*

Keywords: sustainable development, buildings smart management

1. Introduction

The *sustainable development* is a new concept of which determines a different approach from the classical one, which is nowadays used where is raised a building. Today, most of the buildings are considered as a “continuously evolution body”, which during its lifetime have to be monitored, consolidated and optimised to meet the requirements set by the user at different stages. Highly topical are the analyses and interventions regarding the energy saving during maintaining / rising the adequate comfort. This aspect has been named the ***energy efficiency of the building***. In parallel with the reduction of energy needs, two important objectives of sustainable development will be achieved, namely the migration of non-regenerable resources to the sustainable sources and the reduction of polluting emissions into the environment.

It is well known that the existing building fund contributes greatly to greenhouse gas emissions in Europe. Significant reductions in these emissions can be achieved through this domain and the building sector plays an important role in achieving the EU's objectives. To achieve these EU targets, CO₂ emissions and the future buildings energy consumptions will need to be close to zero. This requires to follow the guidelines for the “near-zero energy buildings” concept implementation (nZEB).

The revision of the Building Energy Performance Directive (EPBD2012) introduced, “Near zero energy buildings” (nZEB) as a nowadays requirement to be implemented for public buildings (starting with 2019) and for residential buildings (from 2021). The cited Directive defines buildings with almost zero energy consumption as *“a building with a high energy performance, and this energy requirement of low or almost zero energy should be largely covered from renewable sources, including energy produced on or nearby”*.

Individual and collective residential buildings account for about 95% of the Romanian housing fund. Office buildings account for around 13% of the non-residential building fund, but have seen a high construction rate over the past ten years. The three categories of buildings considered together represent 87% of the building fund in Romania.

Investors and real estate developers have already considered adding smart housing and construction functions to their new residential and commercial developments. Thus, the concept of Smart City has become a "must-accomplish" asset in any important real estate project.

Smart City is more likely a concept and is not very precise defined. Could be widely interpreted and a lot of amendments and additions could be made. This is due to the wide range of components that come under this term's umbrella - Smart City. Taking into consideration the smart building management systems is a compulsory element in a Civil Engineering construction planning, in order to be considered a developing Smart City.

In Romania this concept is very rarely meet. The Alba Iulia city projects and other isolated examples in big cities, demonstrate that this concept is almost unknown or is expensive for local communities.

All stages of a built structure's life-cycle involve energy consumption; efficiency of this consumption is one of the main objectives of the present and future sustainable development programmes of society, through the implementation of programmes for the creation/implementation of renewable energy sources, as well as the protection of the natural environment (through its responsible exploitation).

2. Romanian's Legislation Approaches

Energy efficiency of buildings is a top priority, taking into account the poor quality of most existing buildings, whether old or cheap. Otherwise, the costs related to the thermal rehabilitation of a building are lower than the costs related to the installation of an additional heat capacity for heating. According to statistics, in Romania, the population sector's energy consumption is at the level of 40% of the country consumption's total energy, and this tendency has been found more or less all over the world.

Within the technical regulations valid in Romania in construction, there are minimum requirements only for newly built buildings. As regards minimum energy performance requirements, they do not exist in the form of a global consumption indicator, either in the case of a new building or of the existing building's rehabilitation. However, technical construction regulations in Romania contain normative thermal insulation criteria for building elements and a global thermal transfer coefficient ("G" value). "G" ($\text{W/m}^3 \times \text{K}$), relative to heated volume, is an overall minimum requirement and varies according to the number of building levels and its compactness index.

For residential buildings, the maximum heat requirement (relative to the total heated volume) varies between $15 \text{ kWh/m}^3/\text{year}$ and $37.5 \text{ kWh/m}^3/\text{year}$ depending on the ratio between the envelope's area and the volume of the building (A/V). The maximum heat requirement set does not take into account the efficiency of the installation related to the building. As regards the energy certification system, the categories in the EPC (Energy Performance Certificate) range from A (most efficient) to G (with the highest energy consumption). Category A of the Energy Performance Certificate ranges from $125 \text{ kWh/m}^2/\text{year}$ (heating, domestic hot water and lighting) to $150 \text{ kWh/m}^2/\text{year}$ (all energy facilities). The EPC includes heating, ventilation, cooling, domestic hot water and lighting consumptions. For instance, a building which has no cooling system and no mechanical ventilation system, the energy consumption of "A" Class is less than $125 \text{ kWh/m}^2/\text{year}$.

According to official evaluations, the major majority of buildings in Romania are "C" and "D" classed (in terms of energy performance). There are justified the concerns that this standard assessment might be too optimistic and that in reality most buildings are approaching the "E" standard. The benefits of nZEB's implementing are much broader than energy's saving and reducing CO_2 emissions. It can be punctually described as follows:

- *The quality of life* is much better than in buildings built according to current practices. The almost entirely additional costs of the energy-efficient building type are covered by the cost-saving principles of the building obtained through proper design and high-quality execution. A better thermal comfort increases the quality of life. nZEB buildings ensure good indoor air quality, the ventilation system provides continuously filtered air. Such a building is independent of external conditions (climate, air pollution, etc.).
- *Environmental benefits*: comes from low energy needs which significantly reduce the environmental impact due to energy extraction, production and supply and are also due to quality improvement at local level. Also, by reducing energy consumption in buildings, there is a decrease in energy dependence on fossil fuel extraction and implicitly on future energy prices.
- *Health benefits*: ensuring improved indoor air quality and reduced risk of cold rooms, especially in buildings occupied by low-income families or the elderly.

- *Economic benefits*: the promotion of innovative technologies and the creation of market opportunities for new or more efficient technologies and by providing certain subsidies to encourage pilot projects and market transformation.
- *Private economic benefits*: higher investment costs can be offset by energy savings during the lifetime of the building (buildings are characterized by a low sensitivity to energy prices and political unrest). About 30% resale price is achieved when a high standard new building is sold (by comparing to an ordinary building).
- *Social benefits*: Creating new jobs (generated by developing production and services to increase energy efficiency and install renewable energy technologies); the reduction of energy poverty (energy poverty = the financial impossibility of those on low incomes to provide minimum thermal comfort in housing).

3. Internet of Things (IoT) principles

According to ITU-T's, the "Internet of Things" is a "global infrastructure for the information society, enabling advanced services by interconnecting (physical and virtual) things based on existing and evolving interoperable information and communication technologies" [9].

Starting from the construction stage, going through the housing and continuing with management, IoT reorganizes every aspect of a building. In order to optimize the comfort of the inhabitants, the data provided by IoT are used to make informed decisions

The technologies behind IoT have existed for several years in the construction sector. IoT comes with features like remote access, cloud computing, data storage, office-to-field data exchange a.s.o.

IoT can and must provide the tools to participate at all stages of the life-cycle of a built structure (housing, office and commercial buildings, industrial and services halls, energy facilities (production and energy transport), etc.):

- ⇒ *In the Design stage*: The analysis of the 6th dimension of the BIM concept regarding sustainability (sustainable element monitoring, conceptual / detailed energy analysis, LEED tracking);
- ⇒ *In the Execution stage* (the relationship between all the resources involved in the construction process: the supply of materials, the management of labour, compliance with the requirements imposed by the execution project and the related norms, the ensuring production flows in the construction site, the correct management of transports, etc.);
- ⇒ *In the Exploitation stage* (monitoring of operating behaviour and choosing decisions for the execution of maintenance/repair/rehabilitation works); in this respect, BIM's 7th dimension integrates Facility management applications (Life Cycle BIM Strategies, embedded Q&M manuals, BIM Maintenance Plans and

Technical Support, COBie data population and extraction, BIM file hosting and Lend Lease's Digital Exchange System);

⇒ *In the Ending stage of the building's life-cycle* (post-use decisions for structural reconversion: demolition, destination change, fragmentation).

IoT, brought to the level of households, must be economically profitable. This means that all investments must contribute to the overall efficiency of the household. In other words, IoT technology must become a monitoring and cost-effectiveness centre and not a "black hole" of unnecessary spending. Major global investors (Tesla, Apple, Amazon, Google, etc.) have already invested many billions of dollars in this industry to make the homes of the future to be smart.

Many innovative products, at the time of their placing on the market, have a high purchase and/or maintenance price. Subsequently, after a period of implementation and use, it is proved that the rationale for their introduction was justified in several respects and that the depreciation of the initial investment far exceeds the profit obtained from their use.

At the level of smart homes and consumers (C-IoT) [7], there are many connected devices that contribute to the user's ultimate profit. Within the systems created, each element works as designed, the true value of IoT will be achieved as technology "learns," "matures" and devices are integrated together and driven by "artificial intelligence".

Smart IoT platform approach to facilitate the development of applications and enable communications among systems and solutions in a collaborative manner (C-IoT). Smart IoT as characterized by the:

- 8A's stand for "Automated Remote Provisioning and Management, Augmented Reality, Awareness of Context and Location, Analyse, Take Action, Automate, Anticipate, Predict, Autonomous and Attractive" [8].
- 7S's stand for "Simplicity, Security, Safety, Smart, Scalable, Sustainable and Sleek Appeal".

4. IoT platforms

An IoT platform can contribute to the efficiency of the building through cutting the costs while the energy demands still meeting.

In order to achieve the maximum benefits afforded by the technology, the IoT applications (in conjunction with their renewable energy sources) are used by many companies

In accordance to the need at the time, the IoT platform could provide detailed information that can be selected. The information so collected (Big data), provides options for Descriptive, Predictive and Prescriptive analysis.

IoT Business Model consisted of Sensing, Gateway and Services technologies and protocols that directly relate to IoT for IoT Architecture model (Figure 1):

- **Physical:** Sensors, wireless sensor networks (WSN), radio frequency identification (RFID), micro-electromechanical systems (MEMS), Global Positioning System (GPS), ZigBee, Near Field Communication (NFC), Wi-Fi and 4G/5G;
- **Virtual:** Software Defined anything (SDx), network functions virtualization (NFV), IPv4/IPv6, Geographic Information System (GIS), and body area network (BAN) / Local Area Network (LAN) / wide area network (WAN) (body area network/local area network/wide area network);
- **Cloud:** Big Data / Analytics.

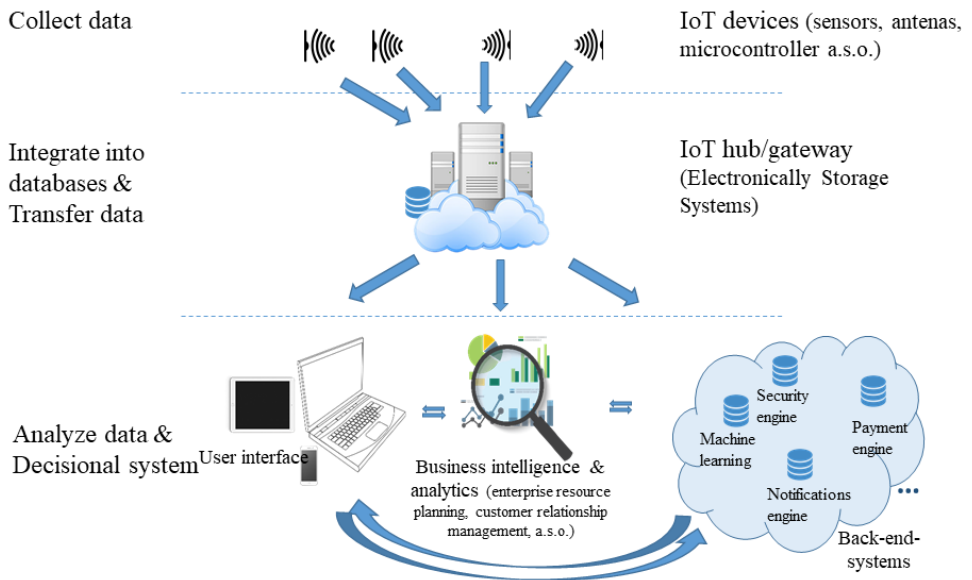


Fig. 1 - The IoT system framework

Watson IoT™ solutions for buildings, Google IoT Core, UbiqiSense, AWS IoT, Microsoft Azure IoT, Power BI, SAP Analytics Cloud, Robustel Cloud Management Service are just some of the IoT platform that can be used for buildings to become „smart” and to obtain lower level of energy consumption and high efficiency.

An IOT platform need to fulfil a few requirements in order to satisfy the clients/users.

Usually, there are used large variety of devices, from more than one producer. From here appears the necessity to develop technology ecosystems into which the vendors could integrate their devices and where the developers support devices extended range

without having to develop vendor-specific code. This manner will increase the flexibility, the scale and, also, the innovation's speed for the IoT platform's developers.

For scaling the system need to be able to connect and support a very large number of sensors, routers, gateways, and data servers.

Sensors (having the capability to send/receive data) allow capturing information required to improve results with real-time data about the site and the workmanship.

The "things" generate a large amount of information, known popularly as "big data" signifying a large volume of data, a large variety and transmitted with high velocity through IoT devices.

The data collected from IoT-enabled products and systems provide information on their most useful and most ignored features. IoT-enabled construction equipment, through the historical data, can help shape patterns of information to understand better the requirements of the customers and contractors, the environment in which they operate, and, ultimately, offer appropriate solutions as per their necessities. Sometimes, as a consequence of a smart decision, building operation changes could be made through a smart, interconnected infrastructure (automatically).

At this can be add more characteristics of it, like:

- veracity, meaning the quality of contained data, in order to avoid biases, noises and abnormality during data analysis;
- validity, that measure the usefulness of data in decision making and policy makings;
- volatility that refers to how long is data valid and also, how long should the data be stored;
- visualisation, that refers to visual graphs, reports, charts, that can be more readable as outcomes of the data processing for users.

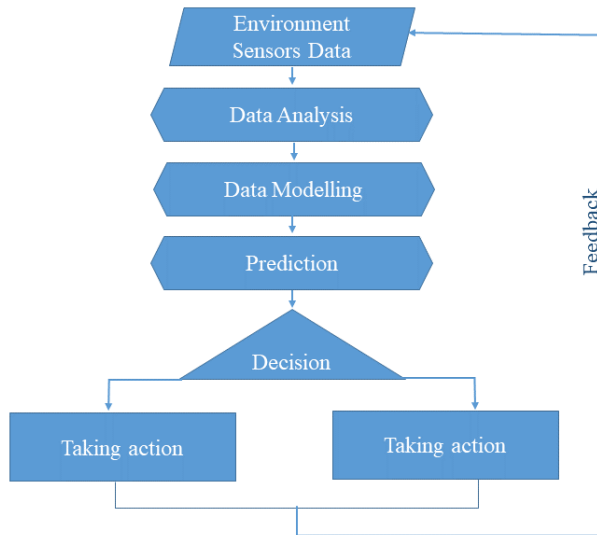


Fig. 2 - IoT platform's Informational framework

For a building where there are different type and/or firms for devices which doesn't „speak the same language” it can be hardly to coordinate the functionality of them. A facility manager or owner expects their Building Management System (BMS) to function effectively. In that manner, IoT platforms allow software applications to optimize the building's performance, by “co-working” processing other building system:

- facility management systems (preventive maintenance, work orders, inventory, etc.);
- business systems,
- smart grids,
- external data (weather and energy markets).

The minimum analytics functions of IoT platform should be able to perform:

- *descriptive analysis*, that can show what's happen at any given moment,
- *predictive analysis* in order to prevent unwanted and costly discontinues in the process
- *prescriptive analysis* used to obtain forecasted ROI values, new business models and ways to maximize output and efficiency.

There are several models for IoT integration platforms that can be used by the customers' application (Figure 3) [9]:

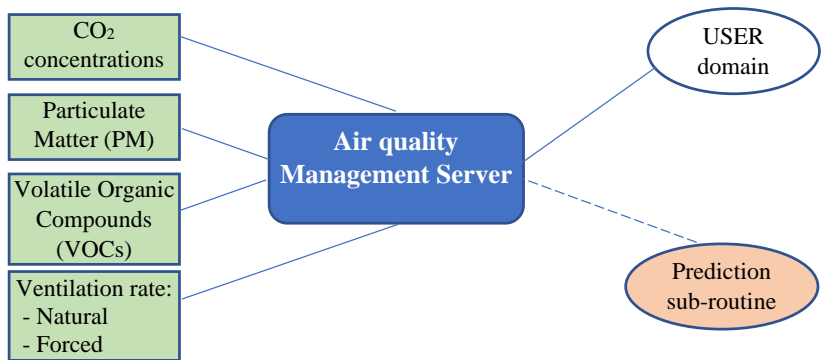
- model 1, where it is a unique provider for application, platform, network and devices
- model 2, where there is one player as device, network and platform provider and a second player as application provider

- model 3, where there one player operates as network and platform provider and the second as device and application provider
- model 4, where device, platform and application are provided by one player and only the network access is provided by the second user
- model 5, where can be multiple players: one as device and application provider, the second as network provider and the third as platform provider.

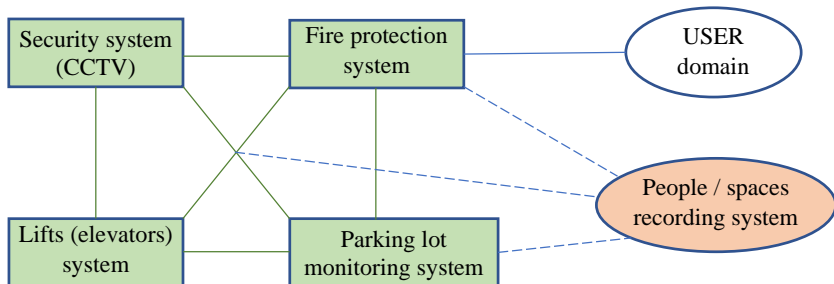
Between the devices that are part of the IoT platform its need to be a good machine socialization (they need to communicate to each other, to follow each other and to collaborate) and to have a relation between them (by sharing / providing the capability to achieve a tack in collaboration.)

The relation's management for machine socialization can have different models:

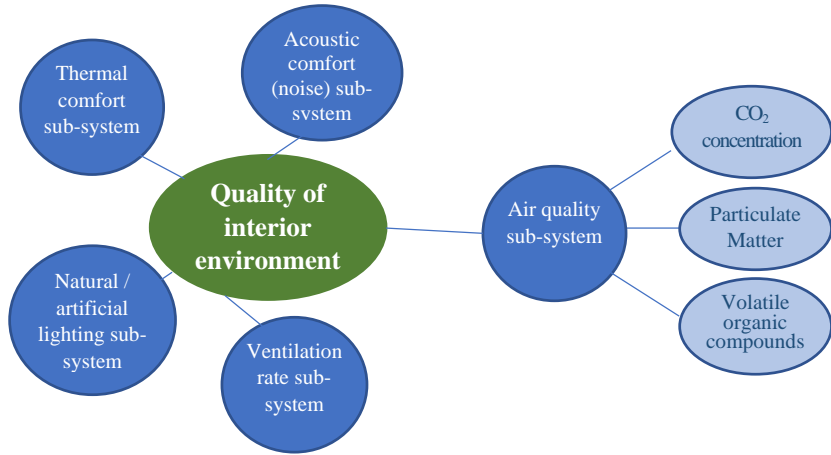
- the centralized model, where is a single relation server and several machines are linked to it (Figure 3a);
- the distributed model (Figure 3b), which have several interconnected machines;
- the nested-centralized model (Figure 3c).



a)



b)



c)

Fig. 3 - The relation management for machine socialization
a) the centralized model; b) the distributed model; c) the nested-centralized model

5. Conclusions

As an integrated tool of the future smart management, IoT contribute to internal and external connections, as follows:

- ⇒ Benefits for internal connections: Safety and Security, Reduced Expenses, Conserve Resources, Optimise Assets.
- ⇒ Benefits for internal connections: Increased Engagements, Enhanced Services, Improved Well-Being, Generate revenues.
- ⇒ Collective benefits: Predictive and proactive maintenance, Resource / Assets optimisation, Remote diagnosis, Real-time Monitoring.

The future of buildings involves projects that combines several concepts, as BIM (Building Information Modelling), Smart Cities, Smart Buildings, IoT, machine learning and future and the practice will show us many more.

References:

- [1] EU's Building Energy Performance Directive (EPBD2012)
- [2] https://ec.europa.eu/energy/topics/energy-efficiency_en
- [3] Law 372/2005 Regarding Buildings Energy Efficiency
- [4] EU's Directive 2010/31/UE
- [5] C 107 / 2005 - *Normativ privind calculul termotehnic al elementelor de construcție ale clădirilor*

- [6] <https://theconstructor.org/building/new-technologies-energy-savings-buildings/1251/>
- [7] Koo D, Piratla K, Matthews J - *Towards Sustainable Water Supply: Schematic Development of Big Data Collection Using Internet of Things (IoT)*, Procedia Engineering 118, 2015, pp. 489÷497
- [8] Behmann F, Wu K – *Collaborative Internet of Things (C-IoT) for Future Smart Connected Life and Bussiness*, Wiley, 2015
- [9] ITU-T, *Unleashing the potential of the Internet of Things*, 2016, <http://handle.itu.int/11.1002/pub/811983d5-en>

STUDY ON THE BEHAVIOUR OF HIGH-DENSITY POLYETHYLENE (HDPE) PIPES BURIED, ON THE EXPLOSION'S EFFECT

Ladislau RADERMACHER¹ and Theodor MATEESCU²

¹Petroșani University, Petroșani, Romania

²Gheorghe Asachi Technical University of Iasi, Romania

Abstract. *Abstract. The behaviour of buried pipes made of HDPE (high density polyethylene) due to an explosion refers to finding a safe distance at which the pipe does not suffer plastic deformations. To solve this problem in this paper, the response of HDPE (high density polyethylene) pipes buried to an explosion due to sabotage or terrorism is analysed by numerical modelling.*

Keywords: TNT explosive, JWL parameters, buried pipeline, gas, FEM

1. Introduction

Due to increased energy's consumption and global changes, natural gas still has an important role in energy production.

In each country, the main method of the natural gas's transportation is through underground pipes. Natural gas pipelines could be destroyed by explosions that can threaten the safety of structures and people.

Used for the distribution of water, gas, etc., the underground pipes in HDPE are considered among the most important elements of the installations.

Existing studies, concerning the explosion reaction of underground pipes, refer to the search for the safety distance in the event of an explosion in which the tube does not undergo plastic deformation

The study of buried pipes that can be destroyed by earthquakes or explosions has been studied by Newmark [1] and M. Mokhtari. et al. [2], M. Hajiazizi et al. [3], O, Adibi et al. [4]

Esparza et al. [5] developed an explosion analysis method to obtain simple methods necessary to determine the maximum stresses and pressures in underground steel pipes. The methods of Esparza et al. [5] applies to the design of pipes that can be subjected to explosions. However, the scale of these problems should be solved by numerical methods [2].

An analysis using numerical modelling of explosions applied to buried structures is presented in [6].

2. Finite element modelling

In the present article, the mechanical behaviour of the HDPE buried pipe is analysed numerically using the finite element method. To this end, a complete 3D model with finite elements was developed using a combined Eulerian-Lagrangian method.

Different models are used to model the behaviour of the used materials (HDPE, soil, explosive, air). These models are briefly explained below.

2.1. The material model for HDPE

The behavioural-modelling of HDPE activity is treated by different authors in [7-15], resulting in various constitutive equations. Starting from those presented in [2] and [16] and through laboratory experiments, the characteristic curve of the HDPE material was obtained (Figure 1) by using HDPE's properties presented in Table 1. The data experimentally obtained were used to model the behaviour of the HDPE pipeline.

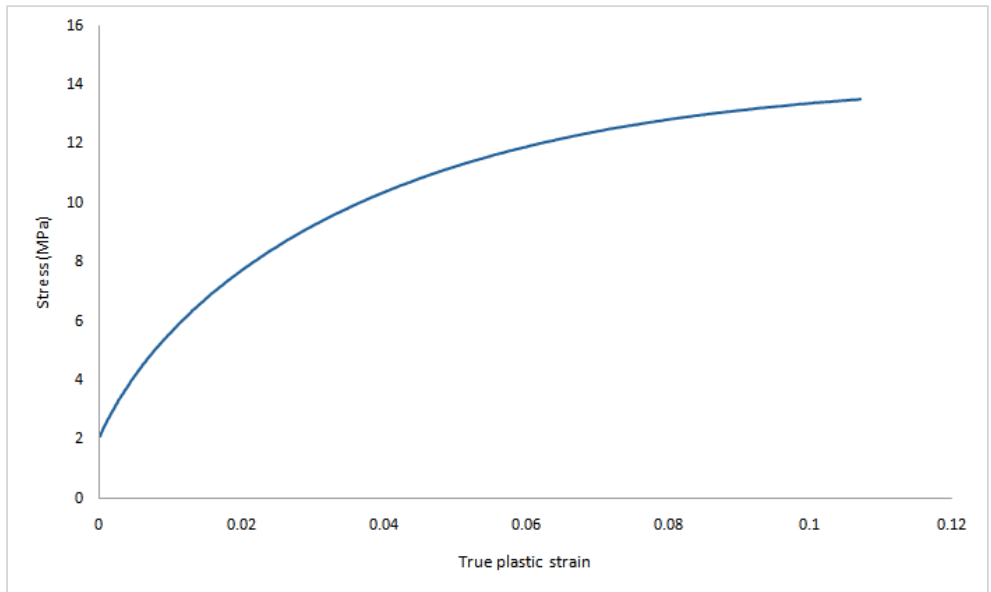


Fig. 1 - The characteristic curve of the HDPE pipeline

Table 1
Properties HDPE

Density [kg/m ³]	Young's Modulus [MPa]	Poisson's ratio
9230	700	0.3

2.2. Modelling of soil behaviour

The tube is placed in clay with the parameters presented in Table 2.

Table 2
Properties for the soil model

Share modulus [MPa]	Density [kg/m ³]	Friction angle [°]	Young's Modulus [MPa]	Poisson's ratio	Cohesion [MPa]
240	2200	24	50	0.3	1

According to [17] the behaviour of the soil influences the propagation of seismic waves in the soil. In this context, the breaking criterion used for the soil is Mohr-Coulomb.

2.3. Modelling of TNT (trinitrotoluene) equivalent

The Jones-Wilkins-Lee (JWL) equation which describes the pressure generated by the explosion of explosive chemicals explosive and has is written as follows [2,18-22]:

$$P = A \left(1 - \frac{\omega}{R_1 \cdot v} \right) \cdot e^{-R_1 \cdot v} + B \left(1 - \frac{\omega}{R_2 \cdot v} \right) \cdot e^{-R_2 \cdot v} + \frac{\omega}{v} \cdot E \quad (1)$$

where v = the specific volume

E = the specific energy.

$v = \rho_e / \rho$ is defined by using ρ_e = density of the explosive (solid part) and ρ = density of the detonation products. The A, B, R₁, R₂, ω constants values (for many common explosives) were determined by dynamic experiments [2]. The parameters of the Jones-Wilkins-Lee equation for TNT (Trinitrotoluene) are given in Table 3:

Table 3
Jones-Wilkins-Lee parameters for TNT (Trinitrotoluene) [2, 24]

Parameter	Value	Parameter	Value
ρ_0 [kg/m ³]	1630	B [GPa]	3747
E [kJ/m ³]	6000000	R ₁	4.15
C _d [m/s]	6930	R ₂	0.9
A [GPa]	373.8	ω	0.35
TNT equivalent [kg] [25]	10		

The ideal gas state equation (in a simplest forms) is used to simulate air [2]:

$$p_h = (\gamma - 1) \cdot \rho \cdot e \quad (2)$$

where p_h = the hydrostatic pressure;

ρ = the density;

e = the specific internal energy;

γ = the adiabatic exponent (Table 4):

Table 4*Air*

Parameter	Value
γ	1.4
ρ_0 , kg/m ³	1.225
T_0 , K	288.2

3. Dimensions, discretization, and general settings

Table 5*Dimensions for the HDPE pipeline [26]*

Parameter	Value
Type	PE100 SDR 11
External diameter, mm	630
Wall thickness, mm	37.4

According to the presentation and builds, the model in shown in Figure 2. The dimensions are beaten by a parametric analysis, consequently, its dimensions do not influence the results. The model is based on the planes symmetry $x, y = 0$ [2].

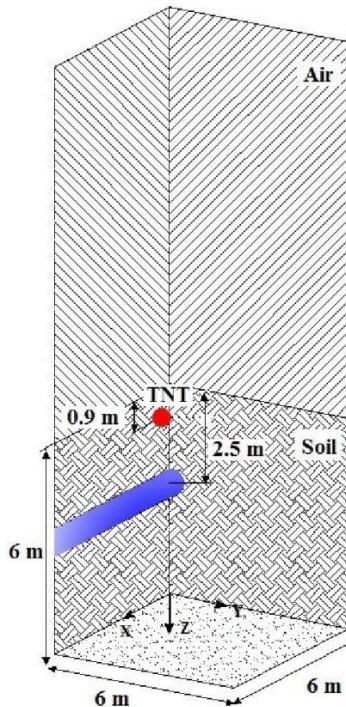


Fig. 2 - The full coupled model

To allow free movement and minimize the reflection of explosion waves, the boundary conditions in the Eulerian environment are unlimited.

The dimensions in Figure 2 are designed so as not to affect the results of the analysis [2]. The pipeline, TNT (trinitrotoluene), air and soil material are modelled from the Lagrangian domain. In critical regions (below the location of the explosive charge) modelling is done with small discretization elements and larger elements in remote regions, this is due to the use of the limited node version of the ABAQUS program (student version) [23].

4. Results, discussions and conclusions

The explosion effect' simulation has been performed following two steps:

1. Before the explosion stage (only the weight of the ground exerted on the model has been considered);
2. The detonation's stage.

The contact between the surrounding ground and the HDPE pipe's exterior is based on the General Contact algorithm. This model of algorithm allows any free movement of the ground pipe.

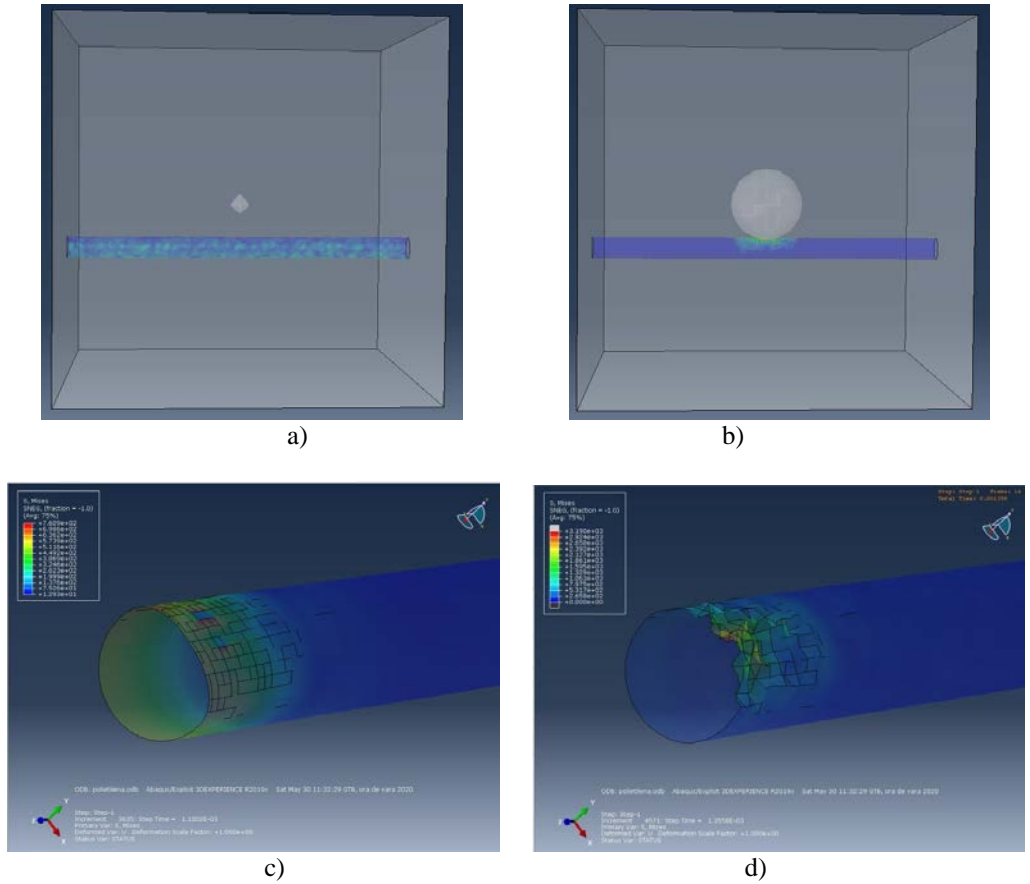
The study of the explosion's effect takes place immediately below the place of the explosive charge where its influence is maximum. The effect of the explosion on the ground surrounding the pipeline before and after the explosion is ignored. In the proposed model, the detonation occurs near the pipe (fig. 3a), so that its effect affects the pipe, the explosive charge of TNT was placed at about 1 m depth and the pipe is buried at 2.5 m depth.

The influence of the explosion begins just below the explosive charge (i.e. point A in Figure 4). As time passes from the moment of explosion to its completion, the tension and deformation of the pipe increase, the damage of the pipe (maximum voltage) moves from point A to point B (i.e. point B in Figure 4), along pipeline. The place where the explosion's effect (i.e. the state of tension and disorientation is maximum) is at point B.

From the analysis of the results in Figure 3 it is observed that the explosion deforms the HDPE pipe over the resistance limit. It is concluded that significant amounts of TNT equivalent can cause significant damage to natural gas pipelines. The crater dimensions for underground explosions coincide with those found in the literature [25].

The results of these studies can help design buried HDPE pipes to avoid damage in the event of an explosion near a natural gas pipeline.

The study can be developed for different gas pressures in the pipeline, the behaviour of HDPE pipes with steel ones can be analysed [2].



a) time 0.0, c) time 1.1×10^{-3} , b) & d) time 1.35×10^{-3} s

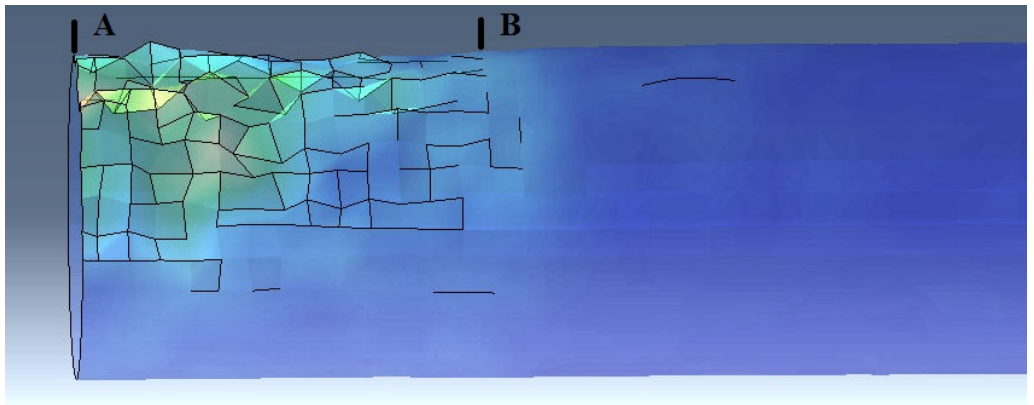


Fig. 4 - State of tension in the pipe due to the explosion, at time 1.35×10^{-3} s

REFERENCES

- [1] N.M. Newmark, *Problems in wave propagation in soil and rock*, in: Proc. International Symposium on Wave Propagation and Dynamic Properties of Earth Materials, August 23–25, University of New Mexico Press, Albuquerque, pp. 7–26, (1968).
- [2] M. Mokhtari, A. Alavi Nia, *A parametric study on the mechanical performance of buried X65 steel pipelines under subsurface detonation*, Archives of Civil and Mechanical Engineering, Volume 15, Issue 3, Pages 668-679, ISSN 1644-9665, <https://doi.org/10.1016/j.acme.2014.12.013>, (2015).
- [3] M.Hajiazizi, R.Kakaei, *Numerical simulation of GFRP blanket effect on reducing the deformation of X65 buried pipelines exposed to subsurface explosion*, International Journal of Pressure Vessels and Piping, Volume 166, Pages 9-23, ISSN 0308-0161, <https://doi.org/10.1016/j.ijpvp.2018.07.013>, (2018).
- [4] O.Adibi, A. Azadi, B. Farhanieh & H. Afshin, *A parametric study on the effects of surface explosions on buried high pressure gas pipelines*. Engineering Solid Mechanics, 5(4), 225-244, doi: 10.5267/j.esm.2017.9.003, (2017).
- [5] E. D. Esparza, P. S. Westine, A.B. Wenzel, *Pipeline Response To Buried explosive detonations*, Southwest Research Institute San Antonio, Texas Report Final Report A.G.A. Project PR-15-109 SwRI Project 02-5567 for The Pipeline Research Committee American Gas Association (August 1981)
- [6] E.E. Hinman, *Effect of deformation on the shock response of buried structures subject to explosions*, in: Structures under Shock and Impact, Elsevier Scientific Publishing Company, New York City, New York, USA, pp. 455–466, (1989).
- [7] M. Khalajmasoumi et al., *Explicit Dynamic Simulation of High Density Polyethylene Beam under Flexural Loading Condition*, Applied Mechanics and Materials, Vols. 229-231, pp. 2150-2154, doi:10.4028/www.scientific.net/AMM.229-231.2150, (2012).
- [8] M. Khalajmasoumi et al., *Hyperelastic Analysis of High Density Polyethylene under Monotonic Compressive Load*, Applied Mechanics and Materials, Vols. 229-231, pp. 309-313, doi:10.4028/www.scientific.net/AMM.229-231.309, (2012).
- [9] V.Filonova, Y. Liu, J. Fish, *Generalized Viscoplasticity Based on Overstress (GVBO) for Large Strain Single-Scale and Multiscale Analyses*, Numerical Simulations of Coupled Problems in Engineering, 3, Computational Methods in Applied Sciences 33, Springer International Publishing Switzerland, pp. 3-27, 2014, DOI: 10.1007/978-3-319-06136-8_1, (2014).
- [10] V.Filonova, Y. Liu and J. Fish, *Singlescale and Multiscale Models of Polyurea and High-Density Polyethylene (HDPE) Subjected to High Strain Rates*, Computational Simulation, Multi Scale Computations, and Issues Related to Behavioral Aspects of HSREP, Editor(s): Roshdy George Barsoum, Elastomeric Polymers with High Rate Sensitivity, William Andrew Publishing, Pages 233-263, ISBN 9780323354004, <https://doi.org/10.1016/B978-0-323-354004.00006-4>, (2015).
- [11] F. Rueda, J.P. Torres, M. Machado, P.M. Frontini, J.L. Otegui, *External pressure induced buckling collapse of high-density polyethylene (HDPE) liners: FEM modeling and predictions*, Thin-Walled Structures, Volume 96, Pages 56-63, ISSN 0263-8231, <https://doi.org/10.1016/j.tws.2015.04.035>, (2015).
- [12] H.J. Kwon, P.-Y.B. Jar, *On the application of FEM to deformation of high-density polyethylene*, International Journal of Solids and Structures, Volume 45, Issues 11–12, pages 3521-3543, ISSN 0020-7683, <https://doi.org/10.1016/j.jisols.2008.02.013>, (2008).
- [13] M.R. Mansouri, H. Darijani, *Constitutive modeling of isotropic hyperelastic materials in an exponential framework using a self-contained approach*, International Journal of Solids and Structures, Volume 51, Issues 25–26, Pages 4316-4326, ISSN 0020-7683, <https://doi.org/10.1016/j.jisols.2014.08.018>, (2014).
- [14] A.V. Amirkhizi, J. Isaacs, J. McGee and S. Nemat-Nasser, *An experimentally-based viscoelastic constitutive model for polyurea, including pressure and temperature effects*, Journal Philosophical Magazine, volume 86, number 36, PP.5847-5866, publisher Taylor & Francis, doi 10.1080/14786430600833198, (2006).
- [15] N.Dusunceli, O.U.Colak, *High density polyethylene (HDPE): Experiments and modelling*, Journal Mechanics of Time-Dependent Materials, Volume 10, Issue 4, pp 331–345, DOI: 10.1007/s11043-007-9026-5, (December 2006).

- [16] R. B. Arieby, H. N. Hameed, *Experimental Investigation and Constitutive Modelling of Volume Strain under Uniaxial Strain Rate Jump*, World Academy of Science, Engineering and Technology International Journal of Materials and Metallurgical Engineering, Volume 8, No:4, ISNI:0000000091950263, pp 748-753, (2014).
- [17] J. Q. Ehrigott Jr., S. A. Akers, J. E. Windham, D. D. Rickman and K. T. Danielson, *The Influence of Soil Parameters on the Impulse and Airblast Overpressure Loading above Surface-Laid and Shallow-Buried Explosives*, journal "Shock and Vibration", Volume 18, number 6, pp. 857-874, issn 1070-9622, doi:10.3233/SAV-2010-0609, (2011).
- [18] E.L. Lee, H.C. Hornig, J.W. Kury, *Adiabatic Expansion of High Explosive Detonation Products*, UCRL-50422, Lawrence Radiation Laboratory, University of California, USA, (1968).
- [19] J. L. Maienschein, *Estimating Equivalency of Explosives Through A Thermochemical Approach* 12th International Conference Symposium, San Diego, California, August 1 1-1 6, (2002).
- [20] L. E Schwer, *Jones-Wilkins-Lee (JWL) Equation of State with Afterburning*, 14th International LS-DYNA Users Conference Session: Constitutive Modelling, (2016).
- [21] R. Castedo, M. Natale, L.M. López, J.A. Sanchidrián, A.P. Santos, J. Navarro, P. Segarra, *Estimation of Jones-Wilkins-Lee parameters of emulsion explosives using cylinder tests and their numerical validation*, International Journal of Rock Mechanics and Mining Sciences, Volume 112, Pages 290-301, ISSN 1365-1609, <https://doi.org/10.1016/j.ijrmms.2018.10.027>, (2018).
- [22] G. Baudin and R. Serradeill, *Review of Jones-Wilkins-Lee equation of state*, EPJ Web of Conferences 10, 00021, DOI: 10.1051/epjconf/20101000021
- [23] ABAQUS/CAE User's Manual, Simulia, Providence, RI, USA, 2018, (2010).
- [24] [https://en.wikipedia.org/wiki/Equation_of_state#Jones%E2%80%93Wilkins%E2%80%93Lee_equation_of_state_for_explosives_\(JWL_equation\)](https://en.wikipedia.org/wiki/Equation_of_state#Jones%E2%80%93Wilkins%E2%80%93Lee_equation_of_state_for_explosives_(JWL_equation)).
- [25] R.D. Ambrosini, B.M. Luccioni, R.F. Danesi, J.D. Riera, M.M. Rocha, *Size of craters produced by explosive charges on or above the ground surface*, Shock Waves, , Volume 12, Issue 1, pp 69–78, (July 2002).
- [26] L. Radermacher L, T. Mateescu, *Study of natural gas pipeline behaviour*, Computational Civil Engineering Conference (CCE2019), IOP Conf. Series: Materials Science and Engineering (2019) doi:10.1088/1757-899X/586/1/012038586

AIRFLOW AND AIRBORNE PATHOGEN TRANSPORT BY HEATING SYSTEMS IN A CARDIAC INTENSIVE CARE UNIT

Florin-Emilian ȚURCANU^{1,*}, Cătălin-George POPOVICI¹, Marina Verdeș¹,
Vasilică CIOCAN¹, Andrei BURLACU¹, Nelu-Cristian CHERECHES¹,
Sebastian-Valeriu HUDIȘTEANU¹, Marius Costel BĂLAN¹, Larisa
ANGHEL^{2,3}

¹*Building Services Department, Faculty of Civil Engineering and Building Services, Gheorghe Asachi Technical University, Iași, Romania*

²*Internal Medicine Department, “Grigore T. Popa” University of Medicine and Pharmacy, Iași, Romania*

³*Cardiology Department, Cardiovascular Diseases Institute “Prof. Dr. George I.M. Georgescu”, Iași, Romania*

Abstract. *Respiratory infections in cardiac intensive care units related with heating systems are a major challenge, as they can lead to deaths but also to higher hospitalization costs. The study investigates the circulation of air currents and the ability to transport pathogens through the air using two different heating systems. The existing and proposed heating system (HVAC) was analyzed. In the investigation methods was modern one’s as computational fluid dynamics method (CFD), using three models of turbulence. It has been shown that the choice of an HVAC system allows adequate thermal comfort and also additional protection against the transmission of airborne infections through proper maintenance.*

Keywords: hospital-acquired respiratory infections; heating system; CFD modelling; particle tracking; intensive cardiac unit.

1. Introduction

Respiratory infections have been a public health concern, which has attracted the attention of researchers in various fields over the years [1,2]. Respiratory tract infections, acquired in cardiac intensive care units and beyond (nosocomial respiratory infections), are proving to be a challenge for physicians. Infections occur due to viruses and are transmitted through contact, drops and aerosol [3,4]. Also, in the same way can be transmitted the viruses [5 - 9].

Experts suggest that transmission by direct contact is most common, but also, there are more than a third hospital in witch infections involves airborne transmission [10]. The danger of threatening of respiratory infection was demonstrated by respiratory

syndrome (SARS) [11,12], the H1N1 [13] and Middle East Respiratory syndrome (MERS) [14-16]. Nowadays we are the witness of coronavirus disease 19 (COVID-19), caused by coronavirus 2 (SARS-CoV-2) [17].

Transmission of viruses by air is higher in indoor environments, given that people spend 90% of their time in buildings [17,18], this aspect also involves the generation, transformation, transport to later reach the inhalation of aerosols. Natural ventilation, especially mechanical ventilation influences the air transmission of aerosols, so that the process of air freshening in order to supply outdoor air and eliminate indoor pollutants, can provide a high quality of indoor air [18]. Distance measures from infected people may not be sufficient and increased ventilation may be helpful, as it may eliminate more infectious particles [19,20].

Patients from intensive care units can contact nosocomial and respiratory infections [21 - 24], which can lead to prolonged hospitalization due to prolonged hospitalization [24,25].

2. Method

The model we selected in the study is located in the Cardiovascular Diseases Institute Iasi. The measured data of indoor climate were taken with a TESTO 480 sensor that is equipped with indoor air quality (IAQ) sensors probe, also for dust fine particle (PM_{10} , $PM_{2.5}$) we used a particle counter from TESTO DiSCmini.

Data were collected during the month of January 2018 in 10 days, with an interval of 10 minute between each measurement, resulting a total of 1443 of measurements. The collection devices were previously calibrated and positioned in fixed points and followed the recommendations expressed in the standards ISO 16000-34:2018 and in ISO 16000-37:2019 [26,27].

The cardiac intensive care unit room geometry is length x width x height = 13.00 m x 6.80 m x 2.75 m and has a number of 7 beds. The studied area has 83 m² and a volume of 229 m³. The outdoor design temperature in winter is -18 °C. The cardiac intensive care unit had a heating system with static heaters (Fig. 1).

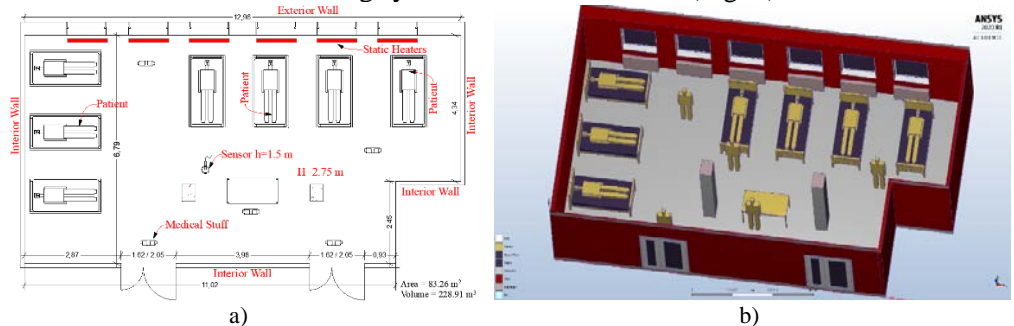


Fig. 1 - a) The floor plan of the studied model b) 3d zone model

Unfortunately, in April 2018 the hospital was involved in a fire, the intensive care unit being severely damaged. For this reason, it was considered to change the heating system, being proposed HVAC system. (Figure 2).

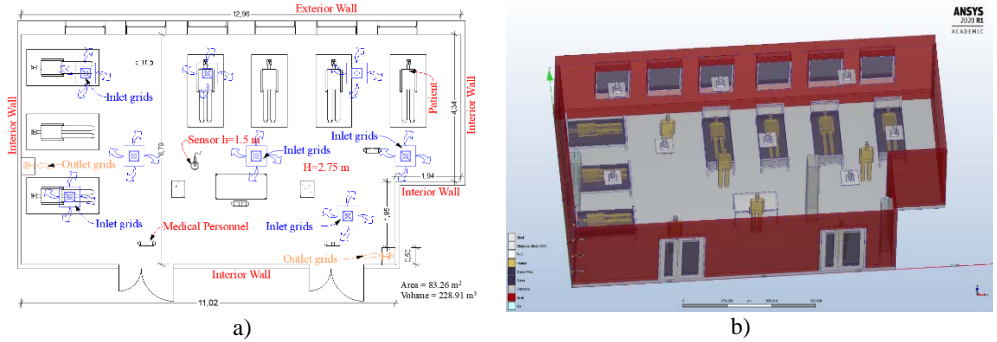


Fig. 2 - a) The floor plan of the proposed heating system b) The 3d zone model

In order to reduce the respiratory tract infections related with heating systems we analyzed the current existing heating system and the proposed one (HVAC). Furthermore, we compared these systems considering the main parameters: temperature, air velocities and particle tracking distribution.

After the indoor and outdoor measurement campaign during wintertime, we determine the boundary conditions in order to compute the (CFD) model for the indoor climate modelling (Table 1).

Table 1.
The boundary conditions for numerical simulation

No.	Envelope element	Heating system	
		Static heaters	HVAC Heating System
Temperature (°C)	Exterior Walls	-16	-16
	Ceiling	+20	+20
	Input grids for hot air		+30
	Floor plate	+20	+20
	Windows and Doors	+18	+18
Pressure (Pa)		Relative pressure	
Heat transfer coefficient U (W/m²K)	Exterior walls	12	12
	Windows and doors	3	3
	Ceiling	3.5	3.5
	Floor plate	3	3
Air velocity(m/s)	Inlet grids for hot air	-	1.2
	Extraction grids	-	1
Heat flux (W/m²)	Static heater	200	-
Heat flow generated by people is imposed at 80 (W)			

We used three different turbulence models: SST-k- ω , k- ϵ and RNG-k- ϵ [15–23], with an unstructured meshing type for our model. The scheme of the simulations analysis is represented in (Fig. 3).

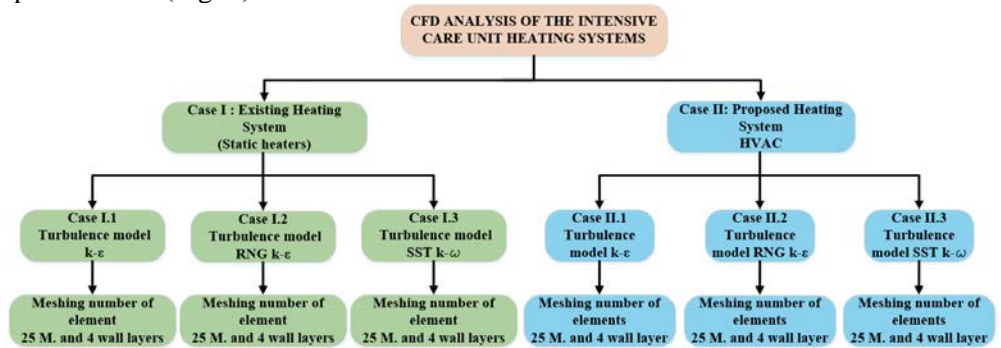


Fig. 3 - CFD analysis scheme of the studies zone.

3. Results and Discussion

The main objective of CFD analysis was a better understanding on the airflow and airborne pathogen transport and on the indoor air of the intensive care unit. The resulting information provide information in response to the high risk of airborne transmission infections in intensive care units.

In the CFD model we observed the transmission of PM 2.5 particles that can carry pathogens down to the lung alveoli.

The data from the three turbulence models and the values of the in situ measurements, were analyzed statistical through boxplot analysis.

Figure 4 shows the results of temperatures for in situ, existing and proposed heating system. Numerical model is valid for the turbulence models k- ϵ and RNG-k- ϵ , with a difference of 10% to 12% from the in situ measurements.

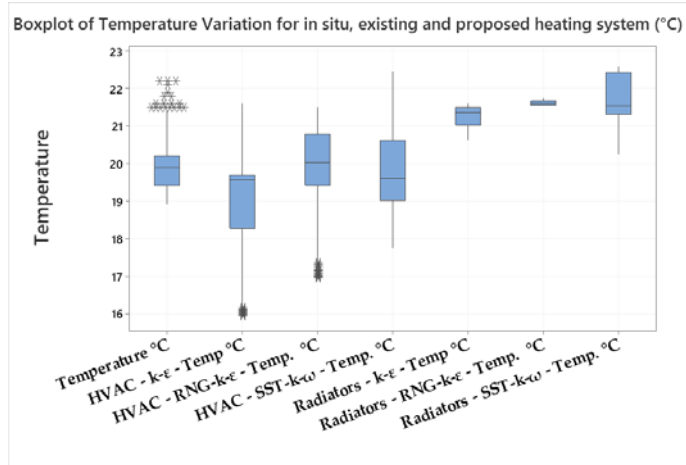


Fig. 4 - Boxplot of temperature variation for in situ, existing and proposed heating system.

The results of the velocities variation for in situ, existing and proposed heating system are presented in Fig. 5.

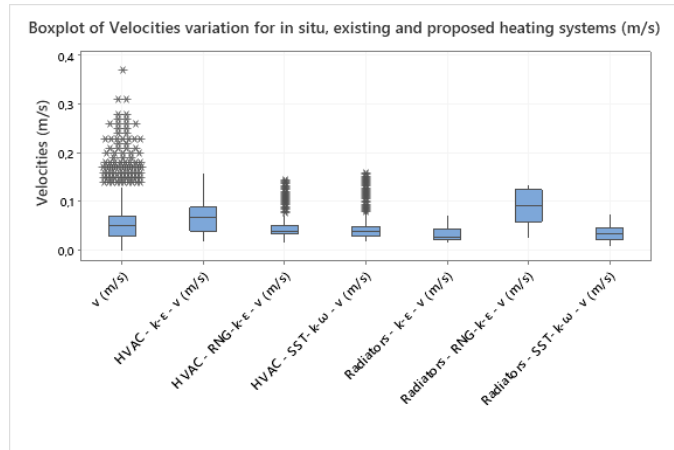


Fig. 5 - Boxplot of velocities variation for in situ, existing and proposed heating system.

We also evaluated the particle density for PM 2.5 and PM 10 and the CO₂ values in the studied unit before the fire, with the static heaters system and we observed a high concentration of PM 10 particles and the values for PM 2.5 were at the upper limit of the normal. Also, the CO₂ values were high for an intensive care unit (Figure 6). All of these values show insufficient ventilation of the space in the intensive care unit, which leads to a high degree of transmission of pathogens.

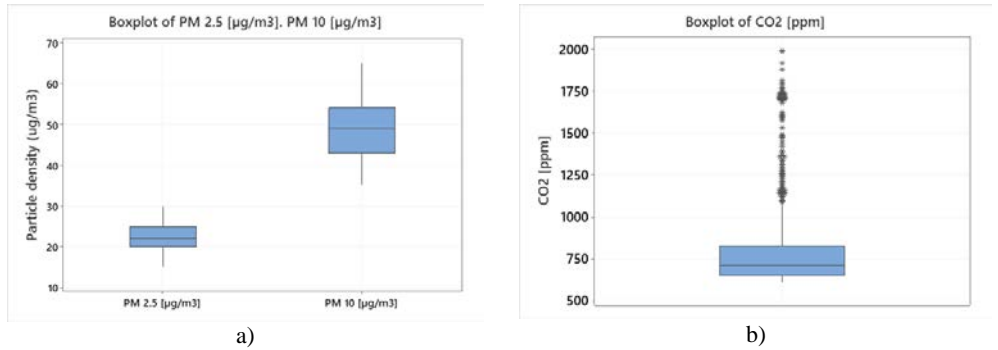


Figure 6. Boxplot of particle density for PM 2.5 and PM 10 (a) and CO₂ values (b).

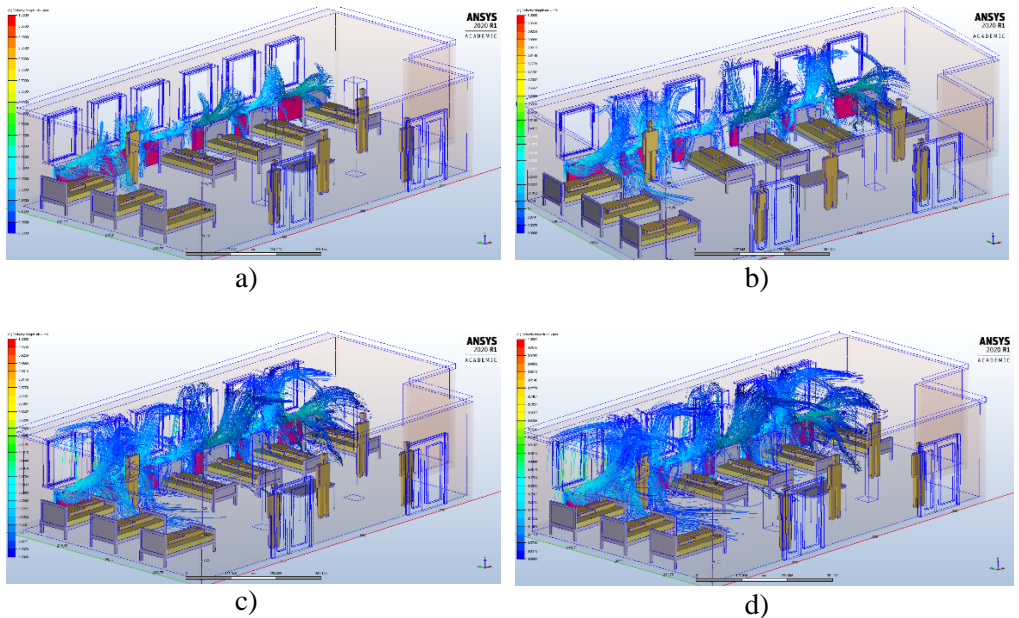


Fig. 7 - Transient analysis of particle tracking a) 5 seconds; b) 10 seconds; c) 15 seconds; d) 20 seconds.

Evaluating the existing heating system in a transient type analysis, we observed that the dispersion of PM 2.5 particles has placed in the upper part of the radiators and also in the upper part of studied unit. The spread of these particles is very fast and, as we can observe, in an interval of less than 20 seconds, they are spreading in more than half of the room (Figure 7).

For the proposed heating system (HVAC) the transient analysis was made for seven inlet design grids. It is observed that the dispersion of PM 2.5 particles is very fast and uniformly distributed around the grids (Fig. 8). Comparing the two heating systems, it is obvious that the HVAC system ensures a much more uniform distribution of particles and a faster spread of the infection. Therefore, for a HVAC heating system, additional safety measures must be taken. These are represented by the additional filtration of the air, the periodic disinfection of the air ducts and a much more frequent replacement of the air filters. These safety measures cannot instead be applied in the case of a static heating system, which is one of its main disadvantages.

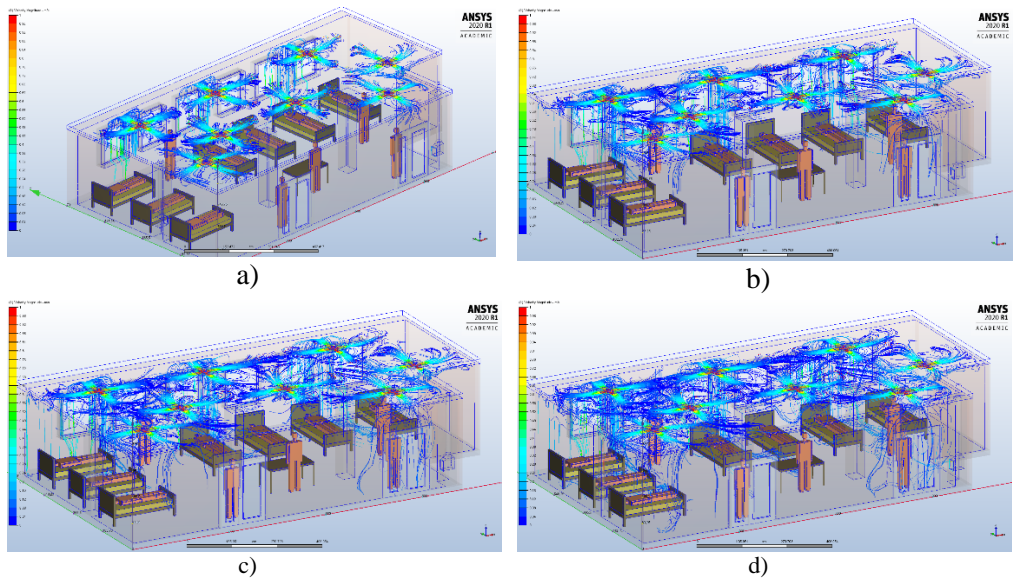


Fig. 8 - Transient analysis of particle tracking a) 5 seconds; b) 10 seconds; c) 15 seconds; d) 20 seconds

4. Conclusions

The result of our study was that, in case of a cardiac intensive care unit, the heating systems, must be carefully selected in order to choose a heating system that does not allow the spread of hospital-acquired respiratory tract infections. In our case, we have demonstrated that the choice of a HVAC system allows an adequate thermal comfort and also an additional protection against the transmission of airborne infections, through an adequate maintenance. Another advantage of this heating system is the possibility of using it during the summer, by permanently admitting a flow of fresh air. Ordinary AC systems and radiator heating systems only recirculate the air inside the room, which allows a faster spread of respiratory infections. In conclusion, the HVAC system is the

most suitable heating system that can be used in an intensive care unit, both to ensure thermal comfort and air quality, but especially to prevent the transmission of hospital-acquired respiratory tract infections, which are unfortunately more common nowadays.

REFERENCES

- [1] W. Filipiak et al., *Breath analysis for in vivo detection of pathogens related to ventilator-associated pneumonia in intensive care patients: a prospective pilot study*, J. Breath Res., vol. 9, no. 1, p. 016004, Jan. 2015, doi: 10.1088/1752-7155/9/1/016004.
- [2] M. R. Moser, T. R. Bender, H. S. Margolis, G. R. Noble, A. P. Kendal, and D. G. Ritter, *An outbreak of influenza aboard a commercial airliner*, Am. J. Epidemiol., vol. 110, no. 1, pp. 1–6, Jul. 1979, doi: 10.1093/oxfordjournals.aje.a112781.
- [3] ASHRAE, *HVAC design manual for hospital and clinics*, ASHRAE Special Project 91, 2003. American Society of Heating, Refrigerating, and Air-conditioning Engineers.
- [4] Y. Li, X. Huang, ITS Yu, et al., *Role of air distribution in SARS transmission during the largest nosocomial outbreak in Hong Kong*, Indoor Air, vol. 15, pp. 83-95, 2005.
- [5] J.M. Vincent, *Aerosol science for industrial hygienists*, in *The motion of airborne particles*. Ed. Oxford, 1995, pp. 72–11
- [6] B. Zhao, Z. Zhang, X. Li, *Numerical study of the transport of droplets or particles generated by respiratory system indoors*, Building and Environment; vol. 40, pp.1032–9, 2004.
- [7] P.V. Nielsen, E. Bjørn, H. Brohus, *Contaminant flow and personal exposure*, Heating/Piping/Air conditioning Engineering, vol.74, pp. 40-45, 2002.
- [8] C. Topp, P.V. Nielsen, D.N. Sorensen, *Application of computer simulated persons in indoor environmental modeling*, ASHRAE Transactions, vol. 108, pp. 1084-1089, 2002.
- [9] 2012 National and State Healthcare-Associated Infections Progress Report. Centers for Disease Control and Prevention (CDC); 2014.
- [10] W. J. Kowalski, *Air-treatment systems for controlling hospital acquired infections*, HPAC Engineering, vol. 79, no. 1, pp. 28–48, 2007.
- [11] H. Qian and X. Zheng, *Ventilation control for airborne transmission of human exhaled bio-aerosols in buildings*, Journal of thoracic disease, vol. 10, pp.S2295, 2018.
- [12] N.S. Zhong, B.J. Zheng, Y.M. Li, et al., *Epidemiology and cause of severe acute respiratory syndrome (SARS) in Guangdong, People's Republic of China*, Lancet, vol. 362, pp.1353-1358, February, 2003.
- [13] M. Balali-Mood, M. Moshiri, L. Etemad, *Medical aspects of bio-terrorism*, Toxicon, vol. 69, pp.131-142, 2013.
- [14] M.D. Van Kerkhove, K.A.Vandemaele, V. Shinde, et al., *Risk factors for severe outcomes following 2009 influenza a (h1n1) infection: a global pooled analysis*, PLoS Med, vol.8, pp. e1001053, 2011.
- [15] C.J. Kim, W.S. Choi, Y. Jung, et al., *Surveillance of the Middle East respiratory syndrome (MERS) coronavirus (CoV) infection in healthcare workers after contact with confirmed MERS patients: incidence and risk factors of MERS-CoV seropositivity*, Clin Microbiol Infect, vol. 22, pp. 880-886, 2016.
- [16] Y. Li, G.M. Leung, J.W. Tang, et al., *Role of ventilation in airborne transmission of infectious agents in the built environment - a multidisciplinary systematic review*, Indoor Air, vol. 17, pp.2-18, 2007.
- [17] X. Gao, J. Wei, H. Lei, et al., *Building ventilation as an effective disease intervention strategy in a dense indoor contact Network in an ideal city*, PLoS One, vol. 11, pp. e0162481, 2016.
- [18] X. Gao, J. Wei, B.J. Cowling, et al., *Potential impact of a ventilation intervention for influenza in the context of a dense indoor contact network in Hong Kong*, Sci Total Environ, vol. 596, pp.373-81, 2016.
- [19] COVID, R., 19. guidance document, April 3, 2020. *How to operate and use buildings services in order to prevent the spread of the corona disease (COVID-19) virus (SARS-CoV-2) in workplaces*.
- [20] G. Greco, W. Shi, R.E. Michler, et al., *Costs associated with health care-associated infections in cardiac surgery*, JACC, vol. 65, pp.15-23, 2015.

- [21] L. Ridderstolpe, H. Gill, H. Granfeldt, et al., *Superficial and deep sternal wound complications: incidence, risk factors and mortality*. European journal of cardio-thoracic surgery: official journal of the European Association for Cardio-thoracic Surgery, vol. 20, pp.1168-1175, 2002.
- [22] V.G. Fowler, S.M. O'Brien, L.H. Muhlbaier, et al., *Clinical predictors of major infections after cardiac surgery*, Circulation, vol. 112, pp. I358-365, 2005.
- [23] F.H. Edwards, T.B. Ferguson. *The Society of Thoracic Surgeons Practice Guidelines*. Ann Thorac Surg, vol. 77, pp. 1140-1151, 2004.
- [24] M.H. Kollef, L. Sharpless, J. Vlasnik, et al. *The impact of nosocomial infections on patient outcomes following cardiac surgery*. Chest, vol. 112, pp. 666-675, 1997.
- [25] P.P. Brown, A.D. Kugelmass, D.J. Cohen, et al. *The frequency and cost of complications associated with coronary artery bypass grafting surgery: results from the United States Medicare program*. Ann Thorac Surg. Vol 85, pp. 1980-1986, 2008.
- [26] ISO 16000-34:2018 Indoor air — Part 34: Strategies for the measurement of airborne particles.
- [27] ISO 16000-37:2019 Indoor air — Part 37: Measurement of PM_{2,5} mass concentration.